Universidad CEU San Pablo
CEINDO – CEU Escuela Internacional de Doctorado

PROGRAMA en CIENCIA Y TECNOLOGÍA DE LA SALUD

Metabolic Phenotyping of Animal Models of Diet-Induced Obesity and its Complications

(Fenotipado metabólico de modelos animales de obesidad inducida por dieta y sus complicaciones)

TESIS DOCTORAL
Presentada por:
Eugenia Carril Carvajal
Dirigida por: Dr. Fco. Javier Rupérez Pascualena
Dr. Joanna Godzien

MADRID
Año 2021

UNIVERSIDAD SAN PABLO CEU

FACULTAD DE FARMACIA
DEPARTAMENTO DE QUÍMICA Y BIOQUÍMICA

METABOLIC PHENOTYPING OF ANIMAL MODELS OF DIET INDUCED OBESITY AND ITS COMPLICATIONS

(FENOTIPADO METABOLICO DE MODELOS ANIMALES DE OBESIDAD INDUCIDA POR DIETA Y SUS COMPLICACIONES)

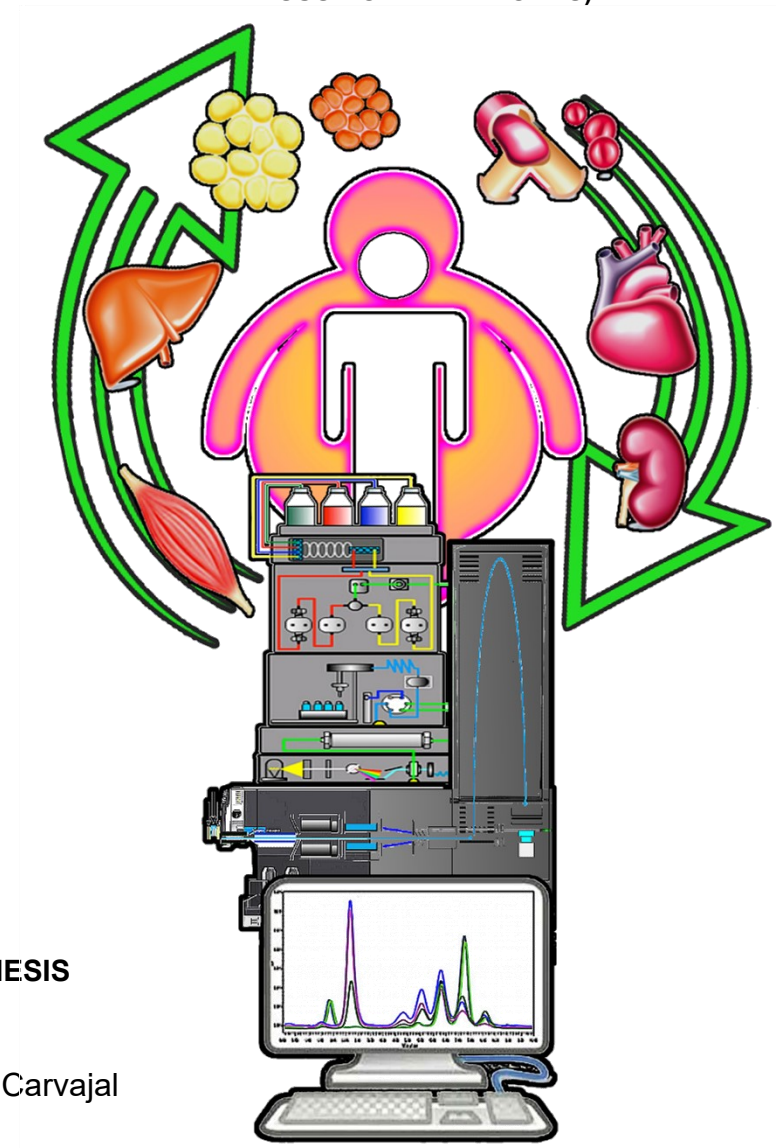

DOCTORAL THESIS

Presented by

Eugenia Carril Carvajal

Supervised by

RUPÉREZ PASCUALENA, FRANCISCO JAVIER
GODZIEN, JOANNA BARBARA

Madrid, 2021

Este trabajo ha sido realizado en el Centro de Metabolómica y Bioanálisis (CEMBIO), Departamento de Química y Bioquímica, Área de Química Analítica de la Facultad de Farmacia de la Universidad San Pablo CEU (Madrid), bajo la dirección del Dr. Francisco Javier Rupérez Pascualena y la Dra. Joanna Godzien.

El Dr. Francisco Javier Rupérez Pascualena y la Dra. Joanna Godzien, director y codirectora de este trabajo; expresan su conformidad para la presentación de este por considerar que reúne los requisitos necesarios y constituye una aportación original al tema tratado.

Fdo. Dr. Fco. Javier Pascualena

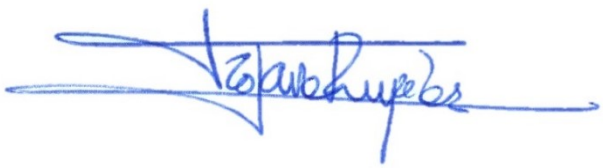

Fdo. Dra. Joanna Godzien

Acknowledgements

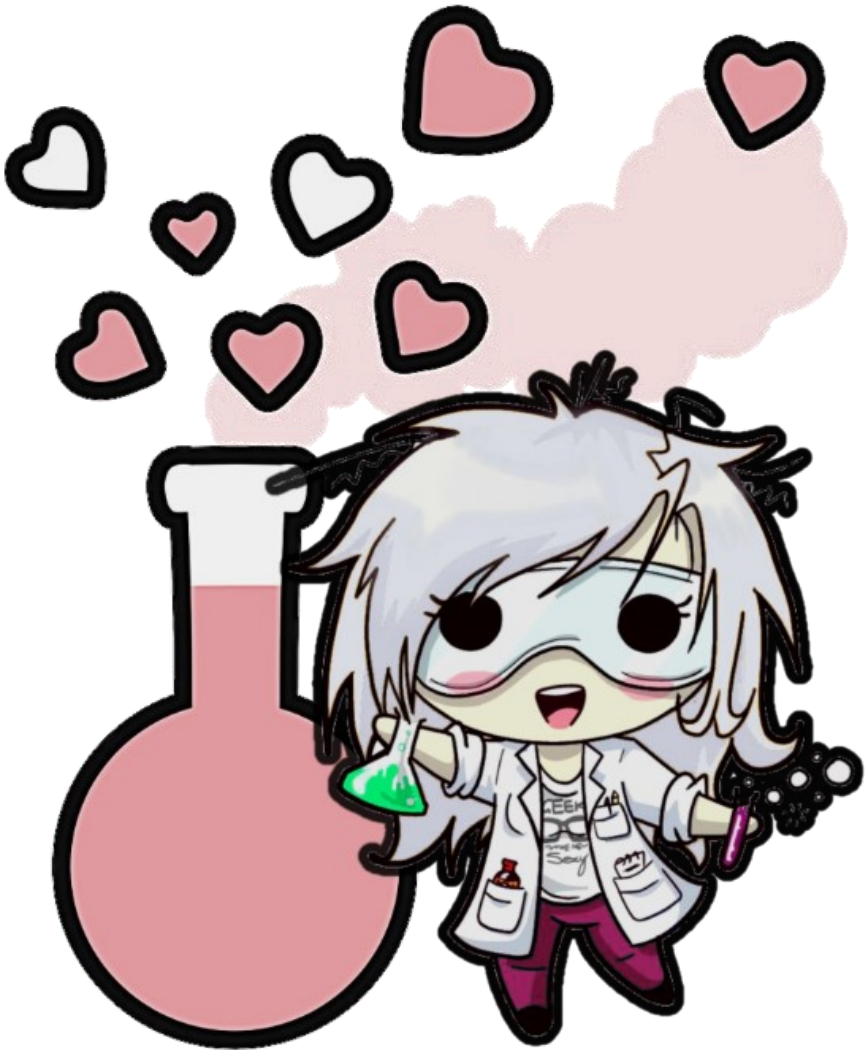

Table of Contents

List of abbreviations

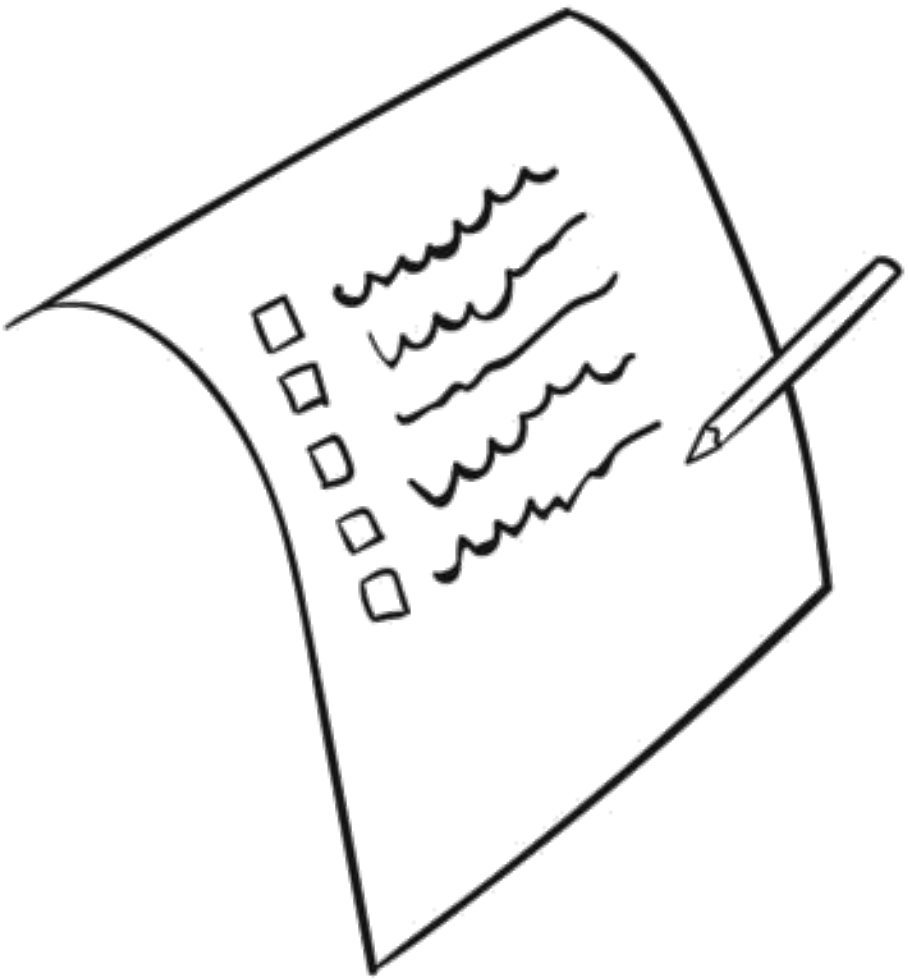

ACN	Acetonitrile
AHT	Arterial Hypertension
ALA	Alpha-linolenic acid
ANOVA	Analysis of variance
ARA	Arachidonic acid
ATGL	Adipose Triglyceride Lipase
BAT	Brown Adipose Tissue
CE-MS	Capillary electrophoresis coupled with mass spectrometry
Cer	Ceramide
CKD	Chronic Kidney Disease
CoAs	Coenzyme A(s)
COX	Cyclooxygenase
CPT	Carnitine palmitoyltransferase
CYP	cytochrome
DIO	Diet-Induced Obesity
DG(s)	Diacylglycerol(s)
DHA	Docosahexaenoic acid
DHAHLA	docosahexaenoic acid ester of hydroxy linoleic acid
DiHETE	Dihydroxy eicosatetraenoic acid
DiHETrE	Dihydroxyeicosatrienoic acid
DIO	Diet-induced obesity
DM	Diabetes Mellitus
DMS	Differential Mobility Spectrometry
EET	Epoxyeicosatrienoic acid
EPA	Eicosapentaenoic acid
EpOME	Epoxyoctadecenoic acid
ER	Endoplasmic reticulum
ESI	Electrospray ionization
EtOH	Ethanol
eWAT	Epididymal White Adipose Tissue
FA	Fatty acyl or fatty acid
FAHFA	Fatty Acid ester of Hydroxyl Fatty Acid
FC	Fold change
FFA	Free Fatty Acid
GC	Gas chromatography
GC-MS	Gas chromatography coupled with mass spectrometry
GFR	Glomerular Filtration Rate
GPL(s)	Glycerophospholipid(s)
H	Heart
HCC	Hepato Cellular Carcinoma
HDL	High-Density lipoproteins
HETE	Hydroxyeicosatetraenoic acid
HMDB	Human metabolome database

HODE	Hydroxy octadecadienoic acid
HPLC	High-performance liquid chromatography
HSL	Hormone-sensitive lipase
IGF	Insulin growth factor
IL	Interleukin
INOS	Inducible nitric oxide synthase
IPA	Isopropanol
IR	Insulin Resistance
IRS	Insulin receptor subtract
iWAT	Inguinal White Adipose Tissue
JNK	Jun N terminal kinase
KEGG	Kyoto Encyclopaedia of Genes and Genomes
K	Kidney
KMD	Kendricks mass defect
KNM	Kendricks nominal mass
LA	Linoleic acid
LC-MS	Liquid chromatography coupled with mass spectrometry
LDL	Low-density lipoproteins
LLE	Liquid-Liquid Extraction
LOX	Lipooxygenase
LP(s)	Lysoglycerophospholipid(s)
LPA(s)	Lysophosphatidic acid(s)
LPC(s)	Lysophosphocholines(s)
LPE(s)	Lysophosphoethanolamine(s)
LSM(s)	Lysosphingomyelin(s)
LT	Leukotriene
m/z	Mass-to-charge ratio
m:n	A fatty acyl chain containing m carbon atoms and n double bonds
MAPK	Mitogen-activated protein kinases
MCD	Methionine Choline Deficient
MD2	Mellitus diabetes type 2
MeOH	Methanol
MFE	Molecular feature extraction
MG(s)	Monoacylglycerol(s)
MS	Mass spectrometric or mass spectrometry
MPP	Mass Profiler Professional
MS/MS	Tandem mass spectrometry
MT	Migration time
MTBE	Methyl-tert-butyl ether
MTHF	Methyltetrahydrofolate
MUFA(s)	Mono-unsaturated fatty acids
N	Number of subjects
N/A	Non- applicable

NAFLD	Non-Alcoholic Fatty Liver Disease
NASH	Non-Alcoholic Steato Hepatitis
NB	Nuclear base
NF-κB	Nuclear factor-kappa B
NO	Nitric Oxygen
P	Plasma
PA(s)	Glycerophosphatidic acid(s)
PC(s)	Glycerophosphocholine(s)
PCA	Principal components analysis
PE(s)	Glycerophosphophatidylethanolamine(s)
PG(s)	Glycerophosphosphatidylglycerol(s)
PH	Partial hepatectomy
PI(s)	Glycerophosphatidylinositol(s)
PI3	Phosphoinositol kinase 3
PIA	Plasminogen inhibitor activator
PIP(s)	Glycerophosphatidylinositol phosphate(s)
PIP2(s)	Glycerophosphatidylinositol diphosphate (or bisphosphate)
PK	Protein kinase
PKC	Protein Kinase C
PNPLA	Patatin like phospholipase domain
PPARs	Peroxisome Proliferator-activated receptor(s)
PPT	Protein precipitation
PRF	Peri Renal Fat
PS(s)	Glycerophosphophatidylserine(s)
PUFA(s)	Poli unsaturated fatty acid (s)
PVAT	Perivascular adipose tissue
pWAT	Perirenal White adipose tissue
QC	Quality control
QqQ	Triple quadrupole mass spectrometer
R2	Goodness of fit of the model
RAAS	Renin-Angiotensin-Aldosterone System
ROS	Reactive oxygen species
RPC	Reactive protein C
RP-LC-MS	Reverse phase liquid chromatography-mass spectrometry
RSF	Renal Sinus Fat
SAH	Systemic arterial hypertension
SFA(s)	Saturated fatty acids (s)
SM(s)	Sphingomyelin(s)
SNS	Sympathetic nervous system
SPE	Solid-phase extraction
TGF	Transforming growth factor
TG(s)	Triacylglycerol(s)
TCA	Tricarboxylic acid cycle (Krebs cycle)

TLR	Toll-like receptors
TMAO	Trimethylamine N-oxide
TMCS	Trimethyl chlorosilane
TNF	Tumour necrosis factor
TOF	Time of flight mass spectrometer
U(H)PLC	Ultra (high)-performance liquid chromatography
UPR	Unfolded protein response
QTOF-MS	quadrupole time-of-flight mass spectrometry
VAT	Visceral Adipose Tissue
VLDL	Very Low-Density Lipoprotein

Abstract

Obesity is the primary cause of insulin resistance that represents one of the main threats to global human health and is increasing every year. In the liver, obesity is manifested by the clinical disorder of the Non-Alcoholic Fatty Liver Disease (NAFLD) that is characterized by insulin resistance and accumulation of triglycerides (hepatic steatosis)

Metabolomics or metabonomics is the study of the metabolic composition of a cell, tissue or biological fluid and the quantitative and multiparametric measurement of the response of a living being to some pathophysiological stimuli of genetic modification.

Nowadays, metabolomics is focused on the resolution of biological challenges by only studying one single tissue. The global purpose of this project is to study through metabolomic a comprehensive approach to evaluating as much as possible the metabolic alterations associated with diet-induced obesity in different organs simultaneously. Also, to study one of the main complications of obesity: non-alcoholic steatohepatitis (NASH) and possible treatment.

There are different dietary animal models relevant to mimic specific pathogenesis and metabolic disorders in the organism. Among the dietary patterns used in this thesis are the High Fat Diet (HFD) (to induce obesity) and Methionine Choline (MCD) diet (to induce NASH).

In the present thesis, we introduce the term “Compartmentomics” as a new omics that focus on the study of metabolic changes caused by obesity (in this case) in the different compartments of the body and then give them a holistic interpretation.

In Chapter 1 we expose results obtained from 8 different tissues under obesity conditions. The real novelty of this chapter is the employed methodology that allowed us to better understand the metabolic impact of obesity in an organism and supposes a new way of studying pathologies.

Multiplatform study through LC-MS, CE-MS and GC-MS was carried out and specific annotations strategies for data from each platform were applied, including database query (CEU Mass Mediator), in-house databases built from standards, MS/MS experiments, and lipid annotation with their Kendrick´s Mass Defect.

We found common trends in many of the significant metabolites (amino acids, short-chain organic acids, lysophospholipids) in plasma, kidney, heart and skeletal muscle. Diglycerides and triglycerides variations between obese and lean mice were similar between WATs but different from BAT. Moreover, the increase in lysophospholipids in plasma of obese mice seems more related to the increase in diglycerides in adipose tissue. Our results highlight the importance of the selection of the biospecimen according to the model under study, and our approach allows us to build a hypothesis about the metabolite flows between organs.

Inside this chapter, one of the tissues (epididymal White Adipose Tissue) was used to study and optimize an extraction methodology for TGs and oxylipins that were performed during my international mobility at the “Adipose Tissue Department from the Institute of Physiology CAS from Prague, Czech Republic” in Prague. Results suggest that there is an enrichment in stearic and oleic acid, a reduction in all PUFA and a noticeable increase in some of the significant lipid and proinflammatory mediators related especially to 2-AG and Arachidonic acid respectively.

In Chapter 2 one of the main complications related to obesity and insulin resistance is studied through metabolomics: Non-Alcoholic Steatohepatitis.

In addition to the metabolic study of NASH and MCD diet, it was wanted to observe liver progression after a partial hepatectomy that is being used as therapy for liver regeneration in cirrhosis and some cancers.

Compound putative identification was performed with CEU Mass Mediator. LC-MS/MS was employed to confirm part of the significant features, and a library of standards and a comprehensive list of compounds was compared in CE-MS.
CE-MS has permitted to see changes in amino acid (proteinogenic and non-proteinogenic) and methylation pathways, whereas lipid metabolism (sphingolipid, phospholipid, neutral lipid, acylcarnitine, etc.) has been evaluated by means of LC-MS.

Results show the great metabolic impact of NASH in the liver but are more remarkable the metabolic changes produced after the Partial Hepatectomy. This study allowed us to elucidate a biological interpretation about metabolic changes due to NASH and also reinforces the previous idea of introducing Partial Hepatectomy as a future therapy for NASH

and other liver complications and will help in the discovery and/or design of possible therapeutic strategies for liver regeneration.

All the data obtained in the studies of this thesis, after exhaustive work, allowed us to increase the information of the metabolic impact of obesity and its complications and obtain the widest metabolite coverage being able to compare results between samples as well as between treatments.

Resumen

La obesidad es la principal causa de la resistencia a la insulina, que representa una de las principales amenazas para la salud mundial y aumenta cada año. En el hígado, la obesidad se manifiesta con el trastorno clínico de la Esteatohepatitis no alcohólica (EHNA) que se caracteriza por la resistencia a la insulina y la acumulación de triglicéridos (esteatosis hepática).

La metabolómica es el estudio de la composición metabólica de una célula, tejido o fluido biológico y la medición cuantitativa y multiparamétrica de la respuesta de un ser vivo a unos estímulos fisiopatológicos de modificación genética.

En la actualidad, la metabolómica se centra en la resolución de retos biológicos mediante el estudio de un único tejido. El propósito global de este proyecto es estudiar a través de la metabolómica una aproximación integral para evaluar al máximo las alteraciones metabólicas asociadas a la obesidad inducida por la dieta en diferentes órganos de forma simultánea. También estudiar una de las principales complicaciones de la obesidad: la esteatohepatitis no alcohólica (EHNA) y su posible tratamiento.

Existen diferentes modelos animales dietéticos relevantes para imitar la patogénesis específica y los trastornos metabólicos en el organismo. Entre los modelos dietéticos utilizados en esta tesis se encuentran la dieta alta en grasas (HFD) (para inducir la obesidad) y la dieta con déficit de metionina y colina (MCD) (para inducir la EHNA).

En la presente tesis introducimos el término "Compartimentómica" como una nueva ómica que se centra en el estudio de los cambios metabólicos causados por la obesidad (en este caso) en los diferentes compartimentos del organismo para luego darles una interpretación holística.

En el capítulo 1 se exponen los resultados obtenidos en 8 tejidos diferentes en condiciones de obesidad. La verdadera novedad de este capítulo es la metodología empleada que nos permitió comprender mejor el impacto metabólico de la obesidad en un organismo y supone una nueva forma de estudiar las patologías.

Se realizó un estudio multiplataforma a través de LC-MS, CEMS y GC-MS y se aplicaron estrategias de anotación específicas para los datos de cada plataforma, incluyendo la

consulta de bases de datos (CEU Mass Mediator), bases de datos propias construidas a partir de estándares, experimentos de MS/MS y anotación de lípidos con su defecto de masa de Kendrick.

Encontramos tendencias comunes en muchos de los metabolitos significativos (aminoácidos, ácidos orgánicos de cadena corta, lisofosfolípidos) en plasma, riñón, corazón y músculo esquelético. Las variaciones de diglicéridos y triglicéridos entre los ratones obesos y delgados fueron similares entre los tejidos adiposos blancos (WAT) pero diferentes de en el tejido adiposo marrón (BAT). Además, el aumento de lisofosfolípidos en el plasma de los ratones obesos parece estar más relacionado con el aumento de diglicéridos en el tejido adiposo. Nuestros resultados ponen de manifiesto la importancia de la selección de la bioespecie en función del modelo estudiado, y nuestro enfoque permite construir una hipótesis sobre los flujos de metabolitos entre órganos.

Dentro de este capítulo, se utilizó uno de los tejidos (tejido adiposo blanco epididimal) para estudiar y optimizar una metodología de extracción de TGs y oxilipinas que se realizó durante mi movilidad internacional en el "Departamento de Tejido Adiposo del Instituto de Fisiología CAS de Praga, República Checa" en Praga. Los resultados sugieren que hay un enriquecimiento en ácido esteárico y oleico, una reducción en todos los PUFA y un aumento notable en algunos de los mediadores lipídicos y proinflamatorios significativos relacionados especialmente con 2-AG y ácido araquidónico respectivamente.

En el capítulo 2 se estudia una de las principales complicaciones relacionadas con la obesidad y la resistencia a la insulina mediante la metabolómica: La esteatohepatitis no alcohólica (EHNA).

Además del estudio metabólico de la EHNA y la dieta MCD, se quiso observar la progresión del hígado después de una hepatectomía parcial que se está utilizando como terapia para la regeneración del hígado en la cirrosis y en algunos cánceres.

La identificación de los compuestos putativos se realizó con CEU Mass Mediator. Se empleó LC-MS/MS para confirmar parte de las características significativas, y se comparó una biblioteca de estándares y una lista completa de compuestos en CE-MS.

La CE-MS ha permitido ver los cambios en las vías de los aminoácidos (proteinogénicos y no proteinogénicos) y de la metilación, mientras que el metabolismo de los lípidos (esfingolípidos, fosfolípidos, lípidos neutros, acilcarnitinas, etc.) se ha evaluado mediante LC/MS.

Los resultados muestran el gran impacto metabólico de la EHNA en el hígado, pero es más notable los cambios metabólicos producidos tras la Hepatectomía Parcial. Este estudio nos ha permitido dilucidar una interpretación biológica sobre los cambios metabólicos debidos a la EHNA y también refuerza la idea previa de introducir la Hepatectomía Parcial como futura terapia para la EHNA y otras complicaciones hepáticas y ayudará en el descubrimiento y/o diseño de posibles estrategias terapéuticas para la regeneración del hígado.

Todos los datos obtenidos en los estudios de esta tesis, tras un exhaustivo trabajo, nos permitieron aumentar la información del impacto metabólico de la obesidad y sus complicaciones y obtener la más amplia cobertura de metabolitos pudiendo comparar los resultados entre muestras, así como entre tratamientos.

General outline

0

Obesity is the primary cause of insulin resistance that represents one of the main threats to global human health and has been increasing worldwide and spreading at a very fast rate over the last 50 years [1].

Obesity is defined as the accumulation of excess fat in one or various compartments of the body, therefore compromising individuals' health. There is a classification system based on the estimation of body fat known as Body Mass Index (consisting of the division of body weight in kilograms by height in meters) and the waist circumference measurement. These methods are convenient and useful to approximate the degree of overweight/obesity. Still, they are far from providing specific information about the composition and the metabolic mechanisms that would help to faster detection of obesity or the future complications derived from it [2].

Obesity is not only considered as a healthy complication but also involve social problems like lack of confidence, physical complex, or social isolation. These make obesity to be considered as a "non-communicable disease" caused by these sociological behaviours.

The metabolic mechanisms involved in body homeostasis, internal body weight control and the new way of social lifestyle added to the lack of control about food intake are responsible for the tendency of obesity to become obese. To summarize, an incorrect control of these mechanisms contributes to unwanted body weight gain and misdistribution of fat, adding to obesity metabolic syndrome and other chronic diseases highly linked to it (diabetes, cardiovascular complications, non-alcoholic fatty liver disease…) [3].

The ectopic accumulation of lipids in other tissues different from adipose tissue is what is known as lipotoxicity. According to the evidence in the lipotoxicity, the more relevant is the type than the quantity of the accumulated ectopic lipids in the other tissues and that it has a substantial negative metabolic impact on individuals' health [4-6].
Also, it has been recently discovered that genetics could be another essential determinant factor for developing this disease [7]. However, the scientific community continues with numerous researches on it to better diagnose, treat and/or prevent its appearance.

Obesity and metabolism

One of the most popular hormones related to obesity metabolism is insulin. Insulin is produced in the pancreas and its role is to keep glucose homeostasis between tissues and blood according to body energy needs. It enhances the entrance of glucose into the tissues when needed and stops the glucose production in the liver when blood glucose levels are enough. In the insulin response failure, body cells do not take up from the blood all the glucose they should. To overcome this scarce glucose income, the pancreas begins to produce more insulin but not always the body's cells can respond to it, and the glucose accumulates in the blood. This lack of insulin response is known as "Insulin Resistance" (IR), and, depending on the degree of response, it can lead to several consequences [8, 9].

The most popular of these consequences are insulin resistance syndrome" or metabolic syndrome. They are characterized by a sum of medical factors and unhealthy costumes, typically linked to obesity. All these together highly promotes the development of type 2 diabetes and several other diseases related to metabolic syndromes such as cardiovascular diseases, Non-alcoholic Fatty Liver Disease (NAFLD), Chronic kidney disease (CKD) and polycystic ovary syndrome [10].

The bigger or smaller adipose tissue capacity for lipid storage also plays a vital role in developing insulin resistance (IR). This is because exceeded capacity results in a leakage of lipids from adipose tissue to other tissues that could interfere with insulin signalling pathways.

In normal conditions, insulin signalling is mediated by activating its specific tyrosine kinase receptor, which directly phosphorylates several tyrosine residues of different insulin receptor substrates (IRS). The two most important IRS associated to glucose transport are IRS 1 and IRS 2 [11, 12].

Mitochondrial dysfunction is also a critical factor in the development of IR by diminished the oxidative capacity of mitochondria, especially of fatty acids (FAs), and promoted acyl CoAs and DGs accumulation [13]. Moreover, mitochondrial activity regulates also the secretion of insulin by pancreatic cells under an increase in blood glucose levels [13, 14].

Age and insulin response was related to the alterations in number, size and capacity of mitochondrion oxidation [14]. Aged people with insulin resistance presented less quantity and capacity of muscular mitochondria oxidation than young people without (IR) [15, 16].

Obesity and inflammation

The growth of adipose tissue is directly linked to an increase in the production of pro-inflammatory cytokines that, together with free fatty acids; seems to be responsible for insulin and leptin resistance [17].

In the last years, it has been discovered that the hypertrophy and hyperplasia of adipose tissue linked to obesity may cause hypoxia and activation of different cellular responses such as oxidative stress, endoplasmic reticulum stress and inflammation. It has been described that obesity-derived inflammation increases the infiltration of macrophages into adipose tissue and changes their polarity from M2 (anti-inflammatory secretion profile) to M1 (proinflammatory secretion profile) [18-20].

JunN terminal kinase (JNK), IKK/NF-κB and protein kinase C (PKC) are some of the most important serine/threonine kinases activated by inflammation or Endoplasmic Reticulum oxidative stress [20-22]

Oxidative stress is manifested by the increase of reactive oxygen species (ROS), resulting from an unbalance between ROS production and elimination through such systems as mitochondrial activity and NADPH oxidase activity. ROS react with a great variety of molecular structures and induce inflammatory responses [23]. High levels of fatty acids frequently found in hypercaloric diets; they can cause, among other things, oxidative stress[24].

Obesity and Non-Alcoholic Fatty Liver Disease (NAFLD)

In the liver, obesity is manifested by the clinical disorder of the Non-Alcoholic Fatty Liver Disease (NAFLD) that is characterized by insulin resistance and accumulation of triglycerides (hepatic steatosis) [25]. NAFLD is characterized by various signs and symptoms, including insulin resistance as mentioned earlier, peripheral lipolysis, increased hepatic absorption of fatty acids, hormonal changes, pro-inflammatory cytokines release and hyperinsulinemia that leads to mitochondrial dysfunction. A proportion of NAFLD patients develop hepatic inflammation, which is a determinant factor for benign steatosis progression to NASH, manifested by an exacerbated intrahepatic inflammation, oxidative stress and hepatocellular damage [26]. NASH could end up in hepatic cirrhosis and, finally, liver death, known as hepatocellular carcinoma (HCC) [27].

To try to prevent the mentioned diseases early diagnose of insulin resistance is essential. Excess weight and lack of physical activity are pointed as primary factors that cause insulin resistance. However, metabolic activity and processes that drive the IR are not fully understood [8].

Metabolomics

The study of the metabolic composition of a cell, tissue or biological fluid is named “Metabolomics” [28]. It was described as the quantitative and multiparametric measurement of a living being’s response to some pathophysiological stimuli or genetic modification [29].

Nowadays, metabolomics is being employed to solve major biological challenges, as the personalization of nutritional treatments [30], the discovery of new drug targets [31], the study of human diseases [32] or the research of biomarkers for the diagnosis or prognosis of the response to treatment [33].

To carry out this measure is essential to perform a statistical, differential, holistic and unbiased comparison between the representative case and control samples. To evaluate the differences, the research must be divided into two well-defined areas: obtaining data in

the laboratory and handling the data. The “wet” part of the workflow is not time-consuming, especially when all protocols are established, and methodologies developed and validated. In contrast, the computational work is lengthy and time-consuming and it covers different processing steps (deconvolution, alignment), pre-treatment (standardization, processing, scaling), treatment (uni- and multivariate analysis), identification (through databases and structural elucidation) and interpretation of biological data (pathway analysis) [33].

This workflow is aimed to give an answer to the initial question postulated at the beginning of the experiment, which must be the ultimate goal of the metabolomics study, either by the elucidation of the biochemical processes modified by the condition under study, or the proposal of possible biomarkers whose determination may be sufficient to diagnose this condition. [Figure 1.1].

Within the metabolomics workflow there are two main bottlenecks: the annotation/identification of the most paramount compounds and the biological interpretation of the results.

As for the identification, different levels of confidence can be distinguished: from the putative databases-based annotation (most of them are free to access on the Internet) to the comparison with a certified standard. Nowadays, proper management of information available in databases and data provided by analytical instrumentation remains a problem. The need to perform very advanced analysts training so they can be able to dismiss the spurious identifications is not less important [34].

In the Centre of Metabolomics and Bioanalysis (CEMBIO), in collaboration with the Laboratory of Bioengineering of the University of San Pablo CEU the CEU Mass Mediator (CMM) tool was developed. CMM allows simultaneous search across five databases simultaneously (HMDB, METLIN, KEGG, Lipid Maps and MINE) [35, 36]. The obtained information is curated to remove redundancies and sorted according to the confidence of compound annotation.

One useful tool to carry out the data analysis in metabolomics is Mass Profiler Professional (MPP) from Agilent Technologies. MPP is a powerful chemometric software designed to take advantage of the information obtained from MS-based metabolomics and determine

the relationship between two or more groups of samples. This program offers various tools and algorithms for advanced statistics and potent visualization of LC-MS, CE-MS and GC-MS datasets.

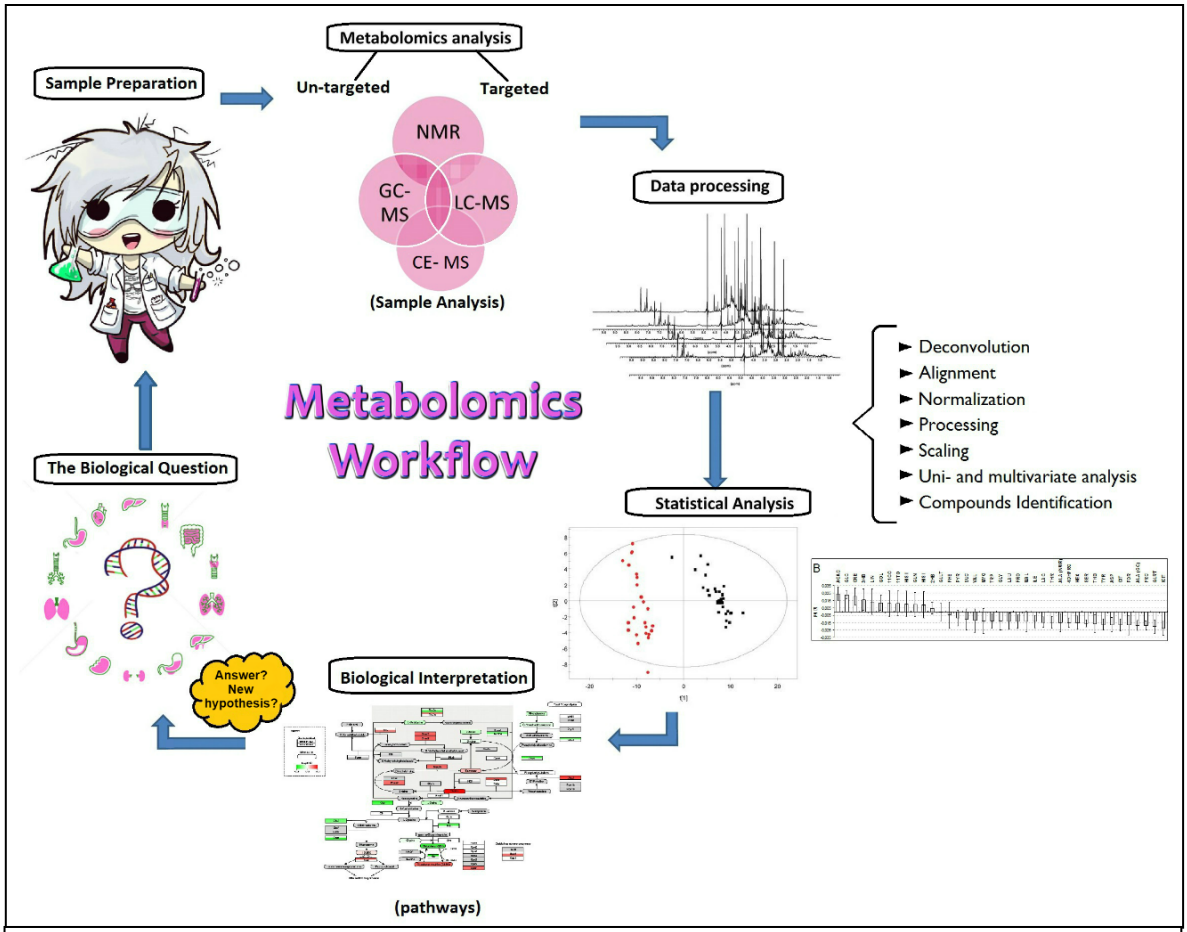

[Figure 1.1]. Scheme representing CEMBIO's multiplatform metabolomics workflow

Dietary animal models

There are different dietary animal models relevant to mimic specific pathogenesis and metabolic disorders, including obesity. As described in a review by Lutz et al. [37], animal models of obesity are mainly divided into monogenic and polygenic models, and most of them use rats or mice. Monogenic models consist of altering a single gene, by deleting or deactivating it in the entire animal, causing specific metabolic modifications that lead to the development of particular characteristic, in this case, obesity, like insulin resistance, hyperglycaemia or hyperphagia. These genetic alterations are related to the inhibition of physiological factors, such as hunger or appetite, by modifying hormones or enzymes involved in these mechanisms (leptin as an example). However, sometimes the simulated obesity induced by these methods is not very similar to human obesity. Polygenic models' strategy is different and is based on the pathology's simulation by feeding the individuals involved in the study with a specific diet. In this study, mice were fed according to the used polygenic model known as the Diet-induced obesity model through a High Fat Diet (HFD) (Teklad high-fat diet TD.06414, Envigo, Madison, Wisconsin USA), consisting of 60% of the lipid content.

In the case of dietary animal models to induce NAFLD and NASH, animals fed with diets rich in lipogenic nutrients (simple sugars [38] and/or saturated fats) develop steatosis instead of steatohepatitis and/or saturated fats [39, 40]. Sometimes High Fat diet is used as a model for NASH, but the provided results vary in terms of levels of steatosis, inflammation and fibrosis [41] and the alterations in the oxidative stress metabolism that occur in NASH [42]. Furthermore, there are monogenic models lacking genes that affect appetite regulation or predisposition to diabetes [43] that are frequently used to mimic NASH but present the same problems as the ones already described in the previous paragraph.

There is evidence of the well-known lipotoxicity caused by the accumulation of lipid excess in different tissues from adipose tissue, in this case, the liver, leading to characteristic hepatocellular injury in NASH [44]. The literature has shown that both the quantity and quality of dietary fat influence liver fatty acid synthesis [45], insulin sensitivity and can induce Insulin Resistance [46].

These reasons justify the need for a model different from the High Fat Diet for the NASH's study. Many studies use the methionine- and choline-deficient-diet (MCD) to establish NASH in the rodent liver as they develop steatohepatitis causing changes in the redox balance and hepatic lesions that mimic the impairment of patients with NASH [47]. It happens because the choline and the methionine are amino acids essential for hepatic β-oxidation and production of VLDL [48], causing a direct increase of oxidative stress, a decrease of phosphatidylethanolamine synthesis and a decrease of the transport of fat from the liver to extrahepatic sites leading to hepatic steatosis [49]. Furthermore, MCD-diet causes the development of inflammation and hepatic fibrosis added to steatosis in these mice [50]. The final reasons for using MCD-diet are easy to purchase and usage [51].

Objectives

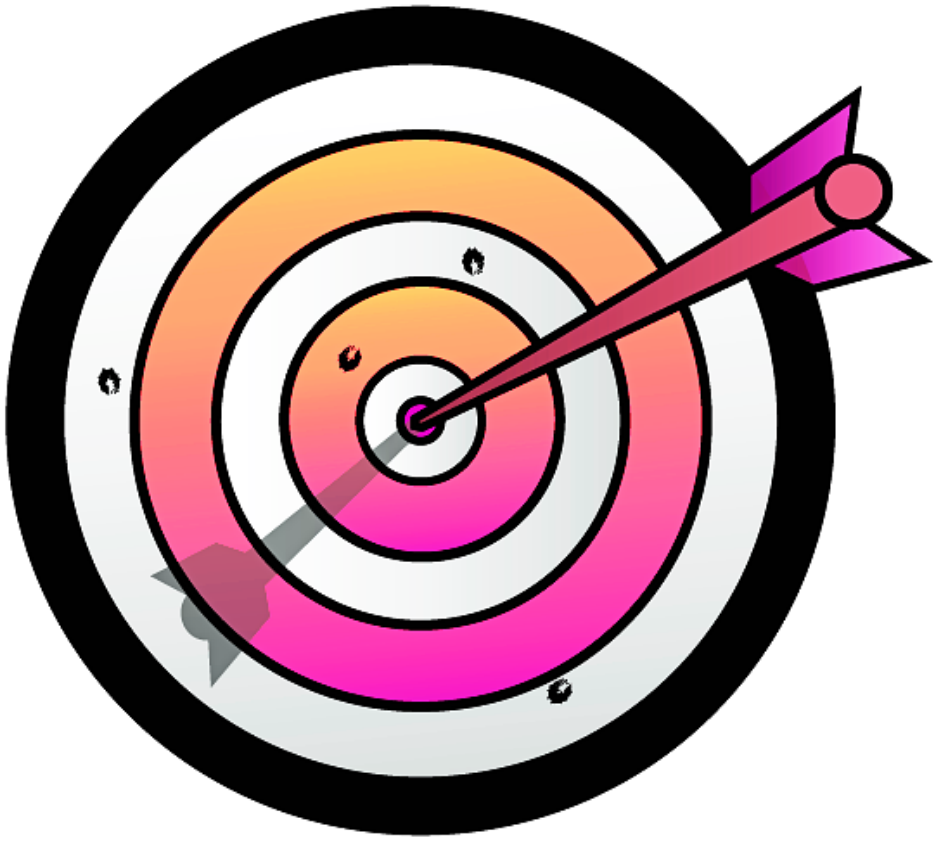

The main objective of this thesis is to study through metabolomics significant metabolic changes occurring in obesity and NASH, two diseases that are highly spread worldwide and suppose a big risk to global human health which are interrelated and linked with the metabolic syndrome.

The present thesis has been structured in two main chapters ordered from a more general study of metabolic impact of obesity (Chapter 1) to a more specific analysis of the metabolic impact of NASH; and possible future treatments (Chapter 2).

The main objectives are:

- The development of a “Compartmentomics” study of Diet-Induced Obesity with a High Fat Diet analysing through Multiplatform metabolomics (RPLC-MS, CE-MS and GC-MS) eight different types of tissues with high metabolic activity, which are plasma (P), kidney (K), heart (H), skeletal muscle (SM), inguinal (iWAT), perirenal (pWAT) and epididymal (eWAT) white adipose tissue and brown adipose tissue (BAT); obtained from mice.

- The processing of the data obtained from the analysis of the eight tissues for the detection and identification of significant compounds between control and DIO mice to elucidate possible metabolic pathways involved in the pathology situation of obesity and give a biochemical holistic interpretation of common significant features in more than one of the studied compartments.

- The optimization of a method for the simultaneous extraction and LC-MS analysis of active and neutral lipids in Adipose tissue.

- The development of a methodology for a comparative study of lipidic profiles by LC-MS and metabolomic profile by CE-MS using liver biopsies (before and after PH) and identification of significant compounds (by analysis of fragmentation MS/MS spectra) to get to the knowledge, understanding of the progression of this disease and the study of the mechanisms involved in liver regeneration as a possible therapy after partial hepatectomy.

Chapter 1: Metabolic and Inflammatory impact of Diet-Induced Obesity (DIO) in Different tissues in mice: A Compartmentomics study

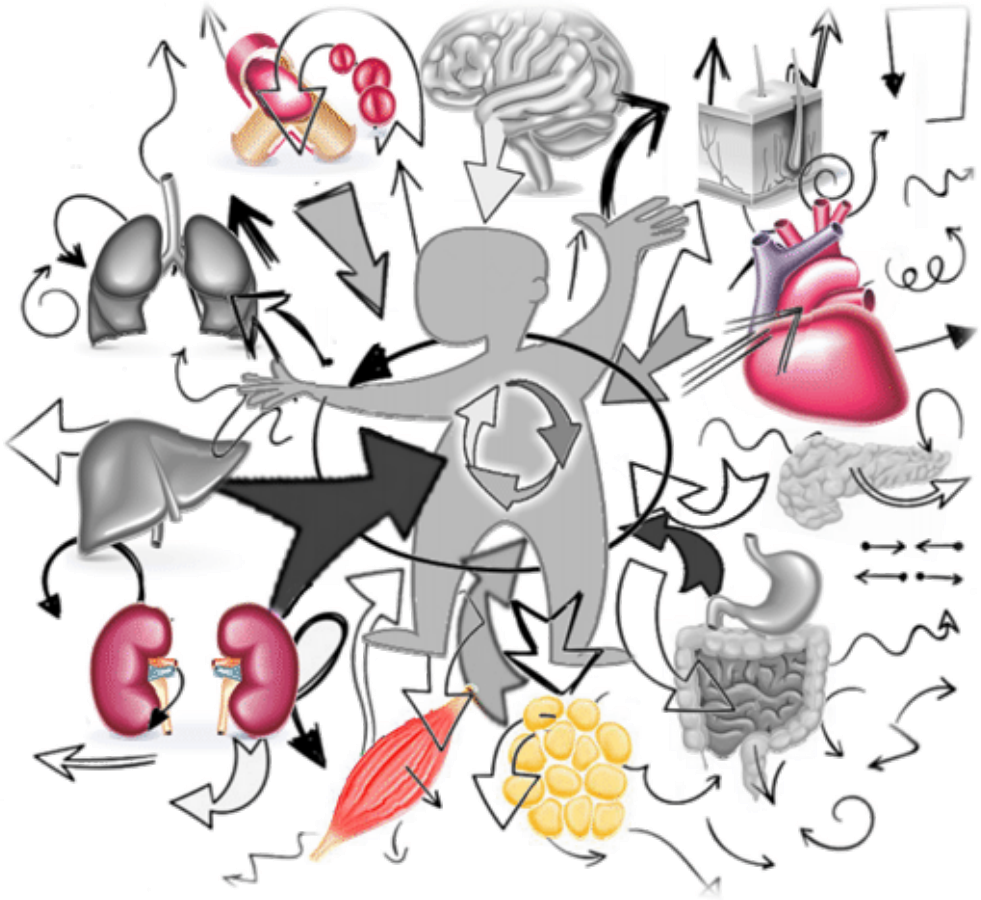

1.1.Compartmentomics of High Fat Diet-Induced Obesity

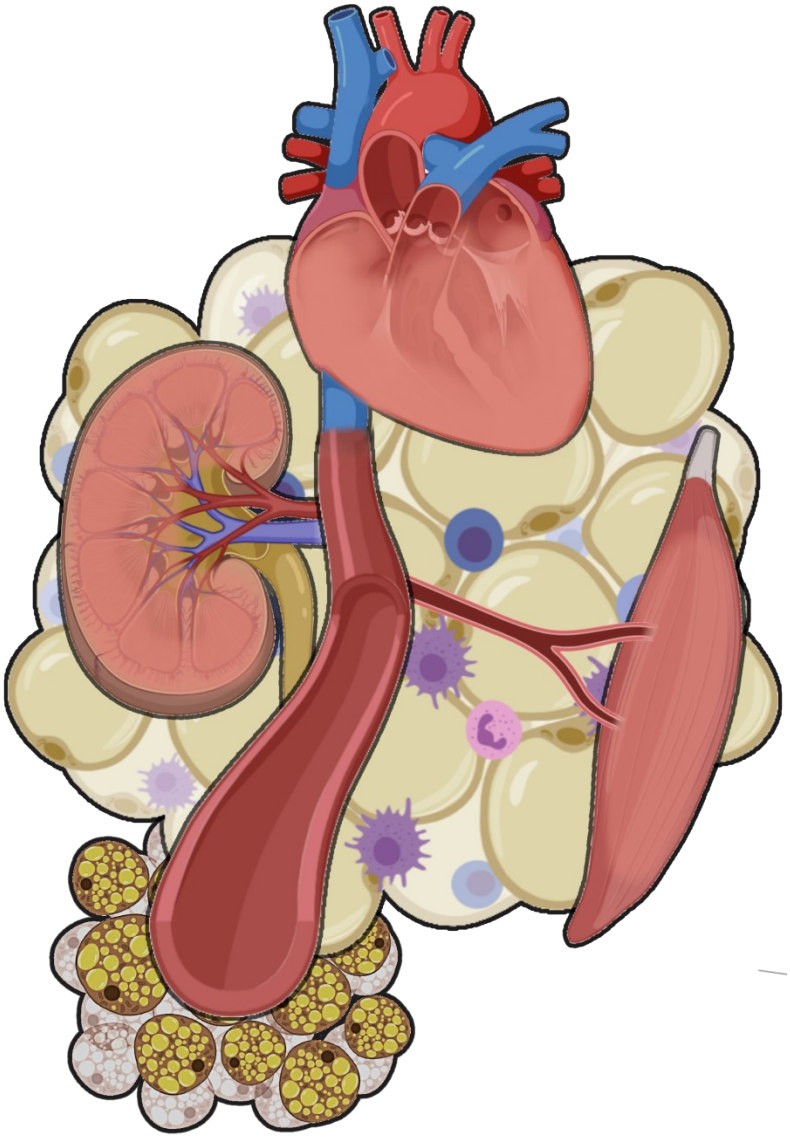

1.1.1-Introduction

As previously mentioned in the outline, obesity is characterized by an excess of fat associated with multiple metabolic disorders that also cause at the same time other health problems.

1.1.1.1- Metabolic alterations in Obese Plasma

Metabolic alterations in plasma are the most studied in any disease. Obesity metabolic impact is also reflected in the plasma metabolic profile.

Obesity alters metabolic and energetic body homeostasis through a complex system controlled by endocrine and nervous factors [52]. These signals can be chronic or acute and are produced from different tissues [53]. Leptin and adiponectin for example are considered chronic signals and are produced by adipocytes and control appetite and energy usage of the body. Examples of acute signals would be insulin (secreted by the pancreas), ghrelin (by the stomach) and peptide YY (by ileum and colon). They combine according to organism necessities. The concentration of all the mentioned hormones is reflected in serum. When serum leptin levels increase, appetite is diminished, and the food intake is null or very scarce. On the other hand, the secretion of ghrelin becomes the signal for starting food intake by enhancing appetite. Finally, to end with the food intake process; peptide YY serum concentration increases producing a satiating effect.

Leptin is a hormone that joins to plasmatic proteins to be transported. As already mentioned, leptin synthesis is regulated mainly by the amount of insulin and other hormones. Its concentration varies according to the circadian rhythm. In Greek, “leptos” means “lean” as this hormone can control brain appetite through chemical mediators[54]. High levels of leptin in obese patients with no manifested physiological effects of leptin suggest a possible leptin resistance.

The unbalance of all these hormones that take place in obese patients normally drive to metabolic syndrome [55]. Plasma levels of TNF-a and resistin in obesity are increased producing insulin resistance while adiponectin plasma concentration, which enhances

insulin sensibility; is decreased. Also, in obese patients, prothrombotic factors as PIA-1 are increased. Adiponectin is also in charge of vascular protection. [56].

It has been demonstrated through the years that there is a direct relationship between obesity and atherosclerosis through mechanisms such as dyslipidaemia, Arterial Hypertension (AHT) and Mellitus Diabetes type 2 (MD2) but it is also influenced by subclinical inflammation processes, high plasma levels of insulin and leptin, high interchange of free fatty acids (FFAs) and specific fat localized depots at intraabdominal and sub-epicardial level [57].

The cardiovascular risk is more influenced by the distribution of fat depots throughout the body (subcutaneous vs. visceral) and the way they increase (hypertrophy vs. hyperplasia) under obesity conditions than the total body fat. The metabolism of a person is altered when the increase of adipose tissue is driven by hypertrophy in visceral adipose tissue depots. [58-61].

The adipocytes are the cells that have the ability to carry out both processes: hypertrophy, which consists of the increase of the size of the cell, in this case, adipocyte; and hyperplasia, by which existing adipocytes create new adipocytes, also known as adipogenesis. This way adipose tissue can increase its capacity for the accumulation of excess energy in form of Triglycerides. The new adipocytes can secrete adipokines and create new lipids [59].

When adipose tissue detects an excess of lipids, it first starts hypertrophy of the adipocytes, which will consequently activate the hyperplasia of them so that adipose tissue maintains its normal functionality. The problem appears when the hypertrophy becomes excessive maintaining hyperplasia permanently activated, which saturates metabolic processes involved in the generation of new cells such as energy substrates oxidation, proteins synthesis; angiogenesis… and this influence in other processes carried out by the adipose tissue-like[58, 59, 62]: deficient protein synthesis inducing intracellular inflammatory response by NFκB factor, the overproduction of oxygen reactive species by activation of enzymes like NADPH that will lead to oxidative stress and inflammation; loss of the regulation in the synthesis of adipokines and increase of pro-inflammatory cytokines (TNFα), IL-6, PIA-1…); decrease of adiponectin and increase of inflammatory cells recruitment. [58, 62, 63].

Also, adipocytes hypertrophy is associated with other pathologies highly linked to obesity such as MD2, insulin resistance, increase of inflammatory factors and decrease of anti-inflammatory factors in blood [58, 59, 62, 64-66].

All these processes are exacerbated in adipocytes of visceral adipose tissue depots and the detectable risk factors associated with these phenomena in serum are hyperinsulinemia, insulin resistance, microalbuminuria, premature atherosclerosis, high oxidable LDL particles, a decrease of HDL particles, increase of TG, fibrinogen and production of PIA-1, an increase of PCR, TNFα, IL-6, blood viscosity and cardiac ventricular hypertrophy [59-61, 67, 68].

Lipotoxicity and inflammation are very common and well-known consequences of obesity that not only affect organs but also plasma tissue. The serum and circulatory system are the transport for all the molecules, compounds, metabolites, nutrients, cells… that make possible the connection between the rest of the tissues. Also is responsible for the accumulation of the excess of free reactive fatty acids that are released from the adipose tissue under obese conditions in the rest of the organs producing lipotoxicity. Because of this, insulin resistance, fatty acid cardiotoxicity and decrease of insulin secretion are produced respectively. [69].

As already mentioned, obese adipose tissue is also characterized by a higher number of infiltrated macrophages. This process is activated and driven by the so-called factors PPAR-γ (Peroxisome Proliferator-activated receptor gamma) that mainly control lipid oxidation and it is also involved in insulin resistance processes. These infiltrated macrophages in adipose and surrounding tissues are activated by free fatty acids starting an inflammatory response that also promotes the well-known insulin resistance. [56].

In obese patients, this inflammatory response becomes chronic and produces vascular damage, which is the first manifestation of atherosclerosis [70].

The leptin also plays an important role in this response as promotes sympathetic activity that will potentiate thrombosis, the increase of arterial pressure and cardiac frequency.

For these reasons, obesity is considered as a pro-inflammatory state and due to this, high serum levels of Reactive Protein C (RPC) are associated with myocardial infarction, cerebrovascular disease and peripheric arterial disease.[57].

The combination of mechanisms such as overproduction of inflammatory factors and decrease of adiponectin (anti-inflammatory hormone) added to the decrease of NO bioavailability and increase in the production of peroxynitrites in obesity leads to the decrease of vasodilation capacity, atherosclerosis, coagulation alterations and arterial hypertension. These malfunctions are manifested by less vasodilatation response of vascular muscle, oxidation of LDL, activation of synthesis and accumulation of collagen, engrossment of vascular walls, vasoconstriction and a systemic proinflammatory state. [71-74].

LDL small particles directly affect the formation of atheroma plaques or atherogenesis when they get oxidized as they penetrate the vascular endothelium. This provokes less NO production, macrophages recruitment, higher inflammatory response and reactive species production, and platelets aggregation. [73, 75].

Dyslipidaemia is another consequence of obesity directly reflected in plasma concentration of certain molecules such as an increase of triglycerides (hypertriglyceridemia), an increase of LDL and a decrease of HDL (due to the overexpression of a hepatic lipase when there is hepatic insulin resistance).[71, 76, 77].

As previously mentioned, adipose tissue also has an important function in the regulation of vascular vasodilatation [78]. There is evidence of a lower response to this vasodilatation in patients that suffer from atherosclerosis and many of these patients have obesity [79]. Furthermore, in some cases, atherosclerosis inhibits vascular function leading to endothelial dysfunction. This endothelial dysfunction is manifested by a decrease of NO and prostacyclin's serum levels, an increase of secretion of endoperoxides and in the production of ROS (Reactive Oxygen Species).[79]. The endothelial dysfunction is also characteristic of AHT and other cardiovascular diseases [80].
It also alters equilibrium between vasodilatation and vasoconstriction, pro and anticoagulant factors, inflammatory and anti-inflammatory mediators, oxidative stress and other several processes [80]. Also, there is a perivascular adipose tissue (PVAT) (adipose tissue that

surrounds the vessels of the blood vessels) related to vascular tone that is affected by endothelial dysfunction [78]. This PVAT reacts in different ways to endothelial dysfunction: in initial obesity induced by food intake, it produces higher dilatator factors as NO to preserve vascular function so that NO can adapt and avoid vascular damage[81] but, as obesity becomes chronic, the PVAT losses its properties due to the increase of inflammatory and oxidative factors, enhancing the endothelial dysfunction.[82].

Oxidative stress produced by obesity also affects the adhesion and activation of leucocytes. When leucocytes are activated, they induce NO synthase that produces high amounts of NO locally. This excess of NO induces more oxidative stress damage and reduces natural endothelial NO becoming a vicious cycle that compromises the healthiness of endothelium [79].

Another system affected by obesity is the coagulation and fibrinolytic process [57]. There is evidence that obese patients present higher serum levels of fibrinogen, VII and VIII coagulant factors, von Willebrand factor and PIA-1, as well as an increase in platelets adhesion. These changes increase thrombotic processes enhancing the atherogenic process characteristic of atherosclerosis [79].

1.1.1.2- Metabolic alterations in Obese Adipose Tissue

According to Encyclopaedia Britannica Adipose tissue or fatty tissue is defined as “connective tissue consisting mainly of fat cells (adipose cells, or adipocytes), specialized to synthesize and contain large globules of fat, within a structural network of fibres”. It has been treated as a huge single organ with homogeneous properties and composition until the late 1940s [83]. Far from this simple idea, adipose tissue results to be a very complex organ with great metabolic activity and diversity of metabolites, functions, and locations.

To better understand obesity is important to know how adipose tissue works apart from the commonly known function of storing energy in the form of lipids. However, in 2005 was discovered that Adipose tissue has also a very important role in energetic metabolism homeostasis [84].

Adipose tissue is an endocrine and paracrine organ that secrets a great amount and diversity of cytokines and bioactive modulators that drives homeostasis, body weight, inflammatory reaction, coagulation, fibrinolysis, insulin resistance, atherosclerosis and some cancers [85, 86].

The adipose tissue is considered to develop endocrine functions as it secretes several hormones (already mentioned and more, such as tumour necrosis factor (TNF -α), adiponectin…) that control insulin sensibility in other organs. Adipose tissue also produces some cytokines (IL1, IL-6) [69] angiotensin and complex factors related to immunity response (adipsin or factor D) and prothrombotic factors (Plasminogen inhibitor activator or PIA-1) [87].

The characteristic cells that form Adipose tissue are known as adipocytes, but other types of cells also belong to it as lymphocytes, macrophages, fibroblasts, and vascular cells. Obesity directly affects the cellular composition, morphology, and secretion of some of the already mentioned cytokines (IL-1 and IL-6) in adipose tissue [18].

Adipose tissue storages and controls Fatty acids depots in the body. These fatty acids reach the adipocyte through blood circulation in 3 main forms: Free Fatty Acids (FFA), associated with serum albumin and joined to very-low-density lipoproteins (VLDL) [88]. There are different mechanisms as membrane receptor or passive diffusion, by which circulating Fatty acids get inside the adipocyte [89]. Once inside the cell, they are esterified by acyl CoA synthase and used for the synthesis of triacylglycerides (TGs) in the rough endoplasmic reticulum. PAT proteins (Perilipin, adipophilin, and the tail-interacting protein of 47 kDa, TIP47) are very important in the storage of mature lipidic bodies as they are in charge of the release of fatty acids by adrenergic stimuli or glucagon. (SC3, TPP47, DRRD y perilipin).

Free Fatty Acids also contribute to this insulin signal inhibition by the activation of Toll-Like Receptors (TLR), which will activate signalling pathways such as Junk N- terminal Kinases (JNK) and this at the same time would interfere with insulin signalling. TLRs are a family of at least 12 different receptors that play a very important role in the innate immune system by detecting the presence of pathogens. TLR4 and TLR2 are the best-characterized ones involved in the expression of proinflammatory cytokines [90-92]. Moreover, intracellular fatty acids allow intracellular signalling pathways related to inflammation [93] such as NFκB

activation or c-Jun N- terminal kinase type 1 (JNK-1) from the already mentioned JNK family, whose also have an important role in the production of pro-inflammatory cytokines [94].

As mentioned above, endoplasmic reticulum and oxidative stress are highly linked to insulin resistance and therefore to obesity. ER is an organelle implicated in the synthesis and transport of proteins that must be perfectly folded by other proteins known as chaperones. Sometimes oxidative stress produced by a strong effort leads to the unproperly folding of proteins by ER (Unfolded protein response, UPR) which directly affects several reactions involved in the synthesis and homeostasis of proteins metabolism. This phenomenon is what is known as ER stress. Calcium, some pathogens, or the availability of certain nutrients may also lead to ER stress. So, ER is like a system that detects cellular homeostasis alterations, and that is why is highly linked to obesity and insulin resistance, as they are diseases in which there are alterations in the synthesis of proteins and lipids and accumulation of the last ones [95]. The peroxisome proliferators activated receptors (PPARs) are transcriptional factors activated by lipidic derivate that regulate certain metabolic reactions such as fatty acids oxidation, adipogenesis and insulin sensitivity [96]. The decrease of PPAR expression in adipose tissue could facilitate the accumulation of lipotoxic species in other surrounding tissues and develop insulin resistance and mitochondrial dysfunction [97, 98].

Lipolysis is exacerbated in obesity resulting in the excessive release of free fatty acids. Intracellular increase of fatty acids and diacylglycerols (DG) activates protein kinase C (PKC), which is involved in the inhibition of intracellular signalling of insulin by the phosphorylation of Insulin Receptor Subtract type 1 and 2 (IRS 1 and 2) [99]. PKC also activates the NADH oxidase enzyme, which increases ROS production and inhibits nitric oxide (NO) production [100, 101]. All these changes are harmful to endothelial cells as they decrease vasodilation of vessels increasing hypertension as a result.

As mentioned in obesity, adipose tissue is very abundant, and this fact leads to a generalized pro-inflammatory situation with a noticeable increment of macrophages migration to adipose tissue. Moreover, the polarization of macrophages is altered and these produce phenotype proteins M-1 instead of M-2, already mentioned in the outline section above [94]. The stimuli of TCD4+ Th-1 cells provokes the polarization of macrophages to phenotype M-1, which produces pro-inflammatory cytokines (such as TNFa and ROS) and this response produces inflammation and tissue damage or destruction. M2 Macrophages release anti-inflammatory

cytokines, as Interleukin 10 (IL-10) or 1- arginase (inhibits inducible nitric oxide synthase INOS) activity*) [102]* anti-inflammatory activity is regulated by T regulatory cells and Th2, which contributes to the homeostasis of adipose tissue.

TNFa is one of the most secreted proinflammatory cytokines in obesity by monocytes and macrophages. Obese patients manifest high serum levels of TNFa while obese patients that are losing weight show decreasing levels of it. It is though that TNFa promotes insulin resistance as it inhibits the activation of IRS-1 in skeletal muscle and adipose tissue [103, 104].

Adiponectin or ACRP30, Adipo q o ApM-1, is a cytokine synthesized by adipocytes [105-107]. Its serum levels are decreased in obese subjects, related to the appearance of chronic diseases. Proinflammatory cytokines, hypoxia and oxidative stress presence stop adipocytes from producing adiponectin [108].

It is known that the most affected tissue in obesity is adipose tissue, but obesity alterations are also manifested in surrounding tissues like the heart, kidney, or skeletal muscle, with harmful and risky pathologies. Furthermore, blood, the tissue that establishes links between all body compartments; transports metabolites throughout the organism producing the manifestation of metabolic changes in the rest of the tissues.

1.1.1.3- Metabolic alterations in Obese Kidney

Excess adiposity, especially when localized in visceral regions and around the kidneys, accounts for 65–75% of the risk of primary hypertension [109, 110]. There is evidence from experimental studies in animals and humans that indicate renal compression due to excess of Peri Renal Fat (PRF), Renal Sinus Fat (RSF) and Visceral Adipose Tissue (VAT), that squeeze the kidneys; activation of the renin-angiotensin-aldosterone system (RAAS); and stimulation of the sympathetic nervous system (SNS), which together mediate increased renal sodium reabsorption and enhances hypertension [111-113]. Adipokines, including leptin, may also contribute to obesity-induced hypertension by activation of the RAAS and SNS. If this situation persists over many years, it could end up in Chronic Kidney Disease (CKD) [114].

Chronic kidney disease (CKD) is currently a worldwide public health problem that brings negative consequences for the quality of life. The incidence and prevalence of CKD are growing and are directly associated with systemic arterial hypertension (SAH) and diabetes mellitus (DM), as the main causes of it [111, 115]. Obesity has been identified as a major cause of kidney disease, including CKD [111, 112, 116, 117].

Insulin resistance, present in CKD; reduces the activity of lipoprotein lipase, which may be implicated in the pathophysiology of dyslipidaemia in CKD. Increased production of endothelin-1 has also been described in obese subjects, which further contributes to the elevation of blood pressure levels and consequently to renal dysfunction [111]. This increase in Blood Pressure associated with Glomerular hyperfiltration and other metabolic alterations such as insulin resistance and Diabetes Mellitus, finally result in kidney damage and reduced Glomerular Filtration Rate (GFR) [111-113].

Kidneys of obese people are also affected by the already mentioned pathophysiological phenomenon “lipotoxicity” caused by an over-intake of nutrients in which the supply of fatty acids to the tissues exceeds the metabolic needs. This leads to a compensatory increase in their oxidation and to the production and release of several substances (from lipid peroxidation and triglycerides for example) that are harmful to the cells of the corresponding tissue, kidney in this case; inducing in many case apoptosis and fibrosis in these non-adipose tissues [111-113].

We have already described in previous paragraphs the direct association between obesity and inflammation mechanisms due to the increase in the production of several adipokines already mentioned. This inflammation derived from obesity is also a risk factor for renal function loss [118, 119].

There is also evidence that obesity itself increases albumin excretion, which progressively increases with obesity severity and, in rare cases, can lead to nephrotic syndrome [112]. Obesity has also shown to be an important risk factor for renal disease progression in patients with glomerulopathies, such as in IgA nephropathy [120].

1.1.1.4- Metabolic alterations in Obese Heart

Cardiac energy metabolism can be mainly summarized in few sequential steps: myocellular substrate uptake/selection, mitochondrial ATP production and ATP transfer from the site of production (mitochondrion) to the site of ATP utilization [121].

Although glycolysis is an ATP generator, the overall ATP production is controlled by the Krebs (tricarboxylic acid) cycle metabolic pathway [122]. Acetyl coenzyme A (CoA), which is produced from the oxidation of fatty acids, ketone bodies, or glucose *via* glycolysis; and the pyruvate dehydrogenase (PDH) enzyme complex [123] enter the Krebs cycle for complete oxidation. When oxidated, they enter into a multistep process producing ATP, which is used for all cardiac cellular processes [124]. ATP is the heart's only immediate source of energy for continuous and unstoppable heart contraction, so cardiac ATP demand is very high[125, 126]. As a result of this large energy requirement, any impairment in ATP production, transfer or utilization can have detrimental effects on cardiac function [127].

It is well known that most obese subjects are at risk of insulin resistance, diabetes and hypertension, all of which are known to independently affect cardiac energy metabolism [125, 126, 128].

Heart failure, a well-documented sequela of obesity [129] is associated with deranged cardiac energetics (decreased efficiency of substrate utilization to create the ATP necessary to drive cardiac contraction) [121].

Cardiac mitochondria contain DNA that encodes some of the proteins required for electron transport complexes involved in ATP production. The remainder of the respiratory subunits, and all of the proteins required for substrate metabolism, are encoded by separate nuclear genes [130]. It is becoming clear that in obesity, changes in both nuclear and mitochondrial transcription are present and are important in the production of the observed changes in cardiac metabolism [131]. The already mentioned Peroxisome proliferator-activated receptors (PPARs) control nuclear gene transcription, regulating therefore myocardial mitochondrial fatty acid oxidation [132]. PPARs when activated, induce peroxisome proliferation that has multiple metabolic roles, which include long- and very-long-chain fatty acid oxidation [133]. There are several PPAR receptors with different tissue expression. In

heart tissue, PPARa is expressed and results to be the most important one for its metabolism [134] and is the primary transcriptional regulator of fat metabolism in tissues with the highest rates of fatty acid oxidation [135]. Activation of PPARa in the heart increases the expression of several genes involved in fatty acid metabolism including the cardiac myocellular fatty acid uptake (fatty acid transport protein, FAT/ CD36, fatty acid-binding protein and acyl-CoA synthetase) [136-138], mitochondrial fatty acid uptake *via* CPT I and mitochondrial and peroxisomal fatty acid b-oxidation *via* medium-chain acyl-CoA dehydrogenase, long-chain acyl-CoA dehydrogenase, very long-chain acyl-CoA dehydrogenase and Acyl-CoA Oxidase, respectively [139].

In obesity-induced insulin resistance, the heart initially adapts to elevated levels of circulating fatty acids by increasing PPARa, resulting in a compensatory increase in myocardial fatty acid uptake and b-oxidation [140], which is believed to limit cardiac ectopic lipid accumulation. However, despite these initial adaptive/protective mechanisms, the potential for cardiac lipotoxicity in obesity has been described [141].

Exposure of the heart to high levels of fatty acids can cause accumulation of lipids within cardiomyocytes increasing the intracellular pool of long-chain fatty acyl-CoA, which provides a fatty acid substrate for non-oxidative processes, including triacylglycerol, diacylglycerol and ceramide synthesis, which can lead to cell dysfunction, insulin resistance and, potentially, apoptotic cell death.

GLUT4 expression is also altered by excessive nutrient intake. In normal cardiac tissue, insulin causes the mobilization of GLUT4 from intracellular stores to the sarcolemma. However, in obesity and insulin resistance this process is reduced [142].

As previously described, adipose tissue secretes a range of adipokines that alter fat metabolism [143]. Leptin and adiponectin have been shown to modulate myocardial substrate metabolism. Adiponectin is believed to act *via* PPARa to stimulate fatty acid metabolism, increase Carnitine palmitoyltransferase 1 (CPT1) activity and decrease malonyl-CoA inhibition of CPT1 activity [144, 145]. However, as adiponectin is significantly lowered by obesity [146] and fatty acid metabolism is increased, the full role of adiponectin in myocardial metabolism in obesity remains unknown. In contrast, leptin increases with increasing obesity [147] and has been shown to increase myocardial fatty acid metabolism

and decrease myocardial glucose metabolism. This increase in fatty acid oxidation occurs independently of the changes in insulin signalling and PPARa transcriptional regulation but may be attributable to increased fatty acid transport proteins on the plasma membrane [148].

Obesity and diabetes have a profound impact on cardiac energetic metabolism leading in many cases to Heart failure. While overall mitochondrial energy production is depressed in the heart, fatty acid β-oxidation rates are increased at the expense of glucose oxidation rates. In addition to this metabolic inflexibility, the accumulation of lipid intermediates can exacerbate cardiac insulin resistance. These metabolic profiles are closely associated with a decrease in cardiac efficiency that can compromise cardiac function and consequently lead to heart failure. Furthermore, lysine acetylation of key metabolic enzymes seems to play a crucial role in the pathophysiology of heart failure related to obesity and diabetes [149].

1.1.1.5- Metabolic alterations in Obese Skeletal muscle

Muscle is highly plastic, undergoes regular remodelling, and is responsible for the majority of total body glucose utilization, which when impaired leads to insulin resistance. Muscle lipotoxicity as a consequence of obesity, insulin resistance and/or metabolic dysfunction; generates a chronic low-level inflammatory environment. In these conditions, muscle is a vulnerable tissue [150-153]. There are also structural alterations that directly affect glucose homeostasis in muscle compromising muscle integrity and leading to complications such as tendinopathy [154], osteoarthritis [155] for example.

As already mentioned in the general outline, Insulin resistance and obesity are highly linked in both ways. Within the mechanisms that are involved in insulin and glucose metabolism, there is an enzyme, 3 phosphoinositol kinase (PI3 kinase) in charge of signalling insulin to regulate glucose transport, FA, and glycogen synthesis. It is also remarkable protein kinase B 2 (PKB2/Akt2) which, at a lower level; regulates the sensibility to insulin in skeletal muscle and liver and is responsible for insulin resistance in these tissues [156].

We have already commented that an increase of lipid accumulation in different tissues from adipose tissue induces the increase of catabolic mediators' levels [157] that damage

tissues. Furthermore, the presence of hypertension may be linked to tissue damage through vasoconstriction and ultimately depriving tissues of appropriate nutrient exchange *[158].*
When muscle mass and quality is lowered and contains increased fat mass over normal levels, this phenomenon is known as Sarcopenic obesity [159-161].

Sarcopenic obesity is directly related to poor physical function [162], weight gain, altered biological function in the muscle and an increase in the risk of developing additional physical disabilities [160] due to lipotoxicity in skeletal muscle [163].

In normal conditions, the muscle is continuously suffering fibre damage as a beneficial stimulus and leading to growth and adaptation through muscle regenerative processes [164]. In this process, muscle is repaired through a series of multistep inflammatory controlled processes involving degeneration, regeneration and remodelling to restore structure and function [165] *i*n which monocyte and macrophage recruitment and phagocytosis of necrotic material are essential in the first 24h [166].

As previously described, the metabolic complications associated with obesity can result in inappropriate temporal recruitment of these cells, which in turn leads to impaired angiogenesis and myocyte formation, while promoting the deposition of fibrotic and adipose tissue, ultimately leading to a reduction in structural integrity and functional capacity of a muscle [164].

Other metabolic alterations derived from this muscle lipotoxicity are elevated levels of leptin that can impair angiogenesis and lead to tissue ischemia [167]. Elevated expression of TGF-b promotes an increased fibrotic tissue deposition [165]. Inflammation related to obesity can also impair myocyte remodelling as a result of a reduction in protein synthesis due to elevated TNF-a levels [167].

Lipid metabolites resulting from impaired mitochondrial function contribute to elevated TNF-a levels, which are known to have inhibitory effects on IGF-1 [166].
Decreases in IGF-1 result in the inhibition of the muscle growth signalling pathway metabolites (IGF-1 P13K Akt mTOR), effectively decreasing muscle protein synthesis [167].

Appropriate levels of pro-inflammatory cytokines are necessary for tissue homeostasis. However, exogenous exposure to pro-inflammatory cytokines, or endogenous high levels of pro-inflammatory cytokines, is associated with damage across all musculoskeletal tissues. In muscle, TNF-a, IL-1b, and IL-6 activate transcription of MuRF-1 and MAFBx/atrogin-1, the key muscle atrophy pathway, through IGF/Akt-1 1 [166].

It is well known that ROS are a by-product of mitochondrial metabolism and homeostasis. Obese muscles undergo cell damage, mitochondrial dysfunction, or oxidative stress. The ROS are accumulated and their levels are associated with the metabolic dysfunction [168] leading to lipid peroxidation and disruption of the cellular membrane; ER stress, resulting in protein misfolding and unfolding, and a decrease in protein synthesis already described in previous sections, and activation of Caspase-3 and cell apoptosis [169].
Also, these high levels of ROS in skeletal muscle result in great susceptibility to fatigue and contractile dysfunction [170] and are associated with reduced muscle repair capacity [171].

Also, muscle lipotoxicity can result in dysfunction in myocyte metabolic pathways. Skeletal muscle is a primary site of glucose uptake and utilization [172].

Fatty acid trafficking in the muscle may also contribute to insulin resistance development by changing the availability of substrates involved in the formation and clearance of harmful lipid intermediates (diacylglycerides and ceramide) [173] from alterations in clearance mechanisms.

Obesity also affects several other pathways in skeletal muscle that may be critical for the onset and progression of systemic inflammation due to metabolic disturbance and musculoskeletal damage. Some of the pathways that could be involved are mitogen-activated protein kinases (MAPK, p38 MAPK, JNK), myeloid differentiation primary response gene 88 (MyD88), NFkB, and the NLRP3 inflammasome [174].

1.1.1.6- Beyond single-organ studies: Compartmentomics

After introducing some of the many different and diverse complications and metabolic changes produced by obesity, it is important to know and continue to discover which are the molecules and mechanisms that play a principal role in the development of this disease so

that we can understand their function and also use them with diagnostic utilities or as therapeutic targets.

In a summary, obese patients' metabolism undergoes at least 3 mechanisms related to chronic diseases. The first one is linked to intracellular excess of free fatty acids and DGs, which could activate intracellular signalling of PKC (intermediary between multiple metabolic signalling pathways in charge of the production of pro-inflammatory cytokines and ROS). The second mechanism is related to pro-inflammatory cytokines, the molecular expression of cellular adhesion and re modelling of vascular endothelium. The last mechanism is involved in the secretion of different immune cellular linkages under obesity conditions: lymphocytes T CD4+ Th-1, activated macrophages M-1 in adipose tissue that promotes inflammatory conditions associated with obesity complications such as hypertension, atheroma plaques, pro-thrombotic activation

Nowadays science tends to study only the target organ in which there is a problem, but it is well known that before pathologies and malfunction of an organ, alterations are not only caused in this; they also appear in other organs and surrounding tissues. This is the reason for the name of this emerging new omics: "Compartmentomics" consists of the study of metabolic changes caused in the different compartments of the body and then give them a holistic interpretation.

As mentioned in the previous paragraph and proceeding with documents research in SCOPUS bibliographic database, it can be observed that most of the studies are focused on only one tissue. As the number of tissues is increased, the number of publications decreases. (See Figure 1.1.2)

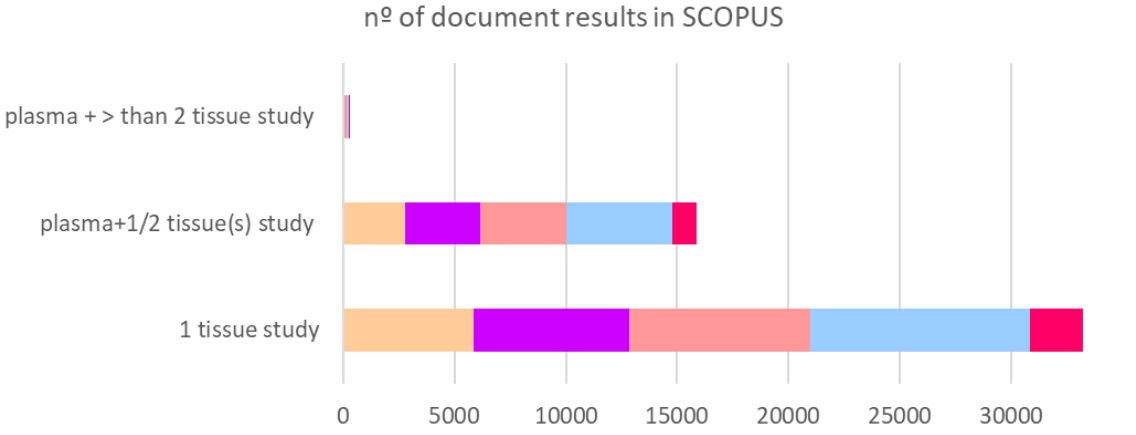

	1 tissue study	plasma+1/2 tissue(s) study	plasma + > than 2 tissue study
2016	5881	2796	31
2017	6945	3351	49
2018	8145	3867	81
2019	9894	4770	72
2020	2372	1114	22

[Figure 1.1.2]. Column chart that represents document search in SCOPUS related to studies of one or more tissues in the last five years. Information given is true as of March 9th, 2020.

All searches were limited to the last five years of publications and English language documents concerning articles, conferences, and all kind of publications. The used queries that lead to the previous column chart are presented in the following table:

1-tissue study	ALL (metabo*omics) AND ALL (plasma OR serum) OR (*tissue*) AND (LIMIT-TO (SUBJAREA , "BIOC") OR LIMIT-TO (SUBJAREA , "MEDI") OR LIMIT-TO (SUBJAREA , "CHEM") OR LIMIT-TO (SUBJAREA , "PHAR")) AND (LIMIT-TO (PUBYEAR , 2020) OR LIMIT-TO (PUBYEAR , 2019) OR LIMIT-TO (PUBYEAR , 2018) OR LIMIT-TO (PUBYEAR , 2017) OR LIMIT-TO (PUBYEAR , 2016)) AND (LIMIT-TO (LANGUAGE , "English"))
plasma+1/2 tissue(s) study	ALL (metabo*omics) AND (ALL (plasma OR serum)) AND (ALL (adipose*) OR (liver) OR (kidney) OR (heart) OR (*muscle)) AND (ALL (adipose*) OR (liver) OR (kidney) OR (heart) OR (*muscle)) AND (LIMIT-TO (SUBJAREA , "BIOC") OR LIMIT-TO (SUBJAREA , "MEDI") OR LIMIT-TO (SUBJAREA , "CHEM") OR LIMIT-TO (SUBJAREA , "PHAR")) AND (LIMIT-TO (PUBYEAR , 2020) OR LIMIT-TO (PUBYEAR , 2019) OR LIMIT-TO (PUBYEAR , 2018) OR LIMIT-TO (PUBYEAR , 2017) OR LIMIT-TO (PUBYEAR , 2016)) AND (LIMIT-TO (LANGUAGE , "English"))
plasma + > than 2 tissue study	ALL (metabo*omics) AND (ALL (plasma OR serum)) AND ALL (adipose*) AND ALL (liver) AND ALL (kidney) AND ALL (heart) AND ALL (*muscle) AND ALL (*tissue*) AND (LIMIT-TO (SUBJAREA , "BIOC") OR LIMIT-TO (SUBJAREA , "MEDI") OR LIMIT-TO (SUBJAREA , "CHEM") OR LIMIT-TO (SUBJAREA , "PHAR")) AND (LIMIT-TO (PUBYEAR , 2020) OR LIMIT-TO (PUBYEAR , 2019) OR LIMIT-TO (PUBYEAR , 2018) OR LIMIT-TO (PUBYEAR , 2017) OR LIMIT-TO (PUBYEAR , 2016)) AND (LIMIT-TO (LANGUAGE , "English"))

Furthermore, there is evidence of the high heterogeneity between the fat depots distributed in the different parts of the body [175, 176] but looking for publications in the last five years involved in the comparison of different white adipose tissues depots and/or brown adipose tissue is scarce. (See Figure 1.1.3)

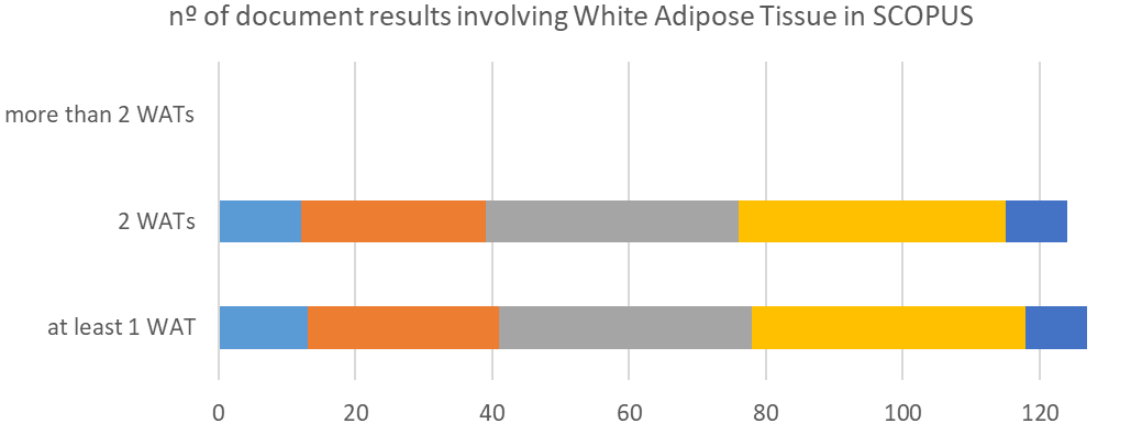

	at least 1 WAT	2 WATs	more than 2 WATs
2016	13	12	0
2017	28	27	0
2018	37	37	0
2019	40	39	0
2020	9	9	0

[Figure 1.1.3]. Column chart that represents document search in SCOPUS related to studies of one or more different types of White Adipose tissues in the last five years. Information given is true as of March 9th, 2020.

Due to the previously presented reasons, this study was designed to compare eight compartments from which four are different types of adipose tissues depots.

In our case, we focused on the observation of these changes in two kinds of the population: Control vs Diet-Induced Obesity (DIO) population through the administration of a High Fat Diet (HFD). This type of diet is characterized by 60% of fats in its composition and has been extensively employed to induce obesity and its consequences have been described. However, the metabolic impact of obesity in different organs and the connections between all the metabolic pathways are still not fully understood.

Some of the tissues with higher metabolic activity in the body were selected to be analysed and compared such as plasma, kidney, heart, skeletal muscle and four types of adipose tissues extracted from different areas of the mouse: inguinal, perirenal, epididymal white adipose tissue and intrascapular brown adipose tissue.

The study of all mentioned tissues will allow building metabolic profiling for these two populations.

The reasons for analysing four different adipose tissue depots are the huge diversity in composition between the different depots and the high relation of this tissue with insulin resistance and the studied diseases in this dissertation: Obesity and NAFLD. Also, it has been observed throughout the years that adipose tissue has a great role in inflammation response and many metabolic reactions involved in the homeostasis of the body [177].

Thanks to the multiplatform analysis of eight different tissues within the same organism/individual, the metabolic impact of obesity is studied.

1.1.1.7- Metabolite Annotation

1.1.1.6.1- Levels of confidence

Compounds detected in GC-MS were identified as describe below (section 1.1.2.7- Data treatment). The statistically significant compounds from CE-MS or LC-MS were putatively annotated by searching their accurate mass against public databases i.e., METLIN (https://metlin.scripps.edu/), KEGG (https://www.genome.jp/kegg/), LIPIDMAPS (https://www.lipidmaps.org/) and HMDB (https://www.hmdb.ca/), all simultaneously accessed through an in-house developed search engine, CEU Mass Mediator (https://www.ceumass.eps.uspceu.es/) [35, 178].

For compounds included in our in-house libraries, retention/migration times were also compared, and improves the annotation confidence. An LC-MS/MS experiment was set up, and the fragmentation pattern was analysed for more profound annotation of some statistically significant features. Therefore, each metabolite was annotated with different level of confidence. We have followed the classification proposed by Schrimpe-Rutledge et al. [179], with five levels of confidence:

- Level 1: highest confidence identification. Validated identification retrieved from reliable databases and confirmed with a pure reference standard.
- Level 2: putative identification. Validated annotation retrieved from reliable databases and confirmed with a MS/MS analysis and spectral matching to the to the predictive or externally acquired spectral libraries (providing information about reliable neutral losses or known fragmentation patterns).

- Level 3: Tentative identification. Validated annotation retrieved from reliable databases, compatible with all the variables (biological, chemical, instrumental) of the study.
- Level 4: Molecular structure candidates: After processing the signal from the instrument, only molecular empirical formula can be provided.
- Level 5: Unknown features: only deconvoluted experimental *m/z*, abundance and retention time could be known.

According to these levels, we can consider that we have annotated a metabolite if we have reached level 2, 3 or 4.. Furthermore, a feature can be considered a compound only if we can propose a molecular formula (level 4).

1.1.1.6.2- Kendrick's Mass Defect

In 1963, the chemist Edward Kendrick introduced the concept of "Kendrick's Mass" (KM) defined by the setting of the mass of a specific molecular fragment (CH_2 is the most commonly used) to an integer value in atomic mass units [180]. Since then, KM has been employed for the identification of compound from the same family of molecules that differs only by a number of an established base unit in high-resolution mass spectra [180]. It is frequently used by scientists working in the area of high-resolution mass spectrometry concerning proteomics, metabolomics [181], polymer analysis[182], environmental analysis [183-185]…etc who make use of mass spectrometers that allow the direct determination of molecular formula of a wide range of different molecular weight analytes. Despite this, the amount of information from spectra that these equipment obtain is increasing exponentially throughout the years and the identification of compounds is becoming more challenging.

The Kendrick's Mass Defect (KMD) method consists of the representation in a two-dimensional plot of the atomic composition of families of compounds spaced by the base units allowing fast recognition and identification of families and, in some cases, specific compounds. This Kendrick's plot is constructed throughout the transformation of the mass spectra representing the X axis KM and the Y-axis KMD. The KM is obtained by converting the exact masses of the unit base (named as Kendrick base, that corresponds to a given group of atoms) to the nearest integer value in the atomic mass unit (amu) changing these units to a different mass unit different from IUPAC amu reference known as Kendrick Nominal Mass (KNM).

[Equation 1]

$$\text{Kendrick-mass} = \text{IUPAC-mass} \times \frac{14.00000}{14.01565}$$

Then, the KMD is calculated by the difference between the KNM values and the KM [Equation 2]

$$\text{Kendrick-mass-(F)} = (\text{observed-mass}) \times \frac{\text{nominal-mass-F}}{\text{exact-mass-F}}.$$

F corresponds to the Base unit of a family of Compounds.

This Kendrick's plot is constructed by plotting KMD at the X-axis and KNM at the Y-axis. This plot shows us aligned in the KMD axis compounds that are chemically related, sharing the same KMD and differing only in KM units, which makes their annotation easier.

As already mentioned, the KMD method is used for the annotation of compounds and can be adjusted to filter data in a non-targeted, semi-targeted and targeted mode. We have made use of this method for the annotation of significant features form Adipose tissue samples because most of the compounds seemed to be lipids. This method has been used in this thesis as a support and a commentary tool to discard multiple annotations for the same features or confirm already putatively annotated compounds.

1.1.1.6.3- MS/MS annotation

To aid the annotation of differentiating signals, structural information is needed. It can be obtained through the fragmentation pattern based on the MS/MS spectra, where ions of interest are isolated and collided with neutral gas under indicated energy. Such a strategy requires a second round of analysis when fragmentation parameters will be set individually for each ion that has to be annotated.

Once all the MS/MS methods are designed and set up, the analysis of the samples takes place. Before spectra are used for the annotation their quality must be evaluated. The

obtained spectra are used to increase and reinforce the annotation of the significant features and to achieve this, each spectrum is inspected and interpreted one by one. In some cases, annotation might be not clear, but it helps to discard other putative identifications retrieved from the databases based on the accurate mass matching to the significative *m/z*. Each compound has specific fragments from its molecular structure that are characteristic of its molecular family. When interpreting spectra, we look for these characteristic fragments. For example Lysophosphocholines spectra acquired in positive ionization mode show fragments that correspond to the head group of the molecule: 124.99 Da, 166.06 Da and 184.07 Da, and usually have a neutral loss of 18.01 Da that corresponds to water molecule [Figure 1.1.4] [34]. The following figures show two examples of spectra interpretation: the first former is a valid and very clear spectrum and can be used for annotation while the latter is a spectrum that must be rejected as it is too noisy and does not provide valuable information.

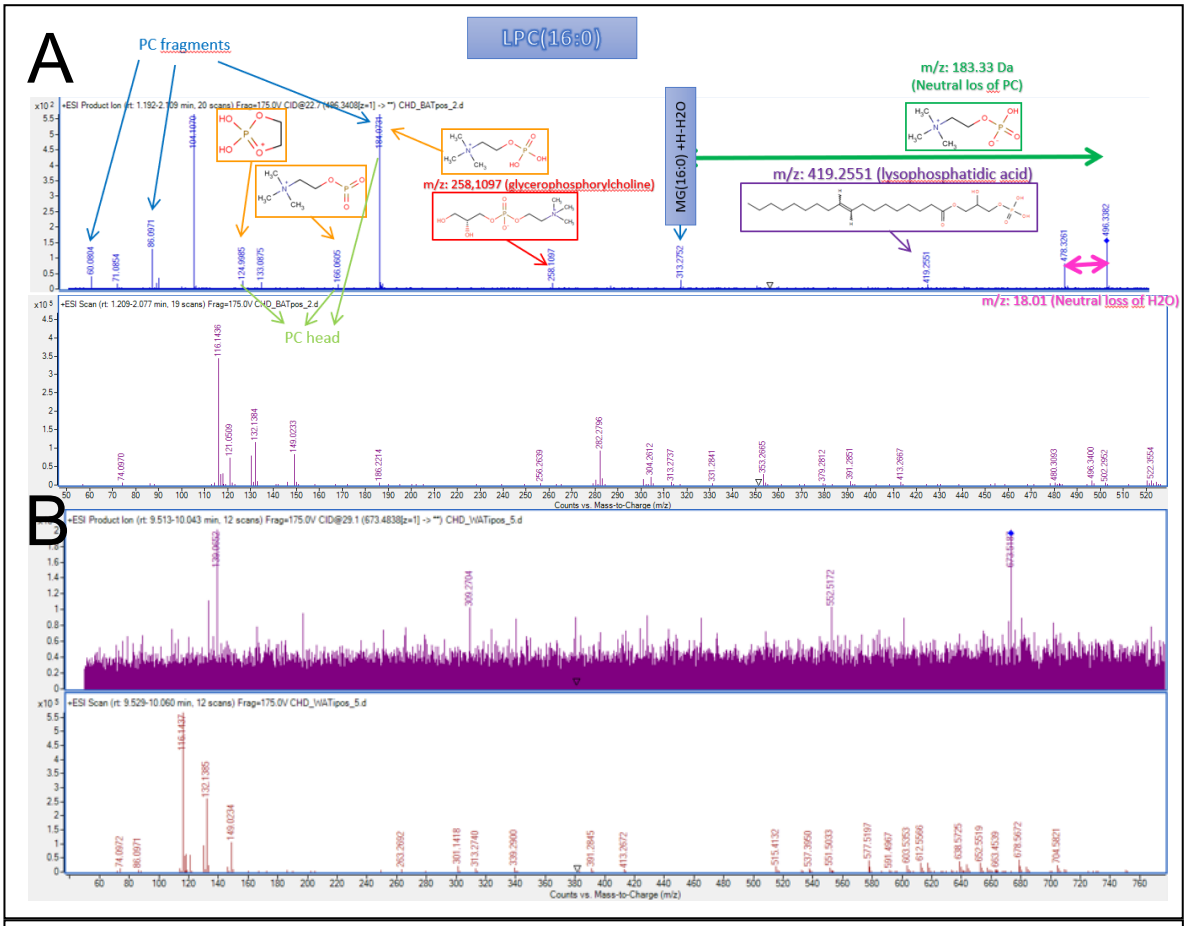

[Figure 1.1.4.]. Screenshots of two examples of MS/MS spectra interpretation from adquired data of compartmentomics study. A: MS/MSspectrum of a feature from BAT (Brown Adipose Tissue) in positive ESI mode which allowed annotation of LPC (16:0) (LPC= Lysophosphatidyl choline). B: MS/MS spectrum of a feature from WATi (inguinal White Adipose Tissue) an unidentified compound as shows a lot of noise and really low signal.

The previous process described is performed parallel to the search of the *m/z* in databases and to other tools that are used for the identification of features.

All these tools are complementary and used together to improve the annotation of significant features and be able to give the highest level of confidence.

1.1.2- Material and methods

1.1.2.1-Animals and sample collection

Twelve 8-week-old male C57Bl6j mice purchased from Charles River Laboratories (Charles River, Barcelona, Spain), were maintained in light/dark (12 h light/12 h dark), temperature (22 °C) and humidity-controlled rooms, fed ad libitum with free access to drinking water.
Mice were fed with a chow diet (Chow; SAFE A04-10 Panlab, Barcelona) or a high-fat diet (Teklad Custom Diet, TD06414, Envigo Teklad Diets, Madison, WI; see annexe 1.1.1) for eighteen weeks [see Figure 1.1.5]. At the final point, animals were anaesthetized with isofluorane and blood was collected in EDTA tubes by intracardiac punction. After that animals were euthanized by cervical dislocation. White adipose tissue depots (inguinal, epididymal and perirenal pads) and intrascapular brown adipose tissue were collected and immediately frozen in liquid nitrogen. Moreover, the main metabolic tissues (muscle, heart and kidney) were removed and frozen in liquid nitrogen. Plasma and all tissues were stored at -80ºC.

All animal experimentation was controlled following the recommendations of the Federation of European Laboratory Animal Science Associations (FELASA) on health monitoring, whereas the use of animals in experimental procedures was approved by the Ethical Committee at Consejo Superior de Investigaciones Científicas (CSIC) Animal Care and Use Committee and the experiment was conducted accordingly to accepted guidelines for animal care of Comunidad de Madrid (Spain). The CNIC Ethics Committee for Animal Experimentation (ECAE) approved all procedures (registration number PROEX 164/15), according to the Spanish laws (Law 32/2007 of 7 November; Royal Decree 53/2013 of 1 February) and European directive 2010/63/EU.

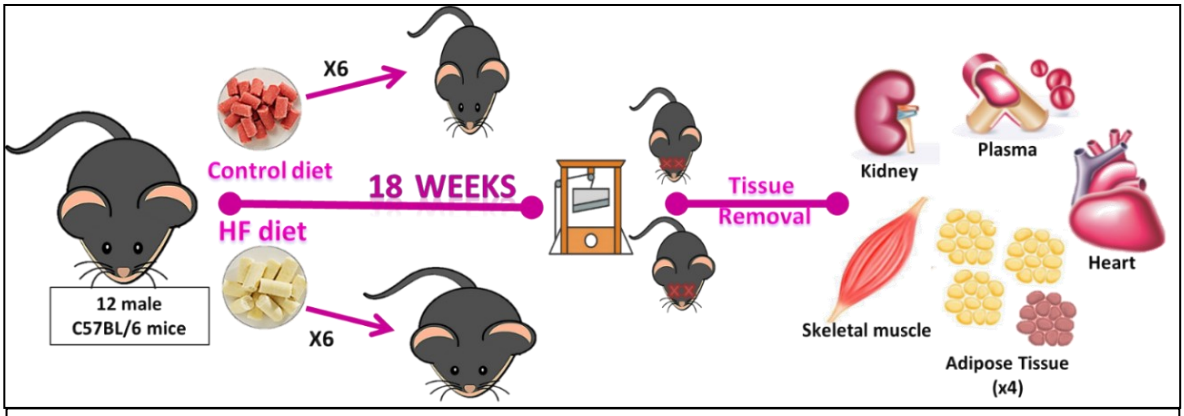

[Figure 1.1.5.]. Scheme representation of study design for the extraction of the eight tissues (plasma, kidney, heart, skeletal muscle and 4 types of adipose tissue). HF= High Fat.

1.1.2.2- Sample treatment and instrumental analysis.

A general overview of sample treatment and instrumental analysis process is depicted in figure 1.1.6. The sample preparation for multiplatform approach is based on a single homogenization step, followed by specific protocols steps to make the extracted sample compatible with the analytical platform. Sample collection and preparation was performed as previously described with slight modifications.

1.1.2.3- Homogenization.

Eight different types of tissues (plasma (P), kidney (K), heart (H), skeletal muscle (SM), Epididymal White adipose tissue (eWAT), Inguinal white adipose tissue (iWAT), Perirenal white adipose tissue (pWAT) and Brown adipose tissue (BAT)) were thawed the same day of the homogenization process and smashed into small pieces using mortar and pestle after dipping them in liquid nitrogen.

Due to the diversity of the tissues, the homogenization process was performed grouping tissues in 2 different processes:

1.1.2.3.1- Homogenization for Kidney, Heart and Skeletal muscle

Water: methanol, 50:50 (WM) was used as a solvent for homogenization. 50 to 60 mg of tissue were collected from each sample and the WM solvent was added at a 1:10 ratio (1mg

of tissue:10µl solvent). Homogenization was performed by adding 3 stainless steel beads of 2.8mm diameter per sample. Samples were homogenized at 50-Hz using 4cycles of 2 min each for kidney samples, 4 cycles of 5min each for heart samples and 8 cycles of 5min each for skeletal muscle samples (Qiagen TissueLyser LT, Germany).

Between each homogenization cycle, closed safety lock microtubes were placed into liquid nitrogen for 10s and into room temperature water for 10s consecutively to help the homogenization process.

1.1.2.3.2- Homogenization for Adipose tissues

To obtain homogenates of the Adipose tissue, homogenization had to be followed by a phase separation and metabolites extraction step due to the high content of lipids in these kinds of tissues and characteristics of the different techniques employed afterwards to analyse the samples.

1st STEP: Water: methanol, 50:50 (WM) was used as a solvent for homogenization. 9 to 10 mg of tissue were collected from each sample and the WM solvent was added at a 1:30 ratio (1mg of tissue:30µl solvent). Homogenization was performed adding 2 stainless steel beads of 2.8mm diameter per sample at 50-Hz speed for 2 cycles of 1 min each followed by 2 cycles of 2 min each (Qiagen TissueLyser: LT, Germany). Between each cycle, locked safety lock microtubes were placed into liquid nitrogen and room T water consecutively to help the homogenization process.

2nd STEP: Methyl tertbutyl ether (MTBE) was first used for lipid extraction.100 µl of MTBE per 1mg of tissue was added to each sample and followed by vortexing for 1h at room T. Afterwards, 20 µl of water per 1mg of tissue was added to each sample and let stand them for 10 min at room temperature. Water helps to promote non-mixable phases formation.

Finally, samples were centrifuged for 15min, 14000×*g* at 4ºC and two obtained phases were separately aliquot for future analysis. Organic phase (upper layer) into glass vials for LC/MS and the aqueous phase (lower layer) in plastic safety locked microtubes for GC/MS and CE/MS.

1.1.2.4- Metabolite's extraction

In this section, 2 different protocols for the preparation of analysis are described, grouping tissues as in the section "1.1.2.3- Homogenization".

1.1.2.4.1- Preparation for analysis of Kidney, Heart and Skeletal Muscle

For LC -QTOF-MS analysis, 100µL of tissue homogenate was vortexed with 100µL of methanol for 2 min. 100µL of MTBE was added and vortexed for 1 h at room T. After that, samples were centrifuged at 4000×*g* for 20 min at 20ºC. Then, 100µL of supernatant was transferred to a vial for LC-MS analysis.

For CE -TOF-MS analysis, 100µL of tissue homogenate was centrifuged at 14000x*g* for 15 min at 15ºC. 80µL of homogenate was transferred to a safety lock microtube and evaporated for 2h in a Savant™ SPD131DDA SpeedVac™ (ThermoFisher Scientific, Waltham, MA USA) at 30ºC. Samples were re-suspended in a 100µL solution of 0.2 mM methionine sulfone (internal standard) and 0.1 mM formic acid. Then, re-suspended samples were vortexed for 5min and transferred to an ultrasound bath for 2min. After that, samples were centrifuged at 16000x*g* for 20min at 20ºC. 100µL of supernatant was collected and transferred to a Chromacol® vial for CE-MS analysis.

For GC -QTOF-MS analysis, 40µL of tissue homogenate was transferred to a safety lock microtube and 120µL of cold acetonitrile was added. Samples were vortexed for 2min and let stand on ice for 5min. Following, liver samples were centrifuged at 15400x *g* for 10min at 4ºC. 100µL of the supernatant was transferred to a GC vial and evaporated for 2h. 10µL of *O*-methoxy amine hydrochloride in pyridine solution (15 mg/ml) was added to the dried samples and vortexed for 1min. Vials were ultra-sonicated for 10s and vortexed for 2min (x3 series). Samples were then incubated in the dark for 1h. 10µL of *N,O*-Bis(trimethylsilyl) trifluoroacetamide (BSTFA) with 1% of trimethylchlorosilane (TMCS) was added to the vials and mixed vigorously for 5min. After that, samples were incubated for 60min at 70ºC. After that, samples were cooled for 1h in a dark place. 100µL of internal standard (10 ppm) was added to each vial and mixed vigorously for 2min. Vials were centrifuged at 2500x*g* for 15min at 18ºC.

1.1.2.4.2- Preparation for analysis of Adipose tissues

For LC -QTOF-MS analysis, 100µL of the organic phase (upper layer) from each adipose tissue was vortexed with 100µL of methanol for 2min. 100µL of MTBE was added and vortexed for 1h at room T. After that, samples were centrifuged at 4000×*g* for 20min at 20ºC. Then, 100µL of supernatant was transferred to a vial for LC-MS analysis.

For CE -TOF-/MS analysis, 100µL of aqueous phase (lower layer) from each adipose tissue was centrifuged at 14000 x *g* for 15 min at 15 ºC. 80µL of homogenate was transferred to a safety lock microtube and evaporated for 2h in a Savant™ SPD131DDA SpeedVac™ (ThermoFisher Scientific, Waltham, MA USA). Samples were re-suspended in a 100µL solution of 0.2 mM methionine sulfone (internal standard) and 0.1 mM formic acid. Then, re-suspended samples were vortexed for 5min and transferred to an ultrasound bath for 2min. After that, samples were centrifuged at 16000x*g* for 20min at 20ºC. 100µL of supernatant was collected and transferred to a Chromacol® vial for CE-MS analysis.

For GC -QTOF-MS analysis, 40µL of aqueous phase (lower layer) from each adipose tissue was transferred to a safety lock microtube and 120µL of cold acetonitrile was added. Samples were vortexed for 2min and let stand on ice for 5min. Following, liver samples were centrifuged at 15400x*g* for 10min at 4ºC. 100µL of the supernatant was transferred to a GC vial and evaporated for 2h. 10µL of *O*-methoxy amine hydrochloride in pyridine solution (15 mg/ml) was added to the dried samples and vortexed for 1min. Vials were ultra-sonicated for 10s and vortexed for 2min (x3 series). Samples were then transferred to a dark place and incubated for 1h. 10µL of BSTFA with 1% of TMCS was added to the vials and mixed vigorously for 5min. After that, samples were incubated for 60min at 70ºC. During incubation, an internal standard (10 ppm solution of C18:0 methyl ester) was injected to confirm the retention time and the peak are in the GC-MS. After that, samples were cooled for 1h in a dark place. 100µL of internal standard (10 ppm) was added to each vial and mixed vigorously for 2min. Vials were centrifuged at 2500x*g* for 15min at 18ºC.

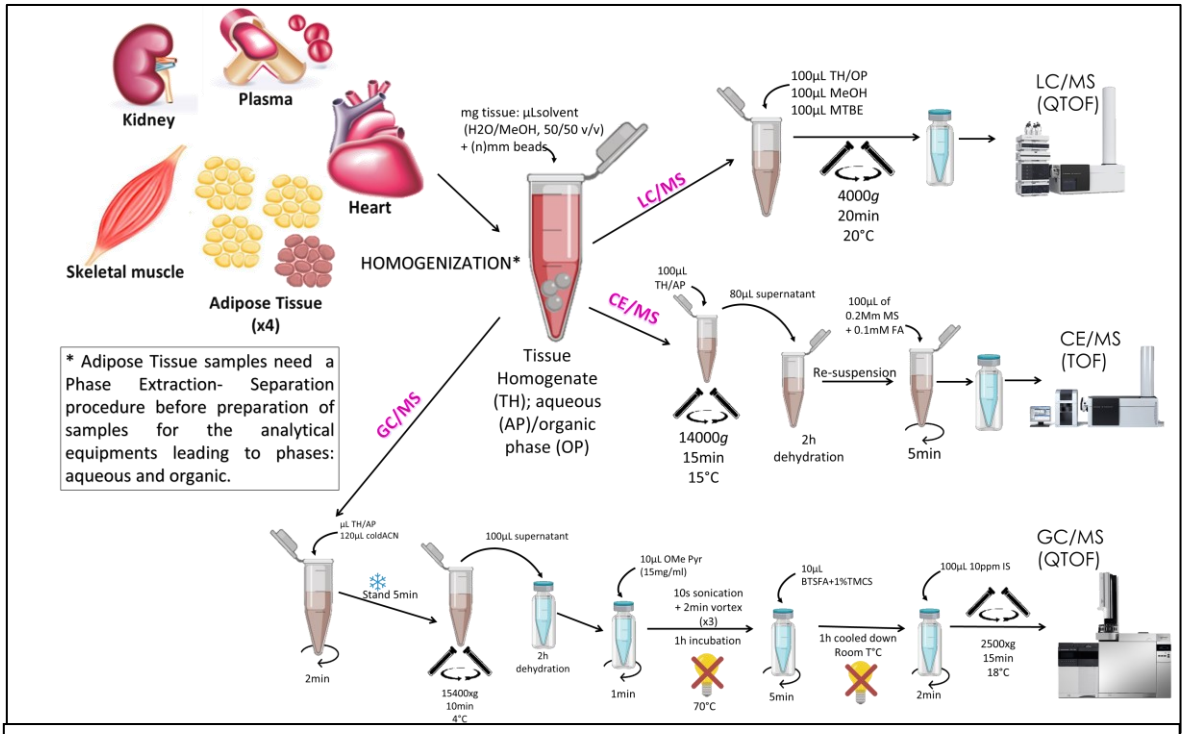

[Figure 1.1.6]. Sample preparation and data acquisition scheme for multiplatform analysis of the eigjht different tissues involved in Compartmentomics study: Plasma, Kidney, Heart, Skeletal muscle and four different Adipose Tissues.

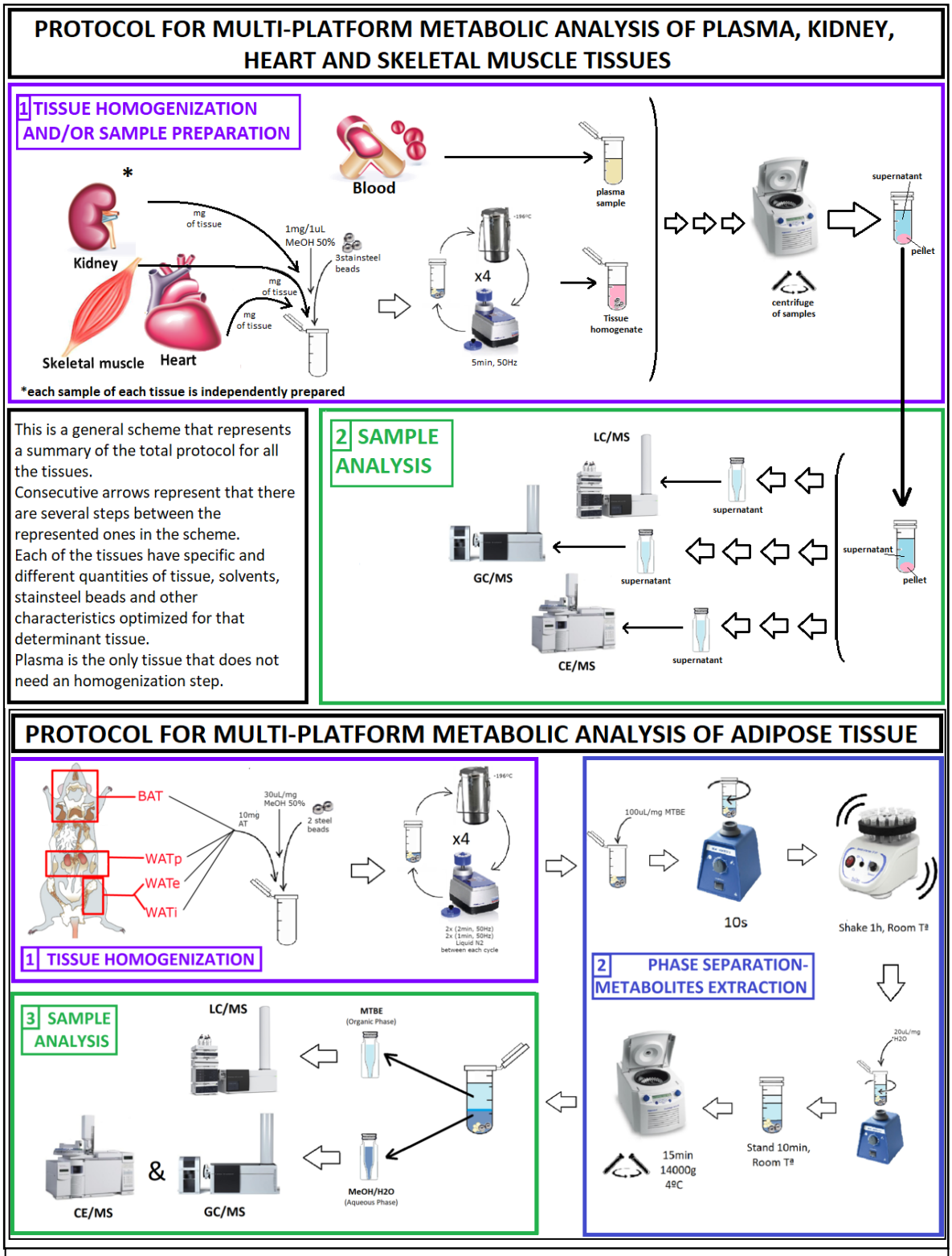

[Figure 1.1.7]. Two scheme comparison between protocol for tissues different from adipose tissue and adipose tissue protocol for multi-platform metabolomics analysis. (BAT=Brown Adipose Tissue; WATp= perirenal White Adipose Tissue; WATe= epididymal White Adipose Tissue; WATi= inguinal White Adipose Tissue; LC/MS= Liquid Chromatography Mass Spectrometry; GC/MS= Gas Chromatography Mass Spectrometry; CE/MS= Capillary Electrophoresis Mass Spectrometry).

1.1.2.5- Instrumental conditions

The final instrumental conditions for the different tissues' samples were optimized from methods for LC-MS; GC-MS and CE-MS previously established in our laboratory [186].

LC-QTOF-MS analysis was carried out with liquid chromatography (LC) system (1200 series, Agilent Technologies, Waldbronn, Germany) consisting of a degasser, two binary pumps, thermostated autosampler and a column oven coupled with 6520 iFunnel QTOF-MS . For the analysis of plasma, kidney, heart and skeletal muscle samples conditions were as follows: 10µL of each sample was injected into Discovery HS C18 column, 15cmx2.1mm 3µm (Supelco) equipped with a guard column Discovery HS C18 2cmx2.1mm 3µm (Supelco) and thermostated at 40ºC. The mobile phases used for the analysis consisted of a A (0.1% ammonium formate in Milli-Q water) and B (0.1 % ammonium formate in acetonitrile) pumped at 0.6mL/min. The gradient started at 95% phase B, decreasing to 25% B in 35min and was maintained until the end of the gradient, taking the total run time to 45min. Data were collected in positive and negative ESI modes, in separate runs, operated in full scan mode from *m/z* 50 to 1000, with a scan rate of 1.2 scans/s in both polarities. The capillary voltage was set to 3000 V for positive and 4000 V for negative ionization mode; the drying gas flow rate was 10.5 L/min at 330°C and nebulizer 52psig, fragmentor voltage 175 V, and octopole radio frequency voltage (OCT RF Vpp) 750 V.

For the analysis of the four types of adipose tissues (eWAT, iWAT, pWAT and BAT) samples conditions were as follows: 1µL of each sample was injected to an Agilent 120 EC_C8; 150 x2.1mm; 2.7µm column placed backwards and thermostated at 60ºC. The mobile phases used for the analysis consisted of a A(40% of 10mM ammonium formate in Milli-Q water + 60% of acetonitrile) and B (90% of isopropanol + 10% of Acetonitrile) pumped at 0.45mL/min. Gradient started with 35% phase B, increasing to 70% B in 11min. This was held until 16.5min. Then gradient increased to 75% B by 22min. Starting conditions were returned by 24.75min and a 10.15 min re-equilibration time was included, taking the total run time to 35 min. Data were collected in positive and negative ESI modes in separate runs, operated in full scan mode from *m/z* 50 to 1200, with a scan rate of 1.05 scans/s in both polarities. The capillary voltage was set to 3500 V for both polarity modes; the drying gas flow rate was 10 L/min at 350°C and nebulizer 40psig, fragmentor voltage 175 V, and OCT RF Vpp 750 V.

Regardless the sample type, two reference masses were used throughout the whole LC-MS analysis: *m/z* 121.0509 (protonated purine) and *m/z* 922.0098 (protonated hexakis, (1H,1H,3H-tetrafluoropropoxy)phosphazine (HP-921)) for the positive ionization mode, and *m/z* 112.9856 (proton-abstracted TFA anion) and *m/z* 966.0007 (formate adduct of HP- 921) for the negative mode. These masses were continuously infused into the system to provide a constant mass correction. Samples were randomly analysed throughout the run.

CE -TOF-MS analysis was performed only on plasma, kidney, heart and skeletal muscle samples. The analysis of these samples was carried out with 7100 capillary electrophoresis (Agilent Technologies) coupled to a 6224 accurate mass TOF-MS (Agilent Technologies), equipped with an ESI source. For metabolite separation, a fused-silica capillary from Agilent Technologies (total length, 96 cm; inner diameter, 50μm) was used, working in normal polarity. Before each analysis, the capillary was flushed for 5min (950 mbar) with background electrolyte (BGE) (0.8 M formic acid solution in 10 % methanol (v/v). Sample injections were performed over 50s at 50 mbar, and to improve the reproducibility of the analysis, the BGE was injected for 10s at 100 mbar after the injection of each sample. The separation was performed with an internal pressure of 25 mbar at a voltage of +30 KV, and a constant temperature of 20°C. The total time of the analytical run was 30min. The MS was operated in positive polarity, with a full scan range from *m/z* 74–1000 at a rate of 1.00 scan/s. The other parameters for the MS were: fragmentor set to 125 V, skimmer to 65 V, OCT RF Vpp to 750 V, drying gas temperature to 200°C, flow rate to 10 L/min, nebulizer to 10psig, and capillary voltage to 3500 V. The sheath liquid consisted of methanol/water (1:1, v:v), formic acid (1 mM) and two reference masses (5μL of purine: *m/z* 121.0509 and 15μL of HP-0921: *m/z* 922.0098) at a flow rate of 0.6 mL/min (1:100 split). Data acquisition was performed with ChemStation software B.04.03 (Agilent Technologies Santa Clara, CA, USA), and Mass Hunter Workstation Data Analysis B.02.01 (Agilent Technologies) controlled the MS performance.

GC-MS fingerprinting analysis was performed on samples from the eight different tissues under the same instrumental conditions carried out with an Agilent GC instrument (7890A) coupled to an inert mass spectrometer with triple-Axis detector (5975C, Agilent Technologies). Summarized conditions are: 2μL of derivatized samples were injected by an Agilent autosampler (7693). Samples were automatically injected in split mode (split ratio 1:10), into an Agilent ultra-inert deactivated glass wool split liner. The compound separation

was achieved using a pre-column (10 m J&W integrated with Agilent 122-5532G) combined with a GC column DB5-MS (length, 30m; inner diameter, 0.25mm; and 0.25µm film of 95% dimethyl/5% diphenylpolysiloxane). The flow rate of helium carrier gas was constant at 1 mL/min through the column. The retention time locking (RTL) to the internal standard (methyl stearate) peak at 19.66 minutes was performed. The column oven temperature was initially set at 60°C (maintained for 1min), then raised by 10°C/min until it reached 325°C, and then was held at this temperature for 10min before cooling down. The injector and the transfer line temperatures were established at 250°C and 280°C, respectively. MS system: the electron ionization operating parameters were set as follows: filament source temperature, 230°C; electron ionization energy, 70 eV. Mass spectra were collected over a mass range of *m/z* 50-600 at a scan rate of 2 spectra/s. Data were acquired using the Agilent MSD ChemStation Software (Agilent Technologies). For retention index determination, a mixture of *n*-alkanes (C8-C28) dissolved in hexane was run before the samples. Data were acquired using Agilent MSD ChemStation Software (Agilent Technologies).

1.1.2.6- Quality control samples:

QCs were prepared for each tissue separately by pooling directly from homogenate equal volumes from each sample from all groups to single safety lock microtube . From this QC pull two QCs samples were prepared following the same steps as the rest of the samples. They were analysed throughout the whole worklist to provide a measurement not only of the system's stability and performance.

1.1.2.7- Data treatment

1.1.2.7.1- LC-QTOF-MS

Chromatograms of resulting data files were analysed with Mass Hunter Qualitative Analysis software (B.08.00, Agilent). Background noise and unrelated ions were cleared, while co-eluting related ions originating from the same molecule were clustered into single value named as feature. This process was performed using the Molecular Feature Extraction (MFE) algorithm through Mass Hunter Profinder Software (B.08.00, Agilent). Features were filtered selecting the data presented in at least 80% of the QCs and 80% of the samples in one of the four groups.

1.1.2.7.2- CE-TOF-MS

An in-house built library of standards and metabolites previously detected by CE/MS [187] was used to perform target search across acquired files. This search was carried out by means of the Find by Formula algorithm available in Mass Hunter Qualitative Analysis software (B.08.00, Agilent). To check the quality of the analysis we used methionine sulfone (MetS) as internal standard (IS). IS was used to correct the signals to minimize the batch effect and to calculate relative MT.

1.1.2.7.3- GC-Q-MS

The identification is assured by the reproducibility of EI mass spectra and the RTL (Retention Time Lock) method. Background noise and unrelated ions were cleared, while co-eluting related ions originating from the same molecule were clustered into single value named as feature. This process was performed using the Molecular Feature Extraction (MFE) algorithm through Mass Hunter Qualitative Analysis Software (B.08.00, Agilent). Deconvolution and compound identification were performed using Mass Hunter Unknown Analysis (B.04.00, Agilent Technologies). Fiehn and NIST libraries were used for the identification. Assignment of selective ion and peak integration were done with Mass Hunter Quantitative Analysis (B.08.00, Agilent Technologies). Mass Profiler Professional software (B.12.00, Agilent Technologies) were used to perform the data filtering (as described in the LC-MS section).

1.1.2.8- Statistical analysis.

Data are reported by all the comparisons of the p-values of estimated means according to the linear regression model that underlies two samples comparison. The p-values are given for all variables detected for all the tissues separately. They correspond to the significant values selected according to the p-value of the Mauchly sphericity contrast with Greenhouse-Geisser correction. All statistical analyses were performed using the MATLAB® R2015a software.

Besides, multivariate analysis (Principal Component Analysis) for all sets of data were performed to check for possible bias or trends of the data, as well as to evaluate the clustering of QCs. This analysis was performed using SIMCA-P+ 14.1 software (Umetrics, Umea, Sweden).

1.1.3- Results

Thanks to our multiplatform approach, we have been able to detect more than 13.000 features. After statistical analysis, 3053 features from the total detected resulted to be significant (p-value <0.05). Each platform was suitable to find differences in a different set of compounds from metabolic families, expanding, therefore, the metabolite coverage of the study. See table 1.2 and table 1.3].

After LC-MS analysis, the total number of detected compounds considering all tissues and both polarities were 9365, from which 2440 resulted to be significant ($p < 0.05$). It is noticeable that LC-MS was the platform that provided more significant features from the three techniques.

Concerning CE-MS analysis, the sum of detected features from four of the eight tissues was 2032 features, from which 473 resulted to be significant. Unfortunately, we could not obtain an adequate CE-MS signal from the aqueous phase of the adipose tissue sample treatment.

About GC-MS analysis, a total of 176 features were detected for all the eight tissues, from which 140 resulted to be significant.

The quality of the methodology was checked by multivariate analysis (PCA; Principal Component Analysis) for all sets of data corresponding to each tissue and platform to check for possible bias or trends of the data, as well as to evaluate the clustering of QCs. [see Annexes 1.1.2 to 1.1.5].

Regarding LC-MS results, after the first analysis of the samples and statistical evaluation of obtained data, methods were designed to perform an MS/MS analysis of the significant features from the first analysis to improve and increase the reliability of the annotations. To perform the methods, *m/z* and retention time windows were needed to be established for each significant feature for the different tissue samples. 269 methods were designed for the analysis of 691 significant features.

Table 1.1.1 summarizes all the data obtained from the different tissues in the 3 platforms:

		GCMS	CEMS	LCMS(+)	LCMS(-)
Plasma	**total**	176	943	881	805
	p<0.05	8	199	263	280
	%	5%	21%	30%	35%
kidney	**total**	176	626	632	563
	p<0.05	14	191	194	190
	%	8%	31%	31%	34%
heart	**total**	176	416	683	607
	p<0.05	60	61	44	144
	%	34%	15%	6%	24%
skeletal muscle	**total**	176	317	519	601
	p<0.05	10	22	66	112
	%	6%	7%	13%	19%
WATi	**total**	176		819	127
	p<0.05	20		208	48
	%	11%		25%	38%
WATp	**total**	176		776	142
	p<0.05	10		285	41
	%	6%		37%	29%
BAT	**total**	176		1008	224
	p<0.05	18		244	83
	%	10%		24%	37%

The corresponding annotation strategies were applied to all significant ($p < 0.05$) features detected by the three platforms, firstly separated by tissues and platform. After the first annotated approach, putative identifications from all the tissues from each technique were placed in the same matrix to perform a comparative study of the differences and similarities between tissues.

Next to this, all significant features from adiposes tissues (already annotated and unknowns by this moment), especially from the LC-MS platform; were processed by Kendricks Mass Defect (KMD) theory by the calculation of Kendricks Nominal Mass and Kendricks Mass Defect and plotted for further annotation. The following Figure 1.1.8 shows the plot of KMD vs. KNM for significant features of the four adiposes tissues:

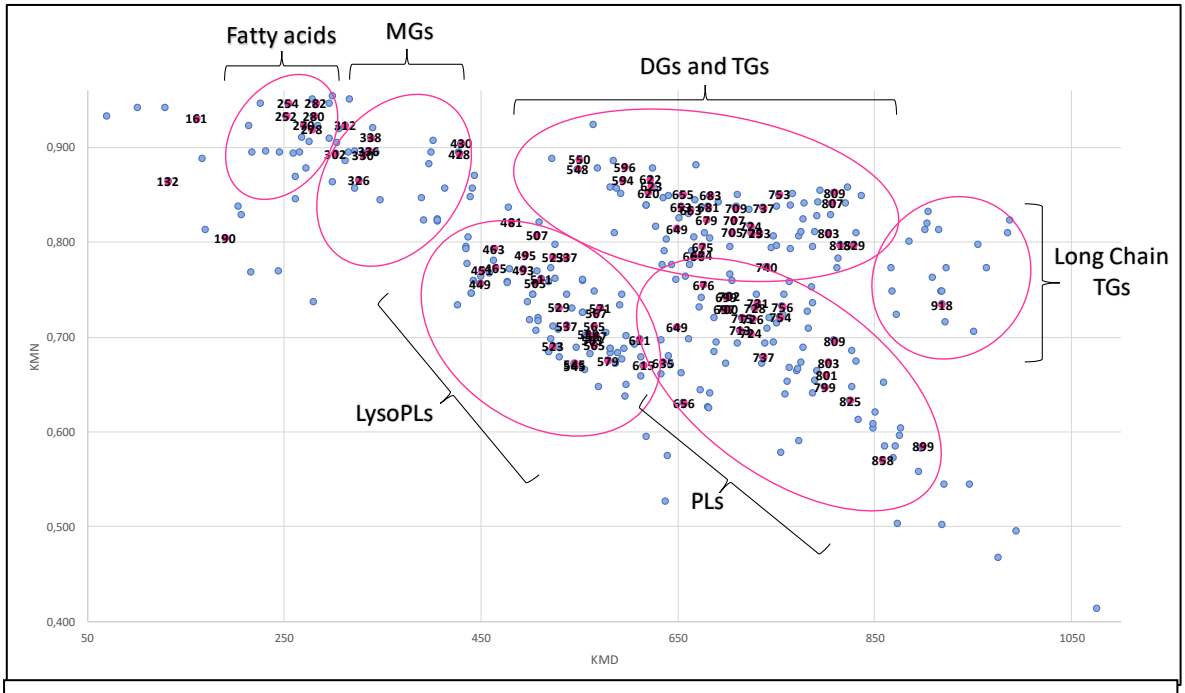

[Figure 1.1.8.]. KMD plot of significant features from the four adipose tissues (WATe, WATi, WATp and BAT). Different molecular families are separated by pink circles. (MGs= Monoglycerides; LysoPLs= Lysophospholipids; DGs= Diglycerides; TGs= Triglycerides; PLs= Phospholipids; WATe=epididimal White Adipose Tissue; WATi= inguinal White Adipose Tissue; WATp= perirenal White Adipose Tissue; BAT= Brown Adipose Tissue).

In figure 1.1.9, there is a representation of some of the molecular families distributed in the KMD plot. We can see how families are aligned according to unsaturation and number of methyl groups in their molecular structure, helping to provide additional information to raise the level of confidence of already annotated compounds and also helping to discard some of the possible putative identifications for those features that matched for more than one annotation provided in databases.

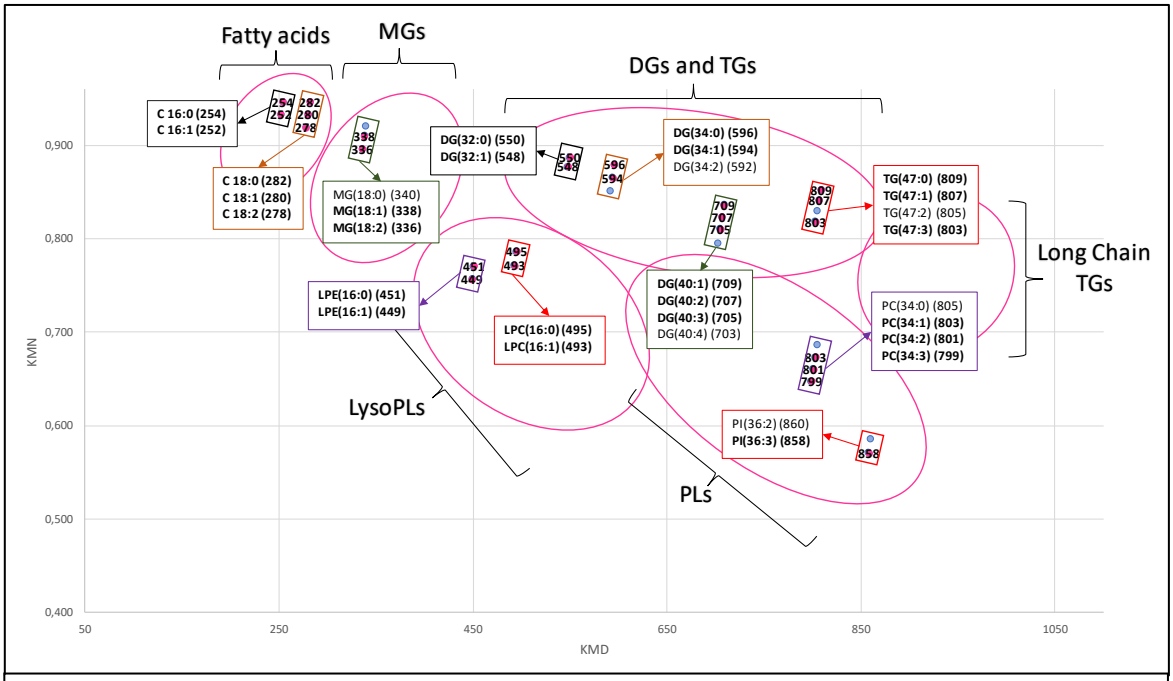

[Figure 1.1.9.]. KMD plot of some of the examples from different molecular families from Figure 1.1.8.. The colours of the squares were randomly selected. (MGs= Monoglycerides; LysoPLs= Lysophospholipids; DGs= Diglycerides; TGs= Triglycerides; PLs= Phospholipids;).

Together with KMD, in House CEMBIO databases already verified with standards; were used to add more reliability to annotations of compounds.

Final annotations were taken to a common table in which only the significant features that were expressed at least in two of the tissues were left to be able to follow, compare and observe the metabolic impact of obesity in each of the common significant features throughout the different tissues and were represented into a table [Table 1.1.4].

We established an internal code so that significant compounds from Table 1.1.4 could be easily found in their corresponding identification results tables (see Table 1.1.2 and Table 1.1.3). It has to be mentioned that this code was only designed for those metabolites which resulted to be significant in more than one tissue, represented all together in Table 1.1.4. For non-common significant features, no code was assigned (in tables 1.1.2 and 1.1.3 N/A = Non-Applicable in Code column).

These non-common features form a long list of metabolites, mainly being lipids. They played an essential role in the annotation process. It is because lipids belonging to the same class behave similarly, according to their class, chain length and unsaturation level. These

properties were used to evaluate the RT order check and to apply Kendricks Mass Defect theory. A larger number of candidates per each class improves the overall annotation confidence

[Table 1.1.2]: (LC-MS identification results in ascending order of mass): *(RT= Retention Time; ID. =identification; CL= Confidence Level; N/A= Non-Applicable)*

CODE	Mass	RT	m/z	PUTATIVE ID	Formula	Adduct	CL	Cathegory	(Sub)Class
N/A	228,2085	1,64	227,2007	Tetradecanoic acid FA 14:0	C14H28O2	M-H	2	Fatty acyls	Fatty Acids and Conjugates
LN009	256,2399	2,32	255,2321	Hexadecanoic acid FA 16:0	C16H32O2	M-H	2	Fatty acyls	Fatty Acids and Conjugates
LN010	254,2242	1,76	253,2164	Hexadecenoic acid FA16:1	C16H30O2	M-H	2	Fatty acyls	Fatty Acids and Conjugates
LN012	284,2706	23,14	283,2628	Octadecanoic acid FA 18:0	C18H36O2	M-H	2	Fatty acyls	Fatty Acids and Conjugates
LN014	282,256	2,51	281,2482	Octadecenoic acid FA 18:1	C18H34O2	M-H	2	Fatty acyls	Fatty Acids and Conjugates
LN015	280,24	1,89	279,2322	Octadecanedioic acid FA 18:2	C18H32O2	M-H	2	Fatty acyls	Fatty Acids and Conjugates
N/A	458,3381	13,78	313,2371	Octadecanedioic acid FA 18:2	C18H34O4	M-H	3	Fatty acyls	Fatty Acids and Conjugates
N/A	278,2242	25,11	277,2164	Octadecatrienoic acid FA 18:3	C18H30O2	M-H	2	Fatty acyls	Fatty Acids and Conjugates
N/A	272,1764	19,77	273,1842	Octadecatriynoic acid FA 18:6	C18H24O2	M+H	2	Fatty acyls	Fatty Acids and Conjugates
N/A	296,271	3,89	297,2788	Nonadecenoic acid FA 19:1	C19H36O2	M+H	2	Fatty acyls	Fatty Acids and Conjugates
N/A	308,2712	31,4	307,2634	Eicosadienoic acid FA 20:2	C20H36O2	M-H	2	Fatty acyls	Fatty Acids and Conjugates
N/A	306,2547	29	305,2469	Eicosatrienoic acid FA 20:3	C20H34O2	M-H	2	Fatty acyls	Fatty Acids and Conjugates
LN017	304,24	1,78	303,2322	Eicosatetraenoic acid FA 20:4	C20H32O2	M-H	2	Fatty acyls	Fatty Acids and Conjugates
LN018	332,2709	30,19	331,2631	Docosatetraenoic acid FA 22:4	C22H36O2	M-H	3	Fatty acyls	Fatty Acids and Conjugates
LN019	328,239	1,62	327,2312	Docosahexaenoic acid FA 22:6	C22H32O2	M-H	2	Fatty acyls	Fatty Acids and Conjugates
N/A	310,25	9,29	311,2578	Hydroxy-octadecadienoic acid methyl ester FA18:2-OH methyl ester	C19H34O3	M+H	3	Fatty acyls	Hydroxy fatty acids
N/A	216,1722	13,52	215,1644	Hydroxy-dodecanoic acid FA 12:0-OH	C12H24O3	M-H	2	Fatty acyls	Hydroxy fatty acids
LN011	272,2348	23,65	271,227	Trihydroxy-hexadecanoic acid FA 16:0-3OH	C16H32O3	M-H	2	Fatty acyls	Hydroxy fatty acids
N/A	244,203	18,66	243,1952	Hydroxy-tetradecanoic acid FA 14:0-OH	C14H28O3	M-H	2	Fatty acyls	Hydroxy fatty acids
N/A	270,2197	20,59	269,2119	Oxo-hexadecanoic acid FA 16:1=O	C16H30O3	M-H	2	Fatty acyls	Oxo fatty acids
LP016	312,266	10,05	313,2738	Oxo-nonadecanoic acid FA 19:1=O	C19H36O3	M+H	2	Fatty acyls	Oxo fatty acids
N/A	298,2494	1,21	297,2416	Oxo-octadecanoic acid FA 18:1=O	C18H34O3	M-H	2	Fatty acyls	Oxo fatty acids
N/A	242,1876	16,53	241,1798	Oxo-tetradecanoic acid FA 14:1=O	C14H26O3	M-H	2	Fatty acyls	Oxo fatty acids
N/A	296,2342	18,01	295,2264	Epoxy-octadecenoic acid EpOME FA18:2=O	C18H32O3	M-H	2	Fatty acyls	Epoxy fatty acids

CODE	Mass	RT	m/z	PUTATIVE ID	Formula	Adduct	CL	Cathegory	(Sub)Class
N/A	324,2661	25,84	323,2583	Epoxy-eicosenoic acid FA 20:0=O	C20H36O3	M-H	2	Fatty acyls	Epoxy fatty acids
N/A	268,2023	17,73	267,1945	Epoxy-hexadecenoic acid FA16:2=O	C16H28O3	M-H	3	Fatty acyls	Epoxy fatty acids
LN002	134,0213	0,74	133,0135	Hydroxybutanedioic acid FA 7:1-OH	C4H6O5	M-H	2	Fatty acyls	Dicarboxylic acids
N/A	72,0212	0,72	71,0134	2-propenoic acid	C3H4O2	M-H	3	Fatty acyls	Unsaturated fatty acids
N/A	217,1303	0,75	218,1381	Propionyl-L-carnitine CAR 3:0	C10H19NO4	M+H	2	Fatty acyls	Fatty acyl carnitines
N/A	231,1486	0,95	232,1564	Butyryl-L-carnitine CAR 4:0	C11H21NO4	M+H	2	Fatty acyls	Fatty acyl carnitines
N/A	245,162	0,98	246,1698	Valeryl-L-carnitine CAR 5:0	C12H23NO4	M+H	2	Fatty acyls	Fatty acyl carnitines
N/A	259,1766	1,01	260,1844	Hexanoyl-L-carnitine CAR 6:0	C13H25NO4	M+H	2	Fatty acyls	Fatty acyl carnitines
N/A	315,2404	8,11	316,2482	Decanoyl-L-carnitine CAR 10:0	C17H33NO4	M+H	3	Fatty acyls	Fatty acyl carnitines
N/A	343,2716	12,26	344,2794	Dodecanoyl-L-carnitine CAR 12:0	C19H37NO4	M+H	3	Fatty acyls	Fatty acyl carnitines
N/A	397,3196	16,98	398,3274	Hexadecenoyl-L-carnitine CAR 16:1	C23H43NO4	M+H	3	Fatty acyls	Fatty acyl carnitines
N/A	427,3653	22,82	428,3731	Octadecanoyl-L-carnitine CAR 18:0	C25H49NO4	M+H	3	Fatty acyls	Fatty acyl carnitines
N/A	261,1552	0,71	262,163	Hydroxy-isovaleryl-L-carnitine CAR 5:0-OH	C12H23NO5	M+H	3	Fatty acyls	Fatty acyl carnitines
N/A	413,3123	13,53	414,3201	Hydroxy-hexadecenoyl-L-carnitine CAR 16:1-OH	C23H43NO5	M+H	2	Fatty acyls	Fatty acyl carnitines
N/A	443,3591	19,35	444,3669	Hydroxy-octadecanoyl-L-carnitine CAR 18:0-OH	C25H49NO5	M+H	3	Fatty acyls	Fatty acyl carnitines
N/A	441,3444	16,93	442,3522	Hydroxy-octadecenoyl-L-carnitine CAR 18:1-OH	C25H47NO5	M+H	3	Fatty acyls	Fatty acyl carnitines
N/A	439,3315	14,8	440,3393	Hydroxy-octadecadienoyl-L-carnitine CAR18:2-OH	C25H45NO5	M+H	3	Fatty acyls	Fatty acyl carnitines
N/A	371,3031	16,04	372,3109	Octadecanoyl-serine NA 21:1;O3	C21H41NO4	M+H	3	Fatty acyls	Fatty amides
N/A	279,256	23,92	280,2638	Hexadecenoyl-ethanolamine NAE 16:1	C18H35NO2	M+H-H2O	2	Fatty acyls	Fatty amides
N/A	297,2665	13,22	298,2743	Hexadecenoyl-ethanolamine NAE 16:1	C18H35NO2	M+H	4	Fatty acyls	Fatty amides
N/A	103,0634	0,69	102,0556	Amino-butanoic acid FA 4:0-NH2	C4H9NO2	M-H	3	Fatty acyls	Amino fatty acids
N/A	299,2821	15,76	300,2899	Amino-octadecanoic acid FA 18:0-NH2	C18H37NO2	M+H	2	Fatty acyls	Amino fatty acids
N/A	323,2811	22,22	324,2889	Anandamide (18:2, n-6)	C20H37NO2	M+H	3	Fatty acyls	N-acyl ethanolamines (endocannabinoids)
N/A	332,2715	30,18	331,2637	Docosatetraenoic acid	C22H36O2	M-H	2	Fatty acyls	Other Docosanoids
N/A	623,2884	23,52	624,2962	S-(PGA2)-glutathione	C30H47N3O10S	M+H-H2O	3	Fatty acyls	Other Octadecanoids
N/A	641,2985	22,55	640,2907	S-(PGA2)-glutathione	C30H47N3O10S	M-H	4	Fatty acyls	Other Octadecanoids

CODE	Mass	RT	m/z	PUTATIVE ID	Formula	Adduct	CL	Cathegory	(Sub)Class
N/A	580,3469	19,06	579,3391	Trehalose-hexadecanoic acid	C28H54O13	M-H-H2O	4	Fatty acyls	Other
N/A	284,235	9,09	285,2428	MG(14:0)	C17H34O4	M+H-H2O	2	Glycerolipids	Monoacylglycerols
N/A	340,294	10,25	341,3018	MG(18:0)	C21H42O4	M+H-H2O	2	Glycerolipids	Monoacylglycerols
LP022	338,282	10,05	339,2898	MG(18:1)	C21H40O4	M+H-H2O	2	Glycerolipids	Monoacylglycerols
LP023	336,266	10,26	337,2738	MG(18:2)	C21H38O4	M+H-H2O	2	Glycerolipids	Monoacylglycerols
N/A	401,3491	19,65	402,3569	MG(20:1)	C23H44O4	M+NH4	3	Glycerolipids	Monoacylglycerols
N/A	399,3343	19,7	400,3421	MG(20:2)	C23H42O4	M+NH4	3	Glycerolipids	Monoacylglycerols
N/A	316,2971	20,89	317,3049	MG(O-16:0)	C19H40O3	M+H	3	Glycerolipids	Monoalkylglycerols
LP024	550,496	10,03	551,5038	DG(32:0)	C35H68O5	M+H-H2O	2	Glycerolipids	Diacylglycerols
N/A	568,507	9,85	569,5148	DG(32:0)	C35H68O5	M+H	3	Glycerolipids	Diacylglycerols
N/A	585,533	10,05	586,5408	DG(32:0)	C35H68O5	M+NH4	2	Glycerolipids	Diacylglycerols
LP025	548,484	14,91	549,4918	DG(32:1)	C35H66O5	M+H-H2O	2	Glycerolipids	Diacylglycerols
N/A	581,502	8,21	582,5098	DG(32:2)	C35H64O5	M+NH4	3	Glycerolipids	Diacylglycerols
N/A	564,549	18,47	565,5568	DG(34:0)	C37H74O4	M+H-H2O	3	Glycerolipids	Diacylglycerols
LP026	596,539	10,78	597,5468	DG(34:0)	C37H72O5	M+H	2	Glycerolipids	Diacylglycerols
N/A	618,523	9,47	619,5308	DG(34:0)	C37H72O5	M+Na	4	Glycerolipids	Diacylglycerols
LP027	594,523	10,04	595,5308	DG(34:1)	C37H70O5	M+H	2	Glycerolipids	Diacylglycerols
N/A	592,507	9,26	593,5148	DG(34:2)	C37H68O5	M+H	2	Glycerolipids	Diacylglycerols
N/A	586,458	8,21	587,4658	DG(34:5)	C37H62O5	M+H	2	Glycerolipids	Diacylglycerols
N/A	590,5234	34,09	589,5156	DG(35:1)	C38H72O5	M-H-H2O	3	Glycerolipids	Diacylglycerols
LP028	623,55	10,03	624,5578	DG(35:2)	C38H70O5	M+NH4	3	Glycerolipids	Diacylglycerols
N/A	624,57	11,61	625,5778	DG(36:0)	C39H76O5	M+H	2	Glycerolipids	Diacylglycerols
N/A	695,611	10,75	642,6028	DG(36:0)	C39H76O5	M+NH4	2	Glycerolipids	Diacylglycerols
LP029	622,555	10,95	623,5628	DG(36:1)	C39H74O5	M+H	2	Glycerolipids	Diacylglycerols
N/A	639,579	10,05	640,5868	DG(36:1)	C39H74O5	M+NH4	2	Glycerolipids	Diacylglycerols

CODE	Mass	RT	m/z	PUTATIVE ID	Formula	Adduct	CL	Cathegory	(Sub)Class
LP031	620,539	10,23	621,5468	DG(36:2)	C39H72O5	M+H	2	Glycerolipids	Diacylglycerols
N/A	659,54	9,27	638,5728	DG(36:2)	C39H72O5	M+NH4	2	Glycerolipids	Diacylglycerols
N/A	618,523	13,01	619,5308	DG(36:3)	C39H70O5	M+H	4	Glycerolipids	Diacylglycerols
N/A	635,55	8,47	636,5578	DG(36:3)	C39H70O5	M+NH4	2	Glycerolipids	Diacylglycerols
N/A	628,512	9,78	629,5198	DG(37:5)	C40H68O5	M+H	3	Glycerolipids	Diacylglycerols
N/A	669,623	11,6	670,6308	DG(38:0)	C41H80O5	M+NH4	2	Glycerolipids	Diacylglycerols
N/A	667,584	11,12	668,5918	DG(38:1)	C41H78O5	M+NH4	2	Glycerolipids	Diacylglycerols
LP033	663,569	9,65	664,5768	DG(38:3)	C41H74O5	M+NH4	2	Glycerolipids	Diacylglycerols
N/A	661,563	10,1	662,5708	DG(38:4)	C41H72O5	M+NH4	2	Glycerolipids	Diacylglycerols
N/A	674,584	12,36	675,5918	DG(40:3)	C43H78O5	M+H	3	Glycerolipids	Diacylglycerols
LP034	666,524	10,1	667,5318	DG(40:7)	C43H70O5	M+H	3	Glycerolipids	Diacylglycerols
LP036	674,5337	37,05	675,5415	DG(42:8)	C45H72O5	M+H-H2O	3	Glycerolipids	Diacylglycerols
N/A	710,625	12,25	711,6328	DG(44:4)	C47H84O5	M+H-H2O	3	Glycerolipids	Diacylglycerols
N/A	522,466	14,15	523,4738	DG(i-30:0)	C33H64O5	M+H-H2O	3	Glycerolipids	Diacylglycerols
N/A	1076,6098	17,51	1077,6176	CDP-DG(40:3)	C52H91N3O15P2	M+NH4	4	Glycerolipids	CDP-diacylglycerols
LP111	815,702	13,13	816,7098	TG (48:4)	C51H90O6	M+NH4	2	Glycerolipids	Triacylglycerols
N/A	641,56	9,77	642,5678	TG(35:0)	C38H72O6	M+NH4	3	Glycerolipids	Triacylglycerols
LP093	655,576	11,37	656,5838	TG(36:0)	C39H74O6	M+NH4	2	Glycerolipids	Triacylglycerols
LP094	653,561	10,69	654,5688	TG(36:1)	C39H72O6	M+NH4	2	Glycerolipids	Triacylglycerols
N/A	651,547	9,95	652,5548	TG(36:2)	C39H70O6	M+NH4	2	Glycerolipids	Triacylglycerols
LP095	649,534	9,25	650,5418	TG(36:3)	C39H68O6	M+NH4	2	Glycerolipids	Triacylglycerols
LP096	683,607	12,12	684,6148	TG(38:0)	C41H78O6	M+NH4	2	Glycerolipids	Triacylglycerols
LP097	681,592	11,54	682,5998	TG(38:1)	C41H76O6	M+NH4	2	Glycerolipids	Triacylglycerols
LP098	679,576	10,84	680,5838	TG(38:2)	C41H74O6	M+NH4	2	Glycerolipids	Triacylglycerols
N/A	677,56	10,18	678,5678	TG(38:3)	C41H72O6	M+NH4	2	Glycerolipids	Triacylglycerols

CODE	Mass	RT	m/z	PUTATIVE ID	Formula	Adduct	CL	Cathegory	(Sub)Class
LP099	675,544	9,42	676,5518	TG(38:4)	C41H70O6	M+NH4	2	Glycerolipids	Triacylglycerols
LP100	709,623	12,24	710,6308	TG(40:1)	C43H80O6	M+NH4	2	Glycerolipids	Triacylglycerols
LP101	707,607	10,86	708,6148	TG(40:2)	C43H78O6	M+NH4	2	Glycerolipids	Triacylglycerols
LP102	705,592	11	706,5998	TG(40:3)	C43H76O6	M+NH4	2	Glycerolipids	Triacylglycerols
N/A	703,575	10,31	704,5828	TG(40:4)	C43H74O6	M+NH4	2	Glycerolipids	Triacylglycerols
N/A	723,636	11,53	724,6438	TG(41:1)	C44H82O6	M+NH4	3	Glycerolipids	Triacylglycerols
LP103	737,654	12,87	738,6618	TG(42:1)	C45H84O6	M+NH4	2	Glycerolipids	Triacylglycerols
LP105	740,595	12,35	741,6028	TG(42:2)	C43H79O6	M+Na	2	Glycerolipids	Triacylglycerols
LP104	733,622	11,75	734,6298	TG(42:3)	C45H80O6	M+NH4	2	Glycerolipids	Triacylglycerols
LP106	731,547	7,72	732,5548	TG(42:4)	C45H78O6	M+NH4	2	Glycerolipids	Triacylglycerols
LP107	753,686	12,78	754,6938	TG(43:0)	C46H88O6	M+NH4	2	Glycerolipids	Triacylglycerols
N/A	751,671	13,17	752,6788	TG(43:1)	C46H86O6	M+NH4	2	Glycerolipids	Triacylglycerols
N/A	747,635	11	748,6428	TG(43:3)	C46H82O6	M+NH4	2	Glycerolipids	Triacylglycerols
N/A	745,621	11,75	746,6288	TG(43:4)	C46H80O6	M+NH4	2	Glycerolipids	Triacylglycerols
N/A	767,703	13,97	768,7108	TG(44:0)	C47H90O6	M+NH4	2	Glycerolipids	Triacylglycerols
N/A	765,687	13,47	766,6948	TG(44:1)	C47H88O6	M+NH4	2	Glycerolipids	Triacylglycerols
N/A	779,706	13,76	780,7138	TG(45:1)	C48H90O6	M+NH4	2	Glycerolipids	Triacylglycerols
N/A	777,687	13,25	778,6948	TG(45:2)	C48H88O6	M+NH4	2	Glycerolipids	Triacylglycerols
N/A	775,671	12,74	776,6788	TG(45:3)	C48H86O6	M+NH4	2	Glycerolipids	Triacylglycerols
N/A	773,664	13,05	774,6718	TG(45:4)	C48H84O6	M+NH4	2	Glycerolipids	Triacylglycerols
N/A	795,737	14,67	796,7448	TG(46:0)	C49H94O6	M+NH4	2	Glycerolipids	Triacylglycerols
N/A	793,723	14,08	794,7308	TG(46:1)	C49H92O6	M+NH4	2	Glycerolipids	Triacylglycerols
N/A	791,705	13,54	792,7128	TG(46:2)	C49H90O6	M+NH4	2	Glycerolipids	Triacylglycerols
N/A	789,687	13,05	790,6948	TG(46:3)	C49H88O6	M+NH4	2	Glycerolipids	Triacylglycerols
N/A	787,669	12,52	788,6768	TG(46:4)	C49H86O6	M+NH4	2	Glycerolipids	Triacylglycerols
LP108	809,75	15,05	810,7578	TG(47:0)	C50H96O6	M+NH4	2	Glycerolipids	Triacylglycerols

CODE	Mass	RT	m/z	PUTATIVE ID	Formula	Adduct	CL	Cathegory	(Sub)Class
LP109	807,737	13,44	808,7448	TG(47:1)	C50H94O6	M+NH4	2	Glycerolipids	Triacylglycerols
N/A	805,723	13,86	806,7308	TG(47:2)	C50H92O6	M+NH4	2	Glycerolipids	Triacylglycerols
LP110	803,701	13,35	804,7088	TG(47:3)	C50H90O6	M+NH4	2	Glycerolipids	Triacylglycerols
N/A	823,772	15,49	824,7798	TG(48:0)	C51H98O6	M+NH4	2	Glycerolipids	Triacylglycerols
N/A	821,753	14,8	822,7608	TG(48:1)	C51H96O6	M+NH4	2	Glycerolipids	Triacylglycerols
N/A	813,686	12,68	814,6938	TG(48:5)	C51H88O6	M+NH4	2	Glycerolipids	Triacylglycerols
N/A	837,779	16,02	838,7868	TG(49:0)	C57H100O6	M+NH4	2	Glycerolipids	Triacylglycerols
N/A	831,733	13,97	832,7408	TG(49:3)	C52H94O6	M+NH4	2	Glycerolipids	Triacylglycerols
LP112	829,718	13,44	830,7258	TG(49:4)	C52H92O6	M+NH4	2	Glycerolipids	Triacylglycerols
N/A	867,735	13,33	868,7428	TG(52:6)	C55H94O6	M+NH4	3	Glycerolipids	Triacylglycerols
N/A	885,784	14,79	886,7918	TG(53:4)	C56H100O6	M+NH4	*	Glycerolipids	Triacylglycerols
N/A	905,838	25,74	906,8458	TG(54:1)	C57H108O6	M+NH4	2	Glycerolipids	Triacylglycerols
N/A	903,824	25,41	904,8318	TG(54:2)	C57H106O6	M+NH4	2	Glycerolipids	Triacylglycerols
N/A	901,814	25,09	902,8218	TG(54:3)	C57H104O6	M+NH4	2	Glycerolipids	Triacylglycerols
N/A	915,83	16,44	916,8378	TG(55:3)	C58H106O6	M+NH4	2	Glycerolipids	Triacylglycerols
N/A	909,773	13,32	910,7808	TG(55:6)	C58H100O6	M+NH4	2	Glycerolipids	Triacylglycerols
N/A	923,798	14,74	924,8058	TG(56:6)	C59H102O6	M+NH4	3	Glycerolipids	Triacylglycerols
N/A	919,769	13,92	920,7768	TG(56:8)	C59H98O6	M+NH4	3	Glycerolipids	Triacylglycerols
N/A	917,767	13,41	918,7748	TG(56:9)	C59H96O6	M+NH4	3	Glycerolipids	Triacylglycerols
N/A	964,845	19,58	965,8528	TG(58:2)	C61H114O6	M+Na	3	Glycerolipids	Triacylglycerols
N/A	955,859	17,11	956,8668	TG(58:4)	C61H110O6	M+NH4	4	Glycerolipids	Triacylglycerols
N/A	922,74	25,1	923,7478	TG(59:10)	C62H100O6	M+H-H2O	3	Glycerolipids	Triacylglycerols
N/A	987,92	21,17	988,9278	TG(60:2)	C63H118O6	M+NH4	3	Glycerolipids	Triacylglycerols
N/A	985,904	19,88	986,9118	TG(60:3)	C63H116O6	M+NH4	3	Glycerolipids	Triacylglycerols
N/A	435,2753	18,87	436,2831	LPC(13:0)	C21H44NO7P	M+H-H2O	3	Glycerophospholipids	Monoacylglycerophosphocholines
LP044	495,333	1,59	496,3408	LPC(16:0)	C24H50NO7P	M+H	2	Glycerophospholipids	Monoacylglycerophosphocholines

CODE	Mass	RT	m/z	PUTATIVE ID	Formula	Adduct	CL	Cathegory	(Sub)Class
N/A	591,3513	19,92	530,3009	LPC(16:0)	C24H50NO7P	M+Cl	3	Glycerophospholipids	Monoacylglycerophosphocholines
LP045	493,3162	16,17	494,324	LPC(16:1)	C24H48NO7P	M+H	3	Glycerophospholipids	Monoacylglycerophosphocholines
N/A	555,3529	20,66	554,3451	LPC(17:0)	C25H52NO7P	M+FA-H	3	Glycerophospholipids	Monoacylglycerophosphocholines
N/A	589,3384	17,57	504,3082	LPC(17:2)	C25H48NO7P	M-H	3	Glycerophospholipids	Monoacylglycerophosphocholines
LN046	569,3689	23,36	568,3611	LPC(18:0)	C26H54NO7P	M+FA-H	2	Glycerophospholipids	Monoacylglycerophosphocholines
N/A	521,348	1,66	522,3558	LPC(18:1)	C26H52NO7P	M+H	3	Glycerophospholipids	Monoacylglycerophosphocholines
LN047	567,3518	1,52	566,344	LPC(18:1)	C26H52NO7P	M+FA-H	2	Glycerophospholipids	Monoacylglycerophosphocholines
LP049	519,3321	17,51	520,3399	LPC(18:2)	C26H50NO7P	M+H	3	Glycerophospholipids	Monoacylglycerophosphocholines
LN048	565,336	1,3	564,3282	LPC(18:2)	C26H50NO7P	M+FA-H	2	Glycerophospholipids	Monoacylglycerophosphocholines
N/A	563,3183	15,19	562,3105	LPC(18:3)	C26H48NO7P	M+FA-H	2	Glycerophospholipids	Monoacylglycerophosphocholines
N/A	555,3527	20,41	590,3435	LPC(20:3)	C28H52NO7P	M+FA-H	3	Glycerophospholipids	Monoacylglycerophosphocholines
N/A	543,3313	15,54	544,3391	LPC(20:4)	C28H50NO7P	M+H	3	Glycerophospholipids	Monoacylglycerophosphocholines
LP050	565,3162	16,09	566,324	LPC(20:4)	C28H50NO7P	M+Na	2	Glycerophospholipids	Monoacylglycerophosphocholines
N/A	589,3377	23,2	588,3299	LPC(20:4)	C28H50NO7P	M+FA-H	3	Glycerophospholipids	Monoacylglycerophosphocholines
N/A	615,3725	21,97	614,3647	LPC(21:0)	C29H58NO8P	M+Cl	3	Glycerophospholipids	Monoacylglycerophosphocholines
LN057	613,3891	23,37	612,3813	LPC(22:1)	C30H60NO7P	M+Cl	4	Glycerophospholipids	Monoacylglycerophosphocholines
LN053	617,367	19,85	616,3592	LPC(22:4)	C30H54NO7P	M+FA-H	2	Glycerophospholipids	Monoacylglycerophosphocholines
N/A	615,3529	17,83	614,3451	LPC(22:5)	C30H52NO7P	M+FA-H	2	Glycerophospholipids	Monoacylglycerophosphocholines
LP054	567,3284	22,56	568,3362	LPC(22:6)	C30H50NO7P	M+H	3	Glycerophospholipids	Monoacylglycerophosphocholines
LN068	453,2843	1,35	452,2765	LPE(16:0)	C21H44NO7P	M-H	2	Glycerophospholipids	Monoacylglycerophosphoethanolamines
LN069	451,268	15,98	450,2602	LPE(16:1)	C21H42NO7P	M-H	3	Glycerophospholipids	Monoacylglycerophosphoethanolamines
LN070	467,3021	20,92	466,2943	LPE(17:0)	C22H46NO7P	M-H	4	Glycerophospholipids	Monoacylglycerophosphoethanolamines
LN076	465,3205	24,34	464,3127	LPE(18:0)	C23H48NO6P	M-H	3	Glycerophospholipids	Monoacylglycerophosphoethanolamines
N/A	481,3161	22,31	480,3083	LPE(18:0)	C23H48NO7P	M-H	3	Glycerophospholipids	Monoacylglycerophosphoethanolamines

CODE	Mass	RT	m/z	PUTATIVE ID	Formula	Adduct	CL	Cathegory	(Sub)Class
N/A	461,2894	18,33	460,2816	LPE(18:1)	C23H46NO7P	M-H-H2O	3	Glycerophospholipids	Monoacylglycerophosphoethanolamines
N/A	539,3215	16,15	478,2923	LPE(18:1)	C23H46NO7P	M-H	3	Glycerophospholipids	Monoacylglycerophosphoethanolamines
N/A	477,2852	17,35	478,293	LPE(18:2)	C23H44NO7P	M+H	3	Glycerophospholipids	Monoacylglycerophosphoethanolamines
N/A	521,274	16,68	520,2662	LPE(18:3)	C23H42NO7P	M+FA-H	3	Glycerophospholipids	Monoacylglycerophosphoethanolamines
N/A	495,3312	21,2	494,3234	LPE(19:0)	C24H50NO7P	M-H	3	Glycerophospholipids	Monoacylglycerophosphoethanolamines
N/A	509,3456	22,55	508,3378	LPE(20:0)	C25H52NO7P	M-H	2	Glycerophospholipids	Monoacylglycerophosphoethanolamines
N/A	555,3529	21,21	554,3451	LPE(20:0)	C25H52NO7P	M+FA-H	3	Glycerophospholipids	Monoacylglycerophosphoethanolamines
LN071	507,3314	23,67	506,3236	LPE(20:1)	C25H50NO7P	M-H	2	Glycerophospholipids	Monoacylglycerophosphoethanolamines
N/A	661,3554	21,11	504,3084	LPE(20:2)	C25H48NO7P	M-H	2	Glycerophospholipids	Monoacylglycerophosphoethanolamines
N/A	501,2858	16,79	500,278	LPE(20:4)	C25H44NO7P	M-H	2	Glycerophospholipids	Monoacylglycerophosphoethanolamines
N/A	583,3471	15,45	582,3393	LPE(21:0)	C26H52NO8P	M+FA-H	3	Glycerophospholipids	Monoacylglycerophosphoethanolamines
LP065	537,3785	25,59	538,3863	LPE(22:0)	C27H56NO7P	M+H	4	Glycerophospholipids	Monoacylglycerophosphoethanolamines
LP074	529,3162	20,34	530,324	LPE(22:4)	C27H48NO7P	M+H	3	Glycerophospholipids	Monoacylglycerophosphoethanolamines
LN075	525,2847	15,38	524,2769	LPE(22:6)	C27H44NO7P	M-H	3	Glycerophospholipids	Monoacylglycerophosphoethanolamines
N/A	428,2184	22,4	427,2106	LPG(12:0)	C18H37O9P	M-H	3	Glycerophospholipids	Monoacylglycerophosphoglycerols
N/A	508,2819	18,76	509,2897	LPG(18:2)	C24H45O9P	M+H	4	Glycerophospholipids	Monoacylglycerophosphoglycerols
N/A	532,2803	20,52	531,2725	LPG(20:4)	C26H45O9P	M-H	4	Glycerophospholipids	Monoacylglycerophosphoglycerols
N/A	556,2807	18,88	557,2885	LPG(22:6)	C28H45O9P	M+H	4	Glycerophospholipids	Monoacylglycerophosphoglycerols
N/A	572,2934	19,84	571,2856	LPI(16:0)	C25H49O12P	M-H	3	Glycerophospholipids	Monoacylglycerophosphoinositols
N/A	600,3266	25,94	599,3188	LPI(18:0)	C27H53O12P	M-H	3	Glycerophospholipids	Monoacylglycerophosphoinositols
N/A	598,3125	21,01	597,3047	LPI(18:1)	C27H51O12P	M+FA-H	3	Glycerophospholipids	Monoacylglycerophosphoinositols
N/A	620,2953	17,11	619,2875	LPI(20:4)	C29H49O12P	M-H	4	Glycerophospholipids	Monoacylglycerophosphoinositols
N/A	525,3055	24,5	524,2977	LPS(18:0)	C24H48NO9P	M-H	3	Glycerophospholipids	Monoacylglycerophosphoserines
N/A	523,2901	20,46	522,2823	LPS(18:1)	C24H46NO9P	M-H	3	Glycerophospholipids	Monoacylglycerophosphoserines
N/A	521,274	18,87	520,2662	LPS(18:2)	C24H44NO9P	M-H	3	Glycerophospholipids	Monoacylglycerophosphoserines

CODE	Mass	RT	m/z	PUTATIVE ID	Formula	Adduct	CL	Cathegory	(Sub)Class
LN085	539,3217	16,16	538,3139	LPS(19:0)	C25H50NO9P	M-H	3	Glycerophospholipids	Monoacylglycerophosphoserines
N/A	266,1552	16,56	530,283	LPS(20:2)	C26H48NO9P	M-H-H2O	3	Glycerophospholipids	Monoacylglycerophosphoserines
N/A	549,3098	23,14	548,302	LPS(20:2)	C26H48NO9P	M-H	3	Glycerophospholipids	Monoacylglycerophosphoserines
LN087	547,288	19,83	546,2802	LPS(20:3)	C26H46NO9P	M-H	3	Glycerophospholipids	Monoacylglycerophosphoserines
LP086	545,2747	17,53	546,2825	LPS(20:4)	C26H44NO9P	M+H	3	Glycerophospholipids	Monoacylglycerophosphoserines
LN088	561,3379	23,37	560,3301	LPS(22:1)	C28H54NO9P	M-H-H2O	3	Glycerophospholipids	Monoacylglycerophosphoserines
N/A	577,343	21,19	578,3508	LPS(22:2)	C28H52NO9P	M+H	4	Glycerophospholipids	Monoacylglycerophosphoserines
N/A	438,2744	24,51	437,2666	LPA(18:0)	C21H43O7P	M-H	2	Glycerophospholipids	Monoacylglycerophosphates
N/A	465,3077	7,29	443,2554	LPA(20:2)	C23H43O7P	M-H-H2O	3	Glycerophospholipids	Monoacylglycerophosphates
N/A	508,2808	20,03	507,273	LPA(20:2)	C23H43O7P	M+FA-H	3	Glycerophospholipids	Monoacylglycerophosphates
N/A	441,2398	10,18	441,2398	LPA(20:3)	C23H41O7P	M-H-H2O	3	Glycerophospholipids	Monoacylglycerophosphates
LP043	481,3525	20,06	482,3603	LPC(O-16:0)	C24H52NO6P	M+H	3	Glycerophospholipids	Monoalkylglycerophosphocholines
N/A	527,3578	20,08	526,35	LPC(O-16:0)	C24H52NO6P	M+FA-H	3	Glycerophospholipids	Monoalkylglycerophosphocholines
LP064	507,3676	20,94	508,3754	LPC(O-18:1)	C26H54NO6P	M+H	3	Glycerophospholipids	Monoalkylglycerophosphocholines
N/A	439,3037	19,84	438,2959	LPE(O-16:0)	C21H46NO6P	M-H	2	Glycerophospholipids	Monoalkylglycerophosphoethanolamines
N/A	525,3776	21,69	526,3854	LPE(O-21:0(OH)	C26H56NO7P	M+H	4	Glycerophospholipids	Monoalkylglycerophosphoethanolamines
N/A	437,2893	1,51	436,2815	LPE(P-16:0)	C21H44NO6P	M-H	2	Glycerophospholipids	1Z-alkenylglycerophosphoethanolamines
LN083	658,3726	16,7	657,3648	LPI(P-20:0)	C29H57O11P	M+FA-H	3	Glycerophospholipids	1Z-alkenylglycerophosphoinositols
LP084	511,3265	9,31	512,3343	LPS(O-18:0)	C24H50NO8P	M+H	3	Glycerophospholipids	Monoalkylglycerophosphoserines
N/A	557,3313	9,32	556,3235	LPS(O-18:0)	C24H38O5	M+Cl	3	Glycerophospholipids	Monoalkylglycerophosphoserines
N/A	643,4057	22,55	642,3979	LPS(2-OMe-22:0)	C29H60NO9P	M+FA-H	3	Glycerophospholipids	Monoalkylglycerophosphoserines
N/A	633,3995	26,92	634,4073	LPS(2-OMe-23:0)	C30H62NO9P	M+Na	4	Glycerophospholipids	Monoalkylglycerophosphoserines
N/A	741,5312	37,04	742,539	PC(33:3)	C41H76NO8P	M+H	3	Glycerophospholipids	Diacylglycerophosphocholines

CODE	Mass	RT	m/z	PUTATIVE ID	Formula	Adduct	CL	Cathegory	(Sub)Class
N/A	537,3393	17,83	538,3471	PC(18:0)	C26H52NO8P	M+H	3	Glycerophospholipids	Diacylglycerophosphocholines
N/A	555,3877	24,53	554,3799	PC(18:0)	C26H56NO6P	M+FA-H	3	Glycerophospholipids	Diacylglycerophosphocholines
N/A	583,3471	16,14	582,3393	PC(18:0)	C26H52NO8P	M+FA-H	3	Glycerophospholipids	Diacylglycerophosphocholines
LN055	581,3315	18,95	580,3237	PC(18:1)	C26H50NO8P	M+FA-H	3	Glycerophospholipids	Diacylglycerophosphocholines
N/A	597,3626	25,71	596,3548	PC(19:0)	C27H54NO8P	M+FA-H	3	Glycerophospholipids	Diacylglycerophosphocholines
N/A	595,3486	24,24	594,3408	PC(19:1)	C27H52NO8P	M+FA-H	3	Glycerophospholipids	Diacylglycerophosphocholines
N/A	565,3732	22,07	566,381	PC(20:0)	C28H56NO8P	M+H	4	Glycerophospholipids	Diacylglycerophosphocholines
N/A	583,342	21,11	582,3342	PC(20:2)	C28H54NO7P	M+Cl	4	Glycerophospholipids	Diacylglycerophosphocholines
N/A	593,4014	26,57	594,4092	PC(22:0)	C30H60NO8P	M+H	3	Glycerophospholipids	Diacylglycerophosphocholines
N/A	591,3877	22,82	592,3955	PC(22:1)	C30H58NO8P	M+H	3	Glycerophospholipids	Diacylglycerophosphocholines
LN059	635,3781	24,72	634,3703	PC(22:2)	C30H56NO8P	M+FA-H	3	Glycerophospholipids	Diacylglycerophosphocholines
N/A	779,567	8,57	778,5592	PC(32:0)	C40H80NO8P	M+FA-H	2	Glycerophospholipids	Diacylglycerophosphocholines
N/A	777,5487	7,42	776,5409	PC(32:1)	C40H78NO8P	M+FA-H	2	Glycerophospholipids	Diacylglycerophosphocholines
LN061	805,58	8,77	804,5722	PC(34:1)	C42H82NO8P	M+FA-H	2	Glycerophospholipids	Diacylglycerophosphocholines
LN060	803,565	7,85	802,5572	PC(34:2)	C42H80NO8P	M+FA-H	2	Glycerophospholipids	Diacylglycerophosphocholines
LN061	801,5494	6,81	800,5416	PC(34:3)	C42H78NO8P	M+FA-H	2	Glycerophospholipids	Diacylglycerophosphocholines
N/A	833,6121	9,81	832,6043	PC(36:1)	C44H86NO8P	M+FA-H	3	Glycerophospholipids	Diacylglycerophosphocholines
N/A	829,5805	7,93	828,5727	PC(36:3)	C44H82NO8P	M+FA-H	3	Glycerophospholipids	Diacylglycerophosphocholines
LN091	827,5643	37,09	826,5565	PC(36:4)	C44H80NO8P	M+FA-H	3	Glycerophospholipids	Diacylglycerophosphocholines
LP062	809,594	9,27	810,6018	PC(38:4)	C46H84NO8P	M+H	*	Glycerophospholipids	Diacylglycerophosphocholines
N/A	853,581	7,87	852,5732	PC(38:5)	C46H82NO8P	M+FA-H	3	Glycerophospholipids	Diacylglycerophosphocholines
N/A	851,563	7,29	850,5552	PC(38:6)	C46H80NO8P	M+FA-H	3	Glycerophospholipids	Diacylglycerophosphocholines
N/A	879,593	8,53	878,5852	PC(40:6)	C48H84NO8P	M+FA-H	3	Glycerophospholipids	Diacylglycerophosphocholines
N/A	877,5837	37,08	876,5759	PC(40:7)	C48H82NO8P	M+FA-H	3	Glycerophospholipids	Diacylglycerophosphocholines

CODE	Mass	RT	m/z	PUTATIVE ID	Formula	Adduct	CL	Cathegory	(Sub)Class
N/A	859,6066	35,41	860,6144	PC(42:7)	C50H86NO8P	M+H		Glycerophospholipids	Diacylglycerophosphocholines
N/A	655,4015	23,78	654,3937	PE(27:1)	C32H62NO8P	M+Cl	4	Glycerophospholipids	Diacylglycerophosphoethanolamines
N/A	689,498	7,38	688,4902	PE(32:1)	C37H72NO8P	M-H	3	Glycerophospholipids	Diacylglycerophosphoethanolamines
N/A	703,546	10,84	704,5538	PE(34:0)	C39H78NO7P	M+H	3	Glycerophospholipids	Diacylglycerophosphoethanolamines
LN077	701,533	9,25	700,5252	PE(34:1)	C39H76NO7P	M-H	2	Glycerophospholipids	Diacylglycerophosphoethanolamines
LN080	717,5287	8,54	716,5209	PE(34:1)	C39H76NO8P	M-H	2	Glycerophospholipids	Diacylglycerophosphoethanolamines
LN078	699,518	8,38	698,5102	PE(34:2)	C39H74NO8P	M-H	2	Glycerophospholipids	Diacylglycerophosphoethanolamines
LN081	715,5132	7,61	714,5054	PE(34:2)	C39H74NO8P	M-H	2	Glycerophospholipids	Diacylglycerophosphoethanolamines
N/A	713,4976	6,66	712,4898	PE(34:3)	C39H72NO8P	M-H	2	Glycerophospholipids	Diacylglycerophosphoethanolamines
N/A	745,5598	9,63	744,552	PE(36:1)	C41H80NO8P	M-H	2	Glycerophospholipids	Diacylglycerophosphoethanolamines
N/A	741,529	7,93	740,5212	PE(36:3)	C41H76NO8P	M-H	2	Glycerophospholipids	Diacylglycerophosphoethanolamines
LN079	739,5125	6,93	738,5047	PE(36:4)	C41H74NO8P	M-H	2	Glycerophospholipids	Diacylglycerophosphoethanolamines
N/A	737,5034	32,33	736,4956	PE(36:5)	C41H72NO8P	M-H	2	Glycerophospholipids	Diacylglycerophosphoethanolamines
N/A	765,529	7,77	764,5212	PE(38:5)	C43H76NO8P	M-H	2	Glycerophospholipids	Diacylglycerophosphoethanolamines
N/A	763,513	7,17	762,5052	PE(38:6)	C45H76NO8P	M-H	2	Glycerophospholipids	Diacylglycerophosphoethanolamines
N/A	761,4973	6,11	760,4895	PE(38:7)	C43H74NO9P	M-H	2	Glycerophospholipids	Diacylglycerophosphoethanolamines
N/A	787,61	10,22	788,6178	PE(39:1)	C44H86NO8P	M+H	2	Glycerophospholipids	Diacylglycerophosphoethanolamines
N/A	783,578	8,11	784,5858	PE(39:3)	C44H82NO8P	M+H	2	Glycerophospholipids	Diacylglycerophosphoethanolamines
N/A	791,546	8,37	790,5382	PE(40:6)	C45H78NO8P	M-H	3	Glycerophospholipids	Diacylglycerophosphoethanolamines
N/A	789,53	7,39	788,5222	PE(40:7)	C45H76NO8P	M-H	3	Glycerophospholipids	Diacylglycerophosphoethanolamines
N/A	510,2948	22,76	509,287	PG(18:1)	C24H47O9P	M-H	4	Glycerophospholipids	Diacylglycerophosphoglycerols
N/A	750,5467	36,97	751,5545	PG(34:0)	C40H79O10P	M+H	4	Glycerophospholipids	Diacylglycerophosphoglycerols
N/A	774,5384	6,12	773,5306	PG(36:2)	C42H79O10P	M-H	3	Glycerophospholipids	Diacylglycerophosphoglycerols
N/A	872,692	24,09	873,6998	PG(44:0)	C57H94O7	M+H-H2O	4	Glycerophospholipids	Diacylglycerophosphoglycerols
N/A	862,5558	6,22	861,548	PI(36:2)	C45H83O13P	M-H	3	Glycerophospholipids	Diacylglycerophosphoinositols

CODE	Mass	RT	m/z	PUTATIVE ID	Formula	Adduct	CL	Cathegory	(Sub)Class
LN082	860,5381	35,72	859,5303	PI(36:3)	C45H81O13P	M-H	3	Glycerophospholipids	Diacylglycerophosphoinositols
N/A	948,6111	19,03	947,6033	PI(44:6)	C53H91O13P	M-H-H2O	4	Glycerophospholipids	Diacylglycerophosphoinositols
N/A	633,3978	23,26	634,4056	PS(16:0)	C32H62NO10P	M+H-H2O	4	Glycerophospholipids	Diacylglycerophosphoserines
LN089	637,3921	21,11	636,3843	PS(25:0)	C31H60NO10P	M-H	3	Glycerophospholipids	Diacylglycerophosphoserines
N/A	683,3963	22,53	682,3885	PS(25:0)	C31H60NO10P	M+FA-H	4	Glycerophospholipids	Diacylglycerophosphoserines
N/A	645,3991	26,71	644,3913	PS(27:1)	C33H62NO10P	M-H-H2O	2	Glycerophospholipids	Diacylglycerophosphoserines
LN090	661,4302	23,43	662,438	PS(28:0)	C34H66NO10P	M+H-H2O	3	Glycerophospholipids	Diacylglycerophosphoserines
N/A	675,406	26,77	674,3982	PS(28:2)	C34H62NO10P	M-H	3	Glycerophospholipids	Diacylglycerophosphoserines
N/A	687,4456	24,05	688,4534	PS(30:1)	C36H68NO10P	M+H-H2O	3	Glycerophospholipids	Diacylglycerophosphoserines
N/A	701,4625	25,94	700,4547	PS(31:1)	C37H70NO10P	M-H-H2O	3	Glycerophospholipids	Diacylglycerophosphoserines
N/A	775,4634	24,97	774,4556	PS(32:3)	C38H68NO10P	M+FA-H	3	Glycerophospholipids	Diacylglycerophosphoserines
N/A	835,5523	35,25	834,5445	PS(36:1)	C42H80NO10P	M+FA-H	4	Glycerophospholipids	Diacylglycerophosphoserines
N/A	757,4314	25,33	756,4236	PS(36:8)	C42H66NO10P	M-H-H2O	4	Glycerophospholipids	Diacylglycerophosphoserines
N/A	873,5685	8,54	872,5607	PS(39:3)	C45H82NO10P	M+FA-H	3	Glycerophospholipids	Diacylglycerophosphoserines
N/A	871,553	7,84	870,5452	PS(39:4)	C45H80NO10P	M+FA-H	3	Glycerophospholipids	Diacylglycerophosphoserines
N/A	875,4884	7,47	874,4806	PS(40:9)	C46H72NO10P	M+FA-H	3	Glycerophospholipids	Diacylglycerophosphoserines
LN092	901,599	9,81	900,5912	PS(41:3)	C47H86NO10P	M+FA-H	2	Glycerophospholipids	Diacylglycerophosphoserines
N/A	899,5938	22,99	898,586	PS(41:4)	C47H84NO10P	M+FA-H	2	Glycerophospholipids	Diacylglycerophosphoserines
N/A	851,5669	37,21	850,5591	PS(41:5)	C47H82NO10P	M-H	3	Glycerophospholipids	Diacylglycerophosphoserines
N/A	897,5682	7,94	896,5604	PS(41:5)	C47H82NO10P	M+FA-H	2	Glycerophospholipids	Diacylglycerophosphoserines
N/A	923,5825	8,67	922,5747	PS(43:6)	C49H84NO10P	M+FA-H	4	Glycerophospholipids	Diacylglycerophosphoserines
N/A	553,3713	20,92	554,3791	PA(24:0)	C27H53O8P	M+NH4	4	Glycerophospholipids	Diacylglycerophosphates
N/A	608,3789	23,4	607,3711	PA(31:4)	C34H59O8P	M-H-H2O	3	Glycerophospholipids	Diacylglycerophosphates
N/A	648,478	10,6	649,4858	PA(32:0)	C35H69O8P	M+H	4	Glycerophospholipids	Diacylglycerophosphates

CODE	Mass	RT	m/z	PUTATIVE ID	Formula	Adduct	CL	Cathegory	(Sub)Class
N/A	684,3973	32,88	683,3895	PA(32:5)	C35H59O8P	M+FA-H	3	Glycerophospholipids	Diacylglycerophosphates
N/A	658,494	10,24	659,5018	PA(34:0)	C37H73O8P	M+H-H2O	3	Glycerophospholipids	Diacylglycerophosphates
LP038	676,505	11,37	677,5128	PA(34:0)	C37H73O8P	M+H	2	Glycerophospholipids	Diacylglycerophosphates
N/A	674,488	10,68	675,4958	PA(34:1)	C37H71O8P	M+H	2	Glycerophospholipids	Diacylglycerophosphates
N/A	672,476	9,94	673,4838	PA(34:2)	C37H69O8P	M+H	2	Glycerophospholipids	Diacylglycerophosphates
LP039	702,522	11,5	703,5298	PA(36:1)	C39H75O8P	M+H	2	Glycerophospholipids	Diacylglycerophosphates
LP037	700,506	10,86	701,5138	PA(36:2)	C39H73O8P	M+H	2	Glycerophospholipids	Diacylglycerophosphates
N/A	730,555	12,24	731,5628	PA(38:1)	C41H79O8P	M+H	2	Glycerophospholipids	Diacylglycerophosphates
LP040	728,538	11,65	729,5458	PA(38:2)	C41H77O8P	M+H	2	Glycerophospholipids	Diacylglycerophosphates
LP041	726,525	11	727,5328	PA(38:3)	C41H75O8P	M+H	2	Glycerophospholipids	Diacylglycerophosphates
LP042	724,507	10,32	725,5148	PA(38:4)	C41H73O8P	M+H	2	Glycerophospholipids	Diacylglycerophosphates
N/A	763,6045	36,23	764,6123	PA(39:0)	C42H83O8P	M+NH4	3	Glycerophospholipids	Diacylglycerophosphates
N/A	757,563	7,86	758,5708	PA(39:3)	C42H77O8P	M+NH4	3	Glycerophospholipids	Diacylglycerophosphates
N/A	758,586	12,87	759,5938	PA(40:1)	C43H83O8P	M+H	4	Glycerophospholipids	Diacylglycerophosphates
LP066	756,571	12,35	757,5788	PC(P-34:3)	C42H78NO7P	M+NH4	2	Glycerophospholipids	1-(1Z-alkenyl),2-acylglycerophosphocholines
LP067	754,558	11,76	755,5658	PC(P-34:4)	C42H76NO7P	M+NH4	2	Glycerophospholipids	1-(1Z-alkenyl),2-acylglycerophosphocholines
N/A	773,535	7,99	772,5272	PE(P-40:7)	C45H76NO7P	M-H	4	Glycerophospholipids	1-(1Z-alkenyl),2-acylglycerophosphoethanolamines
N/A	918,5221	14,6	919,5299	PI(P-34:0)	C43H84O16P2	M+H	4	Glycerophospholipids	1-(1Z-alkenyl),2-acylglycerophosphoinositols
N/A	689,4578	27,81	690,4656	PS(P-30:1)	C36H68NO9P	M+H	3	Glycerophospholipids	1-(1Z-alkenyl),2-acylglycerophosphoserines
N/A	827,6037	36,99	828,6115	PS(P-40:2)	C46H86NO9P	M+H	4	Glycerophospholipids	1-(1Z-alkenyl),2-acylglycerophosphoserines
N/A	509,3845	24,58	510,3923	PC(O-18:0)	C26H56NO6P	M+H	3	Glycerophospholipids	1-alkyl,2-acylglycerophosphocholines
LP073	523,3628	22,51	524,3706	PC(O-18:0)	C26H54NO7P	M+H	3	Glycerophospholipids	1-alkyl,2-acylglycerophosphocholines
N/A	599,3779	23,39	598,3701	PC(O-21:1)	C29H58NO7P	M+Cl	4	Glycerophospholipids	1-alkyl,2-acylglycerophosphocholines
N/A	744,593	12	745,6008	PnC(16:0/18:1)	C42H83NO7P	M+H	4	Glycerophospholipids	Diacylglycerophosphonocholines

CODE	Mass	RT	m/z	PUTATIVE ID	Formula	Adduct	CL	Cathegory	(Sub)Class
N/A	996,6158	17,43	977,5597	PIM1(34:2)	C49H89O18P	M-H-H2O	4	Glycerophospholipid	Diacylglycerophosphoinositol glycans
N/A	565,3382	17,5	995,608	PIM1(35:0)	C50H95O18P	M-H-H2O	4	Glycerophospholipid	Diacylglycerophosphoinositol glycans
N/A	621,3991	21,53	622,4069	PC(23:0(CHO))	C31H60NO9P	M+H	4	Glycerophospholipids	Oxidized glycerophosphocholines
LP063	649,4291	25,52	650,4369	PC(25:0(CHO))	C33H64NO9P	M+H	3	Glycerophospholipids	Oxidized glycerophosphocholines
N/A	685,4136	21,55	684,4058	PC(25:0(CHO))	C33H64NO9P	M+Cl	4	Glycerophospholipids	Oxidized glycerophosphocholines
N/A	812,674	10,98	813,6818	SM(d42:2)	C47H93N2O6P	M+H	4	Sphingolipids	Ceramide phosphocholines (sphingomyelins)
N/A	705,5409	37,02	706,5487	SM(d32:1(OH))	C37H73N2O7P	M+NH4	3	Sphingolipids	Ceramide phosphocholines (sphingomyelins)
N/A	644,49	9,77	645,4978	PE-Cer(d33:2)	C35H69N2O6P	M+H	4	Sphingolipids	Ceramide phosphoethanolamines
N/A	627,551	10,53	628,5588	Cer(d39:2)	C39H75NO3	M+Na	4	Sphingolipids	Ceramides
N/A	693,624	11,34	692,6162	Cer(d42:2)	C42H81NO3	M+FA-H	4	Sphingolipids	Ceramides
N/A	765,642	10,99	766,6498	CerP(d44:2)	C46H90NO6P	M+H-H2O	4	Sphingolipids	Ceramide 1-phosphates
LP114	725,614	11,04	726,6218	N-Glycoloylganglioside GM2	C43H85NO8	M+H-H2O	4	Sphingolipids	Gangliosides
N/A	1089,7495	1,85	1088,7417	Gal-Gal-Glc-Cer(d40:1)	C58H109NO18	M-H-H2O	4	Sphingolipids	Neutral glycosphingolipids
N/A	751,63	11,01	752,6378	GlcCer(d39:1)	C45H87NO8	M+H-H2O	4	Sphingolipids	Neutral glycosphingolipids
N/A	297,2665	19,84	298,2743	Ketosphingosine SPB 18:2;O2	C18H35NO2	M+H	4	Sphingolipids	Sphing-4-enines (Sphingosines)
N/A	661,1733	11,61	350,2091	C16 Sphingosine-phosphate SPBP 16:1;O2	C16H34NO5P	M-H	3	Sphingolipids	Sphingoid base 1-phosphates
N/A	386,2298	13,03	364,2247	C17 Sphingosine-phosphate SPBP 17:1;O2	C17H36NO5P	M-H	3	Sphingolipids	Sphingoid base 1-phosphates
N/A	254,1899	16,06	380,2559	Sphinganine-phosphate SPBP 18:0;O2	C18H40NO5P	M-H	3	Sphingolipids	Sphingoid base 1-phosphates
N/A	297,2664	20,24	298,2742	d18:2 Sphingosine SPB 18:2;O2	C18H35NO2	M+H	2	Sphingolipids	Sphingoid bases
N/A	583,2777	5,28	393,263	Trihydroxy-cholanoic acid ST 23:1;O5	C23H38O5	M-H	3	Sterol lipids	Bile acids and derivatives
N/A	392,2916	11,97	391,2838	Dihydroxy-cholanoic acid ST 24:1;O4	C24H40O4	M-H	3	Sterol lipids	Bile acids and derivatives
N/A	444,2632	7,07	407,2786	Trihydroxy-cholanoic acid ST 24:1;O5	C24H40O5	M-H	2	Sterol lipids	Bile acids and derivatives
N/A	838,5543	8,05	407,2781	Trihydroxy-cholanoic acid ST 24:1;O5	C24H40O5	M-H	3	Sterol lipids	Bile acids and derivatives
N/A	390,2764	8,05	391,2842	Hydroxy-oxo-cholanoic acid ST 24:2;O4	C24H38O4	M+H	3	Sterol lipids	Bile acids and derivatives
N/A	408,2859	8,05	451,2684	Dihydroxy-oxo-cholanoic acid ST 24:2;O5	C24H38O5	M+FA-H	3	Sterol lipids	Bile acids and derivatives

CODE	Mass	RT	m/z	PUTATIVE ID	Formula	Adduct	CL	Cathegory	(Sub)Class
N/A	406,2717	9,47	407,2795	Dihydroxy-oxo-cholanoic acid ST 24:2;O5	C24H38O5	M+H	3	Sterol lipids	Bile acids and derivatives
N/A	442,2476	9,46	441,2398	Oxo-dihydroxy-cholanoic acid ST 24:2;O5	C24H38O5	M+Cl	3	Sterol lipids	Bile acids and derivatives
N/A	469,3757	20,04	470,3835	Cholestanepentol ST 27:0;O5	C27H48O5	M+NH4	4	Sterol lipids	Bile acids and derivatives
N/A	639,247	16,16	638,2392	Hydroxy-estradiol-glutathione	C28H39N3O9S	M+FA-H	4	Sterol lipids	Cholesterol and derivatives
N/A	868,712	12,36	869,7198	22:1-Glc-cholesterol	C55H96O7	M+H	4	Sterol lipids	Cholesterol and derivatives
N/A	472,3176	8,4	498,2943	Taurodeoxycholic acid	C26H45NO6S	M-H	3	Sterol lipids	Sulfates
N/A	516,3225	8,12	517,3303	Taurodeoxycholic acid	C26H45NO6S	M+NH4	3	Sterol lipids	Sulfates
N/A	462,371	6,13	463,3788	Hydroxy-propyl-dihydroxy-norvitamin D3	C29H50O4	M+H	3	Sterol lipids	Vitamin D3 and derivatives
N/A	498,3169	7,54	464,2999	Trihydroxy-cholanoyl-glycine ST 24:1;O5;G	C26H43NO6	M-H	4	Sterol lipids	Glycine conjugates
N/A	268,2187	26,69	269,2265	Anhydroretinol	C20H28	M+H	3	Prenol lipids	Isoprenoids
N/A	155,1668	36,78	156,1746	Dimethyl-octatriene	C10H18	M+NH4	2	Prenol lipids	C10 isoprenoids (monoterpenes)
N/A	172,0129	0,78	171,0051	Glycerol-phosphate	C3H9O6P	M-H	2	Lipids and lipid-like molecules	Glycerophosphates
N/A	218,019	0,95	217,0112	Glycerol -phosphate	C3H9O6P	M+FA-H	2	Lipids and lipid-like molecules	Glycerophosphates
N/A	129,0791	0,6	130,0869	Pipecolic acid	C6H11NO2	M+H	3	Organic acids and derivatives	Amino acids, peptides, and analogues
N/A	147,0527	0,69	146,0449	N-Acetylserine	C5H9NO4	M-H	2	Organic acids and derivatives	Amino acids, peptides, and analogues
N/A	169,0844	0,59	168,0766	Methylhistidine	C7H11N3O2	M-H	2	Organic acids and derivatives	Amino acids, peptides, and analogues
N/A	173,1049	1,14	172,0971	Acetyl-DL-Leucine	C8H15NO3	M-H	2	Organic acids and derivatives	Amino acids, peptides, and analogues
N/A	209,0699	1,01	208,0621	Hydroxyphenylacetylglycine	C10H11NO4	M-H	3	Organic acids and derivatives	Amino acids, peptides, and analogues
N/A	228,1455	0,95	229,1533	Leucylproline	C11H20N2O3	M+H	2	Organic acids and derivatives	Amino acids, peptides, and analogues
N/A	240,1207	0,58	239,1129	N-L-Glutamylhistamine	C10H16N4O3	M-H	2	Organic acids and derivatives	Amino acids, peptides, and analogues
N/A	259,0751	1,04	259,0751	Glutamylmethionine	C10H18N2O5S	M-H-H2O	2	Organic acids and derivatives	Amino acids, peptides, and analogues
N/A	262,1320	0,95	263,1398	Methionyl-Leucine	C11H22N2O3S	M+H	3	Organic acids and derivatives	Amino acids, peptides, and analogues
LN001	192,0265	0,77	191,0187	Citric acid	C6H8O7	M-H	3	Organic acids and derivatives	Carboxylic acids and derivatives
N/A	246,051	0,77	245,0432	Glycerophosphoglycerol	C6H15O8P	M-H	2	Organic acids and derivatives	Organic phosphoric acids and derivatives
LP008	161,1047	0,72	162,1125	Carnitine	C7H15NO3	M+H	2	Organic nitrogen compounds	Quaternary ammonium salts
N/A	150,0525	0,71	149,0447	alpha-L-Arabinose	C5H10O5	M-H	2	Organic oxygen compounds	Carbohydrates and carbohydrate conjugates

CODE	Mass	RT	m/z	PUTATIVE ID	Formula	Adduct	CL	Cathegory	(Sub)Class
N/A	280,0436	15,08	281,0514	(carboxy-trihydroxyoxan-yl)propanedioic acid	C9H12O10	M+H	2	Organic oxygen compounds	Carbohydrates and carbohydrate conjugates
N/A	299,1918	9,19	300,1996	Hexaethylene glycol	C12H26O7	M+NH4	2	Organic oxygen compounds	Organooxygen compounds
N/A	316,2971	20,89	317,3049	Hexadecyl glycerol	C19H40O3	M+H	3	Organic oxygen compounds	Organooxygen compounds
N/A	189,0795	3,48	190,0873	Indole-propionic acid	C11H11NO2	M+H	4	Organoheterocyclic compounds	Indoles and derivatives
N/A	205,0733	1,25	204,0655	Indolelactic acid	C11H11NO3	M-H	2	Organoheterocyclic compounds	Indoles and derivatives
N/A	85,0887	0,95	86,0965	Piperidine	C5H11N	M+H	3	Organoheterocyclic compounds	Piperidines
N/A	179,9852	38,13	178,9774	Methyl-(methylthio)thiophene	C6H8S2	M+Cl	4	Organosulfur compounds	Thioethers
N/A	308,0693	4,82	323,0420	(H-benzodioxole-carbonyloxy)-trihydroxyoxane-carboxylic acid	C14H14O10	M-H-H2O	3	Phenylpropanoids and polyketides	Tannins
N/A	326,1908	37,42	325,1830	Dodecylbenzenesulfonic acid	C18H30O3S	M-H	3	Benzenoids	Benzenesulfonic acids and derivatives
N/A	127,1361	36,81	128,1439	Dimethyl-hexadiene	C8H14	M+NH4	4	Hydrocarbons	Unsaturated hydrocarbons
N/A	141,1514	1,01	142,1592	Isopropyl-hexadiene	C9H16	M+NH4	2	Hydrocarbons	Unsaturated hydrocarbons
N/A	143,0941	0,73	144,1019	Amino-methylene-hexanoic acid	C7H13NO2	M+H	3	unclassified	unclassified
N/A	472,3186	12,81	471,3108	Epoxy-acetoxy-cholest-en-triol	C29H46O6	M-H-H2O	4	unclassified	unclassified
N/A	183,0655	22,54	184,0733	Isopentenyl phosphate	C5H11O4P	M+NH4	4	unclassified	unclassified
N/A	382,1569	0,98	383,1647	N-Acetyl-beta-D-glucosaminyl-D-glucosamine	C14H26N2O10	M+H	3	unclassified	unclassified
N/A	578,3322	16,14	577,3244	NBD-decanoyl-decanoyl-Glycerol	C29H46N4O8	M+FA-H	4	unclassified	unclassified
N/A	266,2607	23,4	267,2685	Octadecadienol	C18H34O	M+H	3	unclassified	unclassified

Lipidic molecules were classified following Lipid Classification System provided by LIPID MAPS, while for small and polar molecules chemical taxonomy provided in HMDB was used.

[Table 1.1.4]: Main metabolite changes associated with obesity, grouped by organ/tissue, and sorted by biochemical relationships. The log2FC (obese/control) of the common significant compounds in more than one of the tissues is shown is a coloured scale: Plasma (P); Kidney (K); Heart (H); Skeletal Muscle (SM); inguinal White Adipose Tissue (Wi); perirenal White Adipose Tissue (Wp) and Brown Adipose Tissue (B). [AA der.= Amino Acids derivative; Acyl-car pre.= Acyl-carnitines precursor; NB der. = Nucleic Base derivative).

CODE	COMPOUND	FAMILY	P	K	H	SM	Wi	Wp	B
MISCELLANEOUS									
G01	Furanose (ribose, fructose?)	Sugar							
G02	Lyxosylamine (hexosamine)	Sugar derivative							
G03	lactic acid	Glycolysis							
G04	Hydroxybutyric acid	Ketone body							
LN001	Citric acid	TCA							
G05	fumaric acid	TCA							
LN002	Malic acid	TCA							
G06	Urea	urea cycle							
G22	adenine	nucleic base							
G23	Uracil	nucleic base							
AMINO ACIDS									
G10	Glycine	amino acid							
G11	Aminomalonic acid	derivative							
G12	serine	amino acid							
G13	Threonine	amino acid							
C01	Serylthreonine	dipeptide							
C02	Leucine	amino acid							
G14	isoleucine	amino acid							
C03	Valine	amino acid							
G15	tyrosine	amino acid							
C04	Cystine	dipeptide							
C05	Methionine	amino acid							
G16	hypotaurine	non-proteinogenic							
C06	Lysine	amino acid							
C07	N-acetyl-lysine	derivative							
C08	N-Methyl-lysine	derivative							
G17	pipecolic acid	derivative							
C09	Pipecolic acid	derivative							
C10	Piperidine	derivative							
C11	Dimethyl-Arginine	derivative							
C12	Homoarginine	non-proteinogenic							
G18	dimethylbenzimidazole	derivative							
C13	hydroxy-methylbutyric acid	derivative							
C14	Methoxytryptamine	derivative							
C15	Acetylcholine	Neurotransmitter							
LP008	Carnitine	AA der./Acyl-car pre.							
C16	Acetylcarnitine	derivative							
C17	Propionyl-carnitine	derivative							
C18	N-Methylalanine	derivative							
C19	hydroxyproline	derivative							
C20	Citrulline	non-proteinogenic							
G19	Tyramine	derivative							
G20	Proline	amino acid							
C21	Proline	amino acid							
C22	Betaine	derivative							
G21	threonic acid	derivative							
C23	Ornithine	non-proteinogenic							

CODE	COMPOUND	FAMILY	P	K	H	SM	Wi	Wp	B
C24	S-Adenosyl-homocysteine (SAM)	AA der./ NB der.							
		LIPIDS							
LN009	C(16:0); Palmitic acid	Fatty acid							
LN010	C(16:1)	Fatty acid							
LN011	Hydroxy palmitic acid	Fatty acid							
LN012	C(18:0); Stearic acid	Fatty acid							
G24	Methyl stearate	Fatty acid							
LN014	C(18:1); oleic acid	Fatty acid							
LN015	C(18:2)	Fatty acid							
LP016	oxo-nonadecanoic acid	Fatty acid							
LN017	C(20:4); Arachidonic acid	Fatty acid							
LN018	C(22:4)	Fatty acid							
LN019	C(22:6); DHA	Fatty acid							
LP020	C(29:4)	Fatty acid							
LP021	C(29:5)	Fatty acid							
G25	Methyl aminoacetate	miscellaneous							
G26	hexenedioic acid	miscellaneous							
LP022	MG(18:1)	GL(MG)							
LP023	MG(18:2)	GL(MG)							
LP024	DG(32:0)	GL(DG)							
LP025	DG(32:2)	GL(DG)							
LP026	DG(34:1)	GL(DG)							
LP027	DG(34:1)	GL(DG)							
LP028	DG(35:2)	GL(DG)							
LP029	DG(36:1)	GL(DG)							
LP031	DG(36:2)	GL(DG)							
LP032	DG(36:2)	GL(DG)							
LP033	DG(38:3)	GL(DG)							
LP034	DG(38:4)	GL(DG)							
LN035	DG(40:0)	GL(DG)							
LP036	DG(42:8)	GL(DG)							
LP037	PA(36:2)	GL(PA)							
LP038	PA(34:0)	GL(PA)							
LP039	PA(36:1)	GL(PA)							
LP040	PA(38:2)	GL(PA)							
LP041	PA(38:3)	GL(PA)							
LP042	PA(38:4)	GL(PA)							
LP043	LPC(O-16:0)	GL(PC)							
LP044	LPC(16:0)	GL(PC)							
LP045	LPC(16:1)	GL(PC)							
LN046	LPC(18:0)	GL(PC)							
LN047	LPC(18:1)	GL(PC)							
LN048	LPC(18:2)	GL(PC)							
LP049	LPC(18:2)	GL(PC)							
LP050	LPC(20:4)	GL(PC)							
LN051	LPC(20:4)	GL(PC)							
LN053	LPC(22:4)	GL(PC)							
LP054	LPC(22:6)	GL(PC)							
LN055	PC(18:1)	GL(PC)							
LN057	LPC(22:1)	GL(PC)							
LP058	PC(22:2)	GL(PC)							
LN059	PC(22:2)	GL(PC)							
LN060	PC(34:1)	GL(PC)							
LN061	PC(34:2)	GL(PC)							
LP062	PC(38:4)	GL(PC)							

CODE	COMPOUND	FAMILY	P	K	H	SM	Wi	Wp	B
LP063	PC(25:0(CHO))	GL(PC)							
LP064	LPC(O-18:1)	GL(PC)							
LP065	PC(O-19:0)//LPE(22:0)	GL(PC)							
LP066	PC(P-34:3)	GL(PC)							
LP067	PC(P-34:4)	GL(PC)							
LN068	LPE(16:0)	GL(PE)							
LN069	LPE(16:1)	GL(PE)							
LN070	LPE(17:0)	GL(PE)							
LN071	LPE(20:1)	GL(PE)							
LP072	LPE(21:0)	GL(PE)							
LP073	LPE(21:0)//PC(O-18:0)	GL(PE)							
LP074	LPE(22:4)	GL(PE)							
LN075	LPE(22:6)	GL(PE)							
LN076	LPE(P-18:0)	GL(PE)							
LN077	PE(34:1)	GL(PE)							
LN078	PE(34:2)	GL(PE)							
LN079	PE(36:4)	GL(PE)							
LN080	PE(P-34:1)	GL(PE)							
LN081	PE(P-34:2)	GL(PE)							
LN082	PI(36:3)	GL(PI)							
LN083	LPI(P-20:0)	GL(PI)							
LP084	LPS(O-18:0)	GL(PS)							
LN085	LPS(19:0)	GL(PS)							
LP086	LPS(20:4)	GL(PS)							
LN087	LPS(20:3)	GL(PS)							
LN088	LPS(22:1)	GL(PS)							
LN089	PS(25:0)	GL(PS)							
LN090	PS(28:0)	GL(PS)							
LN091	PS(39:3)	GL(PS)							
LN092	PS(41:3)	GL(PS)							
LP093	TG(36:0)	GL(TG)							
LP094	TG(36:1)	GL(TG)							
LP095	TG(36:3)	GL(TG)							
LP096	TG(38:0)	GL(TG)							
LP097	TG(38:1)	GL(TG)							
LP098	TG(38:2)	GL(TG)							
LP099	TG(38:4)	GL(TG)							
LP100	TG(40:1)	GL(TG)							
LP101	TG(40:2)	GL(TG)							
LP102	TG(40:3)	GL(TG)							
LP103	TG(42:1)	GL(TG)							
LP104	TG(42:2)	GL(TG)							
LP105	TG(42:3)	GL(TG)							
LP106	TG(42:4)	GL(TG)							
LP107	TG(44:1)	GL(TG)							
LP108	TG(47:0)	GL(TG)							
LP109	TG(47:1)	GL(TG)							
LP110	TG(47:3)	GL(TG)							
LP111	TG(48:4)	GL(TG)							
LP112	TG(49:4)	GL(TG)							
LP113	TG(o-60:11)	GL(TG)							
LP114	N-Glycoloylganglioside GM2	SP(Ganglioside)							
G28	sitosterol	ST(Chol. And der.)							

1.1.4- Discussion

Obesity has become in the last decades one of the most popular and risky diseases spread around the world, especially in the most developed countries. It has been internationally recognized as a chronic disease compromising severely quality of life and obese people health [1].

Is also one of the most studied diseases in the scientific community, but these studies are normally focused on one tissue or area of the organism.

The methodology we have used allowed us to observe and establish links between results obtained from different tissues of the same individual giving us a more complete and holistic interpretation of metabolic changes caused because of obesity state.

The importance of the way we analysed obesity focuses mainly on the observation of the changes that suffers metabolites that are present in every tissue of the organism. This allowed us to verify that the metabolic impact of obesity differs a lot for the same metabolite depending on the tissue.

We also have verified the correlation between results from previous studies with our results, with the difference that in our case and because of the employed methodology; we can observe them all at the same time.

Figure 1.1.11 is a representation of the most significant changes observed in the different tissues and almost all are results that could be expected in obesity metabolic impact.

It is remarkable the difference in the behaviour of PLs from the same family and their derivatives depending on the tissue. These changes in the PLs manifest the increase of phospholipases activity and synthesis of PLs and establish them as possible targets for controlling the physiological and/or pathophysiological processes affecting insulin sensitivity [188].

However, it has been already described by several authors the discrepancy in concentrations of PLs species in plasma, especially LPC 16:0, 18:0, 18:1, 18:2 and 20:4.

[189-192]. This suggests a possible role of LPCs as biomarkers of inflammation in obesity diagnosis and treatment. [193]

The increase of FFA levels in plasma suggests the movement of FFA throughout the organism inducing excess of FFA in other tissues producing lipotoxicity in those tissues and all complications derived from it [194]. Moreover, this increase of FFA in serum justify the well-known chronic inflammation state of obese people as FFAs activate PPAR-γ which induces infiltration of macrophages in adipose and surrounding tissues starting an inflammatory response [55]. This inflammatory response is then responsible for vascular damage and atherosclerosis[68] as a consequence that compromises vascular function and generates endothelial dysfunction [79].

The results show an increase in MGs and DGs in Adipose tissue. This correlates with the storage function control of Fatty acid depots in the body characteristic of Adipose Tissue[86]. In the adipocytes, once FFA had entered they are esterified by acyl CoA synthase and used for lipogenesis of TGs[88]. In our results, TGs seem to be decreased but this is explained because when analysing samples, it was not taken into account the amount of total adipose tissue of the different depots in the different populations (Control vs. HFD). When doing the correlation of total weight of Adipose Tissue, TGs are highly increased in Adipose Tissue, which is what is expected from obese white adipose tissue.

Also, intracellular FA activates TLR, which interfere with insulin signalling and promotes insulin resistance [89-91]; and NFKB or c-Jun N-Terminal kinase type 1 (JNK-1) activations, which promotes the production of proinflammatory cytokines[93].

It is remarkable the already mentioned increase of DGs, which is the most compromising in this case. DGs because of the overexpression of lipases' activity, mainly Adipose triglyceride Lipase (ATGL), also named by different authors since 2004 as desnutrin, calcium-independent phospholipase A2 or patatin-like phospholipase domain-containing protein A1 to A9 (PNPLA1-9); in the TGs[195]. Hormone-Sensitive Lipase (HSL) was previously discovered as ATGL because of its lipolytic activity induced by signals triggered by adipose tissue leading to excess production and accumulation of DGs [195]. These DGs accumulate and trigger signals that are linked with the decrease of PLs (especially phosphatidic acid and phosphatidylethanolamine) that produces the liberation of FFA to blood. These are the

FFAs that travel to the other tissues and produced the already described phenomenon known as “lipotoxicity” and insulin resistance[173]. Also, it has been described that FA derived from lipolysis are important PPAR activators after specific esterification and hydrolysis cycles. This binding reduces significantly PPARa signalling and, consequently, reduces oxidation of substrates of several tissues and cell types, which compromises the severely physiological function of the affected tissues.[195] as already described.

It is not clear if these changes occur inside the adipocytes or in all the cells that make up adipose tissue, but these changes also trigger signals that translate into the liberation of FFAs to circulation.

The decrease of AAs and increase of LPs in the kidney suggest a heavy variation of PLs, and this is directly related to one of the most severe complications of obesity in the kidney: CKD. Alterations in the production of FFAs supposes a misfunction in kidney filtration, which compromises kidney health. This is linked with the effects of AMPK, which is directly involved in energy metabolism and there is evidence that reduced AMPK in the kidney results in proximal tubular cell lipid accumulation, which if takes a long time, can result in CKD [196].

Accumulation of FFAs in the heart is very dangerous. It has been discovered that when there is a large amount of FFA derived from the hydrolysis of TGs, heart uptake lipids through CD36 receptor, which its deficiency leads to increased heart glucose uptake[197] and seems to have an important role in establishing low levels of FFAs in the heart [198]. As already mentioned, one of the main reasons for cardiac dysfunction is the excess accumulation of these lipids in cardiomyocytes together with reduced lipid oxidation. This will lead to all kind of heart complications derived from obesity (atherosclerosis, hypertension…) as cardiomyocytes have a high demand for ATP (heart cells are in continuous and unstoppable contraction)[124, 125].

In the Skeletal muscle, there is a significant decrease in the concentration of Fumaric acid, which suggest changes in glycolytic activity and/or Krebs cycle. This is very important as Skeletal muscle is probably the main responsible for insulin resistance as is where there is a greater number of glucose receptors comparing with other tissues like adipose tissue or brain (there is more skeletal muscle tissue than other and because of its size, glucose demand is higher here) [199]. From this phenomenon and based on other studies, we

deduce that skeletal muscle is trying to maintain oxidative metabolism by replenishing TCA cycle intermediates [200].

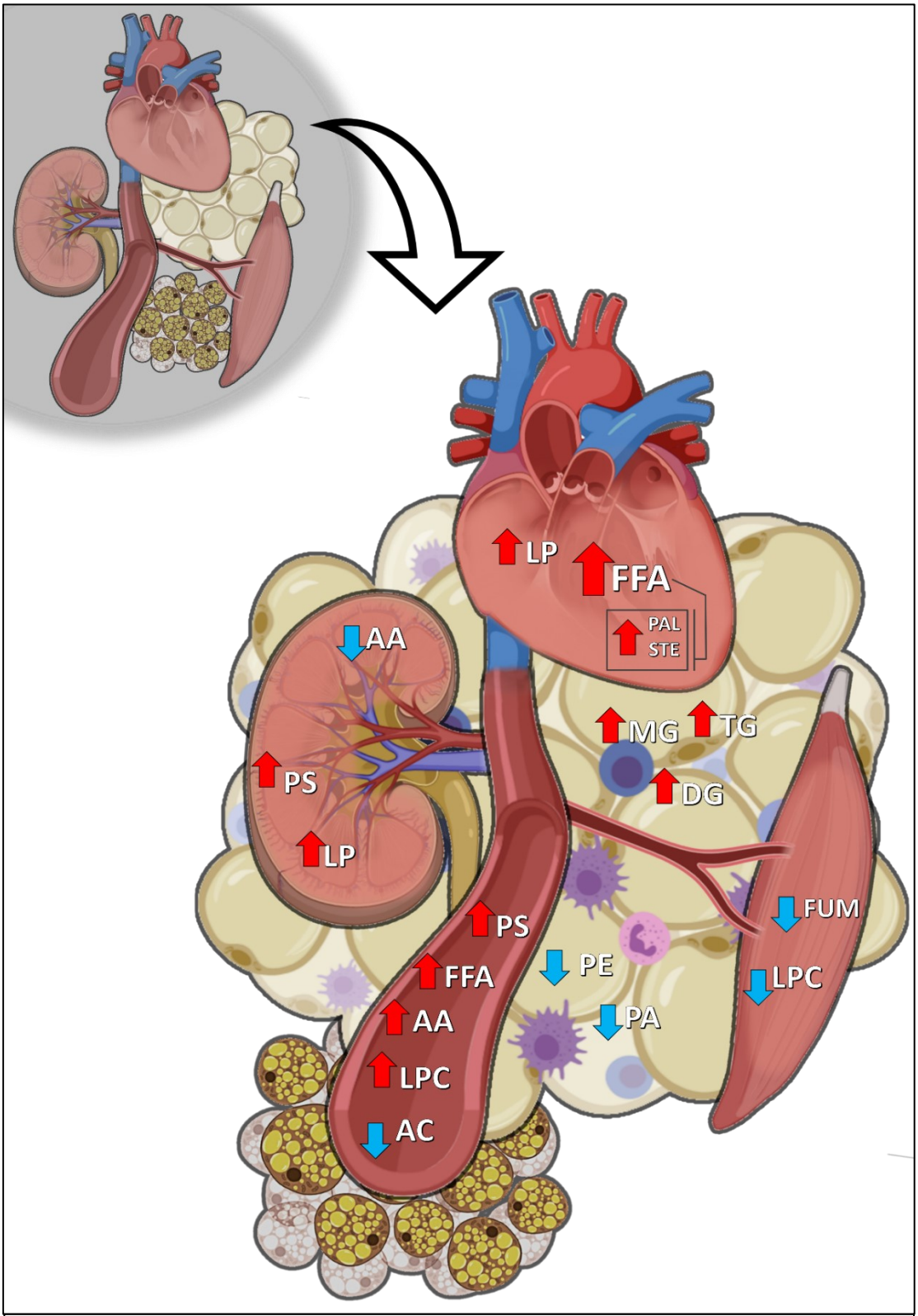

[Figure 1.1.11.]. Scheme representation of metabolic impact of obesity different tissues (Plasma, Kidney, Heart, Skeletal muscle, White adipose tissue and Brown adipose tissue) of the same organism. (PS=Phosphoserines; AA= amino acids; LPC= Lysophosphocholines; PA= Phophatidic acids; PE= Phosphoethanolamines; LP= Lysophospholipids; MG=Monoglycerides; DG= Diglycerides; TG= Triglycerides; FUM= Fumaric Acid; FFA= Free Fatty Acids; AC= Acy carnitines; PAL= palmitic acid; STE= Stearic acid)

1.1.5- Conclusions

We can summarize that this study reinforces what other scientists have already discovered The employed methodology in some way checks everything that other studies have seen in the past about obesity but all together, which allows us to consider the adipose tissue as the origin of all the metabolic changes observed in the rest of the tissues.

The novelty of our study lies fundamentally in the methodology used, which provides a holistic view of the metabolic impact of obesity.

Sample preparation protocols for heart and skeletal muscle have been successfully adapted to work in the most reproducible way under the same conditions as plasma and kidney

Different strategies for structural elucidation using LC/MS and LC/MS/MS, including Kendrick´s Mass Defect plot have allowed us to annotate 415 compounds up to level 2 of confidence

In all techniques, in all compartments, we´ve been able to unveil metabolic differences that were common across compartments for some metabolites or specific and/or characteristic of some compartments.

- Amino acids, their derivatives and related metabolites were found different due to obesity in plasma, kidney and heart, but not in skeletal muscle, the direction of changes (increase/decrease) due to the treatment was completely different between compartments.
- FFA in heart were increased, as well as in plasma and adipose tissues.
- LPC were increased in all obese compartments, as well as PS and LPC
- DGs were increased in white adiposes, but unchanged in BAT. Meanwhile, the significant TGs were those with short fatty acyls, and significantly decreased
- In skeletal muscle there were very few differences, but fumarate and malate were lower in obesity

The study of obesity as a model and a preliminary study of its metabolic alterations opens to the possibility for future studies related to its treatment.

1.2- LC-MS analysis of active and neutral lipids in Adipose Tissue

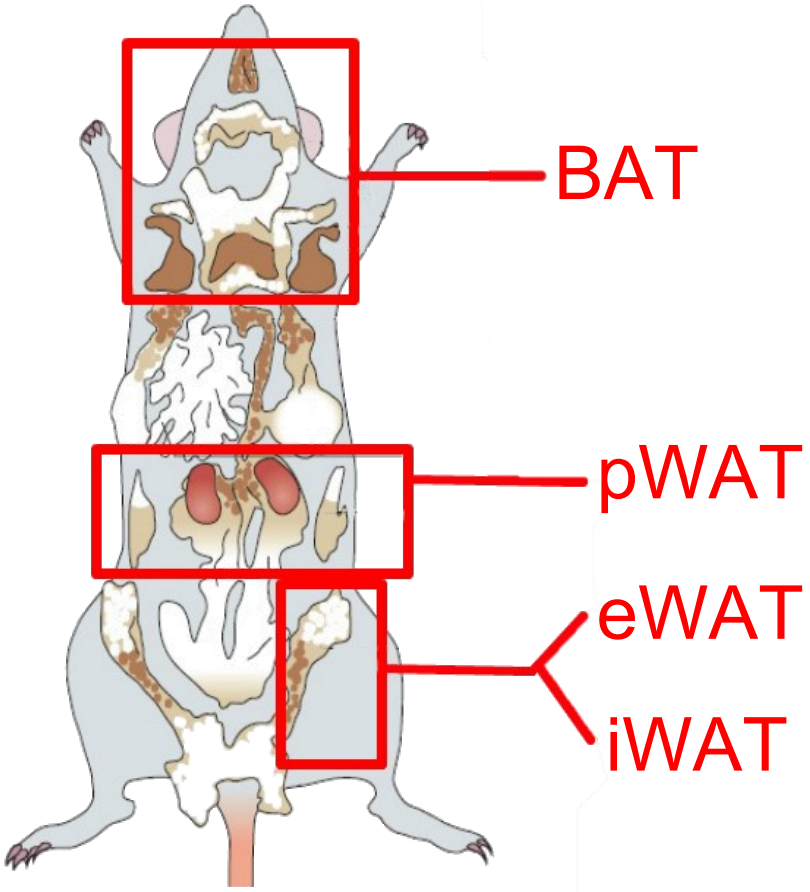

1.2.1-Introduction

1.2.1.1-Oxylipins in adipose tissue

A heterogeneous group of molecules collectively called lipid mediators, common in nature or origin, are of paramount importance in immune regulation and self-defence, as well as in the maintenance of homeostasis [201]. They include endocannabinoids, platelet-activating factor, lysophosphatidic acid, sphingosine 1-phosphate, and oxylipins.

Oxylipins are formed by the oxidation of Fatty Acids, mainly polyunsaturated fatty acids (PUFAs) (including hydroperoxy, hydroxy, oxo and epoxy fatty acids); and have at least one dioxygen-dependent oxidation step [177].

Oxylipins play a major role in regulating inflammatory processes. Depending on the precursor (n-6 or n-3 PUFA), oxylipins can respectively initiate inflammation [202-204] or, on the contrary, be anti-inflammatory agents [91, 205]. In general, traditional endocannabinoids and eicosanoids or prostanoids (from "eicosa-", twenty, by the number of carbons and “prosta-“ because the first were originally identified in prostate tissue), are derived from arachidonic acid and therefore related to omega-6 PUFAs. They are mainly involved in the control of metabolism and inflammation while omega-3 PUFA derivatives exert mainly anti-inflammatory effects [206].

Most of these oxylipins involved in inflammatory reactions are produced by adipocytes. Arachidonic Acid (ARA) and Eicosapentaenoic acid (EPA) are two of the most important long-chain PUFAs precursors of oxylipins that are involved in pro- and anti-inflammatory properties respectively [207-209]. These two PUFAs compete with each other for binding to COX-1 and COX-2, and both at the same time inhibits other reactions involved in the production of other inflammatory eicosanoids such as prostaglandin H2 (PGH2), prostaglandin H3 (PGH3), thromboxane A2 (TXA2), thromboxane A3 (TXA3), prostaglandin I2 (PGI2), prostaglandin I3 (PGI3), PGH2, PGH3…[177].

There are three main enzymatic pathways by which these oxylipins are produced: reactions catalysed by cyclooxygenase (COX), lipoxygenase (LOX), and cytochrome P450 (CYP450) or *via* non-enzymatic autoxidation [177, 210]. Oxylipins formed from PUFAs can be

octadecanoids; whose precursors are linoleic acid (18:2n-6; LA) and α-linolenic acid (18:3n-3; ALA); eicosanoids, derived from dihomo-γ-linolenic acid (20:3n-6; DGLA), arachidonic acid (20:4n-6; ARA) and eicosapentaenoic acid (20:5n-3; EPA); and docosanoids derived from adrenic acid (22:4n-6; AdA) and docosahexaenoic acid (22:6n-3; DHA) [177].

However, ARA is more prevalent than EPA as a precursor for eicosanoids from the oxylipin family [177]. ARA is found in the composition of phospholipids membranes and can be released by phospholipase A2 or formed from diacylglycerol [211]. It is also a precursor for hydroxyeicosatetraenoic acids (HETEs), dihydroxy eicosatetraenoic acids (DiHETEs), epoxyeicosatrienoic acids (EETs), prostaglandins (PGs) and thromboxane (TX). EPA is a precursor of well-known eicosanoids, such as the PG 3-series and TXs (COX) and 5-series leukotrienes (LTs) (LOX) [212].

When inflammation is activated, macrophages migration is promoted. Macrophages suffer polarization changes, already described in the previous section (section 1.1.1.2), that implies the expression of most of the proinflammatory cytokines and molecules responsible for the recruitment of more macrophages in adipose tissue leading to the activation of inflammatory pathways [213]. Some of these cytokines, like tumour necrosis factor alfa (TNF a) induce the phosphorylation of IRS1 into serine, leading to defects in Tyrosine kinase activity or IR, and decreases IRS1 and PI2 kinase activity inhibiting signalling of insulin [214, 215].

Oxylipins in adipose tissue also modulate the production of the so-called adipokines, which are proteins that play a role in adipose tissue homeostasis. They have been identified for their function in energetic metabolic regulation, orexigenic effects and their relationship with the immune system. In general, during Obesity-induced inflammation, different pro-inflammatory adipokines secreted by adipose tissue such as C- Reactive Protein (CRP), TNFα, leptin, IL-6, resistin, RBP4, lipocaline-2, IL-18, ANGPTL2 can be found. Also, some anti-inflammatory cytokines are secreted by AT that are more related to obesity such as adiponectin, IL-10 y SFRP5 [216-218].

Oxylipins from non-enzymatic autoxidation also could be considered as oxidative stress markers in many tissues [219-221]. They also have a large influence on a diverse range of processes, such as kidney function, blood vessel tone, blood coagulation, immune responses… [222, 223], and play a role in pathological processes.

Endocannabinoids are derivatives of PUFAs, produced on demand from membrane phospholipids to act on cannabinoid binding receptors (CBR) in an autocrine or paracrine manner [224]. There are many endocannabinoids, but among them, Arachidonoylethanolamide (anandamide, AEA) and 2-arachidonoylglycerol (2-AG) are the 2 best-known. They both derive from membrane phospholipid precursors and arachidonic acid [225]. For the synthesis of AEA, phosphatidylethanolamine and arachidonic acid are transformed into N-arachidonoyl phosphatidylethanolamine (NAPE) by the enzyme N-acyltransferase (NAT) (6). Then, PLD converts it into AEA and phosphatidic acid [226]. Instead, for 2-AG production, phosphatidylinositol is transformed in 1,2 diacylglycerol (1,2 DG) by the PLC, then in 2-AG by the diacylglycerol lipase (DAGL) [224].

1.2.1.2-Analysis of lipid mediators in adipose tissue

The great diversity and abundance of lipids, especially triglycerides and oxylipins, in some of the adipose tissue depots, make quite challenging the analysis of them in this organ and requires a specific sample pre-treatment for the extraction of these metabolites according to their chemical properties [227]. Additionally, oxylipins are very labile and reactive compounds and are involved in a large number of oxidation pathways that lead to a great diversity of molecules with similar structures, chemical and physical properties [228] that make them even more difficult to be analysed with traditional methods [229-231]. Moreover, most oxylipins are present at low concentrations and their detection and quantification require methods with high sensitivity [232]. All these issues must be taken into account during the collection of samples that must be quickly frozen and properly stored at -80ºC (as some degradation and loss of analytes, like resolvins or prostanoids from DHA and EPA can occur at -20ºC) [233]. It is quite frequent to use some antioxidants to prevent this problem [234].

To normalize the extraction efficiency and instrument response, the internal standard (IS) is added to the sample before extraction. Normally deuterated ISs are used as they undergo the extraction with the same efficiency. This is useful for further calculation of the loss amount of metabolites during the extraction process [235]. For oxylipin analysis by mass spectrometry (MS), a mixture of deuterated species, one IS for each lipid class, is used, selected based on structural similarities. The most commonly used ISs are d4-PGE2, d4-

PGD2, d8-12(S)-HETE, d8-5(S)-HETE, d4-PGF2α, d4-LTB4, d11-14,15-DiHETrE, d4-9(S)-HODE, d4-12(13)-EpOME, d11-14,15-EET, d11-8,9-EET and d11-11,12-EET [236-240].

Due to the aforementioned low concentration, oxylipins must be isolated and concentrated due to their low concentration in the raw sample. To achieve this, two main separation procedures can significantly simplify the analysis and increase its selectivity, eliminating the influence of interfering impurities. These processes are liquid-liquid extraction (LLE) and solid-phase extraction (SPE) [241-243]. Sample preparation includes steps such as adding solvents, acids and antioxidants; extraction; homogenization; centrifugation; the hydrolysis of esterified lipids and/or the derivatization process.

Before the separation procedures (LLE or SPE), protein precipitation (PPT) is needed [234]. Satomi *et al*. compared PPT using different water-soluble organic solvents such as MeOH, ethanol (EtOH), isopropanol (IPA) or acetonitrile (ACN), followed by methyl-*tert*-butyl-ether (MTBE)-based lipid extraction, to determine which would be the best method for sample preparation for LC–MS-based lipidomic analysis. They performed several studies [244] with different PPT protocols, looking for the best one for lipid extraction, which results to be PPT by EtOH, as it seems to cover a wide range of lipid species using a simpler preparation procedure. Once PPT is performed, separation procedures are carried out.

The LLE method is widely used for the extraction of all major classes of lipids, including phospholipids, ceramides, sphingomyelins, and cholesterol esters [245]. Chloroform: MeOH Folch [246] and Bligh and Dyer [247] methods of extraction have been the most common methods used throughout the years. Folch procedure consists of the extraction of lipids through a 2:1 chloroform:MeOH mixture in a volume 20 times higher than that of the sample before adding a saline solution, that allows the formation of a lower layer (lipids are retained here) and an upper layer consisting of water-soluble compounds, proteins, and other molecules different from lipids. At the final stage, solution chloroform:MeOH:water in a ratio of 8:4:3 is used to affirm lipid separation from other sample component into the chloroform layer [246]. Bligh and Dyer's method is similar, but the amount of used solvent is different (3 mL of MeOH:chloroform mixture 2:1 per gram or mL of the sample). After stirring, 1 mL of chloroform 1.8 mL of water is added to separate the solution into two phases. This method decreases the time of extraction and improves lipid yields using chloroform to re-extract tissue compared to the Folch method [248]. However, both methods allow to extract most

lipids, including those that are in very high concentrations in biological tissues (cholesterol, triacylglycerols and phospholipids); and this could be a disadvantage when analysing oxylipins [249]. Various types of organic solvents can be used to extract oxylipins. In the Fleming Laboratory (Frankfurt, Germany), double extraction with ethyl acetate (EA) is used to determine levels of fatty acid epoxides in murine plasma or bone marrow extracellular fluid, obtained from flushed-out femurs. In addition, oxylipins are extracted from plasma with sodium acetate, followed by extraction with EA [250].

The most common LLE method for tissue extraction involving chloroform among the already mentioned is the Bligh and Dyer method [242, 245]. However, due to the wide range of extracted lipids and matrix effects, the authors also used other solvents for lipid LLE from the tissue. To increase the extraction yield of eicosanoids, reduce chemical background noise and reduce the preparation time, Brose *et al.* changed the LLE protocol by replacing acetone:chloroform with MeOH. Using a smaller volume of solvents, modified single-stage extraction with MeOH resulted in much higher extraction efficiency of the internal standard, which may be the result of eliminating analyte loss through transfer/evaporation steps [251].

The basis of the SPE method is the selectivity of the method by the separation of analytes between the liquid and the solid phase. The main objective is to remove the interfering compounds and impurities that cause matrix effects during the analysis and to concentrate the desired analytes which results in increased the sensitivity and improved detection limits. Therefore, the SPE procedure also protects analytical systems and increases efficiency, and when proper solvents are used for elution, tenable selectivity becomes possible [248].

The most used SPE cartridges may be reversed phase (RP) (C18), normal phase (silica) and ion exchange (anion or cation) phase. The basic principle for the use of RP SPE is that aliphatic fragments in oxylipins can interact with non-polar stationary phases. Silica retains polar compounds and is used typically for sample clean-up. Anion-exchange polymer-based resins selectively retain oxylipins based on both hydrophobic and anion-exchange interactions. Polymeric sorbent (containing both lipophilic and hydrophilic functional groups) allows the retention of more lipid metabolites [252].

Usually, the SPE consists of several stages by which cartridges with the solid sorbent are firstly conditioned with one or more suitable solvents. After conditioning, cartridges are

washed to remove impurities and for the last step, analytes are eluted from the cartridge with a specific solvent according to the chemical and physical characteristics of the eluting analytes [253]. Tissue extracts obtained with mid-polar to non-polar solvents can be processed using normal-phase SPE procedures. After centrifugation or filtration to remove the precipitated proteins and solids, the pH of the sample may need to be adjusted. The analyte may adsorb onto the SPE packing or it may simply pass through, without interacting with the sorbent [252]. Solvents for the SPE of eicosanoids from tissue must dissolve the eicosanoids, permeate the matrix of the tissue, destroy the tissue, release the eicosanoids and, finally, cause protein precipitation [254].

When selecting LLE or SPE for sample treatment several considerations must be raised. LLE is a widely used method of sample preparation for the extraction of target compounds from aqueous samples; however, when compared with SPE, in samples prepared by LLE a wider peak of phospholipids appears during the LC-MS analysis [255]. Considering that the SPE method is more suitable for processing a large number of samples, SPE has become a popular method of sample preparation in terms of reproducibility, lower use of organic solvents and ease of use. Besides, SPE is very compatible with automatic analysis systems [255]. Although LLE extraction efficiency is usually higher than SPE, many endogenous impurities are extracted using LLE, which can affect separation and quantification [249]. Among the disadvantages of LLE with organic solvents is the poor extraction of hydrophilic compounds, such as PGs and LTs, compared to SPE [256]. Furthermore, SPE has been shown to provide better purification and enrichment than LLE [248]. The disadvantages of SPE are the high cost of cartridges, the fact that it is time-consuming (depending on the procedure used), and that it may need a long extraction process for accurate analysis of unstable eicosanoids [254]. Nevertheless, LLE is more often used preceding subsequent SPE to improve the purification of oxylipins [257, 258].

The present study aimed to implement a method for the extraction of oxylipins and TGs from adipose tissue samples and analyse them in the epididymal white adipose tissue from obese and control mice described in Chapter 1.1. To achieve this, mobility was done at the Adipose Tissue Department at the Institute of Physiology of the Czech Academy of Sciences in Prague. This department was chosen because of its expertise in analytical aspects related to the manipulation and preparation of adipose tissue.

The finally used optimized protocol for the extraction of Oxylipins and TGs consisted of a 2-step Reverse Phase SPE method that allowed to extract both desired groups of molecules in the same procedure with high sensitivity and reproducibility rate.

1.2.2-Material and methods

1.2.2.1-Animals

Already described in section “1.1.2.1- Animals”.

1.2.2.2- Sample treatment and instrumental analysis.

The methodology followed is a combination of previously described methods by other authors [235, 259, 260] with slight modifications.

1.2.2.2.1- Sample preparation

For homogenization of eWAT samples, 50 to 70mg of tissue were placed into safety lock microtubes containing 650µl of chilled methanol (MeOH with 0.01% BHT) with 1 bead (porcelain, white, around 2mm diameter) and homogenized using MM400 bead mill chilled to -20ºC (Retsch GmbH, Haan, Germany) at 30Hz for 3 minutes. Once homogenized, safety lock microtubes were stored at -80ºC for 30 minutes to allow precipitation of proteins. Before centrifugation at 12000×*g* for 10 minutes at 4ºC, 5µl of internal standard of 5-PAHSA-2H31 and 9-PAHSA-13C4 were added to the homogenate (100 pg/sample). Approximately 3ml of ultrapure water was prepared in disposables glass tubes. While the samples are kept for 10 min at 4ºC, Strata X (RP) 500mg, 6ml SPE columns were prepared according to manufacturer´s (Phenomenex, Torrance CA, USA) instructions. Once centrifugation finished, 650µl of supernatant from the spun samples were added to the disposable glass tubes with water and were vortexed. The next step was the extraction of the sample, performed as written in “Extraction procedure”. After extraction, eluted solvents were evaporated in a Speed-vac (Savant SPD121P; ThermoFisher Scientific) at 35ºC. Finally, parafilm was placed on the tubes with TGs extract and stored at -80ºC and residues of

eicosanoids were dissolved in 200µl of mobile phase, transferred to a new 300µl insert vial and stored at -80ºC until LC/MS analysis took place.

1.2.2.2.2- Preparation of SPE Column

SPE cartridges were activated adding twice 3ml of ethyl acetate under vacuum avoiding dryness of column by leaving a thin layer of the solvent above the sorbent. The next step was the addition of 6ml of methanol under vacuum again avoiding column dryness. Finally, before adding the samples, SPE columns were conditioned by adding 6ml of water under vacuum, this time allowing the columns to completely dry.

1.2.2.2.3- Extraction procedure of TG and lipid mediators from eWAT

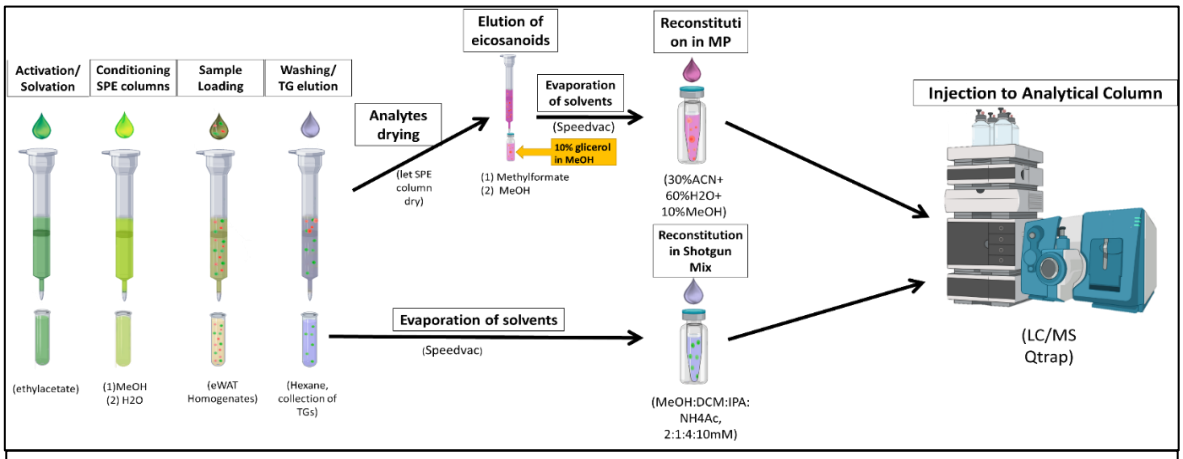

[Figure 1.2.1.]. Scheme of the 2-step RP SPE protocol followed for the extraction of TGs and Oxylipins from Adipose Tissue samples.

After vortexing the disposable tubes containing sample supernatant and water, 300µL of 0.1Mm hydrochloric acid was added and samples were loaded immediately into the SPE column. Tubes were rinsed and poured with 6ml of water into the SPE columns avoiding its dryness by leaving a layer of water on top of the sorbent. Before the addition of hexane, each column was totally dried one by one. Empty tubes were placed into the SPE tank for the collection of the hexane that will contain the TGs. After adding 6mL of hexane, TGs were eluted until columns were dried and tubes were replaced with others containing 10µl of 30% glycerol for the collection of the eicosanoids and docosanoids. Eicosanoids and docosanoids were eluted by the addition of 6ml of methylformate, again avoiding column

dryness. Finally, 2mL of methanol was added to the columns and eluted until full dryness. Samples were stored as described in “Sample preparation”. (See Figure 1.2.1)

1.2.2.2.4- Targeted analysis compounds list

Tables 1.2.1 and 1.2.2 show the corresponding targeted TGs and eicosanoids analysed in the LC-Qtrap-MS :

[Table 1.2.1]: List of Oxylipins/Eicosanoids targeted in LC-Qtrap-MS

	Arachidonic acid (AA)	
	precursor (family)	***name***
1	AA	AA
2	AA	HXA3
3	AA (DHET)	11,12-DHET
4	AA (DHET)	5,6-DHET
5	AA (DHET)	8,9-DHET
6	AA (DHET)	14,15-DHET
7	AA (EET)	14,15-EET
8	AA (EET)	11,12-EET
9	AA (EET)	8,9-EET
10	AA (EET)	5,6-EET
11	AA (HETE)	15-HETE
12	AA (HETE)	9-HETE
13	AA (HETE)	8-HETE
14	AA (HETE)	11-HETE
15	AA (HETE)	20-HETE
16	AA (HETE)	12-HETE
17	AA (HETE)	5-HETE
18	AA (HETrE)	15-HETrE
19	AA (HpETE)	12-HpETE
20	AA (HpETE)	15-HpETE
21	AA (HpETE)	5-HpETE
22	AA (Lipoxin)	LXA4
23	AA (Lipoxin)	LXB4
24	AA (oxo-ETE)	5-oxo-ETE
25	AA (oxo-ETE)	15-oxo-ETE
26	AA (oxo-ETE)	12-oxo-ETE
27	AA (TriHETrE)	11,12,15-TriHETrE
	alfa linolenic acid (ALA)	
	precursor (family)	***name***
28	ALA (EpODE)	15,16-EpODE
29	ALA (EpODE)	9,10-EpODE
30	ALA (EpODE)	12,13-EpODE
31	ALA (diHODE)	9,10-diHODE
32	ALA (diHODE)	12,13-diHODE
33	ALA (diHODE)	15,16-diHODE
34	ALA (HOTrE)	13-HOTrE
35	ALA (HOTrE)	9-HOTrE
	Arachidonic Acid /Eicosapentanoic Acid (AA/EPA)	
	precursor (family)	***name***
36	AA/EPA (Leukotriene)	20-OH-LTB4
37	AA/EPA (Leukotriene)	20-COOH-LTB4
38	AA/EPA (Leukotriene)	LTC4
39	AA/EPA (Leukotriene)	LTD4
40	AA/EPA (Leukotriene)	LTE4
41	AA/EPA (Leukotriene)	LTE4
42	AA/EPA (Leukotriene)	LTD4
43	AA/EPA (Leukotriene)	LTC4
44	AA/EPA (Leukotriene)	LTB5
45	AA/EPA (Leukotriene)	LTB4
46	AA/EPA (Prostaglandin)	6-keto-PGF1a
47	AA/EPA (Prostaglandin)	PGF2a-isoprostanes
48	AA/EPA (Prostaglandin)	PGD2
49	AA/EPA (Prostaglandin)	PGE1
50	AA/EPA (Prostaglandin)	PGJ2+d12-PGJ2
51	AA/EPA (Prostaglandin)	15d-PGJ2
52	AA/EPA (Prostaglandin)	8-iso-PGF2a
53	AA/EPA (Prostaglandin)	PGE3
54	AA/EPA (Prostaglandin)	15d-PGD2
55	AA/EPA (Prostaglandin)	PGE2
56	AA/EPA (Prostaglandin)	PGB2
57	AA/EPA (Prostaglandin)	TXB2
58	AA/EPA (Prostaglandin)	11-dh-TXB2
	Eicosapentanoic acid (EPA)	
	precursor (family)	***name***
59	EPA	EPA
60	EPA (diHETE)	14,15-diHETE
61	EPA (diHETE)	8,15-diHETE
62	EPA (diHETE)	5,15-diHETE
63	EPA (diHETE)	17,18-diHETE
64	EPA (EpETE)	17,18-EpETE
65	EPA (EpETE)	14,15-EpETE
66	EPA (HEPE)	18-HEPE
67	EPA (HEPE)	12-HEPE
68	EPA (HEPE)	15-HEPE
69	EPA (HEPE)	5-HEPE
70	EPA (Resolvin)	RvD3
71	EPA (Resolvin)	RvD5
72	EPA (Resolvin)	RvD6
73	EPA (Resolvin)	RvE2
74	EPA (Resolvin)	RvD1
75	EPA (Resolvin)	RvD6
76	EPA (Resolvin)	RvD2
77	EPA (Resolvin)	RvD2
78	EPA (Resolvin)	RvD1
79	EPA (Resolvin)	RvE1
80	EPA (Resolvin)	RvE3

	Docohexanoic acid (DHA)	
	precursor (family)	***name***
81	DHA	DHA
82	DHA (DiDHA)	10,17-DiHDHA
83	DHA (diHDHA)	7,14 - 13,14-diHDHA
84	DHA (diHDHA)	4,14-diHDHA
85	DHA (diHDHA)	14,21-diHDHA
86	DHA (DiHDPA)	19,20-DiHDPA
87	DHA (EpDPE)	19,20-EpDPE
88	DHA (EpDPE)	16,17-EpDPE
89	DHA (HDHA)	17-HDHA
90	DHA (HDoHE)	7-HDoHE
91	DHA (HDoHE)	14-HDoHE
92	DHA (HDoHE)	4-HDoHE
93	DHA (Maresin)	Maresin1
94	DHA (Protectin)	22-OH-PD1
	N-Ethanolamines (EA)	
	precursor (family)	***name***
95	NEA	N-14:0-EA
96	NEA	N-16:1-EA
97	NEA	N-16:0-EA
98	NEA	N-18:3a-EA
99	NEA	N-18:2-EA
100	NEA	N-18:1-EA
101	NEA	N-18:0-EA
102	NEA	N-20:5-EA
103	NEA	N-20:4-EA
104	NEA	N-22:4-EA
105	NEA	N-22:5-EA
106	NEA	N-22:6-EA
	Glycerolipids (GL)	
	precursor (family)	***name***
107	GL	2-16:0-glycerol
108	GL	2-16:1-glycerol
109	GL	2-18:2-glycerol
110	GL	2-18:1-glycerol
111	GL	2-20:5-glycerol
112	GL	1-20:4-glycerol
113	GL	2-20:4-glycerol
114	GL	2-22:6-glycerol
115	GL	2-22:5-glycerol
	Linoleic Acid (LA)	
	precursor (family)	***name***
116	LA (diHOME)	12,13-diHOME
117	LA (diHOME)	9,10-diHOME
118	LA (EpOME)	12,13-EpOME
119	LA (EpOME)	9,10-EpOME
120	LA (HODE)	9-HODE
121	LA (HODE)	13-HODE
122	LA (HpODE)	13-HpODE
123	LA (HpODE)	9-HpODE
124	LA (oxo- ODE)	9-oxo-ODE
125	LA (oxo- ODE)	13-oxo-ODE
	DEUTERATED Iss	
	precursor (family)	***name***
126	AA	(d8) AA
127	AA (DHET)	(d11)-8,9-DHET
128	AA (EET)	(d11) 8, 9 EET
129	AA (HETE)	(d8) 5-HETE
130	AA (HETE)	(d8) 15-HETE
131	AA (HETE)	(d8) 12-HETE
132	DHA	(d5) DHA
133	EA	(d4)N-20:5-EA
134	EA	(d4)N-20:5-EA
135	EA	(d4)N-22:6-EA
136	EPA	(d5) EPA
137	EPA (Resolvin)	(d5) RvD2
138	EPA (Resolvin)	(d5) RvD1
139	AA/EPA (Leukotriene)	(d4) LTB4
140	EPA/AA (Prostaglandin)	(d4)-6k-PGF1a
141	EPA/AA (Prostaglandin)	(d4) 8-iso-PGF2a
142	EPA/AA (Prostaglandin)	(d9) PGF2a
143	EPA/AA (Prostaglandin)	(d4) PGD2
144	EPA/AA (Prostaglandin)	(d4) 15d-PGJ2
145	EPA/AA (Tromboxane)	(d4) TxB2
146	EPA/AA (Tromboxane)	(d4) 11-dh-TxB2
147	GL	(d8)2-20:4-glycerol
148	LA (HODE)	(d4) 9-HODE

[Table 1.2.2]: List of Triacylglycerides in LC-Qtrap-MS

	SFA	
	FA loss	*TAG*
1	12:0	**TAG 48:2**
2	12:0	**TAG 48:3**
3	14:0	**TAG 46:1**
4	14:0	**TAG 46:2**
5	14:0	**TAG 50:2**
6	14:0	**TAG 50:4**
7	14:0	**TAG 51:10**
8	17:0	**TAG 52:8**
9	17:0	**TAG 52:9**
10	17:0	**TAG 52:10**
11	17:0	**TAG 54:10**
12	18:0	**TAG 50:2**
13	18:0	**TAG 52:2**
14	18:0	**TAG 52:3**
15	18:0	**TAG 54:1**
16	18:0	**TAG 54:2**
17	18:0	**TAG 54:3**
18	18:0	**TAG 54:4**
19	18:0	**TAG 54:5**
20	19:0	**TAG 54:8**
21	19:0	**TAG 54:9**
22	19:0	**TAG 54:10**
23	19:0	**TAG 56:10**
24	20:0	**TAG 56:2**
25	20:0	**TAG 56:3**
26	22:0	**TAG 52:1**
27	22:0	**TAG 54:1**
28	22:0	**TAG 60:9**
	MUFA	
	FA loss	*TAG*
29	14:1	**TAG 50:3**
30	16:1	**TAG 46:1**
31	16:1	**TAG 46:2**
32	16:1	**TAG 48:1**
33	16:1	**TAG 48:2**
34	16:1	**TAG 48:3**
35	16:1	**TAG 50:2**
36	16:1	**TAG 50:3**
37	16:1	**TAG 50:4**
38	16:1	**TAG 50:5**
39	16:1	**TAG 50:10**
40	16:1	**TAG 52:3**
41	16:1	**TAG 52:5**
42	16:1	**TAG 52:10**
43	16:1	**TAG 52:11**
44	18:1	**TAG 38:2**
45	18:1	**TAG 40:2**
46	18:1	**TAG 46:1**
47	18:1	**TAG 46:2**
48	18:1	**TAG 48:1**
49	18:1	**TAG 48:2**
50	18:1	**TAG 48:3**
51	18:1	**TAG 50:1**
52	18:1	**TAG 50:2**
53	18:1	**TAG 50:3**
54	18:1	**TAG 50:4**
55	18:1	**TAG 50:8**
56	18:1	**TAG 52:10**
57	18:1	**TAG 52:2**
58	18:1	**TAG 52:3**
59	18:1	**TAG 52:4**
60	18:1	**TAG 52:5**
61	18:1	**TAG 52:5**
62	18:1	**TAG 52:8**
63	18:1	**TAG 52:9**
64	18:1	**TAG 54:1**
65	18:1	**TAG 54:10**
66	18:1	**TAG 54:11**
67	18:1	**TAG 54:2**
68	18:1	**TAG 54:3**
69	18:1	**TAG 54:4**
70	18:1	**TAG 54:5**
71	18:1	**TAG 54:6**
72	18:1	**TAG 54:6**
73	18:1	**TAG 56:10**
74	18:1	**TAG 56:11**
75	18:1	**TAG 56:2**
76	18:1	**TAG 56:3**
77	18:1	**TAG 56:4**
78	18:1	**TAG 56:5**
79	18:1	**TAG 56:6**
80	18:1	**TAG 58:7**
81	20:1	**TAG 54:4**
82	22:1	**TAG 54:4**
83	20:1	**TAG 56:3**
84	20:1	**TAG 56:4**
85	20:1	**TAG 56:5**

	PUFA	
	FA loss	*TAG*
86	18:2	**TAG 52:4**
87	18:2	**TAG 52:3**
88	18:2	**TAG 54:5**
89	18:2	**TAG 54:4**
90	18:2	**TAG 50:3**
91	18:2	**TAG 52:5**
92	18:2	**TAG 54:6**
93	18:2	**TAG 50:2**
94	18:2	**TAG 50:4**
95	18:2	**TAG 54:3**
96	18:2	**TAG 48:2**
97	18:2	**TAG 48:3**
98	18:2	**TAG 54:7**
99	18:2	**TAG 56:4**
100	18:2	**TAG 56:5**
101	18:2	**TAG 52:10**
102	18:2	**TAG 52:6**
103	18:2	**TAG 54:10**
104	18:2	**TAG 52:11**
105	18:2	**TAG 56:6**
106	18:2	**TAG 54:12**
107	18:2	**TAG 46:2**
108	18:2	**TAG 56:12**
109	18:2	**TAG 56:8**
110	18:2	**TAG 50:9**
111	18:2	**TAG 52:9**
112	18:2	**TAG 56:10**
113	18:2	**TAG 54:2**
114	18:3	**TAG 50:3**
115	18:3	**TAG 50:4**
116	18:3	**TAG 50:5**
117	18:3	**TAG 52:4**
118	18:3	**TAG 52:5**
119	18:3	**TAG 52:6**
120	18:3	**TAG 54:4**
121	18:3	**TAG 54:5**
122	18:3	**TAG 54:7**
123	20:2	**TAG 54:3**
124	20:2	**TAG 56:4**
125	20:2	**TAG 56:6**
126	20:3	**TAG 54:4**
127	20:3	**TAG 54:5**
128	20:3	**TAG 56:5**
129	20:3	**TAG 56:6**
130	20:4	**TAG 54:5**
131	20:4	**TAG 54:6**
132	20:4	**TAG 54:7**
133	20:4	**TAG 56:6**
134	22:4	**TAG 56:6**
135	20:4	**TAG 56:7**
136	20:4	**TAG 56:8**
137	22:4	**TAG 58:7**
138	22:5	**TAG 53:10**
139	22:5	**TAG 56:6**
140	22:5	**TAG 56:7**
141	22:5	**TAG 58:7**
142	22:5	**TAG 58:8**
143	22:6	**TAG 54:6**
144	22:6	**TAG 54:7**
145	22:6	**TAG 56:7**
146	22:6	**TAG 56:8**
147	22:6	**TAG 58:9**

1.2.2.3- Instrumental conditions

Instrumental conditions were based on the published method for FAHFA analysis extraction [261]. Chromatographic separation was carried out in an ultraperformance LC UltiMate 3000 Rapid Separation LC System (Thermo Scientific) coupled to a 5500/SelexION, a hybrid, triple-quadrupole, linear ion trap mass spectrometer equipped with an ion mobility cell (Sciex). Specific parameters of the employed method are described in the previously mentioned paper: 10µL of each sample was injected to Kinetex C18 2.6µm 2.1 x150 mm column (Phenomenex) at 50ºC. The gradient used for the analysis consisted of a mobile phase A (70% Milli-Q water, 30% acetonitrile, 0.01% acetic acid, pH 4 and mobile phase B (50% acetonitrile, 50% isopropanol) pumped at 200 µL/min. The chromatography gradient was as follows: for 1 min (100% solvent A), 5 min (20% solvent A), 18 min (10% solvent A), 20 min (100% solvent A), and 25 min (100% solvent A), while a linear gradient was maintained between the steps. Isocratic elution (20% solvent A, 80% solvent B, for 60 min) was used for structural studies. Data were collected negative ESI mode with the following parameters: decluttering potential, −130; collision energy, −35; collision cell exit potential, −15; curtain gas, 25; collision gas, high; ion-spray voltage, −4500; temperature, 400; ion-source gas 1, 40; and ion source gas 2, 50. Multiple reaction monitoring (MRM) mode with one quantifier and two qualifier transitions per compound were used. Quantifier ion MRM was used as a survey scan for information-dependent acquisition in the linear ion trap for enhanced-resolution MS/MS and 2nd generation (MS/MS/MS) product ion spectra (scan rate 1,000 Da/s, scan mode profile, step size 0.05 Da, linear ion trap fill time 200ms) [262-264].

1.2.2.4- Data treatment

Chromatograms of resulting data files, background data, clearing of unrelated ions, data alignment and data filtering were analysed and processed with Skyline software.(MacCoss Lab Software, http://skyline.ms/).

1.2.2.5- Statistical analysis.

Data are reported by all the comparisons of the p-values of estimated means according to the linear regression model that underlies two-sample comparison. They correspond to the significant values selected according to the p-value of the Mauchly sphericity contrast with

Greenhouse-Geisser correction. All statistical analyses were performed using MATLAB® R2015a.

1.2.3-Results and Discussion

Triacylglycerides in eWAT

With the targeted approach described herein, 147 TGs were found in the samples from both groups. As can be seen in Figure 1.2.1, where the intensity of the transition associated with the fatty acid loss in the MS, depicted by a precursor (TG) and fatty acid, it was possible to measure three main groups of TGs: those with 50 carbon atoms in the acyl groups (for instance, two palmitic, one stearic), those with 52 (*e.g.*, two stearic, one palmitic), and those with 54 (for example, three stearic). The three groups comprised the highest abundance, but the distribution was different in the two groups. It is possible to appreciate that in the HFD group the intensity of the TGs with 52 and 54 carbon atoms in the acyl chains was bigger than in the CD group, whereas the 50 carbon TGs were less prominent.

As shown in table 1.2.3, the difference in 107 out of the 147 TGs turned out to be significant. As the amount of tissue analysed was similar, these differences show up that under obesity produced by a high-fat diet there is a combination of remodelling and lipogenesis that leads to this accumulation of longer chain fatty acids TGs. In the context of increasing obesity, there is an increase in the contribution of the FA from diet *vs*. the *de novo* lipogenesis [265].

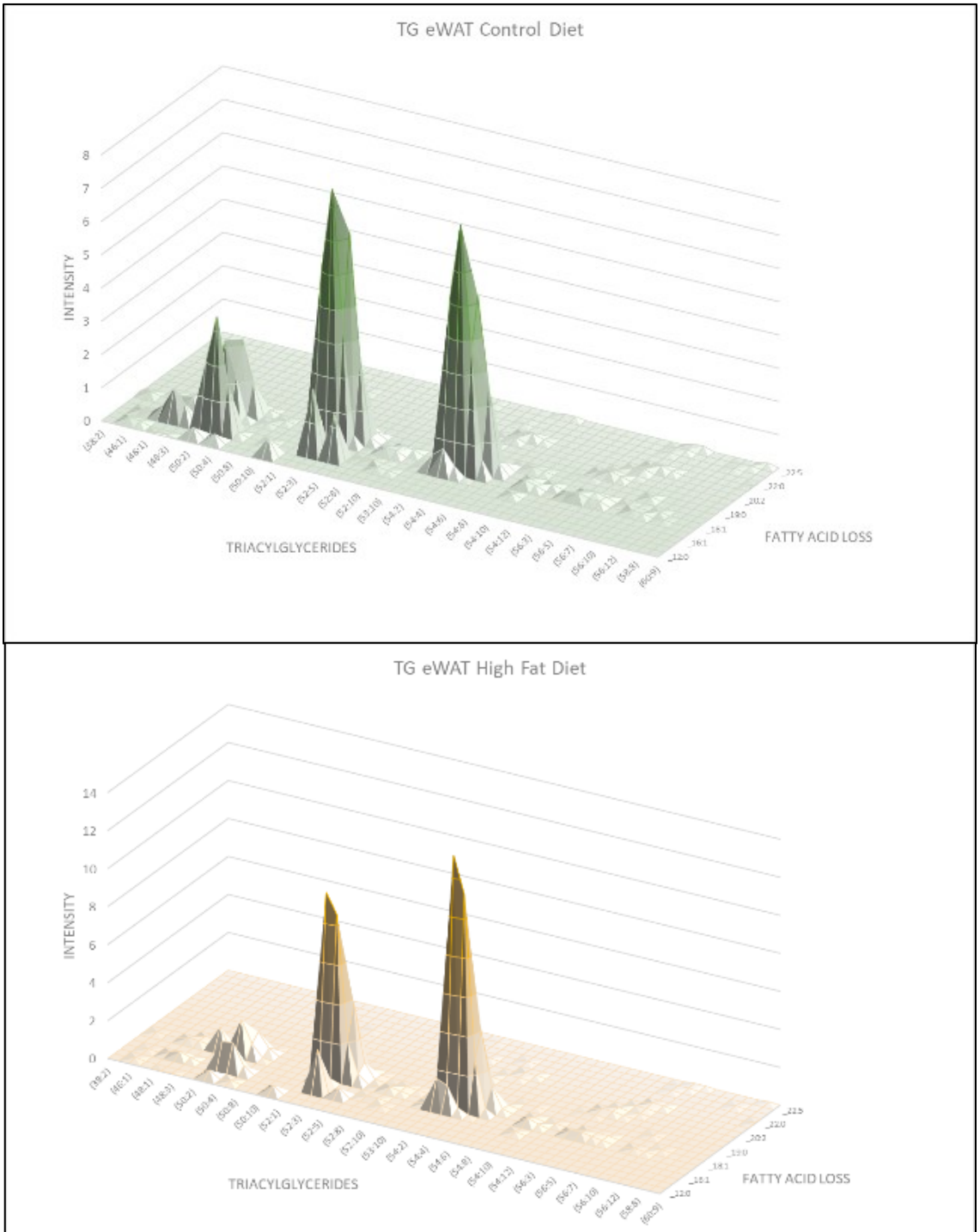

[Figure 1.2.1.]. Average of intensity of the signals of all the TGs identified in Control diet and High Fat Diet

[Table 1.2.4.] Significantly different (HFD vs. CHD) triacylglicerides in eWAT, grouped by their fatty acid loss.

SFA

	FA loss	TAGs	p- value	FC	log2FC	%A
1	14:0	TAG 46:1	0,0022	0,51	-0,97	-95%
2	14:0	TAG 46:2	0,0022	0,08	-3,64	-1145%
3	14:0	TAG 50:4	0,0022	0,39	-1,36	-156%
4	14:0	TAG 51:10	0,0238	0,75	-0,41	-33%
5	17:0	TAG 52:10	0,0043	0,12	-3,10	-760%
6	18:0	TAG 50:2	0,0004	0,66	-0,61	-52%
7	18:0	TAG 52:3	0,0022	0,74	-0,43	-35%
8	18:0	TAG 54:1	0,0000	3,19	1,67	69%
9	18:0	TAG 54:2	0,0000	3,21	1,68	69%
10	18:0	TAG 54:3	0,0000	1,77	0,82	43%
11	19:0	TAG 54:9	0,0022	0,38	-1,38	-160%
12	19:0	TAG 54:10	0,0022	0,07	-3,76	-1252%
13	19:0	TAG 56:10	0,0022	0,48	-1,06	-108%
14	22:0	TAG 54:1	0,0022	2,68	1,42	63%
15	22:0	TAG 60:9	0,0173	1,68	0,75	41%

MUFA

	FA loss	TAGs	p- value	FC	log2FC	%A
16	16:1	TAG 46:1	0,0022	0,48	-1,07	-110%
17	16:1	TAG 46:2	0,0022	0,07	-3,75	-1244%
18	16:1	TAG 48:1	0,0004	0,44	-1,18	-126%
19	16:1	TAG 48:2	0,0022	0,33	-1,60	-203%
20	16:1	TAG 48:3	0,0022	0,25	-2,01	-303%
21	16:1	TAG 50:2	0,0135	0,70	-0,51	-43%
22	16:1	TAG 50:3	0,0022	0,42	-1,24	-136%
23	16:1	TAG 50:4	0,0022	0,26	-1,97	-292%
24	16:1	TAG 50:5	0,0022	0,06	-4,05	-1556%
25	16:1	TAG 50:10	0,0022	0,08	-3,69	-1193%
26	16:1	TAG 52:5	0,0002	0,32	-1,66	-216%
27	16:1	TAG 52:10	0,0001	0,59	-0,77	-70%
28	16:1	TAG 52:11	0,0022	0,10	-3,36	-923%
29	18:1	TAG 38:2	0,0043	0,10	-3,37	-932%
30	18:1	TAG 48:2	0,0043	0,54	-0,90	-86%
31	18:1	TAG 48:3	0,0277	0,68	-0,55	-47%
32	18:1	TAG 50:3	0,0000	0,56	-0,84	-79%
33	18:1	TAG 50:4	0,0001	0,61	-0,72	-65%
34	18:1	TAG 50:8	0,0043	0,14	-2,85	-623%
35	18:1	TAG 52:2	0,0000	1,91	0,93	48%
36	18:1	TAG 52:3	0,0179	1,14	0,19	12%
37	18:1	TAG 52:4	0,0000	0,62	-0,70	-62%
38	18:1	TAG 52:5	0,0000	0,51	-0,98	-97%
39	18:1	TAG 52:5	0,0001	3,58	1,84	72%
40	18:1	TAG 52:8	0,0022	1,64	0,71	39%
41	18:1	TAG 52:10	0,0001	0,64	-0,65	-57%
42	18:1	TAG 54:1	0,0019	2,63	1,40	62%
43	18:1	TAG 54:2	0,0000	3,22	1,68	69%
44	18:1	TAG 54:3	0,0022	2,58	1,37	61%
45	18:1	TAG 54:4	0,0001	1,52	0,60	34%
46	18:1	TAG 54:5	0,0236	0,74	-0,43	-35%
47	18:1	TAG 54:6	0,0381	1,44	0,52	30%
48	18:1	TAG 54:6	0,0012	0,47	-1,08	-112%
49	18:1	TAG 54:10	0,0000	1,49	0,58	33%
50	18:1	TAG 56:3	0,0233	1,41	0,50	29%
51	18:1	TAG 56:4	0,0128	1,24	0,31	19%
52	18:1	TAG 56:5	0,0043	1,27	0,34	21%
53	18:1	TAG 56:6	0,0165	0,81	-0,30	-23%
54	18:1	TAG 56:11	0,0091	0,78	-0,37	-29%
55	18:1	TAG 58:7	0,0087	0,15	-2,70	-552%
56	20:1	TAG 54:4	0,0022	0,11	-3,20	-820%
57	20:1	TAG 56:3	0,0069	1,55	0,63	35%
58	20:1	TAG 56:4	0,0421	0,80	-0,33	-26%
59	20:1	TAG 56:5	0,0001	0,55	-0,87	-83%
60	22:1	TAG 54:4	0,0022	1,70	0,77	41%

DUFA

	FA loss	TAGs	p- value	FC	log2FC	%A
61	18:2	TAG 46:2	0,0022	0,09	-3,44	-985%
62	18:2	TAG 48:2	0,0000	0,54	-0,90	-87%
63	18:2	TAG 48:3	0,0000	0,40	-1,32	-149%
64	18:2	TAG 50:2	0,0060	0,73	-0,46	-37%
65	18:2	TAG 50:3	0,0022	0,49	-1,03	-104%
66	18:2	TAG 50:4	0,0000	0,34	-1,55	-193%
67	18:2	TAG 52:4	0,0000	0,61	-0,70	-63%
68	18:2	TAG 52:5	0,0000	0,35	-1,53	-190%
69	18:2	TAG 52:6	0,0005	0,27	-1,87	-266%
70	18:2	TAG 52:10	0,0000	0,58	-0,77	-71%
71	18:2	TAG 52:11	0,0022	0,35	-1,51	-185%
72	18:2	TAG 54:2	0,0047	1,53	0,61	35%
73	18:2	TAG 54:4	0,0000	1,42	0,51	30%
74	18:2	TAG 54:5	0,0287	0,77	-0,39	-31%
75	18:2	TAG 54:6	0,0043	0,46	-1,12	-117%
76	18:2	TAG 54:3	0,0000	1,75	0,81	43%
77	18:2	TAG 54:7	0,0087	0,43	-1,20	-130%
78	18:2	TAG 54:12	0,0042	0,48	-1,07	-110%
79	18:2	TAG 56:4	0,0139	0,77	-0,37	-29%
80	18:2	TAG 56:5	0,0030	0,66	-0,61	-52%
81	18:2	TAG 56:6	0,0022	0,81	-0,30	-23%
82	18:2	TAG 56:8	0,0022	0,08	-3,71	-1212%
83	18:2	TAG 50:9	0,0022	0,09	-3,42	-972%
84	18:2	TAG 56:10	0,0087	0,15	-2,71	-554%
85	18:2	TAG 56:12	0,0238	0,68	-0,55	-47%
86	20:2	TAG 54:3	0,0016	1,48	0,56	32%
87	20:2	TAG 56:4	0,0000	2,00	1,00	50%

PUFA

	FA loss	TAGs	p- value	FC	log2FC	%A
88	18:3	TAG 50:3	0,0022	0,64	-0,64	-56%
89	18:3	TAG 50:4	0,0022	0,31	-1,68	-220%
90	18:3	TAG 50:5	0,0022	0,07	-3,94	-1438%
91	18:3	TAG 52:4	0,0000	0,58	-0,78	-71%
92	18:3	TAG 52:5	0,0000	0,35	-1,52	-187%
93	18:3	TAG 52:6	0,0022	0,23	-2,14	-342%
94	18:3	TAG 54:5	0,0035	0,78	-0,37	-29%
95	18:3	TAG 54:7	0,0065	0,44	-1,19	-128%
96	20:3	TAG 54:5	0,0022	0,46	-1,12	-117%
97	20:3	TAG 56:5	0,0390	1,25	0,33	20%
98	20:3	TAG 56:6	0,0022	0,62	-0,69	-61%
99	20:4	TAG 54:6	0,0000	0,41	-1,30	-146%
100	20:4	TAG 54:7	0,0022	0,07	-3,78	-1274%
101	20:4	TAG 56:8	0,0022	0,07	-3,83	-1322%
102	22:4	TAG 58:7	0,0037	1,49	0,57	33%
103	22:5	TAG 53:10	0,0249	0,37	-1,42	-168%
104	22:5	TAG 58:7	0,0087	0,16	-2,63	-517%
105	22:5	TAG 58:8	0,0022	0,11	-3,13	-773%
106	22:6	TAG 54:6	0,0065	0,14	-2,82	-608%
107	22:6	TAG 54:7	0,0043	0,12	-3,12	-769%
108	22:6	TAG 56:7	0,0152	0,58	-0,78	-71%
109	22:6	TAG 56:8	0,0087	0,48	-1,05	-107%
110	22:6	TAG 58:9	0,0011	0,63	-0,67	-59%

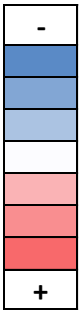

Moreover, it is noteworthy that we show the results obtained in the same amount of tissue, but it has to be considered that the size of adipose tissue from obese mice was almost five times bigger than the control group (data not shown), making this accumulation of

triglycerides even more remarkable. Under these circumstances, the release of free fatty acids due to lipolysis is increased. FFAs are the main contributors to insulin resistance, due to molecular events also linked to the production of inflammatory cytokines, such as the activation of PKC [99], TLRs [90-92], NFκB or JNK1 [94].

Table 1.2.4 shows the results of the 107 TGs that could be found statistically significant between control and obese mice, grouped by the fatty acid loss in the analyser. The intensity associated with these transitions is shown in figure 1.2.2 as a reflection of the proportion of the fatty acids in the respective groups.

In the diet-induced obese mice, we could observe (table 1.2.4, figure 1.2.2) the accumulation of C(18:1) (oleic acid, most probably) and C(18:0) (stearic acid) as the most characteristic increases, together with a decrease in the C(20:4)-containing TGs. We observed that the long and polyunsaturated fatty acids reduce their relative proportion in the obese adipose, indicating that the main contributor to the fat accumulation in the lipid droplets is the fat from the diet, rich in saturated fatty acids (see Annex 1.1.1).

Lipid droplets consist of a neutral lipid core that contains mostly triacylglycerols (TAGs) and cholesteryl esters, covered by a phospholipid monolayer, in which numerous proteins are embedded[266]. Nevertheless, lipid droplets are considered nowadays not only fat storage units, but major regulators of lipid metabolism, trafficking and signalling[267]. They actively control metabolic fluxes and signalling pathways that coordinate lipid uptake, synthesis and breakdown with cellular needs for energy production, biosynthesis, membrane and organelle homeostasis. It has become evident in recent years that the functions of lipid droplets extend beyond lipid metabolism and that they are also an integral part of the cellular stress response[268].

The role of the adipose tissue as an energy storage is undeniable, and our results corroborate it. The abundance of the signal associated to stearic and oleic acid points at a direct incorporation of these fatty acids from the diet, reducing therefore the proportion of the unsaturated fatty acids. Nevertheless, considering the bigger size of the fat depots in the obese mice, the availability of fatty acids as precursors of lipid mediators (mainly arachidonic acid, but also alpha linolenic acid, eicosapentaenoic acid, docosahexaenoic acid) must be considered.

[Figure 1.2.4] Composition of triglycerides in control vs. high fat diet samples of epididymal White Adipose Tissue organized according to the unsaturations of their fatty acids (%TIC by FA loss): A) Triglycerides with SFA; B) Triglycerides with MUFA and DUFA and C)Triglycerides with PUFA. SFA=Saturated Fatty Acids, MUFA= Monounsaturated Fatty Acids; DUFA= Di Unsaturated Fatty Acids; PUFA= Poli Unsaturated Fatty Acids

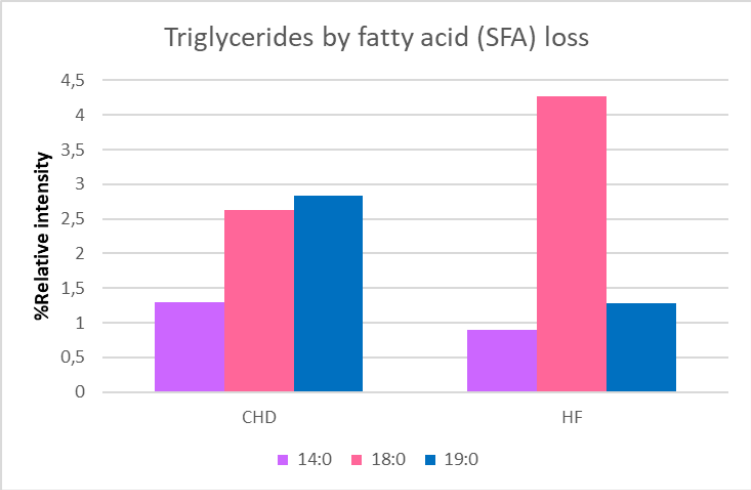

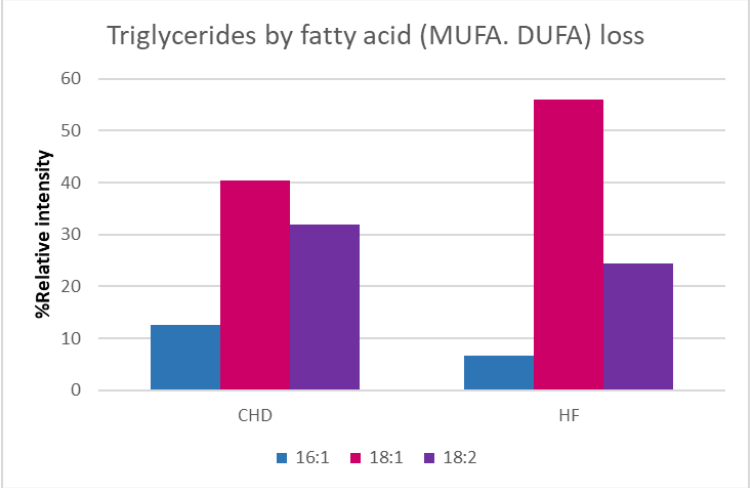

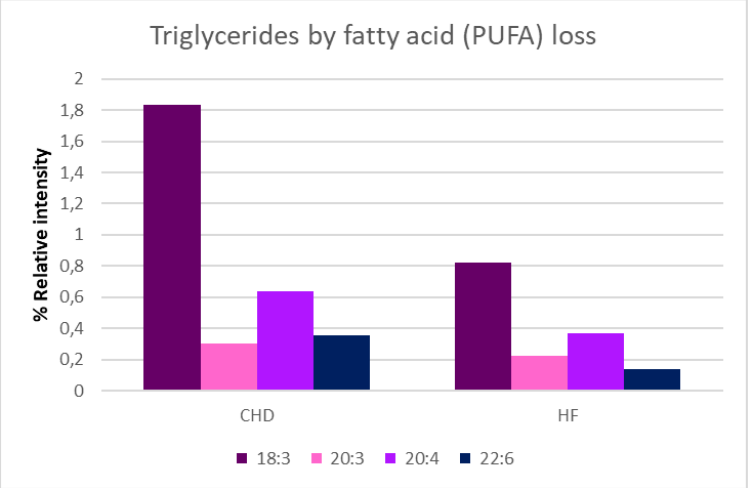

Lipid mediators

We could track 126 transitions (see table 1.2.1, in section1.2.2- materials and methods), and the difference between HFD and CD group was significant for 37 of them, gathered in Table 1.2.4.

As mentioned before, endocannabinoids and eicosanoids or prostanoids involved in the control of metabolism and inflammation, while omega-3 PUFA derivatives exert mainly anti-inflammatory effects. In our study, we could corroborate that the adipose tissue might be the main contributor to systemic inflammation because we found a significant increase in some arachidonic acid-derived oxylipins (8,9-EET, 9-HETE, 8-HETE, 11-HETE, LXA4, LTD4, PGD2) and 2-AG (plus other 6 monoacylglycerols). On the contrary, in obese eWAT we found significantly lower levels of alpha-linolenic acid (ALA) and eicosapentaenoic acid (EPA) oxylipins (15,16-EpODE, 9,10-EpODE, 12,13-EpODE, 9,10-diHODE, 15,16-diHODE, 14,15-diHETE, 17,18-diHETE, RvD2). The changes found are summarized in Figure 1.2.5

There is evidence for the activation of inflammatory lipoxygenase pathways in visceral adipose tissue of obese rats [269]. This activation is not (only) due to the recruitment of activated macrophages in the tissue, but the adipose tissue remodelling may further decrease inflammation, since smaller adipocytes produce less pro-inflammatory cytokines [64].-fat diet showed higher circulating concentrations (plasma) of 5 N-ethanolamides and 2-AG than naïve mice, since the first week of diet consumption [270]. Moreover, they found that there was a continuous increase in the plasma concentration as long as the animals were taking the high-fat diet, and such increase correlated with the increase in body weight and the expression of enzymes related to the synthesis and degradation of 2-AG in the WAT. In our study, we found a dramatic increase in 2-AG in eWAT, together with other MGs. Nevertheless, we did not find significant differences in anandamide, probably due to the low concentration of this metabolite and its liability, but we could observe a moderate decrease in 4 NEAs.

[Table 1.2.4] Significantly different (HFD vs. CHD) lipid mediators in eWAT. (AA= Arachidonic Acid; DHA= Docosahexaenoic acid ; DHET= Dihidroxy Eicosatrienoic Acid; DiHETE= Dihidroxyeicosatetraenoic acid; DiHODE= Dihydroxyoctadecadienoic acid; DiHOME= dihydroxyoctadecenoic acid; EET= epoxyeicosatrienoate; EPA= Eicosapentaenoic acid; EpODE= epoxyoctadecadienoic acid; FC= Fold Change; GL= Glycerolipid; HETE= hydroxyeicosatetraenoic acid; LA= Linoleic acid; LT= Leukotriene; LX= Lipoxin; NEA= N-Ethanolamine; Oxo-ODE= Oxooctadecadienoic acid; PG= Prostaglandin)

precursor (Family)	Compound	p-value	FC	log2FC	%A
AA (DHET)	5,6-DHET	0.026	0.40	-1.34	-60%
AA (DHET)	14,15-DHET	0.041	0.40	-1.33	-60%
AA (EET)	8,9-EET	0.024	2.97	1.57	197%
AA (HETE)	9-HETE	0.043	8.57	3.10	757%
AA (HETE)	8-HETE	0.024	2.97	1.57	197%
AA (HETE)	11-HETE	0.031	3.56	1.83	256%
AA (Lipoxin)	LXA4	0.034	1.70	0.76	70%
AA/EPA (Leukotriene)	LTD4	0.007	1.70	0.77	70%
AA/EPA (Prostaglandin)	PGD2	0.002	9.65	3.27	865%
LA (diHOME)	12,13-diHOME	0.002	0.09	-3.55	-91%
LA (diHOME)	9,10-diHOME	0.002	0.12	-3.02	-88%
LA (oxo- ODE)	9-oxo-ODE	0.031	0.32	-1.63	-68%
ALA (EpODE)	15,16-EpODE	0.009	0.35	-1.50	-65%
ALA (EpODE)	9,10-EpODE	0.026	0.45	-1.16	-55%
ALA (EpODE)	12,13-EpODE	0.014	0.43	-1.20	-57%
ALA (diHODE)	9,10-diHODE	0.002	0.13	-2.95	-87%
ALA (diHODE)	15,16-diHODE	0.002	0.04	-4.56	-96%
EPA (diHETE)	14,15-diHETE	0.014	0.29	-1.77	-71%
EPA (diHETE)	17,18-diHETE	0.008	0.18	-2.49	-82%
DHA (Resolvin)	RvD2	0.031	1.75	0.81	75%
DHA	DHA	0.017	0.90	-0.16	-10%
NEA	N-16:1-EA	0.002	0.23	-2.11	-77%
NEA	N-16:0-EA	0.004	0.43	-1.22	-57%
NEA	N-18:3a-EA	0.043	0.36	-1.49	-64%
NEA	N-22:6-EA	0.002	0.48	-1.06	-52%
Glycerol (GL)	2-16:1-glycerol	0.002	48.51	5.60	4751%
Glycerol (GL)	2-18:2-glycerol	0.002	77.56	6.28	7656%
Glycerol (GL)	2-18:1-glycerol	0.002	80.44	6.33	7944%
Glycerol (GL)	1-20:4-glycerol	0.002	77.23	6.27	7623%
Glycerol (GL)	2-20:4-glycerol	0.002	71.73	6.16	7073%
Glycerol (GL)	2-22:6-glycerol	0.002	22.91	4.52	2191%
Glycerol (GL)	2-22:5-glycerol	0.002	41.60	5.38	4060%

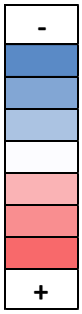

Although Kuipers et al. postulated that the increase in circulation of 2-AG and NEAs was due to the increased production and release from adipose tissue, our results only partially

corroborate this, because the overproduction of 2-AG in eWAT (over 7000%, see Table 1.2.4) is probably also accompanied by an increase in plasma concentration. Therefore, and although all the lipid mediators are assumed to act in an autocrine or paracrine way [224], this overproduction of NEAs in eWAT, in turn, could have an impact on the energy metabolism in distant tissues such as the pancreas [271]. 2-AG mediated signalling has been extensively studied, but in our study, we could see that there are other NEAs with a similar variation, or even bigger. Of particular interest is that we could measure unequivocally differentiated the levels of 1-arachidonoylglycerol, which showed an abundance close to 8000% times higher in obese mice. There is a lack of information in the scientific literature (not only in the field of obesity) about this product of phospholipid remodelling, closely related to 2-AG. Fowler et al proved that 2-AG inhibits C6 glioma cell proliferation as a result of its rapid biotransformation to 1-AG, and that the antiproliferative effects of 1-AG are mediated at least in part by activation of other receptors than the cannabinoid ones[272].

The increase in Resolvin D2 (RvD2) found in eWAT from obese mice is related to the counteraction of both local adipokine production and monocyte accumulation in obesity-induced adipose inflammation, as published by Clària et al.[273] who demonstrated that in adipose, D-series Rvs (RvD1 and RvD2) are potent proresolving mediators. In their study they also found increased concentration of LXA_4 and PGD_2. It is worth emphasizing the increase in PGD2 seen in obese adipose tissue (over 800%), because mice genetically modified to overexpress human hematopoietic prostaglandin D synthase (H-PGDS) with a high-fat diet gained more weight due to increased adipogenesis and increased insulin sensitivity[274].

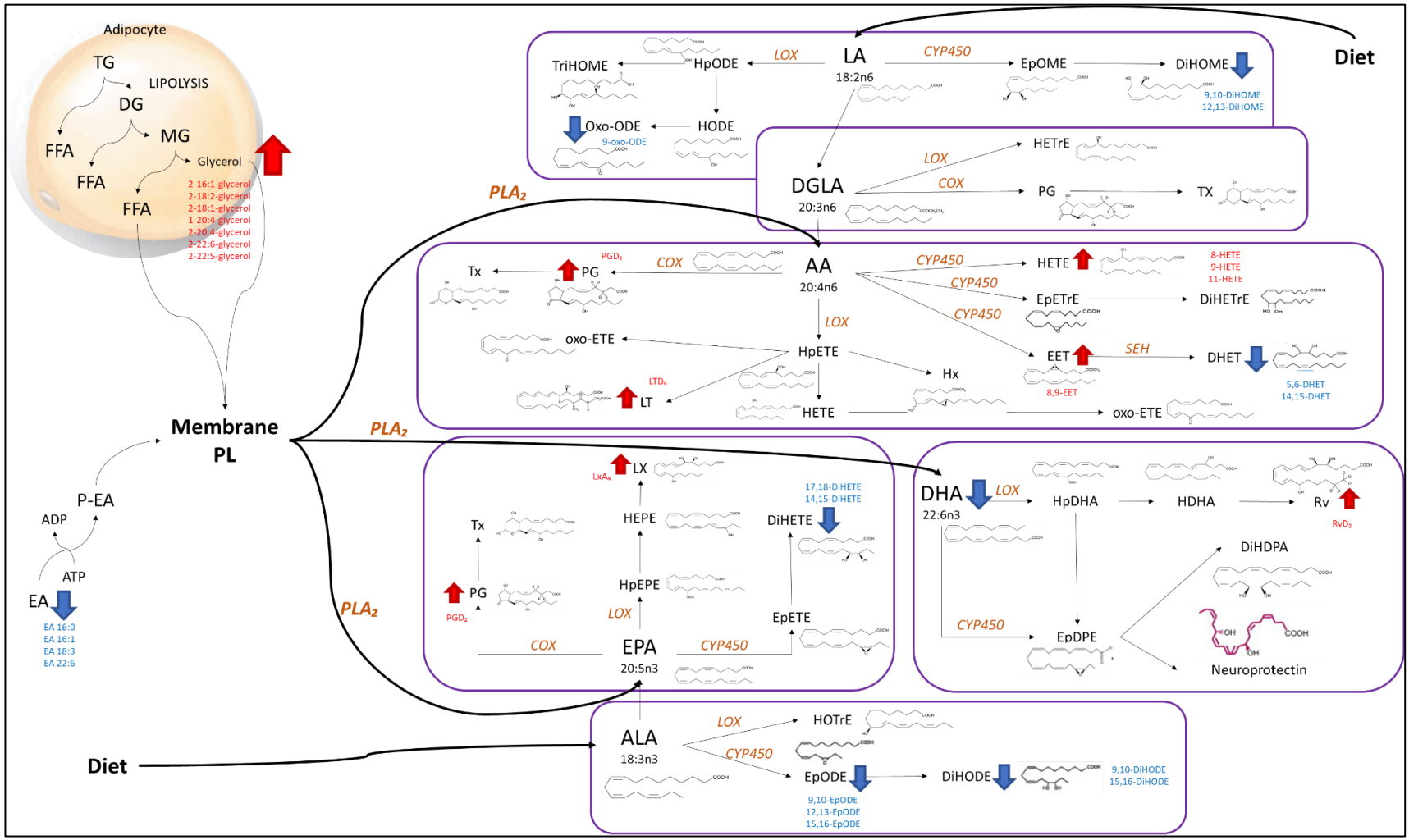

[Figure 1.2.5]: Scheme representation of metabolic alterations and interpretation of obtained results from TG and eicosanoids analysis of eWAT mice samples in HFD vs. CHD populations. (AA= Arachidonic Acid; ALA= Alpha-Linolenic acid; ARA= arachidonicacid; ATP= Adenin tri phosphate; COX= cyclooxygenase; CYP450= cytochrome P450; DG= Digliceride; DGLA= Dihomo-gamma-linolenic acid; DHA= Docosahexaenoic acid; DHET= Dihidroxy Eicosatrienoic Acid; DiHDPA= dihydroxydocosapentaenoic acid; DiHETrE= Dihidroxy Eicosatrienoic Acid; DiHODE= Dihydroxyoctadecadienoic acid; DiHOME= dihydroxyoctadecenoic acid; EA= Ethanolamine; EPA= Eicosapentaenoic acid; EpDPE= epoxydocosapentaenoic acid; EpETE= Epoxyeicosatetraenoic acid; EpETrE= epoxyeicosatrienoic acid; EpODE= epoxyoctadecadienoic acid; EpOME= epoxyoctadecenoic acid; FFA= Free Fatty Acids; HEPE= hydroxyeicosapentaenoic acid; HETE= hydroxyeicosatetraenoic acid; HETrE= hydroxyeicosatrienoic acid; HODE= hydroxyoctadecadienoate; HOTrE= hydroxyoctadecatrienoic acid; HpDHA= hydroperoxydocosahexaenoic acid; HpEPE= hydroperoxyeicosapentaenoic acid; HpETE= hydroperoxyeicosatetraenoic acid; HpODE= hydroperoxyoctadecadienoic acid; LA= Linoleic Acid; LOX= lipoxygenase; LT= leukotriene; LX= lipoxin; oxo-ETE= oxo-eicosatetraenoic acid; Oxo-ODE= Oxooctadecadienoic acid; P-EA= Phosphorilated Ethanolamine; PG= prostaglandin; PL= Phospholipid; PLA2= Phospholipase A2; Rv= resolvin; TG= Triacylglyceride; TriHOME= Trihydroxyoctadecenoic acid;

Whether adipocytes or macrophages are the main contributors to the overproduction of PGD_2 is not completely clear. It is known that the inducible isoform of cyclooxygenase (COX-2) plays a critical role in regulating adipose tissue inflammation and obesity-induced insulin resistance and a wide variety of arachidonic derived lipid mediators including PGD_2 are formed in the adipocytes[275]. Moreover, PGD_2 production was significantly reduced in adipose tissue of COX-2 deficient mice and this was associated with attenuated expression of inflammatory markers and macrophage differentiation [276],[277].

1.2.4- Conclusions

A methodology for the determination of triacylglycerols and lipid mediators in adipose tissue, based on the application of SPE and RP-LC/MS has been successfully applied to the analysis of epididymal adipose tissues from obese and control mice.

We have been able to measure the abundances of 147 TGs by means of their fatty acid loss and 122 lipid mediators by means of their reaction monitoring.

107 TGs have been found significantly expressed between the treatments. As a general overview of the results, smaller TGs show lower relative abundance in obesity than the bigger ones.

The fatty acid profile of the significant TGs shows that there is an enrichment in stearic and oleic acid, whereas there is reduction in all the PUFA measured.

Regarding the significant lipid mediators, we have found a dramatic increase in the monoacylglycerols structurally related to 2-AG, together with other proinflammatory mediators related to arachidonic acid such as PGD2 and other lipoxins and products of the activity of lipoxygenase.

Simultaneously, we found a decrease in several anti-inflammatory mediators, related to ω-3 fatty acids like alpha-linolenic acid and eicosapentaenoic acid. Nevertheless, this decrease is not as pronounced as the increase in the proinflammatory mediators.

With the methodological approach employed, it is impossible to know which cell type is responsible for the production of the compounds found. But a global situation of inflammation which could be partially responsible of insulin resistance in the adipose tissue

can be unequivocally proven. This inflammation goes hand in hand with an accumulation of lipids from the diet, stored in the lipid droplets.

Chapter 2: Metabolic impact of partial hepatectomy in the non-alcoholic steatohepatitis animal model of a methionine-choline deficient diet

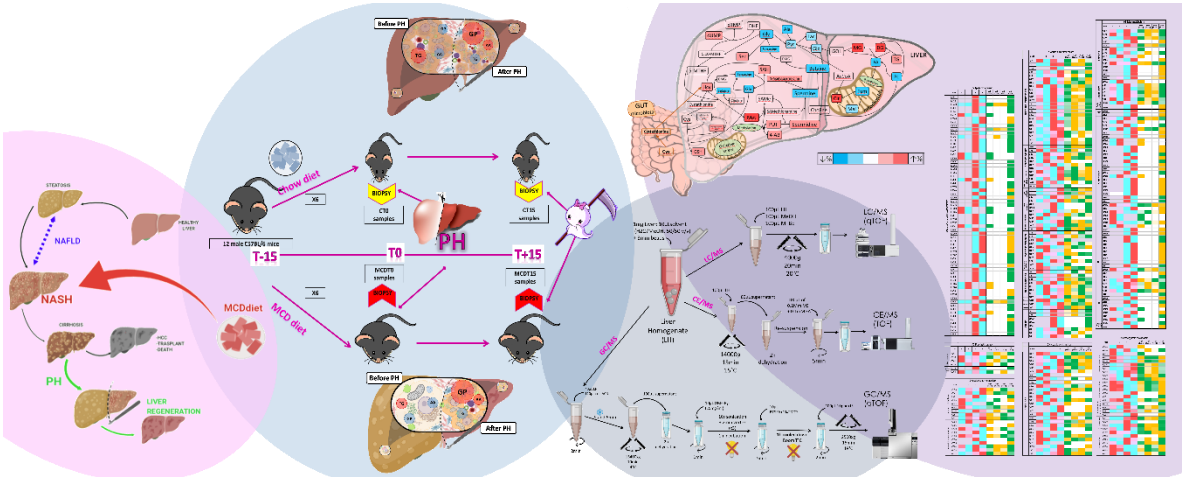

E. Carril, M.P. Valdecantos, B. Lanzón et al., Metabolic impact of partial hepatectomy in the non-alcoholic steatohepatitis animal model of methionine-choline deficient diet, J. Pharm. Biomed. Anal., https://doi.org/10.1016/j.jpba.2019.112958

2.1- Introduction

One of the clinical manifestations of obesity is Non-Alcoholic Fatty Liver Disease (NAFLD). A proportion of NAFLD patients develop hepatic inflammation, known as Non-Alcoholic Steatohepatitis (NASH). NASH is characterized by lobular and portal inflammation, hepatocyte ballooning and variable degrees of fibrosis, which can end up in hepatic cirrhosis and finally to hepatocellular carcinoma (HCC) [278].

The different dietary animal models of NASH are relevant to mimic the pathogenesis of diet-induced obesity and associated metabolic disorders. To directly induce NASH, methionine and choline deficient (MCD) has been extensively used, although it does not perfectly resemble the onset of human NASH linked to obesity due to weight loss and absence of insulin resistance [279]. As lifestyle interventions have limitations when newly diagnosed NASH is in an advanced stage, it is still needed to evaluate new therapeutic strategies. Experimental (animal) models that can emulate human NASH are useful in this preclinical phase [279].

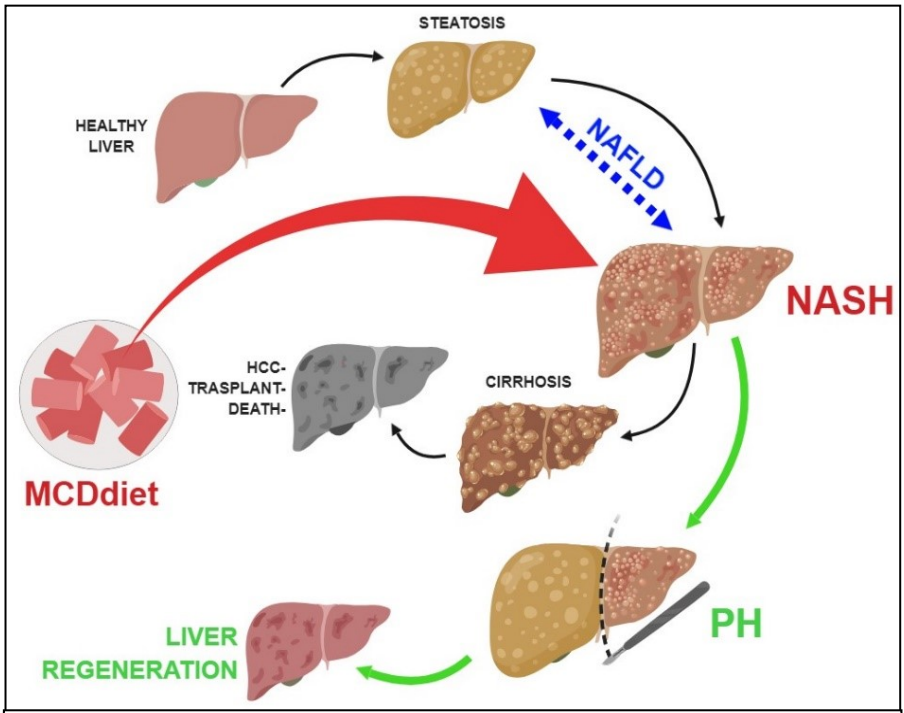

[Figure 2.1.]. Scheme that represent the progression of NAFLD and NASH from a healthy liver that suffers the pathology or induced by MCD diet and two possible developments of the disease: with or without performing Partial Hepatectomy.

Once NAFLD progresses to advanced cirrhosis, liver transplant becomes in many cases necessary. Partial hepatectomy (PH) is an alternative to liver transplant since the liver has the unique capacity to regenerate with healthy hepatocytes. PH does not suffer from the problems associated with the lack of suitable donors, of enough quality, for long waiting periods [280].

In order to get insights on the metabolic regulation of liver regeneration upon resection of 70% of the liver tissue, several studies have evaluated the first hours/days after PH, before the liver structure has been restored mainly in mice or rats [281]. In such conditions, the balance between hepatic glucose and lipid metabolism is essential for energy supply during liver regeneration in mice [282], evolving from initial hypoglycaemia and hepatic triglyceride accumulation towards the restoration of normal liver metabolism. However, many of the metabolic processes involved in the full restoration of size and function are still under active research. Besides, the metabolism of PH under NASH still needs more studies so that might become fully understood. It is known that the NASH condition worsens liver regeneration in patients and animal models [283] and elucidating the metabolic processes involved in the regeneration in naïve and NASH conditions will provide more alternatives to improve the outcome of patients submitted to such therapy.

Metabolomics has already proven its powerful ability to highlight altered routes and help in biomarker discovery in plasma of human patients with NAFLD and/or NASH, even allowing to discriminate different NASH subtypes [284].

Concerning PH, metabolomics with ^{1}H NMR has been applied to the study of the metabolic impact of PH at 24/48 h post-surgery [285], showing the rapid accumulation and disappearance of triglycerides in the liver. Nevertheless, the whole metabolic status of the hepatectomized liver once the size has been restored (beyond 8 days post-surgery), has not been characterized yet.

According to the presented arguments in the General outline, induction of NASH was performed by feeding mice with Methionine Choline-Deficient diet (MCD; TD-90262 Harland-Tecklad, Indianapolis, IN) (MCD diet), as it results to be the most used diet for inducing this pathological situation [286].

We have previously applied a metabolomics approach with GC-MS and CE-MS to respective studies addressed to evaluate potential improvements of the regenerative response of the liver of mice under MCD diet, receiving treatments with either a new glucagon receptor agonist [287] or a glucagon-like peptide 1/glucagon receptor dual agonist [288]. In the context of a complete histological, molecular and physiological characterization of the response, by means of the metabolomics approach, we showed the effect of the treatments in some nucleotides and hydrocarbons, as well as metabolites from the central carbon metabolism and amino acid metabolism, but the detailed changes in lipid composition were not studied.

The objective of the present work was to deepen the knowledge about the metabolites differentially expressed in mice taking MCD diet, before and after (15 days) having been submitted to 70% PH, by means of a multiplatform (GC-MS, CE-MS, RPLC-MS) metabolomics approach

2.2- Material and methods

2.1.1-Animals

Twelve 8-week-old male C57BL/6 mice, purchased to Charles River Laboratories (Charles River, Barcelona, Spain), were maintained in light/dark (12 h light/12 h dark), temperature (22 °C) and humidity-controlled rooms, fed ad libitum with free access to drinking water.

Mice were fed with a chow diet (Chow; SAFE A04-10 Panlab, Barcelona) or methionine choline-deficient diet (MCD; TD-90262 Harland-Tecklad, Indianapolis, IN) for three weeks [see Annex 2.1]. After that, mice were subjected to a standard 70% PH under isoflurane anaesthesia. The animals were maintained for two more weeks with their corresponding diet. At the end of the experiment, animals were sacrificed, and livers were removed and weighed [287, 288].

All animal experimentation was controlled following the recommendations of the Federation of European Laboratory Animal Science Associations (FELASA) on health monitoring, whereas the use of animals in experimental procedures was approved by the Ethical

Committee at Consejo Superior de Investigaciones Científicas (CSIC) Animal Care and Use Committee and was conducted accordingly to accepted guidelines for animal care of Comunidad de Madrid (Spain).

2.2.2- Sample treatment and instrumental analysis.

A general overview of sample treatment and instrumental analysis process is depicted in figure 2.2. The multiplatform approach is based on a single homogenization step, followed by specific steps to make the sample compatible with the analytical conditions. Sample collection and preparation protocol was performed as previously described [186] with slight modifications.

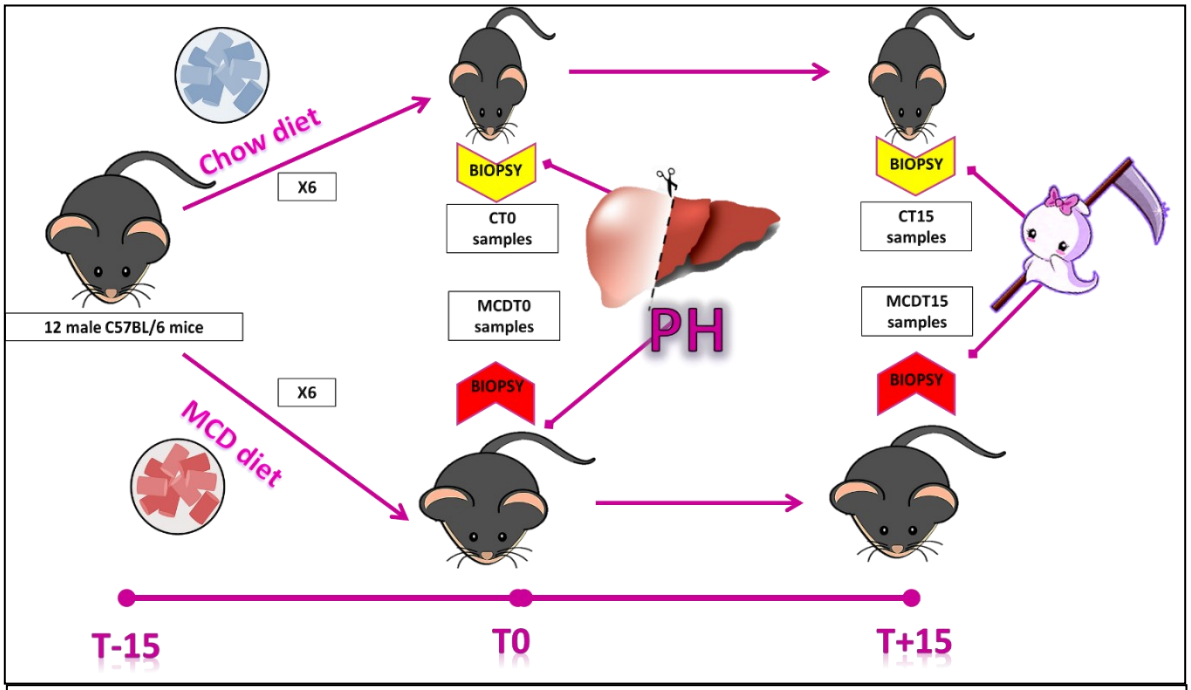

[Figure 2.2.]. Scheme representing the study design

2.2.3- Homogenization.

Livers were frozen in liquid nitrogen immediately after removal and stored at -80ºC. Liver samples were thawed the same day of the analysis and smashed into small pieces using mortar and pestle after dipping them in liquid nitrogen. Water: methanol, 50:50 (WM) was used as a solvent for homogenization. 45-50 mg from each sample were collected and added with a 1:10 ratio (1mg liver tissue:10µl solvent) in WM solvent. Homogenization

(Qiagen TissueLyser LT, Germany) was performed adding 3 mm beads per sample at 50-Hz speed for 2 min and samples were rested on ice for 1-2 min (x4 series).

2.2.4- Preparation for analysis

For LC-MS (QTOF) 100µL of liver homogenate was vortexed with 100µL of methanol for 2 min. 100µL of methyl-tert-butyl ether (MTBE) was added and vortexed for 1 h at room temperature. After that, samples were centrifuged at 4000 × *g* for 20 min at 20 ºC. Then, 100µL of supernatant was transferred to a chromatography vial for LC-MS analysis.

For CE-MS (TOF) 100µL of liver homogenate was centrifuged at 14000 x *g* for 15 min at 15 ºC. 80µL of homogenate was transferred to a safety lock microtube and evaporated for 2 h in a Savant™ SPD131DDA SpeedVac™ (ThermoFisher Scientific, Waltham, MA USA). Samples were re-suspended in a 100µL solution of 0.2 mM methionine sulfone (internal standard) and 0.1 mM formic acid. Then, re-suspended samples were vortexed for 5 min and transferred to an ultrasound bath for 2 min. After that, samples were centrifuged at 16000x *g* for 20 min at 20 ºC. 100µL of supernatant was collected and transferred to a Chromacol® vial for CE-MS analysis.

For GC-MS (QTOF) 40µL of liver homogenate was transferred to a safety lock microtube and 120µL of cold acetonitrile was added. Samples were vortexed for 2 min and let stand on ice for 5 min. Following, liver samples were centrifuged at 15400x *g* for 10 min at 4ºC. 100µL of the supernatant was transferred to a GC vial and evaporated for 2 h. 10µL of O-methoxy amine hydrochloride in pyridine solution (15 mg/ml) was added to the dried samples and vortexed for 1 min. Vials were ultra-sonicated for 10 s and vortexed for 2 min (x3 series). Samples were then transferred for incubation in the dark for 1 h. 10µL of N, O-Bis (trimethylsilyl) trifluoroacetamide (BSTFA) with 1% of trimethylchlorosilane (TMCS) was added to the vials and mixed vigorously for 5 min. After that, samples were incubated for 60 min at 70 ºC. During incubation, an internal standard (10 ppm solution of C18:0 methyl ester) was injected to confirm the retention time and the peak are in the GC-MS. After that, samples were cooled for 1 h in a dark place. 100µL of internal standard (10 ppm) was added to each vial and mixed vigorously for 2 min. Vials were centrifuged at 2500x *g* for 15 min at 18 ºC.

2.2.5- Instrumental conditions

The final instrumental conditions for liver samples were optimized from methods for LC-MS; GC-MS and CE-MS previously established in our laboratory [186].

2.2.6- Quality control samples:

QCs samples for CE were prepared by pooling equal volumes of homogenates from each sample from all groups. QCs were processed as all the samples. In the case of LC, it was decided to run separate experiments for samples before and after PH, and therefore 2 different sets of QCs were prepared. In the case of GC, a larger set of samples was used to prepare the pool, which is not included in the present study. They were analysed throughout the whole worklist to provide a measurement not only of the system's stability and performance but also of the reproducibility of the sample treatment procedure. (see Figure 2.3)

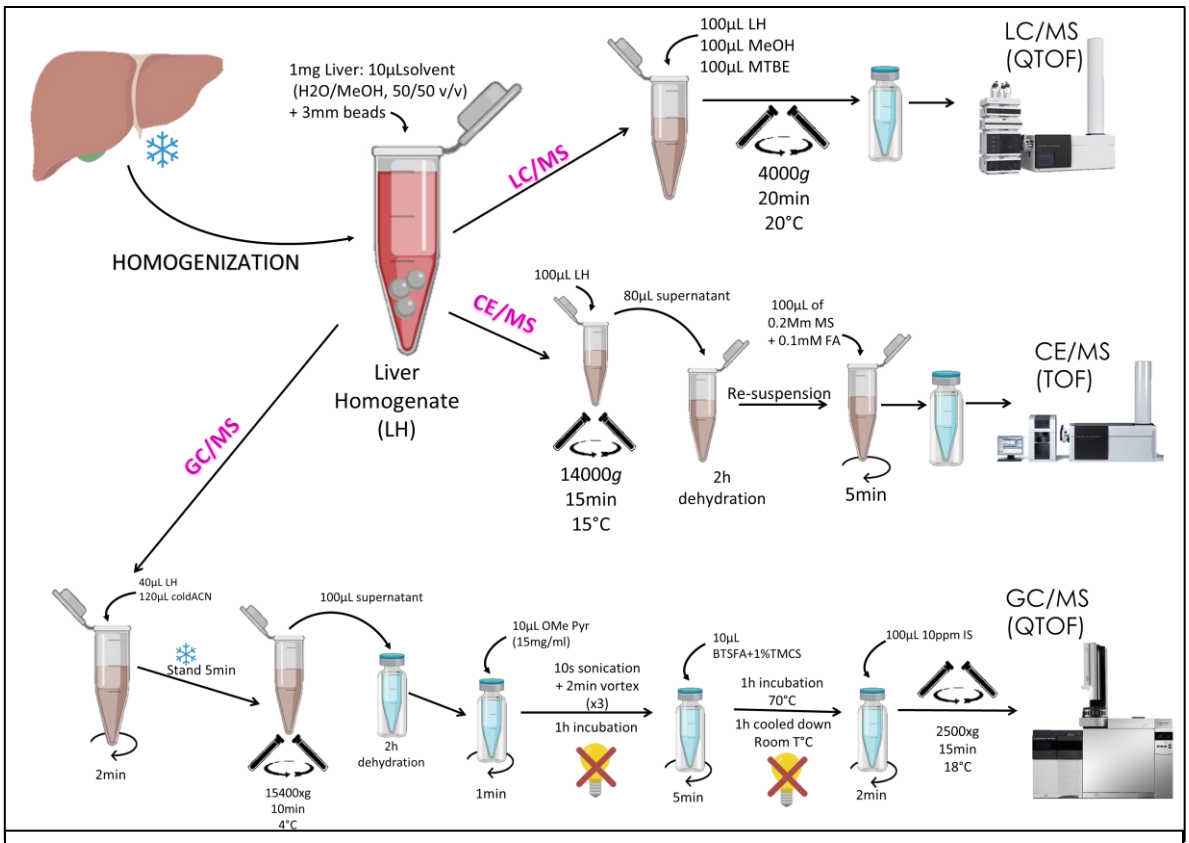

[Figure 2.3.]. Sample preparation and data acquisition scheme for multiplatform analysis of liver samples.

2.2.7- Data treatment

2.2.7.1- LC-QTOF-MS

Chromatograms of resulting data files were analysed with Mass Hunter Qualitative Analysis software (B.04.00, Agilent). Background data and unrelated ions were cleared using the Molecular Feature Extraction (MFE) algorithm included in this software. Data files were processed with Mass Hunter DA Reprocessor (Agilent). Data alignment and filtering were performed with Mass Profiler Professional software (B.12.00, Agilent). Features were filtered selecting the data presented in at least 80% of the QCs and 80% of the samples in one of the four groups.

2.2.7.2- CE-TOF-MS

A library of standards and a comprehensive list of metabolites previously obtained by other authors in CE/MS [187], were used to find features in the data files through the Find by Formula and Extract Ion tools included in Mass Hunter Qualitative Analysis software (B.04.00, Agilent). To check the assurance of the process we used methionine sulfone (MetS) as internal standard (IS), and the signal and migration time (MT) of all compounds are corrected by the abundance and MT of this IS.

2.2.7.3- GC-QTOF-MS

The identification is assured by the reproducibility of EI mass spectra and the RTL method (according to the Internal Standard—C18:0 methyl ester). Background data and unrelated ions were cleared using the Molecular Feature Extraction (MFE) algorithm included in Mass Hunter Qualitative Analysis software (B.04.00, Agilent). Deconvolution and compound identification were performed using Mass Hunter Unknown Analysis (B.04.00, Agilent Technologies). Fiehn and NIST libraries were used in the identification. Mass Profiler Professional software (B.12.00, Agilent Technologies) were used to perform the data alignment and filtering (described in the LC-MS section). Assignment selective ion and integration were done with Mass Hunter Qualitative Analysis (B.04.00, Agilent Technologies).

2.2.8- Statistical analysis.

Data are reported by all the comparisons of the p-values of estimated means according to the linear regression model that underlies ANOVA of repeated measures with correction of Greenhouse-Geisser arising concerning time before and after PH (within variable) and diet (between variable). The p-values are given for all variables, within each group (diet), within each time (PH) and within each group-time (diet-PH). They correspond to the significant values selected according to the p-value of the Mauchly sphericity contrast with Greenhouse-Geisser correction. All statistical analyses were performed using MATLAB® R2015a.

In addition, multivariate analysis (Principal Component Analysis) from all sets of data were performed to check for possible bias or trends of the data, as well as to evaluate the clustering of QCs [Figure 2.4.].

2.2.9- Annotation

The methodology followed for the annotation has been already described in section “1.1.2.9- Annotation” in chapter 1.

[Figure 2.4]: PCA-X scores scattered plot from multiplatform acquisition data. Figure A:PCA-X of CE-MS results; Figure B: PCA-X of GC-MS results; Figure C: PCA-X of LC-MS negative polarity and Figure D: PCA-X of LC/MS positive polarity. Legend of groups:1.green: CHDT0; 2.dark blue: MCDT0; 3.red:CHDT15; 4.yellow: MCDT15; 5.light blue: QCs (Quality Controls)

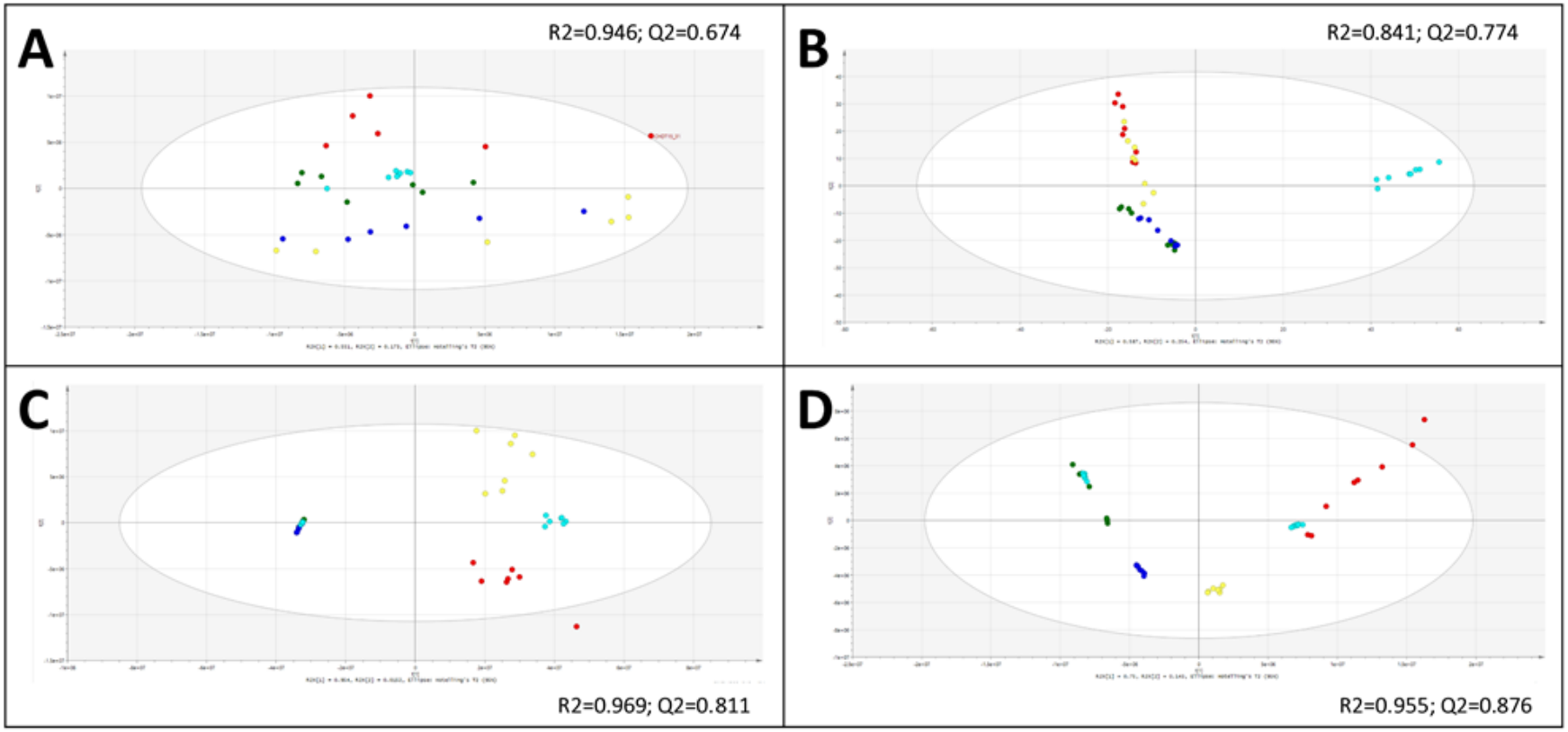

2.3- Results and Discussion

With our multiplatform approach, we have been able to obtain information for more than 3000 features, ideally compounds [Table 2.1]. Each platform was suitable to find differences in a diverse set of compounds from several metabolic families, expanding, therefore, the metabolite coverage of the study. From the total 3297, 1530 resulted significant because of the MCD diet (*i.e.*, 46% of the features) and 2814 were significant due to PH (85% from the total) [Table 2.2]. LC-MS was the platform that provided more significant features, 2819 were significant ($p<0.05$) due to the MCD diet and PH (1353 from the MCD diet, 2509 from PH). 119 from CE-MS were significant ($p<0.05$) due to MCD diet and PH (62 from MCD diet, 82 from PH), whereas GC-MS provided 269 compounds that resulted to be significant ($p<0.05$) (115 from MCD diet, 223 from PH*)* [Table 2].

[Table 2.1]: Total found features, per instrumental technique

	Detected features	
PLATFORM	*total (nº)*	*Total (%)*
CE-MS	207	6.3%
LC-MS.neg	1300	39.4%
LC-MS. Pos	1519	46.1%
GC-MS	271	8.2%
TOTALS	3297	100%

[Table 2.2]: Total significant ($p<0.05$) features, per instrumental technique and factor

	Significant features		
PLATFORM	*MCD Diet*	*PH*	*Interaction*
CE-MS	62	82	40
LC-MS.neg	621	1224	551
LC-MS. Pos	732	1285	572
GC-MS	115	223	56
TOTALS	1530	2814	1219

The corresponding annotation strategies were applied to all significant ($p<0.05$) features detected by CE-MS (49) and GC/MS (183), whereas for LC results, the 174 most significant features ($p<0.0001$) were selected for further annotation. Furthermore, 186 LC-MS/MS spectra were processed, from which 21 showed enough quality to provide additional

information to raise the level of confidence in the annotation from that provided by the coincidence in databases [Table 2.3].

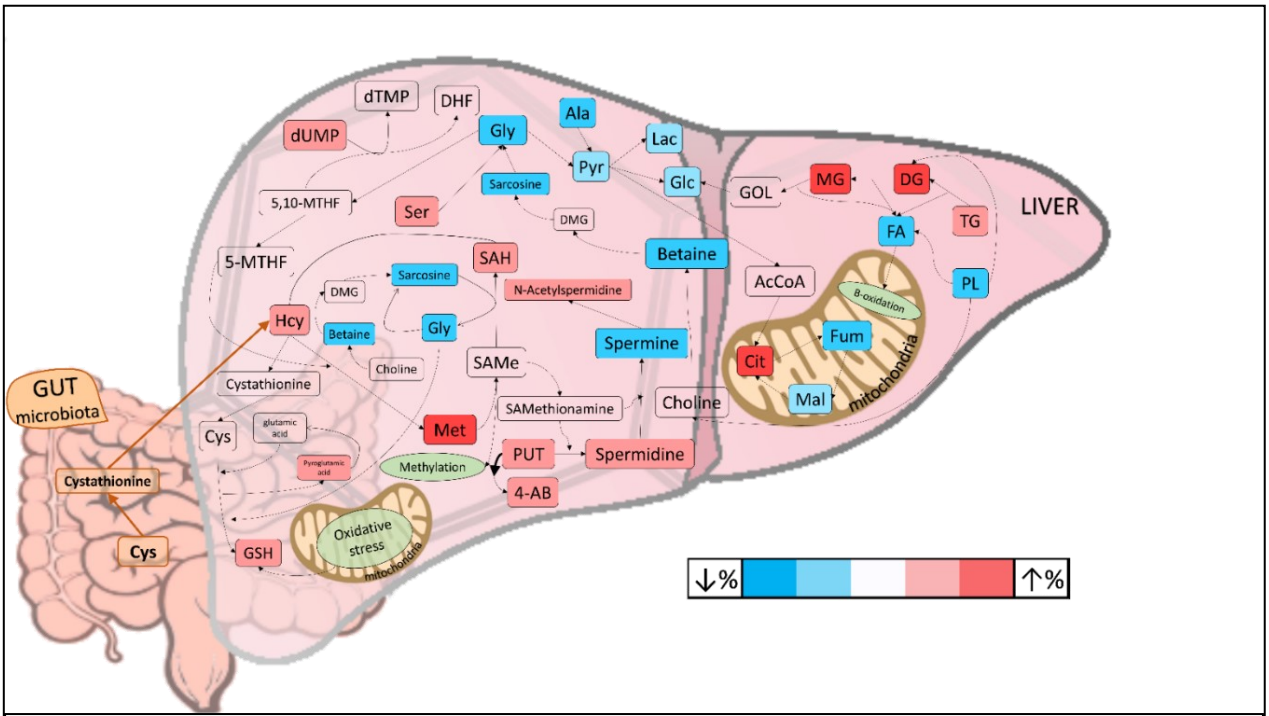

[Figure 2.5.]: Summary of main metabolic differences between MCD diet *vs*. Control diet. Ala: Alanine; Pyr: Pyruvate; Lac: Lactate; Glc: Glucose; AcCoA: Acetyl-CoA; GOL: Glycerol; MG: Monoglycerides; DG: Diglycerides; TG: Triglycerides; PL: Phospholipids; FA: Fatty Acids; Fum: Fumarate; Mal: Malate; Cit: Citrate; DMG: DiMethyl Glycine; Gly: Glycine; Ser: Serine; SAMe: S-Adenosyl Methionine; SAH: S-Adenosyl Homocysteine; Hcy: Homocysteine; Cys: Cysteine; GSH: Glutathione reduced; Met: Methionine; 5-MTHF: 5- Methyl Tetrahydrofolate; 5,10-MTHF: 5,10-Methylenetetrahydrofolate; dUMP: Uridine monophosphate; dTMP: Timidine monophosphate; DHF: Dihydrofolate; SAMethionamine: S-Adenosyl Methionamine; PUT: Putrescine; 4-AB: 4-Amino butyric.

In the case of CE-MS, 43 out of 49 significant compounds were identified making use of the CMM tool and the putative annotation was compared with an in-house database. From the 43 identified, 20 could be confirmed from both sources [Table 2.4].

[Table 2.5] summarizes all the information from all significant putatively annotated compounds (392), grouped by the metabolic route(s) where they can be primarily involved. The average abundance, the p-value associated with each factor under study, as well as the $\log_2$ of the Fold Change (FC) is also included. One code was assigned to each feature in each technique, which is used across the chapter and tables to facilitate the quest for information. It is important to remark that codes assigned in chapter 2 do not correlate with codes given in chapter 1 as the studies were carried out separately and results are not compared between studies.

Part of the changes associated with the MCD diet discussed herein can be seen in Figure 2.5, as a pathway. Table 2.6 contains more detailed information about the annotation parameters for all features, as well as a heat map where the abundances and the fold changes are graphically depicted [Figure 2.6].

[Table 2.7]: Summary of most affected groups of metabolites due to PH. Values are the average of the individual log2 (Fold Change); Fold change = quotient between the average of the signals after PH and before PH, for each diet

Metabolic family	log_2(FC[PHCT vs. CT]) PH in CT	log_2(FC[PHMCD vs MCD]) PH in MCD
Fatty acid	7.0	4.6
GL (DG)	6.6	5.0
GL (MG)	2.3	1.6
GL (TG)	-2.8	-1.7
GP (PC)	-4.0	-5.9
GP (PC//PE)	5.9	6.7
GP (PE)	3.5	3.4
GP (PI)	12.1	9.5
GP (PS)	8.9	8.9
ST (bile acids and der.)	26.7	26.7
ST (Chol. And der.)	2.7	5.4
AA	1.0	0.7

The impact of PH on the biochemical classes is summarized in Table 2.7, which shows the average (within the biochemical class) of log2(FC) of PH in both groups (CT and MCD). We could find common trends and differences mainly in the lipids (Fatty acids, glycerolipids - GL, sterols - ST) and amino acids (AA). Regarding these results, it is noticeable that PH induces the same type of changes (increase/decrease), no matter which diet were the mice taking. The differences between both groups when submitted to PH are in the extent of the changes. The signal of glycerophospholipids (GP) and AAs was in general higher after PH, but a mild decrease of triglycerides (TG) could be seen. Most of the GPs could not be discriminated between glycerophosphatidylcholines (PC) and glycerophosphatidylethanolamines (PE) because of the poor intensity of characteristic adducts and/or fragments in MS, but part of them could be unequivocally identified: All PCs were decreased after PH, whereas all PEs were increased, as previously described by Maldonado EN, et al. [289] [Maldonado E.N, 2014] regardless of the diet. Although the trends can be similar, the relative abundance of the lipids is very different. There is a smaller number of GPs in the MCD group, of any type (except glycerophospholipids, PI), at any

moment (before/after PH). See also [Figure 2.7] for a graphical representation of the changes associated with PH in both diets. These results point to a defective GPs metabolism in mice receiving MCD diet that likely present compromised PC and PE synthesis due to choline/methionine deficiency that impact in the hepatocytes both in quiescent (before PH) and proliferating (after PH) stages. Importantly, this could explain the defective hepatic regeneration of MCD diet-fed mice that requires a boost in PC/PE synthesis in agreement with our previous data [285, 288].

In addition to the changes in the lipidic metabolites, we have seen changes that affect to a similar extent to most of the proteinogenic amino acids: they are mostly decreased due to the MCD diet (as compared to CT), and after PH the levels of amino acids are higher than before, in both groups. But methionine (Met, G063) and threonine (Thr, C11/G041), did not follow this trend: they were higher in MCD groups than in CT, and were lower after PH. Met is one of the 9 essential amino acids and is necessary for the synthesis of S-adenosylmethionine (SAMe), the main methyl donor abundant in the liver. The transfer of the methyl group (for instance, to DNA for epigenetic regulation) is driven by S-adenosyl methyltransferases and produces S-adenosylhomocysteine (SAH). To regenerate SAMe, a cycle of hydrolysis (SAH hydrolase), methylation (Betaine-homocysteine methyltransferase, or 5-methyltetrahydrofolate-homocysteine methyltransferase) and transfer (SAMe synthetase) is carried out. In this cycle, choline is the precursor of betaine and sarcosine, and although it can be obtained from phospholipids, the nutritional needs for this choline are very high, and it is considered essential.

The importance of SAMe in NAFLD and NASH has been revealed in different studies such as those performed in mice lacking SAMe synthetase and Glycine N-methyl transferase (GNMT) that develop NASH, showing that advanced NASH is characterized by the inhibition of SAH hydrolase gene, and increased levels of SAH [290]. In our study, we did not find statistically significant differences in SAMe, although we previously found that the treatment of partially hepatectomized mice under an MCD diet with a dual GLP1 receptor/glucagon receptor induced a dramatic increase of SAMe [288].

[Figure 2.6]: Heat maps representing data from Table 3 results grouped by metabolic families. (1):Control samples before PH; (2): MCD diet samples before PH;(3): Control samples after PH; (4): MCD diet samples after PH; p(DIET).

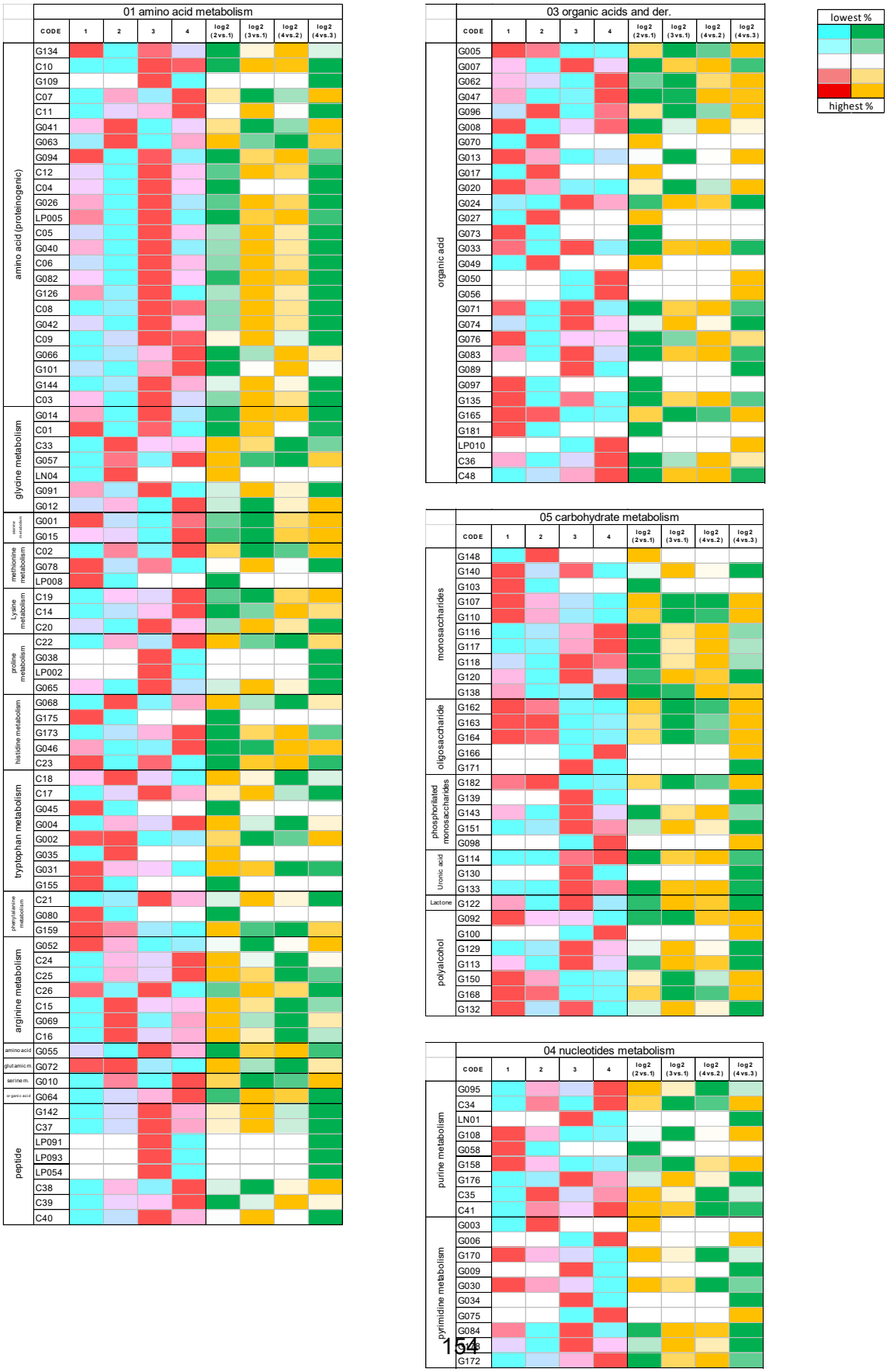


02 lipids metabolism
CODE
1
2
3
4
log2 (2vs.1)
log2 (3vs.1)
log2 (4vs.2)
log2 (4vs.3)
Fatty acid
Acylcarnitine
Fatty amide
CDP
Glycerolipids
SP
ST
Fatty Acyl CoAs
GlyceroPhospholipids (PA/PE/PC)
lowest %
highest %
06 Prosthetic groups
vitamin and der.
Hemoglobin metabolism

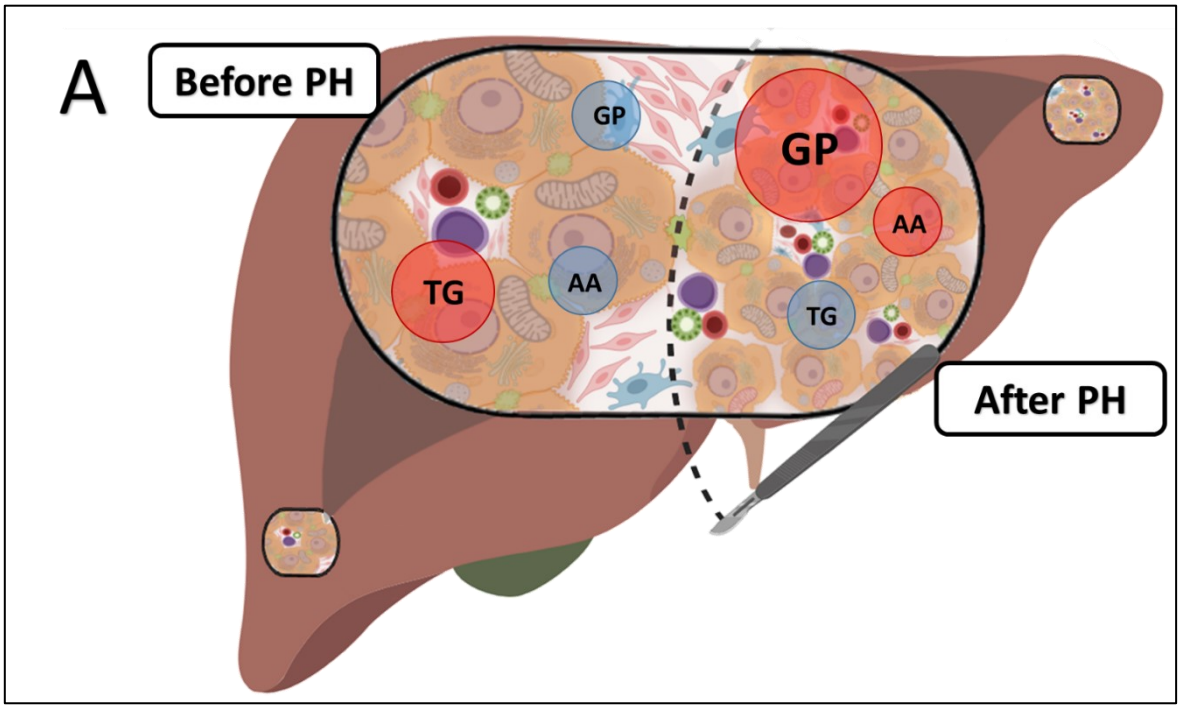

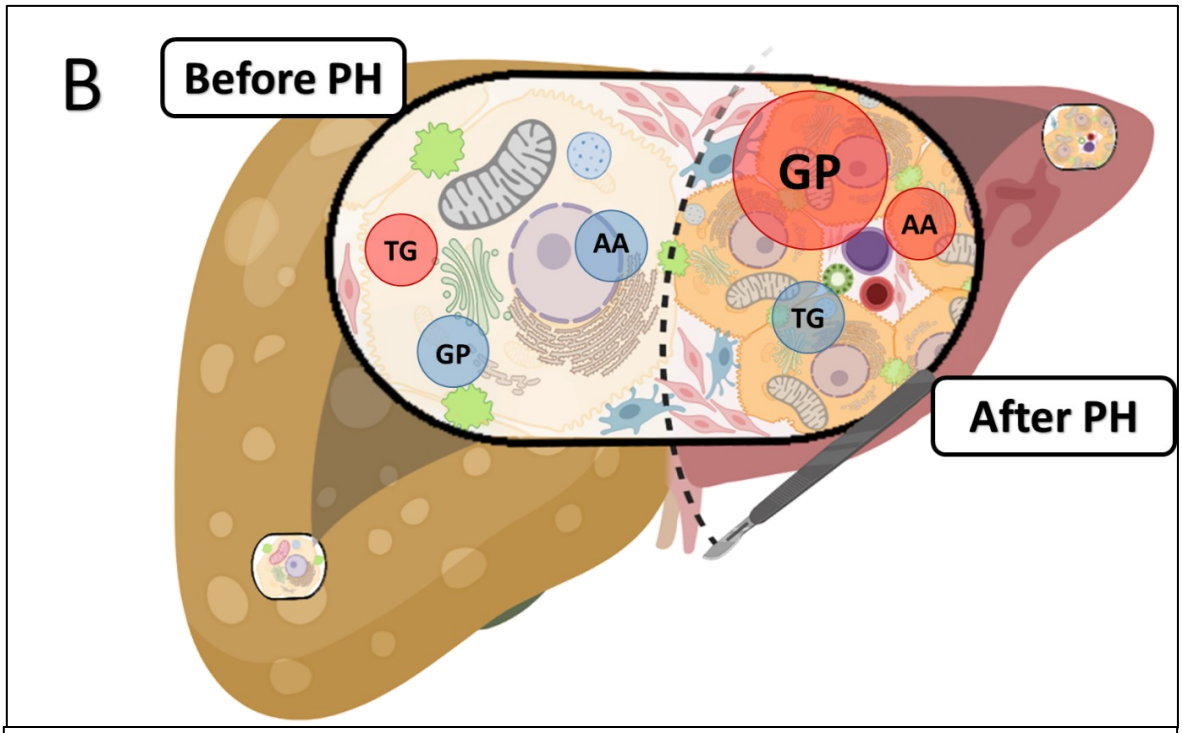

[Figure 2.7.]: Graphical representation of the three most significant molecular features involved in different metabolic changes before and after PH: (Picture A: changes comparing groups fed with control diet; picture B: changes comparing groups fed with MCD diet. GP, Glycerophospholipids; AA, Amino Acids; TG, Triglycerides. Ball size increase proportionally to the logarithm of the relative abundance of these compounds before and after PH. Ball colors represent the metabolic changes within each diet due to PH: blue means a decrease of these compounds while red means an increase).

In our study, we found that the group of mice that received the MCD diet showed increased levels of SAH (C41), versus the control group mice, fed a chow diet. Taking together with the differences in homocysteine (Hcy, C02) and Met (G063), such increase in MCD mice versus the control is pointing to impaired regulation of the cycle. In the context of a diet deficient in Met, it may become paradoxical the presence and variation of Met and Hcy in the liver [Table 2.5]. In absence of supply from the diet, such essential amino acids must come either from the proteolysis of proteins already synthesized before the animals started with the MCD diet and/or the gut microflora activity (see below).

Regarding proteolysis, mice that develop NASH under the MCD diet develop a hypermetabolic state [291] *[Rizki G., 2006]* because they lose weight even though the diet has an adequate caloric supply. Therefore, catabolism of proteins is exacerbated in the liver to provide both energy supply and carbon skeleton for other biomolecules such as glucose (gluconeogenesis). All amino acids can be metabolized to amphibolic intermediates, Acetyl CoA and intermediates of the tricarboxylic acid cycle. Serine (Ser, C07) and Thr (C11) will produce pyruvate (G005), which can be reduced by NADH to lactate (G007) or decarboxylated in the mitochondria to Acetyl CoA. In contrast, amino acids which are catabolized in the mitochondria to Acetyl CoA or one of the intermediates of the TCA cycle, *i.e.*, Valine (Val, C04/G026), Histidine (His, C12), Leucine (Leu, C05), Isoleucine (Ile, G040), Phenylalanine (Phe, C06/G082), Tyrosine (Tyr, G126), proline (Pro, C08), glutamic acid (Glu, C09) and aspartic acid (Asp, G101) were found decreased in MCD group as compared to CT group. The higher levels of citrate (G096), together with the decrease of malic (G062) and fumaric (G047) acids, indicate excessive activity of the TCA cycle, in common with humans with NAFLD [292]. This impaired metabolism of amino acids is related to elevated ALT and AST[293]. With our methodology, we cannot know whether elevated transaminases are a cause or a consequence of the altered levels of amino acids, because there is feedback between the activity of these enzymes and the levels of amino acids and their metabolites.

Despite elevated protein catabolism in the liver of mice fed the MCD diet, it is not enough to supply the needs for an essential amino acid as methionine and gut microflora can provide an extra supply of such amino acid. Of note, the possibility to obtain Hcy from other sulphur sources such as cysteine (through cystathionine) is only present in mammals. Nevertheless, several common bacterial species express cystathionine gamma synthases [294] which

synthesizes cystathionine from cysteine. In such a context, it is worth mentioning that the gut microflora is critical for mice fed an MCD diet because one antibiotic-treatment can produce higher NASH and excessive fibrosis [295].

Hcy must be methylated, and the methyl group may be donated by 5-methyltetrahydrofolate (5-MTHF) or betaine, as previously mentioned. As the MCD diet was deficient in choline, levels of liver betaine (C01) and sarcosine (G014) were found lower in MCD-fed mice as compared to controls [Table 2.5]. In the absence of betaine, glycine is the main source of methyl groups for the synthesis of methionine, because it can be metabolized into 5,10-methylenetetrahydrofolate, which in turn can be converted into 5-MTHF by Methylenetetrahydrofolate reductase. We found a profound decrease in the levels of betaine, and sarcosine, as well as glycine (G134) in the MCD group before PH. Furthermore, the conversion of dUMP (G172) into dTMP was found reduced in the MCD group. 5, 10-MTHF is the source also for such conversion, but in a situation of Met deficiency, this conversion seems under-regulated. We also found differences in the arginine metabolism, and differences between MCD and control groups in putrescine (G052), spermidine (C24) and spermine (C26). As one derivative of SAMe is needed for the conversion of spermidine into spermine, these results indicate that the SAMe pool is not enough to attend to all the reactions where the methyl transfer is needed. In such conditions, putrescine is catabolized through an alternative pathway into 4-amino butanoic acid (C48).

Recently, Dong et al. [296], analysing urine and blood of non-diabetic NAFLD with normal liver function as well as NASH and HC subjects with impairment of liver function, identified biomarkers whose presence was different according to the NAFLD stage. They showed by ROC (Receiver operating characteristic) analysis that 3-indoleacetic acid, L-carnitine, pyroglutamic acid, and indole lactic acid might discriminate NASH from NAFLD. Lake et al. [297] also studied the progression of NAFLD towards NASH by metabolomics and transcriptomic analysis and reported increased levels of leucine, isoleucine, and valine from NAFLD to NASH. Similarly, carnitine metabolites were significantly elevated in NASH compared to NAFLD.

Lipotoxicity, oxidative stress and activation of the immune system are believed to play key roles in the activation and production of pro-inflammatory cytokines as well as in the metabolic adaptations triggered to stop or revert fat accumulation and production of oxygen

reactive species (ROS) from mitochondrial fatty acid oxidation which are main contributors of hepatocyte injury leading to cell death by apoptosis [298].

Oxidative stress promoted by lipid accumulation is a key driver of progression from simple steatosis to NASH [299]. In this regard, inflammation markers such as 11-HETE, oxidative stress-related compounds (glutathione metabolites), bile acids and carbohydrate-related metabolites were found different in the plasma of both types of patients. Different studies have also shown increased primary bile acids in circulation in NASH [300].

In our present study, we could find changes in glutathione (G142) and some metabolites related to either its synthesis (2-hydroxybutyric, G013, pyroglutamic acid, G064) or its further modification (hydroxymethylglutathione, C37) (ophthalmic acid C36) or catabolism [293]. Under the MCD diet, although there is a higher availability of glutathione, its synthesis is lower than in controls, and its depletion is higher. PH involved an increase in the availability of glutathione, but under the MCD diet this increase was lower, and the depletion was higher. A combination of factors: substrate (Cys, Gly, Glu) availability, ROS production (from mitochondria), NADPH synthesis (from pentose phosphate) simultaneously concur to modulate glutathione synthesis and reduction. Therefore, under the MCD diet the amount of GSH available to counteract oxidative stress is lowered, and to be able to increase such availability could provide therapeutic opportunities in NASH, as well as in conditions strongly related to NASH such as HCC[293].

In the liver under physiological conditions, glycogenolysis and gluconeogenesis are activated to maintain body glucose homeostasis when blood glucose levels decrease upon fasting. Coordinated and well-working glucose metabolism is essential for normal liver regeneration. It is long known that after PH the decrease in liver tissue is accompanied by complex hormonal changes producing an increase in glycogenolysis and gluconeogenesis in the remnant liver [301], as well as a shift of glucose utilization towards the pentose phosphate pathway to provide NADPH for lipid and DNA synthesis. Nevertheless, these studies have been carried out mainly in the early stages after PH, before the liver reaches the Hepatostat[302], whereas we show that in our study, even though the liver had reached 100% of the liver weight/body weight[288] differences in the carbohydrate-related metabolism are still present: glucose (G140) and glucose-containing oligosaccharides (sucrose - G162, maltose - G162, lactose - G164, maltotriose - G182) were lower after PH,

whereas phosphorylated sugars (erythrose phosphate G143, glucose phosphate G151), and compounds related to pentose phosphate pathway were increased (gluconolactone G114, galactonolactone G122, galacturonic acid G130, gluconic acid G133). On the other hand, the ribose-phosphate G139 was decreased after PH. Altogether, these results point to an intense activity of nucleic acid synthesis associated with cell replication. In all cases, the MCD diet does not change the trend, or direction of the change (increase/decrease) of each carbohydrate metabolite, associated with PH. The differences between both diets are in the relative abundances.

When mice under the MCD diet were subjected to PH, the aforementioned changes in amino acids due to active protein catabolism, together with the alterations in carbohydrate metabolism led to differences also in the levels of lactic(G007): pyruvic (G005) ratio (lower in MCD than in CT, largely increased after PH in CT, only mild increase after PH in MCD). Under the MCD diet, PH involves more activity of the mitochondrial TCA cycle: whereas citric, malic, and fumaric acids were decreased after PH in the CT group, their levels were increased after PH in the MCD group. In the early stages after PH, there is an increase of the gluconeogenic and decrease of the glycolytic capacity [301], but our results show that after that early adaptation to a large growth activity, new adaptations occur, and glycolysis and lactate production is increased, and the modulation of the metabolic flux towards the mitochondria should be tampered to enhance the efficiency of the PH [288].

Concerning the lipidic content, again we should emphasize that most of the compounds that were found significantly different after PH were lipids (more than 90%) from which we annotated only the 174 most significant. In a recent study Alonso et al. [284], studied metabolomic data obtained from experimental animals as well as human samples and stated that there are two subtypes of NASH according to their circulating pattern of triglycerides, diglycerides, fatty acids, ceramides, and oxidized fatty acids.

With the analytical approach employed, most of the lipids were detected through LC/MS (both positive and negative), and most of the signals detected with our LC/MS method could be attributed to lipids [Figure 2.7]. The intracellular triglyceride accumulation characteristic of NAFLD is usually expressed as corrected by the number of proteins, and in these mice, the ratio of hepatic triglyceride to proteins was shown to be increased [287]. For the sake of the global metabolic interpretation of the results, we decided to not correct any of the

abundances of the metabolites, therefore reflecting the accumulation in the whole organ. With our metabolomics approach we found only a moderate increase in 3 monoglycerides, and a decrease in 5 triglycerides (highly significant, $p<0.0001$), which reflect the behaviour of all those lipids with $p<0.05$. Our results are not as paradoxical as might seem, because mice with MCD diet-induced NASH also develop hepatic fibrosis [303]. Therefore, the ratio of lipids/protein in fibrosis might be increased whereas the total amount of lipids per mass unit of the liver (as reflected by the total abundance) could show a different trend.

Our results show a significant increase in lipid metabolism, particularly glycerophospholipids as the main lipids that constitute cell and organelles membranes; amino acids metabolism and glucose metabolites metabolism, which suggest that liver regeneration is being exacerbated by these pathways to quickly replace the removed damaged tissue, as a fast production of new healthy hepatocytes is needed.

[Table 2.3]: (LC-MS/MS identification results).

CODE	mode	NEUTRAL MASS	m/z EXP	RT	Name	Adduct	MS/MS fragments	Fragments (Metlin)	Formula	Mw	collision energy	Error ppm
LN05	(-)	330.257	329.2492	5.5	C(22:5), Docosapentaenoic acid	M-H	311.23, 285.25, 231.21, 135.11	311.23, 285.25, 231.21, 195.13, 135.11, 59.01	C22H34O2	330.2559	16.7	3.3
N/A	(-)	306.2555	305.2477	5.4	C(20:3) Icosatrienoic acid; linolenic acid	M-H	287.23, 261.25	287.23, 261.25, 59.01	C20H34O2	306.2559	15.9	-1.3
N/A	(-)	332.2712	331.2634	6.2	C(22:4) Adrenic acid/ docosatetraenoic acid	M-H	313.25, 287.27, 127.07	313.25, 287.27, 127.07, 59.01	C22H36O2	332.2715	16.8	N/A
N/A	(-)	451.27	450.2622	2.2	LPE (16:1)	M-H	407.27, 253.21, 214.04, 196.03, 140.01	N/A	N/A	N/A	21.1	N/A
N/A	(-)	302.2244	301.2166	3.6	C(20:5), Eicosapentaenoic acid	M-H	283.20, 257.22, 229.19, 223.16, 203.17, 191.10, 177.09, 149.13, 135.11, 121.10, 107.08	283.20, 257.22, 229.19, 223.16, 203.17, 191.10, 177.08, 149.13, 135.11, 121.10, 107.08	C20H30O2	302.2245	15.7	-0.3
N/A	(-)	316.2407	317.2485	5.5	Eicosapentaenoic Acid methyl ester	M+H	285.21, 267.21, 201.16, 175.14, 161.13, 147.11, 133.11, 95.08, 81.06, 67.05	285.22, 267.21, 201.15, 175.14, 161.13, 147.11, 135.11, 124.10, 109.10, 95.08, 81.06, 67.05	C21H32O2	316.2402	16.3	1.6
N/A	(-)	689.4993	688.4915	15.4	PE(32:1), PE(16:1/16:0)	M-H	452.27, 281.24, 253.21, 196.03, 140.01	N/A	C37H72NO8P	689.4995	29.7	-0.3
N/A	(-)	507.332	506.3242	4.8	LysoPC(20:1) & something else	N/A	Spectrum is a mixture of fragments coming from more than one compounds (e.g., 508.33). Fragments that can be explained are 196.03 and 309.27 give the ID of LPE(20:1) which corresponds to the 506.32 (which is our target). Other signals are not explained but it seems that they are rather related to the second ion (508.33).				23,1	N/A
N/A	(-)	791.549	790.5412	17.5	PE(40:6), PE(18:0/22:6)	M-H	744.54, 579.21, 506.26, 480.30, 327.23, 283.25, 255.23, 229.19, 196.03, 177.16, 140.01	N/A	C45H78NO8P	791.5464	33.3	3.3
N/A	(+)	397.3196	398.3274	2	Hexadec-enoyl carnitine	M+H	339.25, 283.26, 184.07, 144.10, 114.09, 85.02, 60.08	N/A	C23H43NO4	397.3192	19.2	1.0
LP060	(+)	755.5479	756.5557	14.5	PC(34:3), PC(16:1/18:2)	M+H	573.48, 494.32, 184.07, 166.01, 125.00, 86.09, 60.08	N/A	C42H78NO8P	755.5465	32.1	1.9
LP090	(+)	521.664512	522.3577	3.4	LPC (18:1)	M+H	504.34, 339.28, 184.07, 166.06, 124.99, 104.10, 86.09, 60.08	N/A	C26H52NO7P	521.3481	23.7	4.0
LP072	(+)	807.31782	824.7699	27.7	TG(48:0), TG(16:0/16:0/16:0)	M+NH4+	579.53, 551.50, 523.47, 313.27, 239.23, 95.08, 57.07	N/A	C51H98O6	806.7363	34.6	0.08
N/A	(+)	541.3167	542.3245	2.1	LPC (20:5)	M+H	524.31, 361.27, 258.10, 184.07, 166.06, 124.99, 104.10, 86.09, 69.08	N/A	C28H48NO7P	541.3168	24.4	-0.2
N/A	(+)	779.5481	780.5559	14.575	PC (36:5), PC(16:0/20:5)	M+H	597.48, 496.33, 313.27, 184.07, 166.06, 124.99, 86.09, 60.08	N/A	C44H78NO8P	779.5465	33	2.1
N/A	(+)	741.5315	742.5393	16.3	PE (36:3), PE(18:1/18:2)	M+H	601.51, 337.27, 265.25, 184.07, 95.08	N/A	C41H76NO8P	741.5308	31.6	0.9
N/A	(+)	507.3323	508.3401	2.8	LPC (17:0)	M+H	490.32, 339.28, 228.15, 184.07, 166.06, 124.99, 104.10, 86.09, 60.08	N/A	N/A	507.3323	23.2	0.0
LP035	(+)	551.3955	552.4033	6.6	LPC (20:0)	M+H	534.39, 369.33, 184.07, 166.06, 124.99, 104.10, 86.09, 60.08	N/A	C28H58NO7P	551.395	24.8	0.9
N/A	(+)	537.5132	538.521	15.36	N-Palmitoyl sphingosine	M+H	520.50, 282.28, 264.26, 252.26	502.50, 490.50, 439.19, 339.94, 282.28, 264.26, 252.26, 240.88, 196.89, 100.07, 60.05	C34H67NO3	537.512	24.3	2.2
LP058	(+)	743.5485	744.5563	14.7	PC(33:2), PC(15:0/18:2)	M+H	561.40, 482.32, 184.07, 166.06, 124.99, 86.09, 60.08	N/A	C41H78NO8P	743.5465	31.7	2.7
N/A	(+)	777.5328	778.5406	13.45	PC (36:6)	M+H	719.44, 595.46, 357.06, 184.07, 166.06, 124.99, 86.09, 60.03	N/A	C44H76NO8P	777.5308	32.9	2.6
N/A	(+)	729.532	730.5398	13.75	PC (32:2), PC(14:0/18:2)	M+H	547.47, 468.30, 184.07, 166.06, 124.99, 86.09, 60.08	N/A	C40H76NO8P	729.5308	31.2	1.6
N/A	(+)	507.3323	508.3401	2.8	LPC (17:1)	M+H	490.32, 339.28, 184.07, 166.06, 124.99, 104.06, 86.09, 60.08	N/A	C25H50NO7P	507.3325	23.2	-0.4
N/A	(+)	737.5011	738.5089	14.6	PE (36:5), PE(16:1/20:4)	M+H	597.48, 365.26, 311.25, 269.22, 203.17, 95.08	N/A	$C_{41}H_{72}NO_8P$	737.4995	31.5	2.2
LP071	(+)	799.6114	800.6192	18.2	PC(37:2), PC(18:2/19:0)	M+H	538.38, 339.28, 184.07, 166.06, 124.99, 86.09, 60.08	N/A	C45H86NO8P	799.6091	33.7	2.9
LP058	(+)	743.5485	744.5563	14.7	PC(33:2), PC(18:2/15:0)	M+H	561.48, 482.32, 184.07, 166.06, 124.99, 86.09, 60.08	N/A	C41H78NO8P	743.5465	31.7	N/A
LP053	(+)	717.5307	718.5385	16.82	PE (34:1), PE(18:1/16:0)	M+H	604.59, 577.61, 380.31, 308.29, 265.25, 239.23, 184.07, 95.08, 57.07	N/A	$C_{39}H_{76}NO_8P$	717.5308	30.7	-0.1
N/A	(+)	729.532	730.5398	13.75	PE (35:2), PC(14:0/18:2)	M+H	547.47, 468.30, 184.07, 166.06, 124.99, 86.09, 60.08	N/A	C40H76NO8P	729.5309	31.2	1.5

[Table 2.4]: (CE-MS identification results). (MT: Migration Time; DB: Data Base; CMM: CEU Mass Mediator)

CODE	Name	neutral mas	MT	relative MT	Formula	CEMBIO in house DB	CMM
C01	Glycine betaine	117.079	14.38	0.97	C5H11NO2	●	●
C02	Homocysteine	135.035	14.87	1.00	C4H9NO2S	●	●
C03	amino caprylic acid; Amino octanoic acid	159.126	11.17	0.75	C8H17NO2	●	●
C04	Valine	117.079	12.99	0.87	C5H11NO2	●	●
C05	Leucine	131.094	13.23	0.89	C6H13NO2	●	●
C06	Phenylalanine	165.079	13.98	0.94	C9H11NO2	●	●
C07	Serine	105.043	12.96	0.87	C3H7NO3	●	●
C08	Proline	115.063	13.81	0.93	C5H9NO2	●	●
C09	Glutamic acid	147.054	13.91	0.94	C5H9NO4	●	●
C10	Alanine	89.048	10.06	0.68	C3H7NO2		●
C11	Threonine	119.058	13.48	0.91	C4H9NO3	●	●
C12	Histidine	155.069	10.12	0.68	C6H9N3O2	●	●
C13	Aminocyclopropanecarboxylic acid	101.048	13.89	0.94	C4H7NO2	●	●
C14	Saccharopine	276.131	13.82	0.93	C11H20N2O6		●
C15	Creatinine	113.059	10.02	0.67	C4H7N3O	●	●
C16	Creatine	131.069	11.78	0.79	C4H9N3O2	●	●
C17	Indole acrylate	187.063	13.93	0.94	C11H9NO2		●
C18	Formylindolo carbazole	284.096	15.89	1.07	C19H12N2O		●
C19	Aminoadipic acid	161.069	13.88	0.93	C6H11NO4	●	●
C20	Piperidine	85.09	13.22	0.89	C5H11N		●
C21	Phenyl pyruvic acid	164.047	14.26	0.96	C9H8O3	●	●
C22	Pyrrolidine	71.074	6.92	0.47	C4H9N		●
C23	Ergothioneine	229.089	19.39	1.31	C17H11N		●
C24	Spermidine	145.158	6.7	0.45	C7H19N3	●	●
C25	N-Acetyl spermidine	187.169	8.92	0.60	C9H21N3O		●
C26	Spermine	202.216	6.66	0.45	C10H26N4		●
C27	Carnitine	161.105	11.31	0.76	C7H15NO3	●	●
C28	Acetyl carnitine	203.116	11.88	0.80	C9H17NO4	●	●
C29	Propionyl carnitine	217.131	12.16	0.82	C10H19NO4	●	●
C30	Butyryl carnitine	231.148	12.42	0.84	C11H21NO4		●
C31	Hydroxybutyrylcarnitine	247.142	12.75	0.86	C11H21NO5		●
C32	Neurine	103.1	9.45	0.64	C5H13NO		●
C33	Trimethylamine N-oxide (TMAO)	75.069	9.14	0.62	C3H9NO		●
C34	Hypoxanthine	136.038	14.9	1.00	C5H4N4O	●	●
C35	Succinyl adenosine	383.108	17.44	1.17	C14H17N5O8		●
C36	Ophthalmic acid	289.127	15.97	1.08	C11H19N3O6	●	●
C37	Hydroxymethyl)glutathione	337.094	16.19	1.09	C11H19N3O7S		●
C38	Tripeptide	305.123	16.09	1.08	N/A		●
C39	Tripeptide	357.168	10.74	0.72	N/A		●
C40	Tripeptide	490.207	17.04	1.15	N/A		●
C41	S-Adenosylhomocysteine	384.123	11.73	0.79	C14H20N6O5S		●
C42	Unknown*	185.142	11.79	0.79	C10H19NO2		●
C43	Unknown*	877.57	5.99	0.40	C52H80NO8P		●
C44	Unknown*	132.025	13.64	0.92	C5H8O2S		●
C45	Unknown*	125.12	6.93	0.47	C8H15N		●
C46	Unknown*	835.588	5.99	0.40	C44H85NO11S		●
C47	Unknown*	902.497	11.21	0.75	C49H75O13P		●
C48	4-Aminobutyric acid	103.064	10.48	0.71	C4H9NO2	●	●
C49	Thiamine	264.105	9.23	0.62	C12H17N4OS	●	●

**Identifications marked as "Unknown" are because the proposed hit metabolite from CMM does not belong to biological molecules available to appear in this study according to its characteristics.*

*[**Table 2.5**]: Multiplatform results; TENTATIVE id. CL: Confidence Level, CT (1):Control samples before PH; MCD(2): MCD diet samples before PH; CT-PH(3): Control samples after PH; MCD-PH (4): MCD diet samples after PH; p(DIET): p-value (significancy <0.05) for diet impact; p(PH): p-value for Partial Hepatectomy impact; p(Inter).: p-value for interaction between MCD diet and PH impact.*

Metabolism	Metabolic group/category	CODE	Name	CL	CT (1)	MCD(2)	CT-PH(3)	MCD-PH(4)	p (DIET)	p (PH)	p (Inter.)	log2(2/1)	log2(3/1)	log2(4/2)	log2(4/3)
01 amino acid metabolism	amino acid (proteinogenic)	G134	Glycine	2	0.000389	0.000192	0.000378	0.000308	0.02	0.49	0.23	-1.02	-0.04	0.68	-0.29
	amino acid (proteinogenic)	C10	Alanine	2	118707	121484	4377560	4090357	0.03	0.00	0.01	0.03	5.20	5.07	-0.10
	amino acid (proteinogenic)	G109	Alanine	2	.	.	0.005120	0.001677	0.08	0.00	0.08				-1.61
	amino acid (proteinogenic)	C07	Serine	1	501048	871340	579761	1219930	0.00	0.12	0.31	0.80	0.21	0.49	1.07
	amino acid (proteinogenic)	C11	Threonine	1	442001	685873	771610	1061352	0.01	0.00	0.82	0.63	0.80	0.63	0.46
	amino acid (proteinogenic)	G041	Threonine	1	0.002342	0.003333	0.000896	0.002108	0.08	0.01	0.78	0.51	-1.39	-0.66	1.23
	amino acid (proteinogenic)	G063	Methionine	1	0.128741	0.207295	0.119022	0.162749	0.52	0.00	0.52	0.69	-0.11	-0.35	0.45
	amino acid (proteinogenic)	G094	Histidine	2	0.003559	0.001180	0.003472	0.001487	0.01	0.96	0.65	-1.59	-0.04	0.33	-1.22
	amino acid (proteinogenic)	C12	Histidine	1	1809337	1439328	2779497	1918933	0.01	0.03	0.41	-0.33	0.62	0.41	-0.53
	amino acid (proteinogenic)	C04	Valine	1	843933	713673	1430114	859002	0.00	0.00	0.03	-0.24	0.76	0.27	-0.74
	amino acid (proteinogenic)	G026	Valine	1	0.608639	0.442201	0.759269	0.490335	0.00	0.09	0.36	-0.46	0.32	0.15	-0.63
	amino acid (proteinogenic)	LP005	Valine	2	3338545	121558	4585860.00	270359.64	0.00	0.00	0.00	-4.78	0.46	1.15	-4.08
	amino acid (proteinogenic)	C05	Leucine	1	2429289	2120771	4379665	2679711	0.00	0.00	0.03	-0.20	0.85	0.34	-0.71
	amino acid (proteinogenic)	G040	Isoleucine	1	0.338354	0.264005	0.445251	0.276883	0.00	0.01	0.04	-0.36	0.40	0.07	-0.69
	amino acid (proteinogenic)	C06	Phenylalanine	1	707096	611813	1245183	820495	0.00	0.00	0.04	-0.21	0.82	0.42	-0.60
	amino acid (proteinogenic)	G082	Phenylalanine	1	0.049316	0.039872	0.063768	0.049733	0.02	0.05	0.69	-0.31	0.37	0.32	-0.36
	amino acid (proteinogenic)	G126	Tyrosine	1	0.083468	0.057289	0.101688	0.052024	0.04	0.68	0.46	-0.54	0.28	-0.14	-0.97
	amino acid (proteinogenic)	C08	Proline	1	655495	767505	1330486	1253075	0.91	0.00	0.25	0.23	1.02	0.71	-0.09
	amino acid (proteinogenic)	G042	Proline	1	0.494177	0.428723	0.773681	0.531337	0.03	0.00	0.05	-0.20	0.65	0.31	-0.54
	amino acid (proteinogenic)	C09	Glutamic acid	1	3481658	4411492	5336217	5278716	0.26	0.00	0.07	0.34	0.62	0.26	-0.02
	amino acid (proteinogenic)	G066	Glutamic acid	1	0.446312	0.473183	0.532232	0.719306	0.11	0.04	0.29	0.08	0.25	0.60	0.43
	amino acid (proteinogenic)	G101	Aspartic acid	2	0.000206	0.000158	0.000279	0.000367	0.78	0.02	0.21	-0.38	0.44	1.21	0.39
	amino acid (proteinogenic)	G144	Tryptophan	1	0.021993	0.024352	0.040336	0.030132	0.04	0.00	0.00	0.15	0.88	0.31	-0.42
	amino fatty acid	C03	amino caprylic acid; Amino octanoic acid	1	153469	131728	195069	145031	0.11	0.03	0.09	-0.22	0.35	0.14	-0.43
	glycine metabolism	G014	Sarcosine	1	0.004663	0.002046	0.006634	0.002836	0.00	0.33	0.86	-1.19	0.51	0.47	-1.23
	glycine metabolism	C01	Glycine Betaine	1	8797805	511052	8071187	511052	0.00	0.01	0.01	-4.11	-0.12	0.00	-3.98
	glycine metabolism	C33	Trimethylamine N-oxide (TMAO)	2	34280	124718	85986	88640	0.08	0.62	0.02	1.86	1.33	-0.49	0.04
	glycine metabolism	G057	Amino malonic acid	1	0.018955	0.079975	0.025310	0.092241	0.00	0.19	0.67	2.08	0.42	0.21	1.87
	glycine metabolism	LN04	N-Palmitoyl Glycine	2	11051	38112	.	.	0.00	0.00	0.00	1.79			
	glycine metabolism	G091	Acetol [hydroxy acetone]	1	0.038050	0.027919	0.047658	0.024119	0.02	0.51	0.14	-0.45	0.32	-0.21	-0.98
	glycine metabolism	G012	Oxalic acid	1	3.661822	4.044986	3.270381	5.016310	0.03	0.46	0.09	0.14	-0.16	0.31	0.62
	alanine metabolism	G001	Dodecyl ester-Alanine	2	0.840368	0.740941	0.679046	0.824742	0.68	0.51	0.05	-0.18	-0.31	0.15	0.28
	alanine metabolism	G015	N-methyl alanine	1	0.067321	0.064531	0.054717	0.165616	0.00	0.00	0.00	-0.06	-0.30	1.36	1.60
	methionine metabolism	C02	Homocysteine	1	523140	702046	539307	765528	0.02	0.32	0.55	0.42	0.04	0.12	0.51
	methionine metabolism	G078	Hypo taurine	1	0.015136	0.007240	0.013210	0.003392	0.01	0.31	0.73	-1.06	-0.20	-1.09	-1.96
	methionine metabolism	LP008	Farnesyl cysteine	2	713138	114630	.	.	0.00	0.00	0.00	-2.64			
	Lysine metabolism	C19	Aminoadipic acid	1	340758	752488	625830	3141948	0.06	0.04	0.09	1.14	0.88	2.06	2.33
	Lysine metabolism	C14	Saccharopine	2	65624	79666	101264	261914	0.04	0.00	0.02	0.28	0.63	1.72	1.37
	Lysine metabolism	C20	Piperidine	2	969201	826485	1734545	1053259	0.00	0.00	0.03	-0.23	0.84	0.35	-0.72
	proline metabolism	C22	Pyrrolidine	2	87919	469192	209755	899217	0.00	0.00	0.02	2.42	1.25	0.94	2.10
	proline metabolism	G038	9H-Pyrroloindolone	2	.	.	0.019685	0.018650	0.82	0.00	0.82				-0.08
	proline metabolism	LP002	Proline betaine	2	.	.	242825	9080	0.00	0.00	0.00				-4.74
	proline metabolism	G065	Trans-hydroxyproline	1	0.024324	0.019927	0.049423	0.021540	0.00	0.00	0.00	-0.29	1.02	0.11	-1.20
	histidine metabolism	G068	(Trimethylsilyl)oxyimidazolamine	2	0.046693	0.104961	0.049751	0.075534	0.00	0.11	0.06	1.17	0.09	-0.47	0.60
	histidine metabolism	G175	Phenyl-1H-Benzoimidazole	2	0.073659	0.061262	.	.	0.41	0.00	0.41	-0.27			
	histidine metabolism	G173	Benzimidazole	2	0.018567	0.031206	0.052601	0.099571	0.01	0.00	0.06	0.75	1.50	1.67	0.92
	histidine metabolism	G046	Dimethyl imidazoline	2	0.066161	0.048412	0.050576	0.081196	0.38	0.08	0.00	-0.45	-0.39	0.75	0.68
	histidine metabolism	C23	Ergothioneine	2	655541	181026	604237	185662	0.00	0.81	0.77	-1.86	-0.12	0.04	-1.70
	tryptophan metabolism	C18	Formylindolo carbazole	2	97750	133405	93807	79504	0.52	0.04	0.04	0.45	-0.06	-0.75	-0.24
	tryptophan metabolism	C17	Indole acrylate	2	121137	170835	228988	192069	0.42	0.00	0.00	0.50	0.92	0.17	-0.25
	tryptophan metabolism	G045	H-Indole carboxylic acid	2	0.003439	0.002436	.	.	0.22	0.00	0.22	-0.50			
	tryptophan metabolism	G004	Ethyl-hept-yn-yloctahydroindolizine	2	0.426929	0.630322	0.564075	0.770380	0.01	0.01	0.98	0.56	0.40	0.29	0.45
	tryptophan metabolism	G002	N-acetyl-N-formyl-methoxykynurenamine [AFMK]	2	0.001130	0.001143	0.000623	0.000732	0.83	0.04	0.86	0.02	-0.86	-0.64	0.23
	tryptophan metabolism	G035	Serotonin	2	0.046944	0.054111	.	.	0.69	0.00	0.69	0.20			
	tryptophan metabolism	G031	(1H-Indolyl)methylethylpyrrolidinedione	2	1.194801	1.120788	1.102399	0.848368	0.05	0.01	0.19	-0.09	-0.12	-0.40	-0.38
	tryptophan metabolism	G155	H-Pyrido indole	2	0.033998	0.015981	.	.	0.02	0.00	0.02	-1.09			
	phenylalanine metabolism	C21	Phenyl pyruvic acid	1	396083	421350	775151	524805	0.01	0.00	0.02	0.09	0.97	0.32	-0.56
	phenylalanine metabolism	G080	Phenyl lactic acid	2	0.000780	0.000486	.	.	0.22	0.00	0.22	-0.68			
	phenylalanine metabolism	G159	Phenylacetic acid	2	0.018944	0.016397	0.010343	0.008285	0.34	0.00	0.89	-0.21	-0.87	-0.98	-0.32
	serine metabolism	G010	Ethanolamine	2	1.632753	6.366249	1.587577	8.163563	0.00	0.08	0.07	1.96	-0.04	0.36	2.36
	arginine metabolism	G052	Putrescine	2	0.004337	0.002548	0.001363	0.001599	0.38	0.04	0.27	-0.77	-1.67	-0.67	0.23
	arginine metabolism	C24	Spermidine	1	2952931	5364589	4683999	7582437	0.00	0.00	0.57	0.86	0.67	0.50	0.69

Metabolism	Metabolic group/category	CODE	Name	CL	CT (1)	MCD(2)	CT-PH(3)	MCD-PH(4)	p (DIET)	p (PH)	p (Inter.)	log2(2/1)	log2(3/1)	log2(4/2)	log2(4/3)
	arginine metabolism	C25	N-Acetyl spermidine	2	24697	110902	88248	152653	0.00	0.01	0.45	2.17	1.84	0.46	0.79
	arginine metabolism	C26	Spermine	2	1758330	1100318	1855041	1025248	0.00	0.94	0.58	-0.68	0.08	-0.10	-0.86
	arginine metabolism	C15	Creatinine	1	136941	279783	215728	225082	0.00	0.49	0.00	1.03	0.66	-0.31	0.06
	arginine metabolism	G069	Creatinine	1	0.046289	0.104499	0.049016	0.075141	0.00	0.11	0.06	1.17	0.08	-0.48	0.62
	arginine metabolism	C16	Creatine	1	782971	1611502	1161637	1323677	0.00	0.66	0.01	1.04	0.57	-0.28	0.19
	amino acid (non proteinogenic)	G055	Norvaline	2	0.011430	0.006478	0.022056	0.014772	0.00	0.00	0.31	-0.82	0.95	1.19	-0.58
	glutamic metabolism	G072	Oxo proline	2	0.000585	0.000591	0.000378	0.000308	0.21	0.10	0.03	0.02	-0.63	-0.94	-0.29
	organic acid	G064	Pyroglutamic acid	1	2.293261	3.110035	3.677765	4.882255	0.01	0.00	0.52	0.44	0.68	0.65	0.41
	peptide	G142	Glutathione reduced	2	0.021042	0.044576	0.090319	0.060506	0.69	0.00	0.01	1.08	2.10	0.44	-0.58
	peptide	C37	(Hydroxymethyl)glutathione	2	28008	55801	106663	79259	0.37	0.04	0.13	0.99	1.93	0.51	-0.43
	peptide	LP091	Polypeptide	3	.	.	10957	1	0.00	0.00	0.00				-13.42
	peptide	LP093	Polypeptide	3	.	.	17369	1167	0.00	0.00	0.00				-3.90
	peptide	LP054	Tripeptide	3	.	.	48195	1	0.00	0.00	0.00				-15.56
	peptide	C38	Tripeptide	3	42605	73187	47185	147333	0.00	0.03	0.04	0.78	0.15	1.01	1.64
	peptide	C39	Tripeptide	3	12071	22016	24332	50689	0.06	0.04	0.17	0.87	1.01	1.20	1.06
	peptide	C40	Tripeptide	3	28601	35927	69051	45659	0.22	0.04	0.12	0.33	1.27	0.35	-0.60
02 lipids metabolism	Fatty acid	G086	C(12:0); [Lauric acid]; [Dodecanoic acid]	1	0.016083	0.012194	0.019687	0.014573	0.00	0.00	0.44	-0.40	0.29	0.26	-0.43
	Fatty acid	G137	C(16:0); [Palmitic acid]	1	1.398465	0.966238	1.402944	0.775231	0.00	0.34	0.32	-0.53	0.00	-0.32	-0.86
	Fatty acid	G183	C(16:1); [Hexadecenoic acid]	2	0.074728	0.067898	0.133010	0.140764	0.98	0.00	0.58	-0.14	0.83	1.05	0.08
	Fatty acid	G123	ME(16:1); [Methyl ester Hexadecenoic acid]	2	.	.	0.000745	0.000966	0.59	0.00	0.59				0.38
	Fatty acid	G105	C(14:0); [Myristic acid]	1	0.045299	0.039167	0.054286	0.049675	0.29	0.04	0.86	-0.21	0.26	0.34	-0.13
	Fatty acid	G136	C(16:1); [Palmitoleic acid]	1	0.002646	0.001618	.	.	0.03	0.00	0.03	-0.71			
	Fatty acid	G146	C(18:1); [Oleic acid]	1	0.196671	0.144624	0.179688	0.112279	0.00	0.29	0.74	-0.44	-0.13	-0.37	-0.68
	Fatty acid	G154	C(20:4); [Arachidonic acid]	1	0.002780	0.002999	.	.	0.93	0.00	0.93	0.11			
	Fatty acid	LP024	ME(22:4); [Docosatetraenoic Acid methyl ester]	3	.	.	4041	88265	0.00	0.00	0.00				4.45
	Fatty acid	G145	C(18:2); [Linoleic acid]	1	0.150140	0.121494	0.122191	0.087570	0.05	0.03	0.81	-0.31	-0.30	-0.47	-0.48
	Fatty acid	LP012	C(18:2); [Linoleic acid]	3	.	.	634272	1571568	0.00	0.00	0.00				1.31
	Fatty acid	LP026	C(22:3); [Docosatrienoic acid]	3	.	.	2240351	5208993	0.00	0.00	0.00				1.22
	Fatty acid	LN05	C(22:5); [DPA]; [Docosapentaenoic acid]	2	.	.	542924	5080063	0.00	0.00	0.00				3.23
	Fatty acid	LP017	C(22:5); [DPA]; [Docosapentaenoic acid]	3	.	394867	133821	1212245	0.00	0.00	0.00			1.62	3.18
	Fatty acid	LP022	Cholanoic acid	3	26889	138536	.	.	0.00	0.00	0.00	2.37			
	Acylcarnitine	C27	Carnitine	1	1720764	1335914	2715553	1576341	0.00	0.00	0.05	-0.37	0.66	0.24	-0.78
	Acylcarnitine	C28	Acetyl carnitine	1	899548	273401	1532565	259716	0.00	0.00	0.00	-1.72	0.77	-0.07	-2.56
	Acylcarnitine	C29	Propionyl carnitine	1	70005	29027	161164	63194	0.00	0.00	0.00	-1.27	1.20	1.12	-1.35
	Acylcarnitine	C30	Butyryl carnitine	2	23599	10348	211213	25760	0.00	0.00	0.00	-1.19	3.16	1.32	-3.04
	Acylcarnitine	C31	Hydroxybutyrylcarnitine	2	100792	25782	98260	44419	0.00	0.03	0.35	-1.97	-0.04	0.78	-1.15
	Fatty amide	LP016	N-Oleoyl ethanolamine [OEA]	2	58259	1076204	195830	112547	0.00	0.00	0.00	4.21	1.75	-3.26	-0.80
	Fatty Acyl	LP019	O-Arachidonoyl Glycidol	2	.	.	36150	259197	0.00	0.00	0.00				2.84
	GL	G093	Glycerol -phosphate	1	0.299091	0.172390	0.513722	0.331144	0.00	0.00	0.48	-0.79	0.78	0.94	-0.63
	GL	G157	Palmitoyl glycerol	2	0.002325	0.002643	.	.	0.56	0.00	0.56	0.18			
	GL	G169	Stearoyl glycerol	1	.	.	0.098437	0.036736	0.27	0.01	0.27				-1.42
	CDP-DG	LP088	CDP-DG(39:0)	3	.	.	5125	39097	0.00	0.00	0.00				2.93
	CDP-PE	LN08	CDP-Ethanolamine	2	.	.	158545	400599	0.00	0.00	0.00				1.34
	GL (MG)	LP023	MG(18:1)	3	1457468	4294165	1566209	4130337	0.00	0.00	0.00	1.56	0.10	-0.06	1.40
	GL (MG)	LN06	MG(18:2)	3	.	.	173609	380114	0.00	0.00	0.00				1.13
	GL (MG)	LP018	MG(18:2)	2	.	.	6150863	12128571	0.00	0.00	0.00				0.98
	GL (MG)	LP020	MG(20:4)	3	30428	80595	.	.	0.00	0.00	0.00	1.41			
	GL (MG)	LP027	MG(22:5)	3	90537	980292	.	.	0.00	0.00	0.00	3.44			
	GL (MG//DG)	LP028	MG(20:0)//DG(20:0)	3	.	.	1	139833	0.00	0.00	0.00				17.09
	GL (DG)	LN32	DG(34:1)	2	.	.	218415	700024	0.00	0.00	0.00				1.68
	GL (DG)	LP037	DG(34:1)	2	.	.	6377647	2295710	0.00	0.00	0.00				-1.47
	GL (DG)	LN22	DG(36:3)	2	.	.	96094	219786	0.00	0.00	0.00				1.19
	GL (DG)	LP039	DG(36:5)	2	.	.	162177	1	0.00	0.00	0.00				-17.31
	GL (DG)	LP040	DG(36:4)	3	.	.	1	3410007	0.00	0.00	0.00				21.70
	GL (DG)	LN34	DG(38:6)	3	.	.	56893	573809	0.00	0.00	0.00				3.33
	GL (DG)	LP042	DG(38:5)	3	.	.	13049040	2324567	0.00	0.00	0.00				-2.49
	GL (DG)	LP050	DG(38:5)	3	232305	451763	.	.	0.00	0.00	0.00	0.96			
	GL (DG)	LN30	DG(39:4)	2	.	.	12563	47998	0.00	0.00	0.00				1.93
	GL (DG)	LN29	DG(39:5)	2	.	.	34257	106731	0.00	0.00	0.00				1.64
	GL (DG)	LP051	DG(42:10)	3	.	.	56128	427279	0.00	0.00	0.00				2.93
	GL (DG)	LP056	DG(44:12)	3	.	.	44565	190420	0.00	0.00	0.00				2.10
	GL (DG)	LP098	DG(i-48:0)	3			2782517	4625440	0.00	0.00	0.00				0.73
	GL (TG)	LN23	TG(29:0)	2	.	.	123823	23045	0.00	0.00	0.00				-2.43
	GL (TG)	LN27	TG(30:0)	3	.	.	132180	21893	0.00	0.00	0.00				-2.59
	GL (TG)	LP072	TG(48:0)	3	2209711	660934	712912	540225	0.00	0.00	0.00	-1.74	-1.63	-0.29	-0.40
	GL (TG)	LN50	TG(50:0)	3	.	.	10970	20574	0.00	0.00	0.00				0.91
	GL (TG)	LP075	TG(50:4)	3	2818242	807307	387909	319045	0.00	0.00	0.00	-1.80	-2.86	-1.34	-0.28
	GL (TG)	LP078	TG(51:3)	3	429952	74035	.	.	0.00	0.00	0.00	-2.54			

Metabolism	Metabolic group/category	CODE	Name	CL	CT (1)	MCD(2)	CT-PH(3)	MCD-PH(4)	p (DIET)	p (PH)	p (Inter.)	log2(2/1)	log2(3/1)	log2(4/2)	log2(4/3)
	GL (TG)	LP080	TG(54:6)	3	15200000	6063481	.	.	0.00	0.00	0.00	-1.33			
	GL (TG)	LP079	TG(54:7)	3	12150000	5166307	2943639	2741345	0.00	0.00	0.00	-1.23	-2.05	-0.91	-0.10
	GL (TG)	LN74	TG(58:5)	3	11455	34847	.	.	0.00	0.00	0.00	1.61			
	GL (TG)	LP087	TG(61:14)	2	.	.	3647	30505	0.00	0.00	0.00				3.06
	GL (TG)	LP029	TG(O-52:0)	2	.	.	236132	329680	0.00	0.00	0.00				0.48
	GL (TG)	LN63	TG(O-56:7)	3	.	.	14309	6740	0.00	0.00	0.00				-1.09
	GP (PA)	LN07	LPA(16:0)	2	.	.	55470	32661	0.00	0.00	0.00				-0.76
	GP (PC//PE)	LN13	LPC(16:0)//LPE(19:0)	2	.	.	328299	172884	0.00	0.00	0.00				-0.93
	GP (PC//PE)	LP033	LPC(16:0)//PC(O-16:0)//LPE(19:0)	2	11592846	5918532	79262500	42539286	0.00	0.00	0.00	-0.97	2.77	2.85	-0.90
	GP (PC)	LN24	LPC(22:5)	3	.	.	119614	48467	0.00	0.00	0.00				-1.30
	GP (PC)	LP041	LPC(24:1)	2	.	.	101018	37391	0.00	0.00	0.00				-1.43
	GP (PE)	LN12	LPE(22:5)	2	149507	62110	.	.	0.00	0.00	0.00	-1.27			
	GP (PS)	LP083	LPS(12:0)	3	.	.	19893	70561	0.00	0.00	0.00				1.83
	GP (PS)	LN14	LPS(20:2)	3	.	.	107950	185122	0.00	0.00	0.00				0.78
	GP (PC//PE)	LP089	LPS(O-18:0)	3	.	.	171378	15400	0.00	0.00	0.00				-3.48
	GP (PC)	LP034	PC(20:1)	2	96071	38759	655153	132958	0.00	0.00	0.00	-1.31	2.77	1.78	-2.30
	GP (PC//PE)	LN35	PC(20:1)//PE(33:1)	2	.	.	54359	13016	0.00	0.00	0.00				-2.06
	GP (PC//PE)	LN36	PC(32:1)//PE(35:1)	3	8117	14919	60375	23083	0.00	0.00	0.00	0.88	2.89	0.63	-1.39
	GP (PC//PE)	LN49	PC(33:0)//PE(36:0)	3	.	.	222692	133156	0.00	0.00	0.00				-0.74
	GP (PC//PE)	LP061	PC(33:2)//PE(36:2)	3	.	.	51737500	19810714	0.00	0.00	0.00				-1.38
	GP (PC//PE)	LN37	PC(33:5)//PE(36:5)	3	.	.	4944472	2806527	0.00	0.00	0.00				-0.82
	GP (PC//PE)	LN47	PC(34:2)//PE(37:2)	3	.	.	7207278	4149744	0.00	0.00	0.00				-0.80
	GP (PC//PE)	LN52	PC(34:2)//PE(37:2)	3	2986220	499221	.	.	0.00	0.00	0.00	-2.58			
	GP (PC)	LP060	PC(34:3)	2	102275000	41728571	.	.	0.00	0.00	0.00	-1.29			
	GP (PC//PE)	LN45	PC(34:3)//PE(37:3)	3	.	.	10272110	4704263	0.00	0.00	0.00				-1.13
	GP (PC//PE)	LP064	PC(35:1)//PE(38:1)	3	.	.	6390058	745366	0.00	0.00	0.00				-3.10
	GP (PC//PE)	LP062	PC(35:3)//PE(38:3)	3	.	.	5715933	746002	0.00	0.00	0.00				-2.94
	GP (PC//PE)	LP065	PC(36:3)//PE(39:3)	3	.	.	336375000	117464286	0.00	0.00	0.00				-1.52
	GP (PC//PE)	LP071	PC(37:2)//PE(42:5)	3	.	.	1251625	289479	0.00	0.00	0.00				-2.11
	GP (PC//PE)	LN60	PC(37:7)//PE(40:7)	3	37521	94091	.	.	0.00	0.00	0.00	1.33			
	GP (PC//PE)	LN66	PC(38:2)//PE(41:2)	3	.	.	429899	185404	0.00	0.00	0.00				-1.21
	GP (PC//PE)	LP070	PC(38:3)//PE(41:3)	3	.	.	150525000	40425000	0.00	0.00	0.00				-1.90
	GP (PC//PE)	LP069	PC(38:4)//PE(41:4)	3	.	.	190875000	422714286	0.00	0.00	0.00				1.15
	GP (PC//PE)	LN58	PC(38:7)//PE(41:7)	3	.	.	3067821	1079846	0.00	0.00	0.00				-1.51
	GP (PC//PE)	LP066	PC(38:7)//PE(41:7)	3	.	.	656636	2311835	0.00	0.00	0.00				1.82
	GP (PC//PE)	LP074	PC(38:7)//PE(41:7)	3	.	.	251673	92474	0.00	0.00	0.00				-1.44
	GP (PC)	LP076	PC(42:7)	3	.	.	5409752	467873	0.00	0.00	0.00				-3.53
	GP (PI)	LP090	PC(O-18:1)//LPC(18:1)//LPE(20:1)	3	128900	15895	.	.	0.00	0.00	0.00	-3.02			
	GP (PC)	LP035	PC(O-20:0)	3	967791	161104	.	.	0.00	0.00	0.00	-2.59			
	GP (PC)	LN21	PC(P-20:0)//PC(O-20:1)	3	.	.	132083	35741	0.00	0.00	0.00				-1.89
	GP (PE)	LP053	PE(34:1)	2	.	.	1094845	57967	0.00	0.00	0.00				-4.24
	GP (PE)	LP057	PE(36:2)	2	.	.	11514578	3233351	0.00	0.00	0.00				-1.83
	GP (PE)	LP081	PE(48:1)	2	940750	279319	.	.	0.00	0.00	0.00	-1.75			
	GP (PE)	LN40	PE(O-34:0)	2	.	.	82305	49439	0.00	0.00	0.00				-0.74
	GP (PE)	LP059	PE(P-38:6)	3	.	.	40246	337511	0.00	0.00	0.00				3.07
	GP (PG)	LN44	PG(38:4)	3	.	.	164444	302065	0.00	0.00	0.00				0.88
	GP (PG)	LN43	PG(38:6)	3	.	.	447300	2044574	0.00	0.00	0.00				2.19
	GP (PG)	LN51	PG(40:6)	3	.	.	638608	3721939	0.00	0.00	0.00				2.54
	GP (PG)	LN57	PG(42:10)	3	.	.	256918	1632001	0.00	0.00	0.00				2.67
	GP (PG)	LP073	PG(42:10)	3	.	.	1	94433	0.00	0.00	0.00				16.53
	GP (PG)	LP082	PG(43:6)	2	.	.	81216	9439	0.00	0.00	0.00				-3.11
	GP (PG)	LN73	PG(44:8)	2	.	.	124776	75911	0.00	0.00	0.00				-0.72
	GP (PI)	LN55	PI(34:2)	2	.	.	12216800	3835183	0.00	0.00	0.00				-1.67
	GP (PI)	LP030	PI(34:3)	2	.	.	1	261298	0.00	0.00	0.00				18.00
	GP (PI)	LN61	PI(36:3)	2	.	.	34714286	9348031	0.00	0.00	0.00				-1.89
	GP (PI)	LN67	PI(38:5)	2	.	.	55042857	21225000	0.00	0.00	0.00				-1.37
	GP (PI)	LN68	PI(39:5)	2	.	.	752512	209045	0.00	0.00	0.00				-1.85
	GP (PI)	LN70	PI(40:7)	2	.	.	844692	424863	0.00	0.00	0.00				-0.99
	GP (PI)	LP085	PI(44:4)	2	24410	47647	.	.	0.00	0.00	0.00	0.96			
	GP (PIP)	LP084	PIP(36:4)	3	24694	41208	.	.	0.00	0.00	0.00	0.74			
	GP (PS)	LN33	PS(28:2)	2	.	.	8126	61890	0.00	0.00	0.00				2.93
	GP (PS)	LP055	PS(31:3)	3	.	.	6454	79907	0.00	0.00	0.00				3.63
	GP (PS)	LP063	PS(36:0)	3	.	.	230156	57118	0.00	0.00	0.00				-2.01
	GP (PS)	LN42	PS(37:7)	3	13639	8950	6911842	21787500	0.00	0.00	0.00	-0.61	8.99	11.25	1.66
	GP (PS)	LN54	PS(39:1)	3	.	.	5520508	2161453	0.00	0.00	0.00				-1.35
	GP (PS)	LN64	PS(39:3)	3	.	.	1032279	558754	0.00	0.00	0.00				-0.89
	GP (PS)	LN48	PS(39:4)	3	19367	45926	.	.	0.00	0.00	0.00	1.25			
	GP (PS)	LN69	PS(41:4)	3	.	.	292958	130395	0.00	0.00	0.00				-1.17

Metabolism	Metabolic group/category	CODE	Name	CL	CT (1)	MCD(2)	CT-PH(3)	MCD-PH(4)	p (DIET)	p (PH)	p (Inter.)	log2(2/1)	log2(3/1)	log2(4/2)	log2(4/3)
	GP (PS)	LN71	PS(42:9)	3	.	.	21185	41326	0.00	0.00	0.00				0.96
	GP (PS)	LN65	PS(43:6)	3	.	.	1543479	810521	0.00	0.00	0.00				-0.93
	GP (PS)	LN10	PS(O-16:0)	2	.	.	31098	25138	0.00	0.00	0.00				-0.31
	GP (PS)	LN39	PS(O-34:0)	**3**	.	.	8894	5350	0.00	0.00	0.00				-0.73
	GP (PS)	LN59	PS(O-38:1)//PS(P-38:0)	3	.	.	185211	108989	0.00	0.00	0.00				-0.76
	SP (Acidic GSP)	LN76	Ganglioside GM1 (36:2)	2	.	.	167331	114393	0.00	0.00	0.00				-0.55
	SP (Cer.)	LN18	Cer(d33:1)	2	.	.	49478	134677	0.00	0.00	0.00				1.44
	SP (Cer.)	LN20	Cer(d32:2(2OH))	2	.	.	12611	72789	0.00	0.00	0.00				2.53
	SP (Cer.)	LN26	CerP(d34:1)	2	.	.	33096	54922	0.00	0.00	0.00				0.73
	SP (Cer.)	LN28	Cer(d38:2)	2	.	.	19390	50610	0.00	0.00	0.00				1.38
	SP (Cer.)	LP045	Cer(d36:2(2OH))	3	.	.	1	167724	0.00	0.00	0.00				17.36
	SP (CerP)	LP052	CerP(d42:1)	**3**	.	.	67982	118356	0.00	0.00	0.00				0.80
	SP (GlcCer)	LN41	GlcCer(d34:2)	2	.	.	19214286	8906263	0.00	0.00	0.00				-1.11
	SP (Neutral GSP)	LP086	NeuAc-Gal-Cer(d34:0)	3	2823361	581701	676003	146814	0.00	0.00	0.00	-2.28	-2.06	-1.99	-2.20
	SP (PE-Cer.)	LN31	PE-Cer(d34:1)	2	.	.	32348	71526	0.00	0.00	0.00				1.14
	SP (PS)	LN62	PS (39:4)	3	.	.	433420	215531	0.00	0.00	0.00				-1.01
	SP (SM)	LN38	SM(d34:1)	3	5401725	13512500	10828571	18387500	0.00	0.00	0.00	1.32	1.00	0.44	0.76
	SP (Sphingoid base)	G153	Sphingosine	2	0.000186	0.000211	0.000378	0.000308	0.00	0.00	0.81	0.18	1.02	0.55	-0.29
	ST	G179	Cholesterol	1	2.426872	2.408718	3.989900	2.654093	0.18	0.00	0.03	-0.01	0.72	0.14	-0.59
	ST (bile acids and der.)	G177	Cholest-ene	2	0.003351	0.001683	0.002220	0.005670	0.23	0.18	0.02	-0.99	-0.59	1.75	1.35
	ST (bile acids and der.)	LN11	Taurocholic acid	2	.	.	369699	123542	0.00	0.00	0.00				-1.58
	ST (bile acids and der.)	LP025	Hydroxyoxocholenoic acid	2	.	.	2784	57240	0.00	0.00	0.00				4.36
	ST (Chol. And der.)	LN16	Cholesterol glucuronide	2	.	.	19650	6574	0.00	0.00	0.00				-1.58
	ST (Chol. And der.)	LP047	CE(17:1)	2	.	.	10569	94016	0.00	0.00	0.00				3.15
	ST (Chol. And der.)	LP048	CE(18:3)	3	128805	26788	.	.	0.00	0.00	0.00	-2.27			
	ST (Chol. And der.)	LP049	CE(MonoMe(11,3))	3	.	.	1100126	2178346	0.00	0.00	0.00				0.99
	ST (Chol. And der.)	LN19	Cholesteryl-alpha-D-glucoside	2	.	.	328620	164008	0.00	0.00	0.00				-1.00
	ST (Chol. And der.)	LP044	CE(16:0)	2	94969	32957	.	.	0.00	0.00	0.00	-1.53			
	Fatty Acyl CoAs	LP094	CoA (26:0) //Hexacosanoyl-CoA//Cerotoyl-CoA	3	.	.	27797	2948	0.00	0.00	0.00				-3.24
	Fatty Acyl	LP011	Keto pentadecanoic acid	3	.	.	29803	90389	0.00	0.00	0.00				1.60
03 organic acids and der.	organic acid	G005	Pyruvic acid	1	0.227308	0.202825	0.117686	0.119883	0.70	0.00	0.47	-0.16	-0.95	-0.76	0.03
	organic acid	G007	Lactic acid	1	2.123848	1.103529	3.253682	1.964868	0.00	0.00	0.35	-0.94	0.62	0.83	-0.73
	organic acid	G062	Malic acid	1	0.089760	0.082099	0.067764	0.123468	0.07	0.38	0.01	-0.13	-0.41	0.59	0.87
	organic acid	G047	Fumaric acid	1	0.141166	0.108092	0.110535	0.179958	0.25	0.07	0.00	-0.39	-0.35	0.74	0.70
	organic acid	G096	Citric acid	1	0.008433	0.013067	0.005784	0.012203	0.00	0.25	0.55	0.63	-0.54	-0.10	1.08
	organic acid	G008	Dihydroxy propanoic acid	2	0.422216	0.299601	0.401128	0.420004	0.39	0.09	0.02	-0.49	-0.07	0.49	0.07
	organic acid	G070	Trihydroxy butyric acid	2	0.019002	0.023898	.	.	0.31	0.00	0.31	0.33			
	organic acid	G013	Hydroxybutyric acid	1	0.041670	0.035026	0.025909	0.029692	0.81	0.02	0.23	-0.25	-0.69	-0.24	0.20
	organic acid	G017	Propanoic acid	2	0.000331	0.000495	.	.	0.47	0.00	0.47	0.58			
	organic acid	G020	Phosphonomycin	2	0.324303	0.222573	0.135509	0.124595	0.09	0.00	0.14	-0.54	-1.26	-0.84	-0.12
	organic acid	G024	Malonic acid	2	0.047959	0.034972	0.167263	0.101443	0.08	0.00	0.18	-0.46	1.80	1.54	-0.72
	organic acid	G027	Methylmalonic acid	1	0.000336	0.000404	.	.	0.97	0.00	0.97	0.27			
	organic acid	G073	Malonic acid diethyl ester	2	0.006485	0.005994	.	.	0.50	0.00	0.50	-0.11			
	organic acid	G033	Benzoic acid	1	0.012378	0.006976	0.013190	0.007700	0.00	0.50	0.97	-0.83	0.09	0.14	-0.78
	organic acid	G049	Nonanoic acid	2	0.068266	0.107776	.	.	0.06	0.00	0.06	0.66			
	organic acid	G050	Methyl p-tolyloxyacetate	2	.	.	0.004178	0.004275	0.80	0.00	0.80				0.03
	organic acid	G056	Tartronic acid	1	.	.	0.004335	0.024899	0.00	0.00	0.00				2.52
	organic acid	G071	Hydroxy nicotinic acid	2	0.009578	0.003718	0.009978	0.004531	0.00	0.54	0.83	-1.37	0.06	0.29	-1.14
	organic acid	G074	Pentane dioic acid	1	0.010102	0.009660	0.020546	0.010698	0.00	0.00	0.01	-0.06	1.02	0.15	-0.94
	organic acid	G076	Methyl ester iodo Propenoic acid	2	0.041303	0.023832	0.028598	0.028491	0.03	0.38	0.07	-0.79	-0.53	0.26	-0.01
	organic acid	G083	Hydroxybenzoic acid	2	0.008740	0.005712	0.010500	0.007293	0.01	0.11	0.93	-0.61	0.26	0.35	-0.53
	organic acid	G089	Gentisic acid	2	.	.	0.001265	0.000930	0.55	0.00	0.55				-0.44
	organic acid	G097	Phthalic acid, diamide	2	0.007855	0.002249	.	.	0.01	0.00	0.01	-1.80			
	organic acid	G135	Adipic acid	2	0.044740	0.009817	0.037737	0.010881	0.00	0.47	0.33	-2.19	-0.25	0.15	-1.79
	organic acid	G165	Lactobionic acid	1	2.264494	2.160984	0.246842	0.333730	0.98	0.00	0.81	-0.07	-3.20	-2.69	0.44
	organic acid	G181	Dihydroxy dehydroabietic acid	2	0.022820	0.011455	.	.	0.35	0.00	0.35	-0.99			
	organic acid	LP010	Propionyl choline	3	.	.	13724	53804	0.00	0.00	0.00				1.97
	organic acid	C36	Ophthalmic acid	1	174268	47687	126754	245409	0.90	0.07	0.01	-1.87	-0.46	2.36	0.95
	organic acid	C48	4-Aminobutyric acid	2	66131	84990	113506	148054	0.25	0.00	0.99	0.36	0.78	0.80	0.38
04 nucleotides metabolism	purine metabolism	G095	Hypoxanthine	1	0.005058	0.031189	0.018855	0.050962	0.00	0.02	0.66	2.62	1.90	0.71	1.43
	purine metabolism	C34	Hypoxanthine	1	74752	248622	73795	308788	0.02	0.48	0.46	1.73	-0.02	0.31	2.07
	purine metabolism	LN01	Methyl hypoxanthine	3	.	.	383609	267878	0.00	0.00	0.00				-0.52
	purine metabolism	G108	Adenine	1	0.054221	0.028194	0.014250	0.015517	0.03	0.00	0.02	-0.94	-1.93	-0.86	0.12
	purine metabolism	G058	Tetrahydro methyl(nitrophenyl)oxazolopurinedione	2	0.295012	0.239222	.	.	0.21	0.00	0.21	-0.30			
	purine metabolism	G158	Inosine	1	0.041493	0.019631	0.014660	0.015489	0.05	0.00	0.01	-1.08	-1.50	-0.34	0.08
	purine metabolism	G176	Inosine -monophosphate	1	0.028650	0.045024	0.167972	0.105720	0.31	0.00	0.00	0.65	2.55	1.23	-0.67
	purine metabolism	C35	Succinyl adenosine	2	66576	133161	96225	119654	0.03	0.61	0.21	1.00	0.53	-0.15	0.31
	purine metabolism	C41	S-Adenosylhomocysteine; [SAM]	2	115310	294059	276295	303099	0.00	0.01	0.01	1.35	1.26	0.04	0.13

Metabolism	Metabolic group/category	CODE	Name	CL	CT (1)	MCD(2)	CT-PH(3)	MCD-PH(4)	p (DIET)	p (PH)	p (Inter.)	log2(2/1)	log2(3/1)	log2(4/2)	log2(4/3)
	pyrimidine metabolism	G003	Pyridine carboxylic acid methyl ester	2	0.004458	0.005391	.	.	0.48	0.00	0.48	0.27			
	pyrimidine metabolism	G006	Hydroxy pyridine	1	.	.	0.002601	0.004441	0.05	0.00	0.05				0.77
	pyrimidine metabolism	G170	Cytidine	2	0.015193	0.007938	0.005588	0.001767	0.01	0.00	0.39	-0.94	-1.44	-2.17	-1.66
	pyrimidine metabolism	G009	Dioxide Pyrazine	2	.	.	0.000556	0.000356	0.04	0.00	0.04				-0.64
	pyrimidine metabolism	G030	Aminotrimethylenepyridine	2	1.311042	1.243430	1.177514	0.933654	0.06	0.00	0.18	-0.08	-0.15	-0.41	-0.33
	pyrimidine metabolism	G034	Aminocyanobutyltrimethylenepyrimidine	2	.	.	1.228879	0.899112	0.05	0.00	0.05				-0.45
	pyrimidine metabolism	G075	4H-Pyridopyrimidinecarboxylic acid	2	.	.	0.008175	0.009092	0.35	0.00	0.35				0.15
	pyrimidine metabolism	G084	Aminophenyldiphenylpyrimidine	2	0.015555	0.006930	0.018339	0.007802	0.00	0.05	0.28	-1.17	0.24	0.17	-1.23
	pyrimidine metabolism	G178	Tetramethyl -pyridinetetracarboxylate	2	2.219387	1.996421	3.467864	2.300218	0.09	0.01	0.06	-0.15	0.64	0.20	-0.59
	pyrimidine metabolism	G172	Uridine -monophosphate	2	0.030910	0.053306	0.085896	0.165582	0.01	0.00	0.07	0.79	1.47	1.64	0.95
05 carbohydrate metabolism	monosaccharide (pentose)	G148	Ribose	2	0.011554	0.023793	.	.	0.05	0.00	0.05	1.04			
	monosaccharide (hexose)	G140	Glucose	2	0.005875	0.004467	0.005748	0.003516	0.03	0.59	0.68	-0.40	-0.03	-0.35	-0.71
	monosaccharide (hexose)	G103	Tagatose	1	0.018436	0.014102	.	.	0.36	0.00	0.36	-0.39			
	monosaccharide (hexose)	G107	Sorbose	1	0.207562	0.094964	0.048641	0.022271	0.03	0.00	0.13	-1.13	-2.09	-2.09	-1.13
	monosaccharide (heptose)	G110	Methyl galactoside	1	0.798318	0.424045	0.173196	0.101818	0.03	0.00	0.14	-0.91	-2.20	-2.06	-0.77
	monosaccharide (hexose)	G116	Mannose	2	4.758267	6.151832	9.383475	14.235447	0.02	0.00	0.23	0.37	0.98	1.21	0.60
	monosaccharide (hexose)	G117	Galactose	1	4.451449	4.930993	9.129128	13.855603	0.02	0.00	0.11	0.15	1.04	1.49	0.60
	monosaccharide (hexose)	G118	Altrose	1	4.269702	2.850666	6.138355	5.794370	0.41	0.01	0.51	-0.58	0.52	1.02	-0.08
	monosaccharide (hexose)	G120	Talose	1	4.507889	2.592739	7.058928	3.638885	0.01	0.02	0.30	-0.80	0.65	0.49	-0.96
	monosaccharide (hexose)	G138	Allose	2	0.005039	0.004256	0.004412	0.005675	0.71	0.44	0.06	-0.24	-0.19	0.42	0.36
	oligosaccharide (disaccharide)	G162	Sucrose	1	0.006889	0.005991	0.002868	0.002729	0.76	0.05	0.82	-0.20	-1.26	-1.13	-0.07
	oligosaccharide (disaccharide)	G163	Maltose	1	0.174269	0.175042	0.034118	0.055809	0.78	0.00	0.76	0.01	-2.35	-1.65	0.71
	oligosaccharide (disaccharide)	G164	Lactose	1	0.187140	0.175733	0.039023	0.053237	0.97	0.00	0.68	-0.09	-2.26	-1.72	0.45
	oligosaccharide (disaccharide)	G166	Trehalose	2	.	.	0.065082	0.086269	0.04	0.00	0.04				0.41
	oligosaccharide (disaccharide)	G171	Sophorose	2	.	.	0.003049	0.001966	0.09	0.00	0.09				-0.63
	polysaccharide (trisaccharide)	G182	Maltotriose	2	0.033663	0.040824	0.002242	0.005319	0.40	0.00	0.40	0.28	-3.91	-2.94	1.25
	phosphorylated monosaccharide (pentose)	G139	Ribose-phosphate	1	.	.	0.002708	0.002513	0.13	0.00	0.13				-0.11
	phosphorylated monosaccharide (tetrose)	G143	Erythrose-phosphate	2	0.015164	0.005842	0.020714	0.012912	0.00	0.00	0.65	-1.38	0.45	1.14	-0.68
	phosphorylated monosaccharide (hexose)	G151	Glucose-phosphate	2	0.000160	0.000194	0.000378	0.000308	0.04	0.00	0.42	0.28	1.24	0.67	-0.29
	phosphorylated amino monosaccharide (hexose)	G098	Glucosamine phosphate	1	.	.	0.034246	0.056088	0.09	0.00	0.09				0.71
	Uronic acid	G114	Gluconic acid lactone		5.995464	6.018586	13.318696	14.922985	0.60	0.00	0.69	0.01	1.15	1.31	0.16
	Lactone	G122	Galactonolactone	1	1.378505	0.717951	1.850678	0.880756	0.02	0.34	0.64	-0.94	0.42	0.29	-1.07
	Uronic acid	G130	Galacturonic acid	1	.	.	0.069275	0.044063	0.15	0.00	0.15				-0.65
	Uronic acid	G133	Gluconic acid	1	0.000213	0.000149	0.002128	0.001602	0.78	0.01	0.85	-0.51	3.32	3.43	-0.41
	polyalcohol	G092	Arabitol	1	0.025395	0.012520	0.012218	0.009126	0.04	0.03	0.18	-1.02	-1.06	-0.46	-0.42
	polyalcohol	G100	Anhydrohexitol	2	.	.	0.017038	0.037512	0.00	0.00	0.00				1.14
	polyalcohol	G129	Mannitol	1	0.021926	0.031460	0.256354	0.063611	0.01	0.00	0.01	0.52	3.55	1.02	-2.01
	polyalcohol	G113	Inositol	2	0.384284	0.237686	0.628737	0.354931	0.00	0.00	0.23	-0.69	0.71	0.58	-0.82
	polyalcohol	G150	Scyllo-Inositol der.		0.099258	0.058752	0.019631	0.022771	0.28	0.00	0.13	-0.76	-2.34	-1.37	0.21
	polyalcohol	G168	Lactitol	2	0.083606	0.074956	0.007824	0.010396	0.84	0.00	0.72	-0.16	-3.42	-2.85	0.41
	polyalcohol	G132	Glucitol	2	0.287541	0.184936	0.283259	0.133534	0.03	0.52	0.59	-0.64	-0.02	-0.47	-1.08
06 Prosthetic groups	vitamin	C49	Thiamine	2	61519	50135	111929	65709	0.01	0.00	0.05	-0.30	0.86	0.39	-0.77
	vitamin	G059	Nicotinamide	1	0.378913	0.264668	0.292879	0.236685	0.00	0.01	0.01	-0.52	-0.37	-0.16	-0.31
	vitamin der.	G061	Methyl nicotinamide	2	0.527005	0.362772	0.393060	0.236729	0.00	0.00	0.86	-0.54	-0.42	-0.62	-0.73
	vitamin der.	G124	Dehydroascorbic acid	1	0.139537	0.240028	0.192737	0.271342	0.00	0.01	0.45	0.78	0.47	0.18	0.49
	Hemoglobin metabolism	G032	Ethylpyrrolidinol	2	.	.	0.005092	0.004891	0.98	0.00	0.98				-0.06
	Hemoglobin metabolism	G060	(1H)Pyrrole carbonitrile	2	0.069135	0.046712	0.056088	0.044276	0.00	0.01	0.05	-0.57	-0.30	-0.08	-0.34
07 other metabolism and der.	inorganic acid	G037	Phosphoric acid	1	8.471409	11.329063	16.541242	16.983202	0.34	0.00	0.32	0.42	0.97	0.58	0.04
	inorganic acid	G088	Pyrophosphate	1	0.316424	0.246719	0.610648	0.509663	0.26	0.00	0.77	-0.36	0.95	1.05	-0.26
	nitrogenated compounds	G016	Lactamide	1	.	.	0.000563	0.000588	0.90	0.00	0.90				0.06
	nitrogenated compounds	G021	N- methyl-N'-phenylthiourea	2	.	.	0.000610	0.000839	0.52	0.00	0.52				0.46
	organic acid	G087	Methoxy-N-phenylTriazinamine	2	.	.	0.035895	0.030252	0.41	0.00	0.41				-0.25
	nitrogenated compounds	G111	Ethyl-N-allylbenzamide	2	1.239316	0.661130	0.212970	0.118040	0.03	0.00	0.13	-0.91	-2.54	-2.49	-0.85
	organic compound	G156	(Phenylmethyl)amino benzaldehyde	2	0.017489	0.022480	0.008430	0.009606	0.49	0.02	0.65	0.36	-1.05	-1.23	0.19
	natural monoamine alkaloid	G147	N-Benzyl phenethylamine	2	0.010259	0.065184	0.007370	0.054290	0.00	0.14	0.38	2.67	-0.48	-0.26	2.88
	contaminant? From coal	G128	Pyrenamine	2	0.021491	0.013441	.	.	0.01	0.00	0.01	-0.68			
	choline der.	C32	Neurine	2	2196773	1692174	3141592	1374894	0.00	0.28	0.05	-0.38	0.52	-0.30	-1.19
	organic compound	G149	Hydroxyanthraquinone	2	.	.	0.000621	0.001400	0.03	0.00	0.03				1.17
	natural monoterpenoid	G043	Thymol	2	0.029232	0.023555	0.030790	0.024453	0.02	0.61	0.89	-0.31	0.07	0.05	-0.33
	enzyme	G077	Hydroxy biphenyl	2	0.324985	0.209241	0.248276	0.182659	0.00	0.09	0.39	-0.64	-0.39	-0.20	-0.44
	organic compound	G131	Hydroxyheptene	2	0.004170	0.002605	0.006250	0.003138	0.01	0.12	0.35	-0.68	0.58	0.27	-0.99
	monoterpenoid	LP001	Dimethyl octatriene	3	72636	78387	1168788	15510	0.00	0.00	0.00	0.11	4.01	-2.34	-6.24
	organic compound	LP009	Phenyl heptane	3	.	.	55485	135358	0.00	0.00	0.00				1.29
	organic compound	G054	Undecane	2	.	.	0.001000	0.000863	0.79	0.00	0.79				-0.21
	sulfonated compounds	G011	Ethylthiomethylpentane	2	0.005820	0.025717	0.005101	0.029433	0.00	0.57	0.40	2.14	-0.19	0.19	2.53
	sulfonated compounds	G039	Ethyl methanesulphonyl acetate	2	.	.	0.025650	0.024393	0.87	0.00	0.87				-0.07
	etilene metabolite	C13	Aminocyclopropanecarboxylic acid	1	496448	589761	750574	722149	0.51	0.00	0.18	0.25	0.60	0.29	-0.06
	hydrocarbon	G023	Acetylmethylthiophenecarbaldehyde	2	.	.	0.001319	0.002492	0.02	0.00	0.02				0.92

Metabolism	Metabolic group/category	CODE	Name	CL	CT (1)	MCD(2)	CT-PH(3)	MCD-PH(4)	p (DIET)	p (PH)	p (Inter.)	log2(2/1)	log2(3/1)	log2(4/2)	log2(4/3)
	hydrocarbon	G025	Morpholino propanediol	2	.	.	0.001267	0.001831	0.30	0.00	0.30				0.53
	hydrocarbon	G028	MethylButenol	2	0.010843	0.008693	0.010921	0.012016	0.59	0.04	0.05	-0.32	0.01	0.47	0.14
	hydrocarbon	G029	Dimethoxyphenyl propane	2	.	.	0.394542	0.357968	0.76	0.00	0.76				-0.14
	Fatty alcohol	G044	Pentadecanol	2	0.002612	0.010935	.	.	0.04	0.00	0.04	2.07			
	hydrocarbon	G051	Amino acetaldehyde dimethyl acetal	1	0.001357	0.000803	.	.	0.08	0.00	0.08	-0.76			
	hydrocarbon	G053	Propanoldimethoxyacetate	2	0.007768	0.010730	.	.	0.31	0.00	0.31	0.47			
	hydrocarbon	G081	aminomethylpropanediol	2	0.066844	0.053733	0.088592	0.068712	0.02	0.03	0.67	-0.31	0.41	0.35	-0.37
	hydrocarbon	G106	Methyl-But-yn-ol	2	0.054150	0.028152	0.014250	0.015517	0.03	0.00	0.02	-0.94	-1.93	-0.86	0.12
	hydrocarbon	G141	Octadecanol	2	0.034614	0.026055	0.040662	0.031533	0.01	0.06	0.92	-0.41	0.23	0.28	-0.37
	hepatotoxicity marker	G127	Methyl mercaptopurine	2	0.000546	0.000562	0.000811	0.000991	0.72	0.20	0.73	0.04	0.57	0.82	0.29
	N/A	LN15	Unknown	4	.	.	80771	42870	0.00	0.00	0.00				-0.91
08 Unknown	N/A	LP015	Unknown	4	42042	32534	84656	395611	0.00	0.00	0.00	-0.37	1.01	3.60	2.22
	N/A	LN46	unknown	4	.	.	469742	231906	0.00	0.00	0.00				-1.02
	N/A	LN53	unknown	4	.	.	144000	267910	0.00	0.00	0.00				0.90
	N/A	LN56	unknown	4	.	.	121861	75126	0.00	0.00	0.00				-0.70
	N/A	LN75	unknown	4	.	.	142206	85213	0.00	0.00	0.00				-0.74
	N/A	LP006	Unknown	4	3338545	121558	.	.	0.00	0.00	0.00	-4.78			
	N/A	LP021	Unknown	4	.	19561	.	.	0.00	0.00	0.00				
	N/A	LP043	Unknown	4	.	.	122480	18204	0.00	0.00	0.00				-2.75
	N/A	LP046	Unknown	4	10721	18776	.	.	0.00	0.00	0.00	0.81			
	N/A	LP068	Unknown	4	637143	121734	.	.	0.00	0.00	0.00	-2.39			
	N/A	LP095	Unknown	4	19871	9233	.	.	0.00	0.00	0.00	-1.11			
	N/A	LP096	Unknown	4	25859	8246	.	.	0.00	0.00	0.00	-1.65			
	N/A	LP097	Unknown	4	.	.	9327920	1015645	0.00	0.00	0.00				-3.20
	N/A	C42	Unknown	4	94954	207424	69659	73090	0.05	0.02	0.11	1.13	-0.45	-1.50	0.07
	N/A	C43	Unknown	4	63193	64290	75632	75139	0.47	0.00	0.40	0.02	0.26	0.22	-0.01
	N/A	C44	Unknown	4	947	2151	11210	5777	0.00	0.20	0.11	1.18	3.57	1.43	-0.96
	N/A	C45	Unknown	4	332457	262178	443522	354061	0.00	0.00	0.21	-0.34	0.42	0.43	-0.33
	N/A	C46	Unknown	4	37964	38224	48798	46310	0.61	0.01	0.64	0.01	0.36	0.28	-0.08
	N/A	C47	Unknown	4	31025	38092	37293	51132	0.02	0.20	0.30	0.30	0.27	0.42	0.46

[Table 2.6]: Spectrometric parameters of tentative identification of multiplatform analysis results. MT: for CE-MS platform data ; RT: Retention time for LC-MS and GC-MS platforms data; TI: Target Ion for CE/MS platform data; CL: Confidence Level; MW: Molecular Weight.

Analytical platform	CODE	Formula	Name	MT/RT	Adduct (LC/MS&CE/MS)	Neutral mass/TI m/z	PPM Error	CL	MW
CE/MS	C01	C5H11NO2	Betaine	14.380	M+H	117.079	0	1	117.14554
	C02	C4H9NO2S	Homocysteine	14.870	M+H	135.035	3	1	135.18396
	C03	C8H17NO2	amino caprylic acid; Amino octanoic acid	11.170	M+H	159.126	0	1	159.22528
	C04	C5H11NO2	Valine	12.990	M+H	117.079	0	1	117.14554
	C05	C6H13NO2	Leucine	13.230	M+H	131.094	4	1	131.17212
	C06	C9H11NO2	Phenylalanine	13.980	M+H	165.079	0	1	165.18834
	C07	C3H7NO3	Serine	12.960	M+H	105.043	4	1	105.09138
	C08	C5H9NO2	Proline	13.810	M+H	115.063	2	1	115.12966
	C09	C5H9NO4	Glutamic acid	13.910	M+H	147.054	6	1	147.12766
	C10	C3H7NO2	Alanine	10.060	M+H	89.048	4	3	89.09238
	C11	C4H9NO3	Threonine	13.480	M+H	119.058	1	1	119.11796
	C12	C6H9N3O2	Histidine	10.120	M+H	155.069	3	1	155.15376
	C13	C4H7NO2	Aminocyclopropanecarboxylic acid	13.890	M+H	101.048	3	1	101.10308
	C14	C11H20N2O6	Saccharopine	13.820	M+H	276.131	4	3	276.2839
	C15	C4H7N3O	Creatinine	10.020	M+H	113.059	1	1	113.11748
	C16	C4H9N3O2	Creatine	11.780	M+H	131.069	3	1	131.13236
	C17	C11H9NO2	Indole acrylate	13.930	M+H	187.063	1	3	187.19386
	C18	C19H12N2O	Formylindolo carbazole	15.890	M+H	284.096	4	3	284.31098
	C19	C6H11NO4	Aminoadipic acid	13.880	M+H	161.069	1	1	161.15424
	C20	C5H13NO	Piperidine	13.220	M+H	85.09	2	3	85.14754
	C21	C9H8O3	Phenyl pyruvic acid	14.260	M+H	164.047	2	1	164.15682
	C22	C4H9N	Pyrrolidine	6.920	M+H	71.074	7	3	71.12096
	C23	C9H15N3O2S	Ergothioneine	19.390	M+H	229.089	2	3	229.27594
	C24	C7H19N3	Spermidine	6.700	M+H	145.158	1	1	145.24586
	C25	C9H21N3O	N-Acetyl spermidine	8.920	M+H	187.169	3	3	187.28214
	C26	C10H26N4	Spermine	6.660	M+H	202.216	1	3	192.26084
	C27	C7H15NO3	Carnitine	11.310	M+H	161.105	1	1	161.1977
	C28	C9H17NO4	Acetyl carnitine	11.880	M+H	203.116	1	1	203.23398
	C29	C10H19NO4	Propionyl carnitine	12.160	M+H	217.131	2	1	217.26056
	C30	C11H21NO4	Butyryl carnitine	12.420	M+H	231.148	4	3	231.28714
	C31	C11H21NO5	Hydroxybutyrylcarnitine	12.750	M+H	247.142	0	3	247.28614
	C32	C5H13NO	Neurine	9.450	M+H	103.1	3	3	103.16242
	C33	C3H9NO	Trimethylamine N-oxide (TMAO)	9.140	M+H	75.069	8	3	75.10926
	C34	C5H4N4O	Hypoxanthine	14.900	M+H	136.038	4	1	136.11106
	C35	C14H17N5O8	Succinyl adenosine	17.440	M+H	383.108	1	3	383.31028
	C36	C11H19N3O6	Ophthalmic acid	15.970	M+H	289.127	1	1	289.28266
	C37	C11H19N3O7S	(Hydroxymethyl)glutathione	16.190	M+H	337.094	1	3	337.34666
	C38	C11H19N3O7	Tripeptide	16.090	M+H	305.123	2	3	N/A
	C39	C14H23N5O6	Tripeptide	10.740	M+H	357.168	9	3	N/A
	C40	C18H30N6O10	Tripeptide	17.040	M+H	490.207	10	3	N/A
	C41	C14H20N6O5S	S-Adenosylhomocysteine	11.730	M+H	384.123	4	3	416.4738
	C42	N/A	Unknown	11.790	N/A	185.142	N/A	5	N/A
	C43	N/A	Unknown	5.990	N/A	877.57	N/A	5	N/A
	C44	N/A	Unknown	13.640	N/A	132.025	N/A	5	N/A
	C45	N/A	Unknown	6.930	N/A	125.12	N/A	5	N/A
	C46	N/A	Unknown	5.990	N/A	835.588	N/A	5	N/A
	C47	N/A	Unknown	11.210	N/A	902.497	N/A	5	N/A
	C48	C4H9NO2	4-Aminobutyric acid	10.480	M+H	103.064	7	3	103.11896
	C49	C12H15N4OS	Thiamine	9.230	M+H	264.105	6	3	265.35
GC/MS	G001	C20H39NO5	Dodecyl ester-Alanine	5.661	N/A	77.0242	N/A	2	373.52536
	G002	C13H16N2O4	N-acetyl-N-formyl-methoxykynurenamine [AFMK]	6.210	N/A	248.0585	N/A	2	264.27554
	G003	C9H9NO2	Pyridine carboxylic acid methyl ester	6.244	N/A	163.073	N/A	2	163.17246
	G004	C17H29N	Ethyl-hept-yn-yloctahydroindolizine	6.391	N/A	152.0486	N/A	2	247.41886
	G005	C3H4O3	Pyruvic acid	6.497	N/A	174.06	N/A	1	88.06086

Analytical platform	CODE	Formula	Name	MT/RT	Adduct (LC/MS&CE/MS)	Neutral mass/TI m/z	PPM Error	CL	MW
	G006	C5H5NO	Hydroxy pyridine	6.500	N/A	152.0517	N/A	1	95.0989
	G007	C3H6O3	Lactic acid	6.700	N/A	133.0423	N/A	1	90.07674
	G008	C3H6O4	Dihydroxy propanoic acid	7.300	N/A	59.0311	N/A	2	106.07574
	G009	C4H4N2O2	Dioxide Pyrazine	7.397	N/A	112.0751	N/A	2	112.08596
	G010	C2H7NO	Ethanolamine	7.527	N/A	102.071	N/A	2	205.44492
	G011	C8H18S2	Ethylthiomethylpentane	7.581	N/A	55.0008	N/A	2	178.35852
	G012	C2H2O4	Oxalic acid	7.837	N/A	147.0625	N/A	1	90.03328
	G013	C4H8O3	Hydroxybutyric acid	7.864	N/A	131.09	N/A	1	104.10332
	G014	C3H7NO2	Sarcosine	7.900	N/A	117.08	N/A	1	89.09238
	G015	C4H9NO2	N-methyl alanine	8.291	N/A	130.1035	N/A	1	103.11896
	G016	C3H7NO2	Lactamide	8.300	N/A	233	N/A	1	89.09238
	G017	C3H6O2	Propanoic acid	8.365	N/A	69.9688	N/A	2	189.2832
	G018	H3PO4	Phosphoric acid	8.387	N/A	241.0423	N/A	1	256.382372
	G019	C4H8O3	Hydroxybutyric acid	8.396	N/A	131.088	N/A	1	248.46556
	G020	C3H7O4P	Phosphonomycin	8.406	N/A	211.0272	N/A	2	138.057412
	G021	C8H10N2S	N- methyl-N'-phenylthiourea	8.521	N/A	92.9915	N/A	2	166.2434
	G022	C3H7NO3	Serine	8.547	N/A	116.0492	N/A	2	249.45362
	G023	C8H8O2S	Acetylmethylthiophenecarbaldehyde	8.751	N/A	100.021	N/A	2	168.21212
	G024	C3H4O4	Malonic acid	8.900	N/A	147.0635	N/A	2	104.05986
	G025	C7H15NO3	Morpholino propanediol	8.909	N/A	100.0224	N/A	2	161.1977
	G026	C5H11NO2	Valine	8.929	N/A	144.1192	N/A	1	117.14554
	G027	C4H6O4	Methylmalonic acid	9.088	N/A	247	N/A	1	118.08644
	G028	C5H10O	MethylButenol	9.221	N/A	71.0486	N/A	2	86.1319
	G029	C11H16O2	Dimethoxyphenyl propane	9.230	N/A	75.0258	N/A	2	180.24274
	G030	C11H14N2	Aminotrimethylenepyridine	9.272	N/A	173.0673	N/A	2	174.24226
	G031	C15H16N2O2	(1H-Indolyl)methylethylpyrrolidinedione	9.274	N/A	130.0472	N/A	2	256.29894
	G032	C6H13NO	Ethylpyrrolidinol	9.354	N/A	115.0606	N/A	2	115.17312
	G033	C7H6O2	Benzoic acid	9.420	N/A	105.0339	N/A	1	122.12054
	G034	C12H16N4	Aminocyanobutyltrimethylenepyrimidine	9.666	N/A	149.057	N/A	2	216.28224
	G035	C10H12N2O	Serotonin	9.677	N/A	174.1123	N/A	2	176.21468
	G037	H3O4P	Phosphoric acid	9.725	N/A	299.0721	N/A	1	97.993552
	G038	C12H9NO	9H-Pyrroloindolone	9.938	N/A	182.0021	N/A	2	183.20556
	G039	C5H10O4S	Ethyl methanesulphonyl acetate	9.985	N/A	120.9871	N/A	2	166.1939
	G040	C6H13NO2	Isoleucine	10.021	N/A	158.135	N/A	1	131.17212
	G041	C4H9NO3	Threonine	10.045	N/A	130.0847	N/A	1	119.11796
	G042	C5H9NO2	Proline	10.101	N/A	142.1012	N/A	1	115.12966
	G043	C10H14O	Thymol	10.475	N/A	207.0339	N/A	2	150.21716
	G044	C15H32O	Pentadecanol	10.583	N/A	75.0263	N/A	2	300.5947
	G045	C9H7NO2	H-Indole carboxylic acid	10.660	N/A	101.041	N/A	2	160.14864
	G046	C5H10N2	Dimethyl imidazoline	10.790	N/A	83.0317	N/A	2	98.1463
	G047	C4H4O4	Fumaric acid	10.800	N/A	75.0263	N/A	1	116.07056
	G048	C9H11NO3	Tyrosine	10.934	N/A	218.1024	N/A	2	397.7307
	G049	C9H18O2	Nonanoic acid	10.961	N/A	75.0262	N/A	2	272.49808
	G050	C10H12O3	Methyl p-tolyloxyacetate	11.541	N/A	180.0229	N/A	2	180.19928
	G051	C4H11NO2	Amino acetaldehyde dimethyl acetal	11.545	N/A	74.0484	N/A	1	105.13484
	G052	C4H12N2	Putrescine	11.611	N/A	174.1077	N/A	2	376.87596
	G053	C7H14O4	Propanoldimethoxyacetate	11.941	N/A	75.0258	N/A	2	162.18206
	G054	C11H24	Undecane	11.984	N/A	57.0698	N/A	2	156.30826
	G055	C5H11NO2	Norvaline	12.252	N/A	75.0263	N/A	2	373.52536
	G056	C3H4O5	Tartronic acid	12.300	N/A	292.132	N/A	1	120.05886
	G057	C3H5NO4	Amino malonic acid	12.374	N/A	147.0629	N/A	1	335.61786
	G058	C14H9N5O5	Tetrahydro methyl(nitrophenyl)oxazolopurinedione	12.438	N/A	326.9582	N/A	2	327.24976
	G059	C6H6N2O	Nicotinamide	12.558	N/A	78.0346	N/A	1	122.127
	G060	C5H5N2	(1H)Pyrrole carbonitrile	12.558	N/A	105.0462	N/A	2	106.12524
	G061	C7H9N2O	Methyl nicotinamide	12.563	N/A	75.0262	N/A	2	123.15206
	G062	C4H6O5	Malic acid	12.599	N/A	233.1	N/A	1	134.08544
	G063	C5H11NO2S	Methionine	13.005	N/A	128.0879	N/A	1	149.21054

Analytical platform	CODE	Formula	Name	MT/RT	Adduct (LC/MS&CE/MS)	Neutral mass/TI m/z	PPM Error	CL	MW
	G064	C5H7NO3	Pyroglutamic acid	13.030	N/A	156.0802	N/A	1	129.11278
	G065	C5H9NO3	Trans-hydroxyproline	13.091	N/A	230.1327	N/A	1	131.12866
	G066	C5H9NO4	Glutamic acid	13.170	N/A	84.0433	N/A	1	147.12766
	G067	C9H11NO2	Phenylalanine	13.409	N/A	91.0534	N/A	1	165.18834
	G068	C13H31N3OSi3	(Trimethylsilyl)oxyimidazolamine	13.413	N/A	115.0761	N/A	2	329.66084
	G069	C4H7N3O	Creatinine	13.447	N/A	115.0797	N/A	1	113.11748
	G070	C4H8O5	Trihydroxy butyric acid	13.492	N/A	147.0651	N/A	2	424.8258
	G071	C6H5NO3	Hydroxy nicotinic acid	13.551	N/A	268.0829	N/A	2	139.1076
	G072	C5H7NO3	Oxo proline	13.591	N/A	156.084	N/A	2	273.47502
	G073	C7H12O4	Malonic acid diethyl ester	13.645	N/A	243.2107	N/A	2	279.32994
	G074	C5H8O4	Pentane dioic acid	13.677	N/A	147.0663	N/A	1	364.65538
	G075	C11H14N2O3	4H-Pyridopyrimidinecarboxylic acid	13.913	N/A	93.0409	N/A	2	222.23926
	G076	C4H5IO2	Methyl ester iodo Propenoic acid	13.979	N/A	212.0006	N/A	2	85.0805
	G077	C12H10O	Hydroxy biphenyl	13.986	N/A	211.0016	N/A	2	170.2068
	G078	C2H7NO2S	Hypo taurine	14.006	N/A	188.1275	N/A	1	109.14668
	G079	C2H2O4	Oxalic acid	14.285	N/A	136.0205	N/A	2	361.517
	G080	C9H10O3	Phenyl lactic acid	14.300	N/A	193.1	N/A	2	166.1727
	G081	C4H11NO2	aminomethylpropanediol	14.307	N/A	218.1	N/A	2	105.13484
	G082	C9H11NO2	Phenylalanine	14.310	N/A	192.1194	N/A	1	309.55058
	G083	C7H6O3	Hydroxybenzoic acid	14.335	N/A	193.1147	N/A	2	138.11954
	G084	C22H17N3	Aminophenyldiphenylpyrimidine	14.476	N/A	323.1834	N/A	2	323.39048
	G085	C12H24O2	Dodecanoic acid	14.607	N/A	257.1916	N/A	2	271.49014
	G086	C12H24O2	Lauric acid	14.626	N/A	129.0367	N/A	1	200.31696
	G087	C10H9N7O	Methoxy-N-phenylTriazinamine	14.675	N/A	466.1075	N/A	2	300.235749
	G088	H4O7P2	Pyrophosphate	14.676	N/A	451.068	N/A	1	180.996044
	G089	C7H6O4	Gentisic acid	14.762	N/A	266.9942	N/A	2	154.11854
	G090	C5H10O5	Ribose	14.878	N/A	73.046	N/A	1	150.1279
	G091	C3H6O2	Acetol	15.225	N/A	217.1047	N/A	1	74.07774
	G092	C5H12O5	Arabitol	15.420	N/A	217.1049	N/A	1	152.14378
	G093	C3H9O6P	Glycerol -phosphate	15.818	N/A	299.066	N/A	1	172.071292
	G094	C6H9N3O2	Histidine	16.300	N/A	82.0526	N/A	2	155.15376
	G095	C5H4N4O	Hypoxanthine	16.309	N/A	265.0918	N/A	1	136.11106
	G096	C6H8O7	Citric acid	16.448	N/A	273.0942	N/A	1	192.12072
	G097	C22H20N2O2	Phthalic acid, diamide	16.489	N/A	238.1286	N/A	2	344.4056
	G098	C6H14NO8P	Glucosamine phosphate	16.523	N/A	217.1052	N/A	1	259.147792
	G099	C3H4O4	Malonic acid	16.622	N/A	249	N/A	2	304.52842
	G100	C6H12O5	Anhydrohexitol	16.649	N/A	147.0656	N/A	2	452.87896
	G101	C4H7NO4	Aspartic acid	16.690	N/A	70.0655	N/A	2	349.64444
	G102	C6H6O6	Dehydroascorbic acid	16.738	N/A	157.0542	N/A	1	174.10584
	G103	C6H12O6	Tagatose	16.742	N/A	217.104	N/A	1	180.15348
	G104	C16H30O2	Hexadecenoic acid	16.770	N/A	75.0258	N/A	2	326.58852
	G105	C14H28O2	Myristic acid	16.788	N/A	117.0365	N/A	1	228.37012
	G106	C5H8O	Methyl-But-yn-ol	16.995	N/A	264.1078	N/A	2	279.256689
	G107	C6H12O6	Sorbose	17.000	N/A	217.1038	N/A	1	180.15348
	G108	C5H5N5	Adenine	17.000	N/A	264.1083	N/A	1	65.0932
	G109	C5H5N5	Alanine	17.075	N/A	100.0553	N/A	2	233.45462
	G110	C7H14O6	Methyl galactoside	17.077	N/A	189.0791	N/A	1	482.90454
	G111	C12H15NO	Ethyl-N-allylbenzamide	17.100	N/A	133.0596	N/A	2	189.2532
	G112	C9H11NO3	Tyrosine	17.177	N/A	179.0886	N/A	1	181.18734
	G113	C6H12O6	Inositol	17.245	N/A	318.14	N/A	2	180.15348
	G114	C6H10O6	Gluconic acid lactone	17.248	N/A	319.1782	N/A	1	178.1376
	G115	C6H13NO6	Glucose oxime	17.255	N/A	74.0517	N/A	2	628.25484
	G116	C6H12O6	Mannose	17.273	N/A	205.1143	N/A	2	570.1003
	G117	C6H12O6	Galactose	17.275	N/A	217.1147	N/A	1	180.15348
	G118	C6H12O6	Altrose	17.291	N/A	321.163	N/A	1	180.15348
	G119	C6H6O6	Dehydroascorbic acid	17.376	N/A	244.1	N/A	1	174.10584
	G120	C6H12O6	Talose	17.450	N/A	205.1015	N/A		180.15348

Analytical platform	CODE	Formula	Name	MT/RT	Adduct (LC/MS&CE/MS)	Neutral mass/TI m/z	PPM Error	CL	MW
	G121	C6H10O6	Gluconic acid lactone	17.430	N/A	217.1049	N/A	1	178.1376
	G122	C6H10O6	Galactonolactone	17.526	N/A	189.0785	N/A	1	178.1376
	G123	C17H34O2	Methyl ester Hexadecanoic acid	17.595	N/A	270.256	N/A	2	270.44986
	G124	C6H6O6	Dehydroascorbic acid	17.620	N/A	244.1	N/A	1	174.10584
	G125	C6H12O6	Galactose	17.662	N/A	319.1529	N/A	2	180.15348
	G126	C9H11NO3	Tyrosine	17.704	N/A	218.1017	N/A	1	181.18734
	G127	C6H6N4S	Methyl mercaptopurine	17.800	N/A	92.9893	N/A	1	110.17684
	G128	C16H11N	Pyrenamine	17.802	N/A	217.1067	N/A	2	217.26524
	G129	C6H14O6	Mannitol	17.810	N/A	217.104	N/A	1	182.16936
	G130	C6H10O7	Galacturonic acid	17.917	N/A	333.1292	N/A	1	194.1366
	G131	C7H14	Hydroxyheptene	17.974	N/A	171.0825	N/A	2	186.36618
	G132	C6H14O6	Glucitol	18.132	N/A	217.103	N/A	2	615.25608
	G133	C6H12O7	Gluconic acid	18.297	N/A	319.16	N/A	1	196.15248
	G134	C2H5NO2	Glycine	18.394	N/A	52.0305	N/A	2	219.42804
	G135	C6H10O4	Adipic acid	18.582	N/A	129.0359	N/A	2	426.6712
	G136	C16H30O2	Palmitoleic acid	18.728	N/A	311.23	N/A	1	254.4074
	G137	C16H32O2	Palmitic acid	18.846	N/A	117.0365	N/A	1	256.42328
	G138	C6H12O6	Allose	19.058	N/A	319.16	N/A	2	180.15348
	G139	C5H11O8P	Ribose-phosphate	19.548	N/A	299.0727	N/A	1	230.106572
	G140	C6H12O6	Glucose	19.691	N/A	204.0957	N/A	2	831.56092
	G141	C18H38O	Octadecanol	19.824	N/A	327.3034	N/A	2	342.67444
	G142	C10H17N3O6S	Glutathione reduced	19.880	N/A	213.0999	N/A	2	307.32108
	G143	C4H7O7P	Erythrose-phosphate	20.110	N/A	357.113	N/A	2	198.065112
	G144	C11H12N2O2	Tryptophan	20.263	N/A	202.1052	N/A	1	204.22438
	G145	C18H32O2	Linoleic acid	20.324	N/A	67.0536	N/A	1	280.44468
	G146	C18H34O2	Oleic acid	20.377	N/A	75.0255	N/A	1	282.46056
	G147	C15H17N	N-Benzyl phenethylamine	20.781	N/A	91.0544	N/A	2	211.30218
	G148	C5H10O5	Ribose	20.827	N/A	147.0663	N/A	2	620.053392
	G149	C14H8O3	Hydroxyanthraquinone	20.965	N/A	281.0507	N/A	2	224.21032
	G150	C6H12O6	Scyllo-Inositol der.	21.075	N/A	217.1031	N/A	2	613.2402
	G151	C6H13O9P	Glucose-phosphate 1	21.394	N/A	387	N/A	2	260.132152
	G152	C6H12O6	Mannose	21.992	N/A	147.0663	N/A	2	722.260092
	G153	C18H37NO2	Sphingosine	22.100	N/A	132.0395	N/A	2	299.49108
	G154	C20H32O2	Arachidonic acid	22.210	N/A	75.0258	N/A	1	376.6472
	G155	C11H8N2	H-Pyrido indole	22.433	N/A	58.065	N/A	2	351.39784
	G156	C21H19NO	(Phenylmethyl)amino benzaldehyde	22.465	N/A	91.0533	N/A	2	301.38126
	G157	C19H38O4	Palmitoyl glycerol	23.196	N/A	218.11	N/A	2	474.86326
	G158	C10H12N4O5	Inosine	23.473	N/A	230.116	N/A	1	556.94856
	G159	C8H8O2	Phenylacetic acid	23.687	N/A	58.0652	N/A	2	207.26808
	G160	H3PO4	Phosphoric acid	23.750	N/A	133.0115	N/A	2	460.795772
	G161	C10H14O	Thymol	23.840	N/A	59.0316	N/A	2	222.39828
	G162	C12H22O11	Sucrose	23.988	N/A	217.107	N/A	1	342.29208
	G163	C12H22O11	Maltose	24.312	N/A	204.1	N/A	1	948.78226
	G164	C12H22O11	Lactose	24.386	N/A	361.1675	N/A	1	342.29208
	G165	C12H22O12	Lactobionic acid	24.583	N/A	204.0961	N/A	1	358.29108
	G166	C12H22O11	Trehalose	24.752	N/A	361.169	N/A	2	342.29208
	G167	C12H22O11	Maltose	24.802	N/A	361.1681	N/A	2	342.29208
	G168	C12H24O11	Lactitol	24.877	N/A	319.1517	N/A	2	344.30796
	G169	C21H42O4	Glycerol monostearate	24.894	N/A	147.0651	N/A	1	502.91642
	G170	C9H13N3O5	Cytidine	25.061	N/A	217.1078	N/A	2	243.21462
	G171	C12H22O11	Sophorose	25.189	N/A	217.1067	N/A	2	342.29208
	G172	C9H13N2O9P	Uridine -monophosphate	25.600	N/A	315.0953	N/A	2	324.177652
	G173	C7H6N2	Benzimidazole	25.612	N/A	299.066	N/A	2	382.52058
	G174	C12H22O11	Maltose	26.574	N/A	204.1003	N/A	2	948.78226
	G175	C13H10N2	Phenyl-1H-Benzoimidazole	26.666	N/A	207.0275	N/A	2	314.38002
	G176	C10H13N4O8P	Inosine -monophosphate	26.822	N/A	169.0682	N/A	1	348.202752
	G177	C27H46	Cholest-ene	26.970	N/A	91.0515	N/A	2	370.65414

Analytical platform	CODE	Formula	Name	MT/RT	Adduct (LC/MS&CE/MS)	Neutral mass/TI m/z	PPM Error	CL	MW
	G178	C18H25NO9	Tetramethyl -pyridinetetracarboxylate	27.523	N/A	105.0656	N/A	2	399.3888
	G179	C27H46O	Cholesterol	27.555	N/A		N/A	1	458.83426
	G180	C4H6O5	Malic acid	28.424	N/A	401.0475	N/A	2	350.6288
	G181	C20H28O4	Dihydroxy dehydroabietic acid	29.701	N/A	135.0647	N/A	2	490.82114
	G182	C18H32O16	Maltotriose	29.884	N/A	204.0955	N/A	2	504.43068
	G183	C16H30O2	Hexadecenoic acid	32.460	N/A	311.2757	N/A	2	368.66826
LC/MS (-)	LN01	C6H6N4O	Methyl hypoxanthine	1.068	M+Cl	186.0307	1	4	150.13764
	LN03	C16H32O3	C(16:0(OH); [Hydroxy palmitic ac	3.047	M-H	272.2350	1	3	272.42228
	LN04	C18H35NO3	N-Palmitoyl Glycine	3.859	M-H	313.2611	2	3	313.4742
	LN05	C22H34O2	C(22:5); [DPA]; [Docosapentaenoic acid]	6.016	M-H	330.2570	3	2	330.50336
	LN06	C21H38O4	MG(18:2)	3.759	M+FA-H	400.2825	0	4	354.52242
	LN07	C19H39O7P	LPA(16:0)	3.136	M-H	410.2438	1	3	410.479692
	LN08	C11H20N4O11P2	CDP-Ethanolamine	1.752	M-H	446.0596	2	3	446.239764
	LN10	C22H46NO8P	PS(O-16:0)	2.917	M-H-H2O	465.2852	0	3	483.573072
	LN11	C26H45NO7S	Taurocholic acid	1.152	M-H-H2O	497.2813	1	3	515.7002
	LN12	C27H46NO7P	LPE(22:5)	3.269	M-H	527.3002	2	3	527.627572
	LN13	C24H50NO7P	LPC(16:0)//LPE(19:0)	3.125	M+Cl	531.3093	0	3	495.627232
	LN14	C26H48NO9P	LPS(20:2)	4.807	M-H	549.3041	5	4	549.630752
	LN15	N/A	Unknown	8.052	N/A	552.3660	N/A	5	N/A
	LN16	C33H54O7	Cholesterol glucuronide	7.745	M-H	562.3861	2	3	562.77486
	LN18	C33H65NO3	Cer(d33:1)	15.190	M+FA-H	569.5015	1	3	523.8729
	LN19	C32H54O6	Cholesteryl-alpha-D-glucoside	10.514	M+FA-H	580.3974	0	3	534.76516
	LN20	C32H61NO4	Cer(d32:2(2OH))	13.766	M-H+HCOONa	591.4524	9	3	523.82944
	LN21	C28H56NO7P	PC(P-20:0)//PC(O-20:1)	5.402	M+FA-H	595.3841	2	2?	549.717672
	LN22	C39H70O5	DG(36:3)	16.145	M-H-H2O	600.5074	6	3	618.9681
	LN23	C32H60O6	TG(29:0)	8.826	M-H+HCOONa	608.4283	3	3	540.8128
	LN24	C30H52NO7P	LPC(22:5)	3.069	M+FA-H	615.3549	2	4	569.707312
	LN26	C34H68NO6P	CerP(d34:1)	15.080	M-H	617.4774	2	3	617.878152
	LN27	C33H62O6	TG(30:0)	9.661	M-H+HCOONa	622.4439	3	4	554.83938
	LN28	C38H73NO3	Cer(d38:2)	18.659	M+FA-H	637.5636	2	3	591.98992
	LN29	C42H72O5	DG(39:5)	16.197	M-H	656.5377	0	3	657.01608
	LN30	C42H74O5	DG(39:4)	16.308	M-H	658.5520	3	3	659.03196
	LN31	C36H73N2O6P	PE-Cer(d34:1)	15.058	M-H	660.5195	2	3	660.945952
	LN32	C37H70O5	DG(34:1)	18.458	M+FA-H	662.5120	0	3	594.9467
	LN33	C34H62NO10P	PS(28:2)	10.325	M-H	674.3993	7	3	675.826512
	LN34	C39H70O5	DG(38:6)	18.417	M-H	686.5117	1	4	618.9681
	LN35	C38H74NO8P	PC(20:1)//PE(33:1)	16.810	M-H	703.5144	1	3	703.966592
	LN36	C40H78NO8P	PC(32:1)//PE(35:1)	14.611	M-H	731.5537	10	4	732.019752
	LN37	C41H72NO8P	PC(33:5)//PE(36:5)	15.550	M-H	737.5008	2	4	737.982812
	LN38	C39H80N2O6P	SM(d34:1)	15.883	M+FA-H	748.5745	2	4	704.033632
	LN39	C40H80NO9P	PS(O-34:0)	4.238	M-H	749.5534	5	4	750.034632
	LN40	C39H80NO7P	PE(O-34:0)	3.141	M+FA-H	751.5711	2	3	706.025932
	LN41	C40H75NO8	GlcCer(d34:2)	17.178	M-H+HCOONa	765.5332	5	3	698.0222
	LN42	C43H70NO10P	PS(37:7)	2.597	M-H	791.4753	2	4	791.986332
	LN43	C44H75O10P	PG(38:6)	17.325	M-H	794.5111	2	4	795.030032
	LN44	C44H79O10P	PG(38:4)	21.612	M-H	798.5410	0	4	799.061792
	LN45	C42H78NO8P	PC(34:3)//PE(37:3)	15.307	M+FA-H	801.5537	2	4	756.081632
	LN46	N/A	unknown	15.301	N/A	801.7425	N/A	5	N/A
	LN47	C42H80NO8P	PC(34:2)//PE(37:2)	16.353	M+FA-H	803.5697	3	4	758.057032
	LN48	C45H80NO10P	PS(39:4)	5.364	M-H-H2O	807.5357	6	4	826.087132
	LN49	C41H82NO8P	PC(33:0)//PE(36:0)	16.198	M+FA-H	815.5668	1	4	748.062212
	LN50	C53H102O6	TG(50:0)	15.081	M-H	816.7504	8	3	835.37098
	LN51	C46H79O10P	PG(40:6)	19.030	M-H	822.5420	1	4	823.083192
	LN52	C42H80NO8P	PC(34:2)//PE(37:2)	15.702	M+FA-H	825.5513	1	4	758.057032
	LN53	N/A	unknown	16.763	N/A	827.7607	N/A	5	N/A
	LN54	C45H86NO10P	PS(39:1)	18.166	M-H	831.6005	2	4	832.134772
	LN55	C43H79O13P	PI(34:2)	18.464	M-H	834.5273	2	3	835.048092

Analytical platform	CODE	Formula	Name	MT/RT	Adduct (LC/MS&CE/MS)	Neutral mass/TI m/z	PPM Error	CL	MW
	LN56	N/A	unknown	3.129	N/A	842.3944	N/A	5	N/A
	LN57	C48H75O10P	PG(42:10)	17.159	M-H	842.5104	1	4	843.072832
	LN58	C46H78NO8P	PC(38:7)//PE(41:7)	15.260	M+FA-H	849.5513	1	4	804.083952
	LN59	C44H86NO9P	PS(O-38:1)//PS(P-38:0)	17.706	M+FA-H	849.6069	3	4	804.125072
	LN60	C45H76NO8P	PC(37:7)//PE(40:7)	17.737	M-H+HCOONa	857.5189	1	4	790.057372
	LN61	C45H81O13P	PI(36:3)	19.123	M-H	860.5440	3	3	861.085372
	LN62	C45H80NO10P	PS (39:4)	16.359	M+FA-H	871.5559	2	4	826.087132
	LN63	C59H102O5	TG(O-56:7)	16.359	M-H-H2O	871.7518	3	4	891.43618
	LN64	C45H82NO10P	PS(39:3)	17.665	M+FA-H	873.5707	3	4	828.103012
	LN65	C49H84NO10P	PS(43:6)	16.886	M-H	877.5839	1	4	878.161692
	LN66	C46H88NO8P	PC(38:2)//PE(41:2)	18.751	M-H+HCOONa	881.6128	1	4	814.163352
	LN67	C47H81O13P	PI(38:5)	19.132	M-H	884.5441	3	3	885.106772
	LN68	C48H83O13P	PI(39:5)	19.408	M-H	898.5573	0	3	899.133352
	LN69	C47H84NO10P	PS(41:4)	18.173	M+FA-H	899.5879	1	4	854.140292
	LN70	C49H81O13P	PI(40:7)	19.037	M-H	908.5436	2	3	909.128172
	LN71	C50H74NO10P	PS(42:9)	16.994	M-H+HCOONa	925.5077	1	4	880.092992
	LN72	C45H81O13P	PI(36:3)	19.120	M+FA-H	928.5281	4	3	861.085372
	LN73	C50H83O10P	PG(44:8)	17.698	M-H+HCOONa	941.5572	5	3	875.157752
	LN74	C61H108O6	TG(58:5)	21.136	M+Na-2H	957.7804	9	4	937.50422
	LN75	N/A	unknown	24.764	N/A	1484.2823	N/A	5	N/A
	LN76	C73H129N3O31	Ganglioside GM1 (36:2)	24.782	M+Hac-H	1603.8676	9	3	1544.79446
LC/MS (+)	LP001	C10H16	Dimethyl octatriene	6.371	M+H	136.1247	3	4	136.23404
	LP002	C7H13NO2	Proline betaine	0.995	M+H	143.0944	1	3	143.18282
	LP005	C5H11NO2	Valine	0.971	M+K	155.0343	5	4	117.14554
	LP006	N/A	Unknown	0.970	N/A	155.0374	N/A	5	N/A
	LP008	C18H31NO2S	Farnesyl cysteine	22.385	M+H+NH4	172.1249	4	3	325.50844
	LP009	C13H20	Phenyl heptane	7.132	M+H	176.1553	7	4	176.2979
	LP010	C15H24O2	Propionyl choline	7.240	M+NH4	178.1681	3	4	160.23322
	LP011	C15H28O3	Keto pentadecanoic acid	7.236	M+H-H2O	238.1923	4	4	256.37982
	LP012	C18H32O2	C(18:2); [Linoleic acid]	7.247	M+H-H2O	262.2296	2	4	280.44468
	LP015	N/A	Unknown	0.930	N/A	335.9486	N/A	5	N/A
	LP016	C20H39NO2	N-Oleoyl ethanolamine [OEA]	6.115	M+Na	347.2827	8	3	325.52836
	LP017	C22H34O2	C(22:5); [DPA]	6.180	M+NH4	347.2828	1	4	326.51876
	LP018	C21H38O4	MG(18:2)	3.854	M+H	354.2776	2	3	354.52242
	LP019	C23H38O4	O-Arachidonoyl Glycidol	13.005	M+H	360.2669	1	3	378.54382
	LP020	C23H36O4	MG(20:4)	3.899	M+H-H2O	360.2680	4	4	376.52794
	LP021	N/A	Unknown	8.047	N/A	375.4471	N/A	5	N/A
	LP022	C24H40O2	C(24:4); [Cholanoic acid]	9.242	M+NH4	377.3287	5	4	360.5724
	LP023	C21H40O4	MG(18:1)	3.853	M+H	378.2770	1	4	356.5383
	LP024	C23H38O2	Docosatetraenoic Acid methyl ester	9.371	M+K	384.2448	5	4	346.54582
	LP025	C24H36O4	Hydroxyoxocholenoic acid	16.327	M+H	388.2619	1	3	388.53864
	LP026	C22H38O2	C(22:3); [Docosatrienoic acid]	3.760	M+H+HCOONa	402.2774	1	4	334.53512
	LP027	C25H40O4	MG(22:5)	4.830	M+H	404.2930	1	4	404.5811
	LP028	C23H46O4	MG(20:0)//DG(20:0)	5.624	M+Na	408.3238	6	4	386.60734
	LP029	C55H108O5	TG(O-52:0)	15.720	M+2H	424.4065	8	3	849.44102
	LP030	C43H77O13P	PI(34:3)	1.498	M+H+NH4	424.7678	1	3	833.032212
	LP032	C24H50NO7P	LPC(16:0)//PC(O-16:0)//LPE(19:0)	3.205	M+H	495.3341	3	3	N/A
	LP033	C24H50NO7P	LPC(16:0)//PC(O-16:0)//LPE(19:0)	2.874	M+H	495.3341	3	3	N/A
	LP034	C28H56NO7P	PC(20:1)	5.561	M+H	549.3797	1	3	549.717672
	LP035	C28H58NO7P	PC(O-20:0)	7.434	M+H	551.3950	0	2?	551.733552
	LP037	C37H70O5	DG(34:1)	15.612	M+H-H2O	576.5127	1	3	594.9467
	LP039	C39H66O5	DG(36:5)	13.053	M+H-H2O	596.4799	1	3	614.93634
	LP040	C39H70O4	DG(36:4)	16.277	M+H	602.5281	1	4	602.9691
	LP041	C32H64NO7P	LPC(24:1)	10.336	M+H	605.4425	1	3	605.823992
	LP042	C41H70O5	DG(38:5)	14.895	M+H-H2O	624.5129	2	4	642.9895
	LP043	N/A	Unknown	17.138	N/A	628.7137	N/A	5	N/A
	LP044	C43H76O2	C(16:0) Cholesteryl ester	28.542	M+Na	646.5650	2	3	625.06154

Analytical platform	CODE	Formula	Name	MT/RT	Adduct (LC/MS&CE/MS)	Neutral mass/TI m/z	PPM Error	CL	MW
	LP045	C36H69NO4	Cer(d36:2(2OH))	16.036	M+H+HCOONa	647.5117	3	4	579.93576
	LP046	N/A	Unknown	14.386	N/A	650.6623	N/A	5	N/A
	LP047	C44H76O2	CE(17:1)	18.191	M+Na	658.5608	9	3	637.07224
	LP048	C45H74O2	CE(18:3)	27.005	M+Na	668.5504	1	4	647.06706
	LP049	C46H76O3	CE(MonoMe(11,3))	16.263	M+H	676.5754	6	4	677.09264
	LP050	C41H70O5	DG(38:5)	19.831	M+K	680.4784	0	4	642.9895
	LP051	C45H68O5	DG(42:10)	18.368	M+NH4	705.5332	0	4	689.01642
	LP052	C42H84NO6P	CerP(d42:1)	17.996	M+H-H2O	711.5981	7	4	730.090792
	LP053	C39H76NO8P	PE(34:1)	15.099	M+H	717.5307	0	3	717.993172
	LP054	C18H28N4O4	Tripeptide	18.992	2M+H	728.4197	3	3	364.43772
	LP055	C37H66NO10P	PS(31:3)	12.339	M+NH4	732.4756	9	4	715.890372
	LP056	C47H68O5	DG(44:12)	13.262	M+Na	734.4883	0	4	713.03782
	LP057	C41H78NO8P	PE(36:2)	15.748	M+H	743.5478	2	3	744.030452
	LP059	C43H74NO7P	PE(P-38:6)	17.137	M+H	747.5220	2	4	748.021092
	LP060	C42H78NO8P	PC(34:3)	16.005	M+H	755.5483	2	2	756.041152
	LP061	C41H78NO8P	PC(33:2)//PE(36:2)	17.320	M+Na	765.5324	5	4	744.030452
	LP062	C43H80NO8P	PC(35:3)//PE(38:3)	16.360	M+H	769.5629	1	4	770.067732
	LP063	C42H82NO10P	PS(36:0)	14.458	M+H-H2O	773.5552	2	4	792.070912
	LP064	C43H84NO8P	PC(35:1)//PE(38:1)	18.635	M+H	773.5934	0	4	774.099492
	LP065	C44H82NO8P	PC(36:3)//PE(39:3)	17.267	M+H	783.5804	3	4	784.094312
	LP066	C46H78NO8P	PC(38:7)//PE(41:7)	16.908	M+H	803.5442	3	4	804.083952
	LP067	C46H78NO8P	PC(38:7)//PE(41:7)	15.474	M+H	803.5484	3	4	804.083952
	LP068	N/A	Unknown	27.697	N/A	807.7522	N/A	5	N/A
	LP069	C46H84NO8P	PC(38:4)//PE(41:4)	18.472	M+H	809.5976	5	4	810.131592
	LP070	C46H86NO8P	PC(38:3)//PE(41:3)	19.070	M+H	811.6104	2	4	812.147472
	LP071	C47H84NO8P	PC(37:2)//PE(42:5)	18.115	M+H	821.5920	2	4	822.142292
	LP072	C51H98O6	TG(48:0)	29.260	M+NH4	823.7621	1	4	807.31782
	LP073	C48H75O10P	PG(42:10)	12.865	M+H-H2O	824.5017	3	4	843.072832
	LP074	C46H78NO8P	PC(38:7)//PE(41:7)	15.321	M+K	841.5022	0	4	804.083952
	LP075	C53H94O6	TG(50:4)	27.059	M+Na	848.6875	1	4	827.30746
	LP076	C50H86NO8P	PC(42:7)	18.719	M+H	859.6090	0	4	860.190272
	LP078	C54H98O6	TG(51:3)	28.491	M+H	864.7172	4	4	843.34992
	LP079	C57H96O6	TG(54:7)	28.282	M+H	876.7232	3	4	877.36614
	LP080	C57H98O6	TG(54:6)	29.233	M+H	878.7354	1	4	879.38202
	LP081	C53H104NO8P	PE(48:1)	25.742	M+H-H2O	895.7406	1	3	914.365292
	LP082	C49H85O10P	PG(43:6)	14.899	M+K	902.5520	9	3	865.162932
	LP083	C18H36NO9P	LPS(12:0)	15.654	2M+Na	904.4127	6	4	441.449872
	LP084	C47H84O16P2	PIP(36:4)	17.649	M+H-H2O	948.5049	8	4	967.101324
	LP085	C53H95O13P	PI(44:4)	16.303	M+NH4	987.6772	0	3	971.282132
	LP086	C51H94N2O16	NeuAc-Gal-Cer(d34:0)	3.167	M+H	990.6639	4	4	991.28946
	LP087	C64H96O6	TG(61:14)	4.933	M+2Na-H	1004.6789	6	3	961.44104
	LP088	C51H95N3O15P2	CDP-DG(39:0)	16.067	M+H-H2O	1033.6125	1	4	1052.252564
	LP089	C24H50NO8P	LPS(O-18:0)	6.826	2M+NH4	1039.6865	5	4	511.626232
	LP090	C26H52NO7P	PC(O-18:1)//LPC(18:1)//LPE(20:1)	3.701	2M+H	1042.6934	3	4	521.664512
	LP091	C26H41N5O7	Polypeptide	3.173	2M+H	1070.6030	2	4	535.63024
	LP093	C30H35N5O7	Polypeptide	3.177	M+K	1154.5002	6	4	577.6254
	LP094	C47H86N7O17P3S	CoA(26:0)//Hexacosanoyl-CoA//Cerotoyl-CoA	3.189	M+NH4	1162.5186	8	4	1146.201836
	LP095	N/A	Unknown	3.686	N/A	1164.5344	N/A	5	N/A
	LP096	N/A	Unknown	3.700	N/A	1190.5455	N/A	6	N/A
	LP097	N/A	Unknown	17.740	N/A	1523.5426	N/A	5	N/A
	LP098	C51H100O5	DG(i-48:0)	16.673	2M+H-H2O	1567.5165	8	4	793.3347

2.4- Conclusion

In a mouse model of NASH, decreased hepatocyte damage and enhanced liver mass recovery after PH are likely related to multiple homeostatic mechanisms and adaptive metabolic responses including glucose metabolism. Such adaptation allows the regenerating liver to mainly focus on the synthesis of lipids and DNA.

In our previous studies, we showed that part of these changes could be counteracted by a dual GLP1 receptor/glucagon receptor agonist [288], and to a lesser extent by a GLP1 receptor agonist[287]. In those studies, we focused mainly on the compounds that were different, associated with the treatments. In the present study, we have deepened in the metabolic alterations under the MCD diet ant eh impact of PH.

Both MCD diet and PH have a profound impact on liver metabolism, although we found greater metabolic changes due to PH than to MCD diet. The multiplatform metabolomics approach has expanded the metabolite coverage, and CE/MS has allowed detecting changes in amino acid (proteinogenic and non-proteinogenic) and methylation pathways, whereas lipid metabolism (sphingolipids, phospholipids, neutral lipids, acylcarnitines, etc.) has been evaluated through LC/MS, and GC/MS has provided data about several carbohydrates and related small non-aminated compounds.

The present study has provided solid evidence of the metabolomics profile of the regenerating liver in the context of MCD-induced NASH. We have expanded the number of annotated compounds to a number close to 400, among those that significantly changed associated with NASH development and advanced liver regeneration after PH. This work will facilitate the study of the animal model of PH under the MCD diet, in the quest for better therapeutic approaches to liver regeneration.

This study has permitted to enlarge the knowledge about the metabolic routes that are involved in the advanced stages of liver regeneration after PH, especially in an animal model of NASH.

Final Conclusions

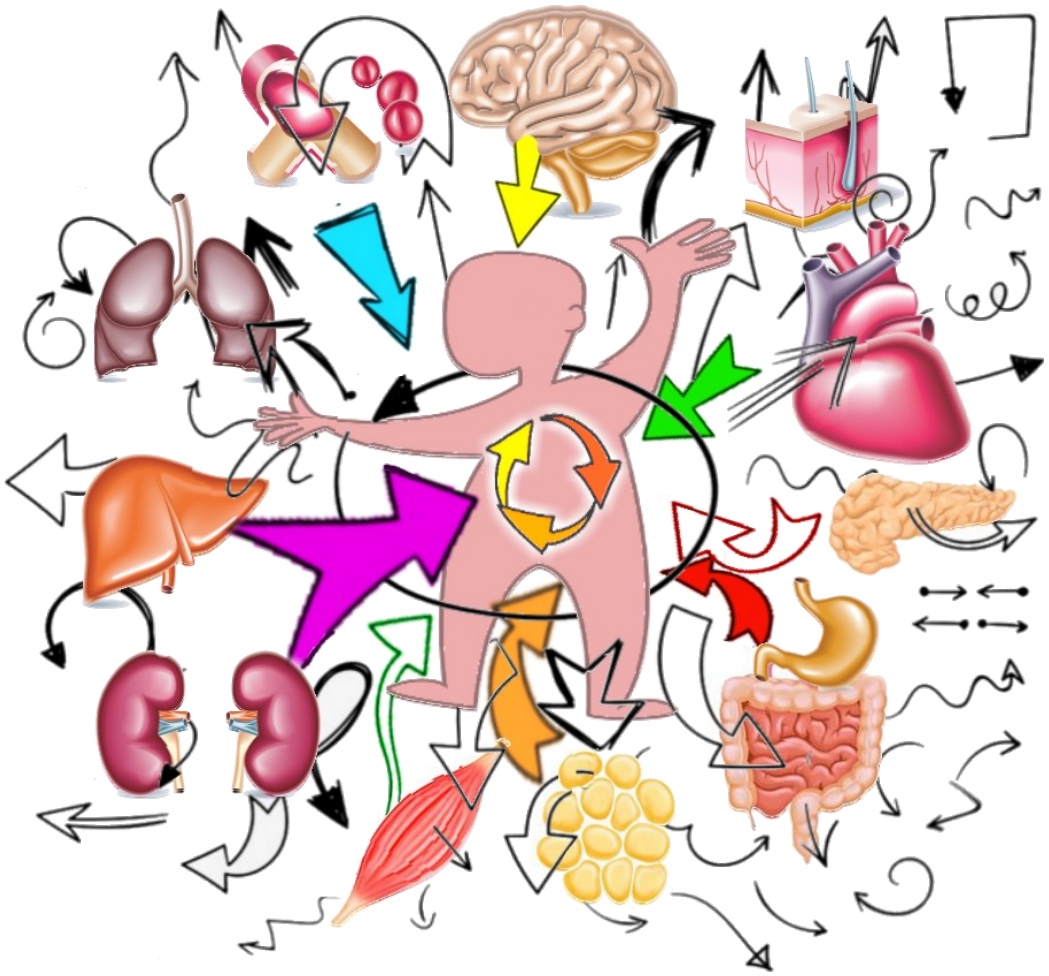

The results obtained have been discussed within each section, and partial conclusions have been respectively included. Some global, summarizing conclusions can be extracted:

- A global, holistic, and comprehensive multiplatform mass spectrometry (GC/MS, CE/MS, LC/MS) metabolomics study has been successfully performed analysing the metabolic phenotype of the differences associated with diet-induced obesity in 8 physiological compartments in mice.

- A thorough study of the differences due to diet-induced obesity in the abundance of 147 triacylglycerides and 122 lipid mediators in epididymal adipose tissue through LC/MS was accomplished.

- Taken altogether, our results show up the metabolic impact and/or alterations of obesity in different organs, beyond the WAT. WAT gains importance as the place where changes associated with the diet (i.e., SFA TGs) are accumulated and then become the origin of signalling molecules (lipid mediators) which exert their effect first locally, then spread to the body as signalling themselves, or through secondary inflammation-related compounds (LPs)

- A global, holistic and comprehensive multiplatform mass spectrometry (GC/MS, CE/MS, LC/MS) metabolomics study has been successfully performed analysing the metabolic phenotype of the differences in livers of mice subjected to a methionine-choline deficient diet, as a model of NASH (a common complication of obesity), and the impact of partial hepatectomy under these conditions.

All the information gathered in the present Thesis becomes a starting point to study potential therapies for obesity pandemic or its complications. From the knowledge acquired through different metabolomic strategies, the metabolic impact of the potential treatment(s) can be tackled straightforwardly.

Conclusiones finales

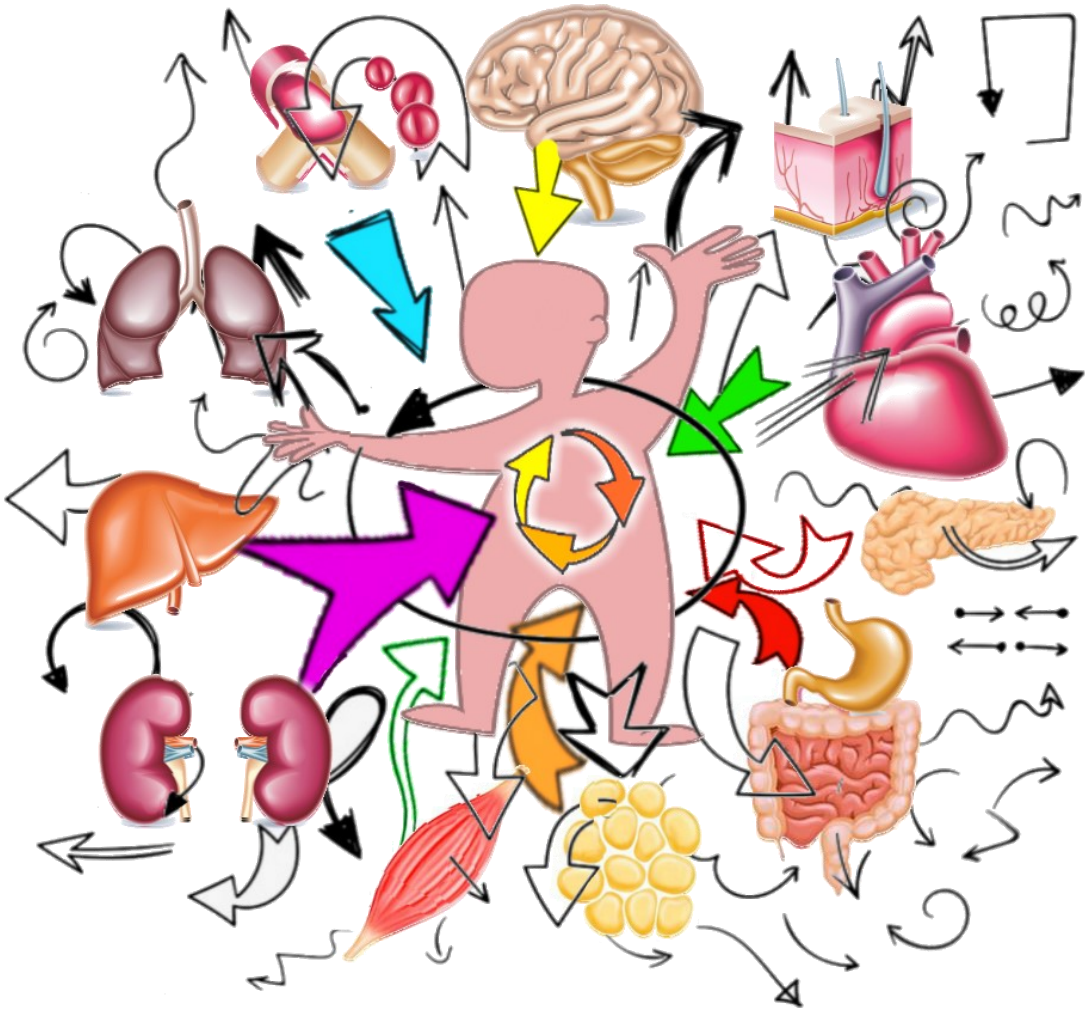

Los resultados obtenidos se han discutido dentro de cada sección, y se han incluido conclusiones parciales respectivamente. Se pueden extraer algunas conclusiones globales y resumidas:

- Se ha realizado con éxito un estudio global, holístico y exhaustivo de metabolómica multiplataforma (GC/MS, CE/MS, LC/MS) que analiza el fenotipo metabólico de las diferencias asociadas a la obesidad inducida por la dieta en 8 compartimentos fisiológicos en ratones.

- Se ha realizado un estudio exhaustivo de las diferencias debidas a la obesidad inducida por la dieta en la abundancia de 147 triacilglicéridos y 122 mediadores lipídicos en el tejido adiposo epididimal mediante LC/MS.

- En conjunto, nuestros resultados ponen de manifiesto el impacto metabólico y/o las alteraciones de la obesidad en diferentes órganos, más allá del Tejido Adiposo Blanco. El Tejido Adiposo adquiere importancia como el lugar donde se acumulan los cambios asociados a la dieta (es decir, los ácidos grasos saturados) y luego se convierten en el origen de las moléculas de señalización (mediadores lipídicos) que ejercen su efecto primero localmente, y luego se extienden al organismo como señalización propia, o a través de compuestos secundarios relacionados con la inflamación (Lisofosfolípidos).

- Se ha realizado con éxito un estudio global, holístico y exhaustivo de espectrometría de masas multiplataforma (GC/MS, CE/MS, LC/MS) que analiza el fenotipo metabólico de las diferencias en hígados de ratones sometidos a una dieta deficiente en metionina-colina, como modelo de EHNA (una complicación común de la obesidad), y el impacto de la hepatectomía parcial en estas condiciones.

Toda la información recopilada en la presente Tesis se convierte en un punto de partida para estudiar potenciales terapias para la pandemia de la obesidad o sus complicaciones. A partir de los conocimientos adquiridos a través de las diferentes estrategias metabolómicas, se puede abordar directamente el impacto metabólico de los posibles tratamientos.

References

[1] J.Q. Purnell, Definitions, Classification, and Epidemiology of Obesity, in: Feingold, K.R., Anawalt, B., Boyce, A., Chrousos, G., Dungan, K., Grossman, A., Hershman, J.M., Kaltsas, G., Koch, C., Kopp, P., Korbonits, M., McLachlan, R., Morley, J.E., New, M., Perreault, L., Purnell, J., Rebar, R., Singer, F., Trence, D.L., Vinik, A. and Wilson, D.P. (Eds.), Endotext, MDText.com, Inc., South Dartmouth (MA), 2000.

[2] World Health Organization, "Mean Body Mass Index (BMI)", https://www.who.int/gho/ncd/risk_factors/bmi_text/en/ (2019).

[3] I. Kyrou, H.S. Randeva, C. Tsigos, G. Kaltsas, M.O. Weickert, Clinical Problems Caused by Obesity, in: Feingold, K.R., Anawalt, B., Boyce, A., Chrousos, G., Dungan, K., Grossman, A., Hershman, J.M., Kaltsas, G., Koch, C., Kopp, P., Korbonits, M., McLachlan, R., Morley, J.E., New, M., Perreault, L., Purnell, J., Rebar, R., Singer, F., Trence, D.L., Vinik, A. and Wilson, D.P. (Eds.), Endotext, MDText.com, Inc., South Dartmouth (MA), 2000.

[4] R.H. Unger, Minireview: Weapons of Lean Body Mass Destruction: The Role of Ectopic Lipids in the Metabolic Syndrome, Endocrinology. 144 (2003) 5159-5165, doi: 10.1210/en.2003-0870.

[5] R. Unger, L. Orci, Lipotoxic diseases of nonadipose tissues in obesity, International Journal of Obesity. 24 (2000) S28-S32, doi: 10.1038/sj.ijo.0801498.

[6] S. Virtue, A. Vidal-Puig, It's Not How Fat You Are, It's What You Do with It That Counts, PLOS Biology. 6 (2008) e237, doi: 10.1371/journal.pbio.0060237.

[7] I.S. Farooqi, S. O'Rahilly, The Genetics of Obesity in Humans, in: Feingold, K.R., Anawalt, B., Boyce, A., Chrousos, G., Dungan, K., Grossman, A., Hershman, J.M., Kaltsas, G., Koch, C., Kopp, P., Korbonits, M., McLachlan, R., Morley, J.E., New, M., Perreault, L., Purnell, J., Rebar, R., Singer, F., Trence, D.L., Vinik, A. and Wilson, D.P. (Eds.), Endotext, MDText.com, Inc., South Dartmouth (MA), 2000.

[8] Insulin Resistance & Prediabetes | NIDDK, https://www.niddk.nih.gov/health-information/diabetes/overview/what-is-diabetes/prediabetes-insulin-resistance. 2020.

[9] G.M. Reaven, The Insulin Resistance Syndrome: Definition and Dietary Approaches to Treatment, Annu. Rev. Nutr. 25 (2005) 391-406, doi: 10.1146/annurev.nutr.24.012003.132155.

[10] Y.T. Wondmkun, Obesity, Insulin Resistance, and Type 2 Diabetes: Associations and Therapeutic Implications, Diabetes Metab Syndr Obes. 13 (2020) 3611-3616, doi: 10.2147/DMSO.S275898.

[11] K.M. Kriauciunas, M.G. Myers, C.R. Kahn, Cellular compartmentalization in insulin action: altered signaling by a lipid-modified IRS-1, Mol. Cell. Biol. 20 (2000) 6849-6859, doi: 10.1128/mcb.20.18.6849-6859.2000.

[12] A.R. Saltiel, C.R. Kahn, Insulin signalling and the regulation of glucose and lipid metabolism, Nature. 414 (2001) 799-806, doi: 10.1038/414799a.

[13] B.B. Lowell, G.I. Shulman, Mitochondrial dysfunction and type 2 diabetes, Science. 307 (2005) 384-387, doi: 10.1126/science.1104343.

[14] J. Kim, Y. Wei, J.R. Sowers, Role of mitochondrial dysfunction in insulin resistance, Circ. Res. 102 (2008) 401-414, doi: 10.1161/CIRCRESAHA.107.165472.

[15] K.F. Petersen, D. Befroy, S. Dufour, J. Dziura, C. Ariyan, D.L. Rothman, L. DiPietro, G.W. Cline, G.I. Shulman, Mitochondrial dysfunction in the elderly: possible role in insulin resistance, Science. 300 (2003) 1140-1142, doi: 10.1126/science.1082889.

[16] M. Mogensen, K. Sahlin, M. Fernström, D. Glintborg, B.F. Vind, H. Beck-Nielsen, K. Højlund, Mitochondrial respiration is decreased in skeletal muscle of patients with type 2 diabetes, Diabetes. 56 (2007) 1592-1599, doi: 10.2337/db06-0981.

[17] C. Sánchez-Lasheras, A. Christine Könner, J.C. Brüning, Integrative neurobiology of energy homeostasis-neurocircuits, signals and mediators, Frontiers in Neuroendocrinology. 31 (2010) 4-15, doi: 10.1016/j.yfrne.2009.08.002.

[18] S.P. Weisberg, D. McCann, M. Desai, M. Rosenbaum, R.L. Leibel, A.W. Ferrante, Obesity is associated with macrophage accumulation in adipose tissue, J Clin Invest. 112 (2003) 1796-1808, doi: 10.1172/JCI19246.

[19] M.T.A. Nguyen, S. Favelyukis, A. Nguyen, D. Reichart, P.A. Scott, A. Jenn, R. Liu-Bryan, C.K. Glass, J.G. Neels, J.M. Olefsky, A subpopulation of macrophages infiltrates hypertrophic adipose tissue and is activated by free fatty acids via Toll-like receptors 2 and 4 and JNK-dependent pathways, J. Biol. Chem. 282 (2007) 35279-35292, doi: 10.1074/jbc.M706762200.

[20] J.M. Olefsky, C.K. Glass, Macrophages, inflammation, and insulin resistance, Annu. Rev. Physiol. 72 (2010) 219-246, doi: 10.1146/annurev-physiol-021909-135846.

[21] J. Hirosumi, G. Tuncman, L. Chang, C.Z. Görgün, K.T. Uysal, K. Maeda, M. Karin, G.S. Hotamisligil, A central role for JNK in obesity and insulin resistance, Nature. 420 (2002) 333-336, doi: 10.1038/nature01137.

[22] G.D. Frank, S. Eguchi, E.D. Motley, The role of reactive oxygen species in insulin signaling in the vasculature, Antioxid. Redox Signal. 7 (2005) 1053-1061, doi: 10.1089/ars.2005.7.1053.

[23] Y. Lin, A.H. Berg, P. Iyengar, T.K.T. Lam, A. Giacca, T.P. Combs, M.W. Rajala, X. Du, B. Rollman, W. Li, M. Hawkins, N. Barzilai, C.J. Rhodes, I.G. Fantus, M. Brownlee, P.E. Scherer, The hyperglycemia-induced inflammatory response in adipocytes: the role of reactive oxygen species, J. Biol. Chem. 280 (2005) 4617-4626, doi: 10.1074/jbc.M411863200.

[24] J.L. Evans, I.D. Goldfine, B.A. Maddux, G.M. Grodsky, Are oxidative stress-activated signaling pathways mediators of insulin resistance and beta-cell dysfunction?, Diabetes. 52 (2003) 1-8, doi: 10.2337/diabetes.52.1.1.

[25] G. Marchesini, E. Bugianesi, G. Forlani, F. Cerrelli, M. Lenzi, R. Manini, S. Natale, E. Vanni, N. Villanova, N. Melchionda, M. Rizzetto, Nonalcoholic fatty liver, steatohepatitis, and the metabolic syndrome, Hepatology. 37 (2003) 917-923, doi: 10.1053/jhep.2003.50161.

[26] C. Duval, U. Thissen, S. Keshtkar, B. Accart, R. Stienstra, M.V. Boekschoten, T. Roskams, S. Kersten, M. Muller, Adipose tissue dysfunction signals progression of hepatic steatosis towards nonalcoholic steatohepatitis in C57Bl/6 mice, Diabetes (2010) 3181.

[27] D. Schuppan, M.D. Gorrell, T. Klein, M. Mark, N.H. Afdhal, The challenge of developing novel pharmacological therapies for non-alcoholic steatohepatitis, Liver International. 30 (2010) 795-808, doi: 10.1111/j.1478-3231.2010.02264.x.

[28] G.J. Patti, O. Yanes, G. Siuzdak, Innovation: Metabolomics: the apogee of the omics trilogy, Nature Reviews Molecular Cell Biology. 13 (2012) 263-269, doi: 10.1038/nrm3314.

[29] J.C. Lindon, J.K. Nicholson, E. Holmes, Chapter 1 - Metabonomics and Metabolomics Techniques and Their Applications in Mammalian Systems, in: Anonymous , The Handbook of Metabonomics and Metabolomics, Elsevier Science, Amsterdam, 2007, pp. 1-33.

[30] H. Gibbons, A. O'Gorman, L. Brennan, Metabolomics as a tool in nutritional research, Curr. Opin. Lipidol. 26 (2015) 30-34, doi: 10.1097/MOL.0000000000000140.

[31] D.G. Robertson, U. Frevert, Metabolomics in drug discovery and development, Clin. Pharmacol. Ther. 94 (2013) 559-561, doi: 10.1038/clpt.2013.120.

[32] M. Mamas, W.B. Dunn, L. Neyses, R. Goodacre, The role of metabolites and metabolomics in clinically applicable biomarkers of disease, Arch. Toxicol. 85 (2011) 5-17, doi: 10.1007/s00204-010-0609-6.

[33] E.G. Armitage, C. Barbas, Review: Metabolomics in cancer biomarker discovery: Current trends and future perspectives, J. Pharm. Biomed. Anal. 87 (2014) 1-11, doi: 10.1016/j.jpba.2013.08.041.

[34] J. Godzien, M. Ciborowski, M.P. Martínez-Alcázar, P. Samczuk, A. Kretowski, C. Barbas, Rapid and Reliable Identification of Phospholipids for Untargeted Metabolomics with LC–ESI–QTOF–MS/MS, J. Proteome Res. 14 (2015) 3204-3216, doi: 10.1021/acs.jproteome.5b00169.

[35] Gil de la Fuente, Alberto, J. Godzien, M. Fernández López, F.J. Rupérez, C. Barbas, A. Otero, Knowledge-based metabolite annotation tool: CEU Mass Mediator, Journal of Pharmaceutical and Biomedical Analysis. 154 (2018) 138-149, doi: 10.1016/j.jpba.2018.02.046.

[36] A. Gil-de-la-Fuente, J. Godzien, S. Saugar, R. Garcia-Carmona, H. Badran, D.S. Wishart, C. Barbas, A. Otero, CEU Mass Mediator 3.0: A Metabolite Annotation Tool, J. Proteome Res. 18 (2019) 797-802, doi: 10.1021/acs.jproteome.8b00720.

[37] T.A. Lutz, S.C. Woods, Overview of animal models of obesity, Curr Protoc Pharmacol. Chapter 5 (2012) Unit5.61, doi: 10.1002/0471141755.ph0561s58.

[38] R. Kohli, M. Kirby, S.A. Xanthakos, S. Softic, A.E. Feldstein, V. Saxena, P.H. Tang, L. Miles, M.V. Miles, W.F. Balistreri, S.C. Woods, R.J. Seeley, High-fructose, medium chain trans-fat diet induces liver fibrosis and elevates plasma coenzyme Q9 in a novel murine model of obesity and nonalcoholic steatohepatitis, Hepatology. 52 (2010) 934-944, doi: 10.1002/hep.23797.

[39] T. Kawasaki, K. Igarashi, T. Koeda, K. Sugimoto, K. Nakagawa, S. Hayashi, R. Yamaji, H. Inui, T. Fukusato, T. Yamanouchi, Rats fed fructose-enriched diets have characteristics of nonalcoholic hepatic steatosis, J. Nutr. 139 (2009) 2067-2071, doi: 10.3945/jn.109.105858.

[40] M.S. Winzell, B. Ahrén, The high-fat diet-fed mouse: a model for studying mechanisms and treatment of impaired glucose tolerance and type 2 diabetes, Diabetes. 53 Suppl 3 (2004) 215, doi: 10.2337/diabetes.53.suppl_3.s215.

[41] R.M. London, J. George, Pathogenesis of NASH: animal models, Clin Liver Dis. 11 (2007) 55-74, viii, doi: 10.1016/j.cld.2007.02.010.

[42] W. Syn, L. Yang, D.J. Chiang, Y. Qian, Y. Jung, G. Karaca, S.S. Choi, R.P. Witek, A. Omenetti, T.A. Pereira, A.M. Diehl, Genetic differences in oxidative stress and inflammatory responses to diet-induced obesity do not alter liver fibrosis in mice, Liver Int. 29 (2009) 1262-1272, doi: 10.1111/j.1478-3231.2009.02036.x.

[43] L.A. Campfield, F.J. Smith, P. Burn, The OB protein (leptin) pathway--a link between adipose tissue mass and central neural networks, Horm. Metab. Res. 28 (1996) 619-632, doi: 10.1055/s-2007-979867.

[44] R.H. Unger, The Physiology of Cellular Liporegulation, Annu. Rev. Physiol. 65 (2003) 333-347, doi: 10.1146/annurev.physiol.65.092101.142622.

[45] R. Buettner, K.G. Parhofer, M. Woenckhaus, C.E. Wrede, L.A. Kunz-Schughart, J. Schölmerich, L.C. Bollheimer, Defining high-fat-diet rat models: metabolic and molecular effects of different fat types, J. Mol. Endocrinol. 36 (2006) 485-501, doi: 10.1677/jme.1.01909.

[46] M. Manco, M. Calvani, G. Mingrone, Effects of dietary fatty acids on insulin sensitivity and secretion, Diabetes Obes Metab. 6 (2004) 402-413, doi: 10.1111/j.1462-8902.2004.00356.x.

[47] G. Serviddio, A.M. Giudetti, F. Bellanti, P. Priore, T. Rollo, R. Tamborra, L. Siculella, G. Vendemiale, E. Altomare, G.V. Gnoni, Oxidation of hepatic carnitine palmitoyl transferase-I (CPT-I) impairs fatty acid beta-oxidation in rats fed a methionine-choline deficient diet, PLoS ONE. 6 (2011) e24084, doi: 10.1371/journal.pone.0024084.

[48] M.K. Pickens, H. Ogata, R.K. Soon, J.P. Grenert, J.J. Maher, Dietary fructose exacerbates hepatocellular injury when incorporated into a methionine-choline-deficient diet, Liver Int. 30 (2010) 1229-1239, doi: 10.1111/j.1478-3231.2010.02285.x.

[49] S. Pelz, P. Stock, S. Brückner, B. Christ, A methionine-choline-deficient diet elicits NASH in the immunodeficient mouse featuring a model for hepatic cell transplantation, Exp. Cell Res. 318 (2012) 276-287, doi: 10.1016/j.yexcr.2011.11.005.

[50] Q.M. Anstee, R.D. Goldin, Mouse models in non-alcoholic fatty liver disease and steatohepatitis research, Int J Exp Pathol. 87 (2006) 1-16, doi: 10.1111/j.0959-9673.2006.00465.x.

[51] Y. Takahashi, Y. Soejima, T. Fukusato, Animal models of nonalcoholic fatty liver disease/nonalcoholic steatohepatitis, World J. Gastroenterol. 18 (2012) 2300-2308, doi: 10.3748/wjg.v18.i19.2300.

[52] A. Schultz, C.M. D Angelo, I. Bringhenti, S. Barbosa da Silva, T. da Silva Faria, V. Souza Mello, Nonalcoholic steatohepatitis: lessons from different diet-induced animal models, Journal of Diabetes, Metabolic Disorders & Control. Volume 1 (2014), doi: 10.15406/jdmdc.2014.01.00014.

[53] V. Kumar, A.K. Abbas, J.C. Aster, Robbins Patología Humana, Elsevier, 2018.

[54] V. Kumar, A.K. Abbas, J.C. Aster, Robbins Y Cotran Patología Estructural Y Funcional, Elsevier, 2015.

[55] J. Marx, Cellular warriors at the battle of the bulge, Science. 299 (2003) 846-849, doi: 10.1126/science.299.5608.846.

[56] E. Alegría Ezquerra, J.M. Castellano Vázquez, A. Alegría Barrero, [Obesity, metabolic syndrome and diabetes: cardiovascular implications and therapy], Rev Esp Cardiol. 61 (2008) 752-764.

[57] C.R. Borstnar, F. Cardellach, Farreras Rozman. Medicina Interna, Elsevier Health Sciences, 2020.

[58] F. López-Jiménez, M. Cortés-Bergoderi, Obesidad y corazón, Revista Española de Cardiología. 64 (2011) 140-149.

[59] S. de Ferranti, D. Mozaffarian, The perfect storm: obesity, adipocyte dysfunction, and metabolic consequences, Clin. Chem. 54 (2008) 945-955, doi: 10.1373/clinchem.2007.100156.

[60] H.E. Bays, J.M. González-Campoy, G.A. Bray, A.E. Kitabchi, D.A. Bergman, A.B. Schorr, H.W. Rodbard, R.R. Henry, Pathogenic potential of adipose tissue and metabolic consequences of adipocyte hypertrophy and increased visceral adiposity, Expert Rev Cardiovasc Ther. 6 (2008) 343-368, doi: 10.1586/14779072.6.3.343.

[61] J. Després, I. Lemieux, Abdominal obesity and metabolic syndrome, Nature. 444 (2006) 881-887, doi: 10.1038/nature05488.

[62] J. Després, I. Lemieux, J. Bergeron, P. Pibarot, P. Mathieu, E. Larose, J. Rodés-Cabau, O.F. Bertrand, P. Poirier, Abdominal obesity and the metabolic syndrome: contribution to global cardiometabolic risk, Arterioscler. Thromb. Vasc. Biol. 28 (2008) 1039-1049, doi: 10.1161/ATVBAHA.107.159228.

[63] M. Blüher, Adipose tissue dysfunction in obesity, Exp. Clin. Endocrinol. Diabetes. 117 (2009) 241-250, doi: 10.1055/s-0029-1192044.

[64] H.E. Bays, J.M. González-Campoy, R.R. Henry, D.A. Bergman, A.E. Kitabchi, A.B. Schorr, H.W. Rodbard, Is adiposopathy (sick fat) an endocrine disease?, Int J Clin Pract. 62 (2008) 1474-1483, doi: 10.1111/j.1742-1241.2008.01848.x.

[65] T. Skurk, C. Alberti-Huber, C. Herder, H. Hauner, Relationship between adipocyte size and adipokine expression and secretion, J. Clin. Endocrinol. Metab. 92 (2007) 1023-1033, doi: 10.1210/jc.2006-1055.

[66] M. Jernås, J. Palming, K. Sjöholm, E. Jennische, P. Svensson, B.G. Gabrielsson, M. Levin, A. Sjögren, M. Rudemo, T.C. Lystig, B. Carlsson, L.M.S. Carlsson, M. Lönn, Separation of human adipocytes by size: hypertrophic fat cells display distinct gene expression, FASEB J. 20 (2006) 1540-1542, doi: 10.1096/fj.05-5678fje.

[67] M. Pasarica, H. Xie, D. Hymel, G. Bray, F. Greenway, E. Ravussin, S.R. Smith, Lower Total Adipocyte Number but No Evidence for Small Adipocyte Depletion in Patients With Type 2 Diabetes, Diabetes Care. 32 (2009) 900-902, doi: 10.2337/dc08-2240.

[68] L.F. Van Gaal, I.L. Mertens, C.E. De Block, Mechanisms linking obesity with cardiovascular disease, Nature. 444 (2006) 875-880, doi: 10.1038/nature05487.

[69] M.M. Ibrahim, Subcutaneous and visceral adipose tissue: structural and functional differences, Obes Rev. 11 (2010) 11-18, doi: 10.1111/j.1467-789X.2009.00623.x.

[70] T.R. Harrison, A.S. Fauci, Principios De Medicina Interna, McGraw-Hill Interamericana, 2009.

[71] A. Pires, E. Castela, C. Sena, R. Seiça, [Obesity: Paradigm of Endothelial Dysfunction in Paediatric Age Groups], Acta Med Port. 28 (2015) 233-239.

[72] A. Bakhai, Adipokines—targeting a root cause of cardiometabolic risk, QJM. 101 (2008) 767-776, doi: 10.1093/qjmed/hcn066.

[73] G. Fantuzzi, T. Mazzone, Adipose tissue and atherosclerosis: exploring the connection, Arterioscler. Thromb. Vasc. Biol. 27 (2007) 996-1003, doi: 10.1161/ATVBAHA.106.131755.

[74] N.R. Madamanchi, A. Vendrov, M.S. Runge, Oxidative stress and vascular disease, Arterioscler. Thromb. Vasc. Biol. 25 (2005) 29-38, doi: 10.1161/01.ATV.0000150649.39934.13.

[75] A. Avogaro, S.V. de Kreutzenberg, Mechanisms of endothelial dysfunction in obesity, Clin. Chim. Acta. 360 (2005) 9-26, doi: 10.1016/j.cccn.2005.04.020.

[76] K.C. Zalesin, B.A. Franklin, W.M. Miller, E.D. Peterson, P.A. McCullough, Impact of obesity on cardiovascular disease, Endocrinol. Metab. Clin. North Am. 37 (2008) 663-684, ix, doi: 10.1016/j.ecl.2008.06.004.

[77] V. Bamba, D.J. Rader, Obesity and atherogenic dyslipidemia, Gastroenterology. 132 (2007) 2181-2190, doi: 10.1053/j.gastro.2007.03.056.

[78] C.A. Aguilar-Salinas, Mesa redonda XXV. Adiposidad abdominal como factor de riesgo para enfermedades crónicas, Salud Pública de México. 49 (2007) 311-316.

[79] M.S. Fernández-Alfonso, Regulation of vascular tone: the fat connection, Hypertension. 44 (2004) 255-256, doi: 10.1161/01.HYP.0000140056.64321.f9.

[80] A. Esteller Pérez, Biología de la pared vascular y síndrome metabólico, Nutrición Hospitalaria. 20 (2005) 5-17.

[81] O. Rosas-Carrasco, A. GE, G. CHA, E. JJ, O. MA, Endothelial Dysfunction and Hypertension, Medicina Interna de Mexico. 19 (2003) 221-42.

[82] M. Gil-Ortega, P. Stucchi, R. Guzmán-Ruiz, V. Cano, S. Arribas, M.C. González, M. Ruiz-Gayo, M.S. Fernández-Alfonso, B. Somoza, Adaptative nitric oxide overproduction in perivascular adipose tissue during early diet-induced obesity, Endocrinology. 151 (2010) 3299-3306, doi: 10.1210/en.2009-1464.

[83] M.S. Fernández-Alfonso, M. Gil-Ortega, C.F. García-Prieto, I. Aranguez, M. Ruiz-Gayo, B. Somoza, Mechanisms of perivascular adipose tissue dysfunction in obesity, Int J Endocrinol. 2013 (2013) 402053, doi: 10.1155/2013/402053.

[84] E. Rosen, B. Spiegelman, What We Talk About When We Talk About Fat, Cell. 156 (2014) 20-44, doi: //doi.org/10.1016/j.cell.2013.12.012.

[85] D.C.W. Lau, B. Dhillon, H. Yan, P.E. Szmitko, S. Verma, Adipokines: molecular links between obesity and atheroslcerosis, Am. J. Physiol. Heart Circ. Physiol. 288 (2005) 2031, doi: 10.1152/ajpheart.01058.2004.

[86] P.G. Kopelman, Obesity as a medical problem, Nature. 404 (2000) 635-643, doi: 10.1038/35007508.

[87] V. Mohamed-Ali, J.H. Pinkney, S.W. Coppack, Adipose tissue as an endocrine and paracrine organ, International Journal of Obesity. 22 (1998) 1145-1158, doi: 10.1038/sj.ijo.0800770.

[88] F. Gomes, D.F. Telo, H.P. Souza, J.C. Nicolau, A. Halpern, C.V. Serrano Jr, Obesidad y enfermedad arterial coronaria: papel de la inflamación vascular, Arquivos Brasileiros de Cardiologia. 94 (2010) 273-279, doi: 10.1590/S0066-782X2010000200021.

[89] B. Meissburger, Molecular mechanisms of adipogenesis in obesity and the metabolic syndrome (2010), doi: 10.3929/ethz-a-006214330.

[90] K.B. Misra, K.C. Kim, S. Cho, M.G. Low, A. Bensadoun, Purification and characterization of adipocyte heparan sulfate proteoglycans with affinity for lipoprotein lipase, J. Biol. Chem. 269 (1994) 23838-23844.

[91] A.C. Könner, J.C. Brüning, Toll-like receptors: linking inflammation to metabolism, Trends Endocrinol. Metab. 22 (2011) 16-23, doi: 10.1016/j.tem.2010.08.007.

[92] N. Kumar, G. Gupta, K. Anilkumar, N. Fatima, R. Karnati, G.V. Reddy, P.V. Giri, P. Reddanna, 15-Lipoxygenase metabolites of α-linolenic acid, [13-(S)-HPOTrE and 13-(S)-HOTrE], mediate anti-inflammatory effects by inactivating NLRP3 inflammasome, Sci Rep. 6 (2016) 31649, doi: 10.1038/srep31649.

[93] H. Kumar, T. Kawai, S. Akira, Toll-like receptors and innate immunity, Biochem. Biophys. Res. Commun. 388 (2009) 621-625, doi: 10.1016/j.bbrc.2009.08.062.

[94] Y. Shi, P. Burn, Lipid metabolic enzymes: emerging drug targets for the treatment of obesity, Nature Reviews Drug Discovery. 3 (2004) 695-710, doi: 10.1038/nrd1469.

[95] C.N. Lumeng, J.L. Bodzin, A.R. Saltiel, Obesity induces a phenotypic switch in adipose tissue macrophage polarization, J. Clin. Invest. 117 (2007) 175-184, doi: 10.1172/JCI29881.

[96] U. Ozcan, Q. Cao, E. Yilmaz, A. Lee, N.N. Iwakoshi, E. Ozdelen, G. Tuncman, C. Görgün, L.H. Glimcher, G.S. Hotamisligil, Endoplasmic reticulum stress links obesity, insulin action, and type 2 diabetes, Science. 306 (2004) 457-461, doi: 10.1126/science.1103160.

[97] C. Sewter, A. Vidal-Puig, PPARγ and the thiazolidinediones: molecular basis for a treatment of 'Syndrome X'?, Diabetes, Obesity and Metabolism. 4 (2002) 239-248, doi: 10.1046/j.1463-1326.2002.00187.x.

[98] M. Slawik, A.J. Vidal-Puig, Adipose tissue expandability and the metabolic syndrome, Genes Nutr. 2 (2007) 41-45, doi: 10.1007/s12263-007-0014-9.

[99] T. Tchkonia, T. Pirtskhalava, T. Thomou, M.J. Cartwright, B. Wise, I. Karagiannides, A. Shpilman, T.L. Lash, J.D. Becherer, J.L. Kirkland, Increased TNFalpha and CCAAT/enhancer-binding protein homologous protein with aging predispose preadipocytes to resist adipogenesis, Am. J. Physiol. Endocrinol. Metab. 293 (2007) 1810, doi: 10.1152/ajpendo.00295.2007.

[100] R. Ray, A.M. Shah, NADPH oxidase and endothelial cell function, Clin Sci (Lond). 109 (2005) 217-226, doi: 10.1042/CS20050067.

[101] S. Pilz, W. März, Free fatty acids as a cardiovascular risk factor, Clin. Chem. Lab. Med. 46 (2008) 429-434, doi: 10.1515/CCLM.2008.118.

[102] B.T. Noronha, J. Li, S.B. Wheatcroft, A.M. Shah, M.T. Kearney, Inducible nitric oxide synthase has divergent effects on vascular and metabolic function in obesity, Diabetes. 54 (2005) 1082-1089, doi: 10.2337/diabetes.54.4.1082.

[103] K. Nakamura, J.J. Fuster, K. Walsh, Adipokines: a link between obesity and cardiovascular disease, J Cardiol. 63 (2014) 250-259, doi: 10.1016/j.jjcc.2013.11.006.

[104] K.T. Uysal, S.M. Wiesbrock, M.W. Marino, G.S. Hotamisligil, Protection from obesity-induced insulin resistance in mice lacking TNF-alpha function, Nature. 389 (1997) 610-614, doi: 10.1038/39335.

[105] G.S. Hotamisligil, A. Budavari, D. Murray, B.M. Spiegelman, Reduced tyrosine kinase activity of the insulin receptor in obesity-diabetes. Central role of tumor necrosis factor-alpha, J. Clin. Invest. 94 (1994) 1543-1549, doi: 10.1172/JCI117495.

[106] E. Hu, P. Liang, B.M. Spiegelman, AdipoQ is a novel adipose-specific gene dysregulated in obesity, J. Biol. Chem. 271 (1996) 10697-10703, doi: 10.1074/jbc.271.18.10697.

[107] K. Maeda, K. Okubo, I. Shimomura, T. Funahashi, Y. Matsuzawa, K. Matsubara, cDNA Cloning and Expression of a Novel Adipose Specific Collagen-like Factor, apM1 (AdiposeMost Abundant Gene Transcript 1), Biochemical and Biophysical Research Communications. 221 (1996) 286-289, doi: 10.1006/bbrc.1996.0587.

[108] P.E. Scherer, S. Williams, M. Fogliano, G. Baldini, H.F. Lodish, A novel serum protein similar to C1q, produced exclusively in adipocytes, J. Biol. Chem. 270 (1995) 26746-26749, doi: 10.1074/jbc.270.45.26746.

[109] Y. Arita, Reprint of “Paradoxical Decrease of an Adipose-Specific Protein, Adiponectin, in Obesity”, Biochemical and Biophysical Research Communications. 425 (2012) 560-564, doi: 10.1016/j.bbrc.2012.08.024.

[110] J.E. Hall, J.M. do Carmo, A.A. da Silva, Z. Wang, M.E. Hall, Obesity-induced hypertension: interaction of neurohumoral and renal mechanisms, Circ. Res. 116 (2015) 991-1006, doi: 10.1161/CIRCRESAHA.116.305697.

[111] R.J. Garrison, W.B. Kannel, J. Stokes, W.P. Castelli, Incidence and precursors of hypertension in young adults: the Framingham Offspring Study, Prev Med. 16 (1987) 235-251, doi: 10.1016/0091-7435(87)90087-9.

[112] J.D. Kopple, Obesity and Chronic Kidney Disease, Journal of Renal Nutrition. 20 (2010) S29-S30, doi: 10.1053/j.jrn.2010.05.008.

[113] J.E. Hall, J.R. Henegar, T.M. Dwyer, J. Liu, A.A. Da Silva, J.J. Kuo, L. Tallam, Is obesity a major cause of chronic kidney disease?, Adv Ren Replace Ther. 11 (2004) 41-54, doi: 10.1053/j.arrt.2003.10.007.

[114] J.D. Kopple, U. Feroze, The effect of obesity on chronic kidney disease, J Ren Nutr. 21 (2011) 66-71, doi: 10.1053/j.jrn.2010.10.009.

[115] J.E. Hall, J.M. do Carmo, A.A. da Silva, Z. Wang, M.E. Hall, Obesity, kidney dysfunction and hypertension: mechanistic links, Nat Rev Nephrol. 15 (2019) 367-385, doi: 10.1038/s41581-019-0145-4.

[116] T. Ecder, Early diagnosis saves lives: focus on patients with chronic kidney disease, Kidney Int Suppl. 3 (2013) 335-336, doi: 10.1038/kisup.2013.70.

[117] A. Chang, L. Van Horn, D.R. Jacobs, K. Liu, P. Muntner, B. Newsome, D.A. Shoham, R. Durazo-Arvizu, K. Bibbins-Domingo, J. Reis, H. Kramer, Lifestyle-related factors, obesity, and incident microalbuminuria: the CARDIA (Coronary Artery Risk

Development in Young Adults) study, Am. J. Kidney Dis. 62 (2013) 267-275, doi: 10.1053/j.ajkd.2013.02.363.

[118] Y. Song, J. Sung, K. Lee, Longitudinal relationships of metabolic syndrome and obesity with kidney function: Healthy Twin Study, Clin. Exp. Nephrol. 19 (2015) 887-894, doi: 10.1007/s10157-015-1083-5.

[119] L.D. Bash, T.P. Erlinger, J. Coresh, J. Marsh-Manzi, A.R. Folsom, B.C. Astor, Inflammation, hemostasis, and the risk of kidney function decline in the Atherosclerosis Risk in Communities (ARIC) Study, Am. J. Kidney Dis. 53 (2009) 596-605, doi: 10.1053/j.ajkd.2008.10.044.

[120] J. Lin, F.B. Hu, C. Mantzoros, G.C. Curhan, Lipid and inflammatory biomarkers and kidney function decline in type 2 diabetes, Diabetologia. 53 (2010) 263-267, doi: 10.1007/s00125-009-1597-z.

[121] M. Praga, E. Hernández, J.C. Herrero, E. Morales, Y. Revilla, R. Díaz-González, J.L. Rodicio, Influence of obesity on the appearance of proteinuria and renal insufficiency after unilateral nephrectomy, Kidney Int. 58 (2000) 2111-2118, doi: 10.1111/j.1523-1755.2000.00384.x.

[122] S. Neubauer, The Failing Heart, New England Journal of Medicine. 356 (2007) 2544-2546, doi: 10.1056/NEJMc071013.

[123] W.C. Stanley, M.P. Chandler, Energy metabolism in the normal and failing heart: potential for therapeutic interventions, Heart Fail Rev. 7 (2002) 115-130, doi: 10.1023/a:1015320423577.

[124] P.J. Randle, P.B. Garland, C.N. Hales, E.A. Newsholme, The Glucose fatty-acid cycle. Its role in insulin sensitivity and the metabolic disturbances of Diabetes Mellitus, The Lancet. 281 (1963) 785-789, doi: 10.1016/S0140-6736(63)91500-9.

[125] E.N. Dedkova, L.A. Blatter, Measuring mitochondrial function in intact cardiac myocytes, J. Mol. Cell. Cardiol. 52 (2012) 48-61, doi: 10.1016/j.yjmcc.2011.08.030.

[126] H. Ashrafian, M.P. Frenneaux, L.H. Opie, Metabolic mechanisms in heart failure, Circulation. 116 (2007) 434-448, doi: 10.1161/CIRCULATIONAHA.107.702795.

[127] L.H. Opie, Substrate Utilization and Glycolysis in the Heart, CRD. 56 (1971) 2-21, doi: 10.1159/000166613.

[128] N. Varma, F.R. Eberli, C.S. Apstein, Increased diastolic chamber stiffness during demand ischemia: response to quick length change differentiates rigor-activated from calcium-activated tension, Circulation. 101 (2000) 2185-2192, doi: 10.1161/01.cir.101.18.2185.

[129] D. An, B. Rodrigues, Role of changes in cardiac metabolism in development of diabetic cardiomyopathy, Am. J. Physiol. Heart Circ. Physiol. 291 (2006) 1489, doi: 10.1152/ajpheart.00278.2006.

[130] S. Kenchaiah, J.C. Evans, D. Levy, P.W.F. Wilson, E.J. Benjamin, M.G. Larson, W.B. Kannel, R.S. Vasan, Obesity and the risk of heart failure, N. Engl. J. Med. 347 (2002) 305-313, doi: 10.1056/NEJMoa020245.

[131] S. Mv, L. T, D. Am, S. Re, B. Gm, Relationship of mitochondrial DNA depletion and respiratory chain activity in preadipocytes treated with nucleoside reverse transcriptase inhibitors., Antivir Ther. 12 (2007) 205-216.

[132] S. Boudina, S. Sena, H. Theobald, X. Sheng, J.J. Wright, X.X. Hu, S. Aziz, J.I. Johnson, H. Bugger, V.G. Zaha, E.D. Abel, Mitochondrial energetics in the heart in obesity-related diabetes: direct evidence for increased uncoupled respiration and activation of uncoupling proteins, Diabetes. 56 (2007) 2457-2466, doi: 10.2337/db07-0481.

[133] J. Berger, D.E. Moller, The mechanisms of action of PPARs, Annu. Rev. Med. 53 (2002) 409-435, doi: 10.1146/annurev.med.53.082901.104018.

[134] J.M. Huss, D.P. Kelly, Nuclear receptor signaling and cardiac energetics, Circ. Res. 95 (2004) 568-578, doi: 10.1161/01.RES.0000141774.29937.e3.

[135] M. Chandran, S.A. Phillips, T. Ciaraldi, R.R. Henry, Adiponectin: more than just another fat cell hormone?, Diabetes Care. 26 (2003) 2442-2450, doi: 10.2337/diacare.26.8.2442.

[136] P.M. Barger, D.P. Kelly, PPAR signaling in the control of cardiac energy metabolism, Trends Cardiovasc. Med. 10 (2000) 238-245, doi: 10.1016/s1050-1738(00)00077-3.

[137] K. Motojima, P. Passilly, J.M. Peters, F.J. Gonzalez, N. Latruffe, Expression of putative fatty acid transporter genes are regulated by peroxisome proliferator-activated receptor alpha and gamma activators in a tissue- and inducer-specific manner, J. Biol. Chem. 273 (1998) 16710-16714, doi: 10.1074/jbc.273.27.16710.

[138] M. Van Bilsen, J.E. de Vries, Van der Vusse, G. J., Long-term effects of fatty acids on cell viability and gene expression of neonatal cardiac myocytes, Prostaglandins Leukot. Essent. Fatty Acids. 57 (1997) 39-45, doi: 10.1016/s0952-3278(97)90491-9.

[139] van der Lee, K. A., M.M. Vork, J.E. De Vries, P.H. Willemsen, J.F. Glatz, R.S. Reneman, Van der Vusse, G. J., M. Van Bilsen, Long-chain fatty acid-induced changes in gene expression in neonatal cardiac myocytes, J. Lipid Res. 41 (2000) 41-47.

[140] F. Djouadi, J.M. Brandt, C.J. Weinheimer, T.C. Leone, F.J. Gonzalez, D.P. Kelly, The role of the peroxisome proliferator-activated receptor alpha (PPAR alpha) in the control of cardiac lipid metabolism, Prostaglandins Leukot. Essent. Fatty Acids. 60 (1999) 339-343, doi: 10.1016/s0952-3278(99)80009-x.

[141] Pagamp. C, Calcagno. A, Granzotto. M, Calabrese. F, Thiene. G, Federspil. G, Vettor. R, Heart lipid accumulation in obese non-diabetic rats: effect of weight loss., Nutr Metab Cardiovasc Dis. 18 (2007) 189-197, doi: 10.1016/j.numecd.2006.05.009.

[142] H.C. Chiu, A. Kovacs, D.A. Ford, F.F. Hsu, R. Garcia, P. Herrero, J.E. Saffitz, J.E. Schaffer, A novel mouse model of lipotoxic cardiomyopathy, J. Clin. Invest. 107 (2001) 813-822, doi: 10.1172/JCI10947.

[143] S.L.M. Coort, D.M. Hasselbaink, D.P.Y. Koonen, J. Willems, W.A. Coumans, A. Chabowski, Vusse, Ger J. van der, A. Bonen, J.F.C. Glatz, Luiken, Joost J. F. P., Enhanced sarcolemmal FAT/CD36 content and triacylglycerol storage in cardiac myocytes from obese zucker rats., Diabetes (2004), doi: 10.2337/diabetes.53.7.1655.

[144] R.S. Ahima, Adipose tissue as an endocrine organ, Obesity (Silver Spring). 14 Suppl 5 (2006) 242S-249S, doi: 10.1038/oby.2006.317.

[145] L. Li, L. Wu, C. Wang, L. Liu, Y. Zhao, Adiponectin modulates carnitine palmitoyltransferase-1 through AMPK signaling cascade in rat cardiomyocytes, Regul. Pept. 139 (2007) 72-79, doi: 10.1016/j.regpep.2006.10.007.

[146] R. Palanivel, X. Fang, M. Park, M. Eguchi, S. Pallan, S. De Girolamo, Y. Liu, Y. Wang, A. Xu, G. Sweeney, Globular and full-length forms of adiponectin mediate specific changes in glucose and fatty acid uptake and metabolism in cardiomyocytes, Cardiovasc. Res. 75 (2007) 148-157, doi: 10.1016/j.cardiores.2007.04.011.

[147] Y. Arita, S. Kihara, N. Ouchi, M. Takahashi, K. Maeda, J. Miyagawa, K. Hotta, I. Shimomura, T. Nakamura, K. Miyaoka, H. Kuriyama, M. Nishida, S. Yamashita, K. Okubo, K. Matsubara, M. Muraguchi, Y. Ohmoto, T. Funahashi, Y. Matsuzawa, Paradoxical decrease of an adipose-specific protein, adiponectin, in obesity, Biochem. Biophys. Res. Commun. 257 (1999) 79-83, doi: 10.1006/bbrc.1999.0255.

[148] R.V. Considine, M.K. Sinha, M.L. Heiman, A. Kriauciunas, T.W. Stephens, M.R. Nyce, J.P. Ohannesian, C.C. Marco, L.J. McKee, T.L. Bauer, Serum immunoreactive-leptin concentrations in normal-weight and obese humans, N. Engl. J. Med. 334 (1996) 292-295, doi: 10.1056/NEJM199602013340503.

[149] G.D. Lopaschuk, C.D.L. Folmes, W.C. Stanley, Cardiac energy metabolism in obesity, Circ. Res. 101 (2007) 335-347, doi: 10.1161/CIRCRESAHA.107.150417.

[150] A. Fukushima, G.D. Lopaschuk, Cardiac fatty acid oxidation in heart failure associated with obesity and diabetes, Biochimica et Biophysica Acta (BBA) - Molecular and Cell Biology of Lipids. 1861 (2016) 1525-1534, doi: 10.1016/j.bbalip.2016.03.020.

[151] J.G. Tidball, Inflammatory processes in muscle injury and repair, Am. J. Physiol. Regul. Integr. Comp. Physiol. 288 (2005) 345, doi: 10.1152/ajpregu.00454.2004.

[152] L.N. Fink, S.R. Costford, Y.S. Lee, T.E. Jensen, P.J. Bilan, A. Oberbach, M. Blüher, J.M. Olefsky, A. Sams, A. Klip, Pro-inflammatory macrophages increase in skeletal muscle of high fat-fed mice and correlate with metabolic risk markers in humans, Obesity (Silver Spring). 22 (2014) 747-757, doi: 10.1002/oby.20615.

[153] D.M. D'Souza, K.E. Trajcevski, D. Al-Sajee, D.C. Wang, M. Thomas, J.E. Anderson, T.J. Hawke, Diet-induced obesity impairs muscle satellite cell activation and muscle repair through alterations in hepatocyte growth factor signaling, Physiol Rep. 3 (2015), doi: 10.14814/phy2.12506.

[154] K.H. Collins, D.A. Hart, R.A. Reimer, R.A. Seerattan, C. Waters-Banker, S.C. Sibole, W. Herzog, High-fat high-sucrose diet leads to dynamic structural and inflammatory alterations in the rat vastus lateralis muscle, J. Orthop. Res. 34 (2016) 2069-2078, doi: 10.1002/jor.23230.

[155] G.A. Meyer, S.R. Ward, Developmental Biology and Regenerative Medicine: Addressing the Vexing Problem of Persistent Muscle Atrophy in the Chronically Torn Human Rotator Cuff, Phys Ther. 96 (2016) 722-733, doi: 10.2522/ptj.20150029.

[156] S. Lee, T. Kim, S. Kim, Sarcopenic obesity is more closely associated with knee osteoarthritis than is nonsarcopenic obesity: a cross-sectional study, Arthritis Rheum. 64 (2012) 3947-3954, doi: 10.1002/art.37696.

[157] H. Cho, J.L. Thorvaldsen, Q. Chu, F. Feng, M.J. Birnbaum, Akt1/PKBalpha is required for normal growth but dispensable for maintenance of glucose homeostasis in mice, J. Biol. Chem. 276 (2001) 38349-38352, doi: 10.1074/jbc.C100462200.

[158] L. Fontana, J.C. Eagon, M.E. Trujillo, P.E. Scherer, S. Klein, Visceral fat adipokine secretion is associated with systemic inflammation in obese humans, Diabetes. 56 (2007) 1010-1013, doi: 10.2337/db06-1656.

[159] W.G. McMaster, A. Kirabo, M.S. Madhur, D.G. Harrison, Inflammation, immunity, and hypertensive end-organ damage, Circ. Res. 116 (2015) 1022-1033, doi: 10.1161/CIRCRESAHA.116.303697.

[160] R.N. Baumgartner, K.M. Koehler, D. Gallagher, L. Romero, S.B. Heymsfield, R.R. Ross, P.J. Garry, R.D. Lindeman, Epidemiology of sarcopenia among the elderly in New Mexico, Am. J. Epidemiol. 147 (1998) 755-763, doi: 10.1093/oxfordjournals.aje.a009520.

[161] R.N. Baumgartner, Body Composition in Healthy Aging, Annals of the New York Academy of Sciences. 904 (2000) 437-448, doi: 10.1111/j.1749-6632.2000.tb06498.x.

[162] S. Stenholm, T.B. Harris, T. Rantanen, M. Visser, S.B. Kritchevsky, L. Ferrucci, Sarcopenic obesity: definition, cause and consequences, Curr Opin Clin Nutr Metab Care. 11 (2008) 693-700, doi: 10.1097/MCO.0b013e328312c37d.

[163] M. Zamboni, G. Mazzali, F. Fantin, A. Rossi, V. Di Francesco, Sarcopenic obesity: a new category of obesity in the elderly, Nutr Metab Cardiovasc Dis. 18 (2008) 388-395, doi: 10.1016/j.numecd.2007.10.002.

[164] M.J. Ormsbee, C.M. Prado, J.Z. Ilich, S. Purcell, M. Siervo, A. Folsom, L. Panton, Osteosarcopenic obesity: the role of bone, muscle, and fat on health, J Cachexia Sarcopenia Muscle. 5 (2014) 183-192, doi: 10.1007/s13539-014-0146-x.

[165] M. Karalaki, S. Fili, A. Philippou, M. Koutsilieris, Muscle regeneration: cellular and molecular events, In Vivo. 23 (2009) 779-796.

[166] T. Laumonier, J. Menetrey, Muscle injuries and strategies for improving their repair, J Exp Orthop. 3 (2016) 15, doi: 10.1186/s40634-016-0051-7.

[167] D. Akhmedov, R. Berdeaux, The effects of obesity on skeletal muscle regeneration, Front Physiol. 4 (2013) 371, doi: 10.3389/fphys.2013.00371.

[168] L.A. Brown, D.E. Lee, J.F. Patton, R.A. Perry, J.L. Brown, J.I. Baum, N. Smith-Blair, N.P. Greene, T.A. Washington, Diet-induced obesity alters anabolic signalling in mice at the onset of skeletal muscle regeneration, Acta Physiol (Oxf). 215 (2015) 46-57, doi: 10.1111/apha.12537.

[169] D. Serra, P. Mera, M.I. Malandrino, J.F. Mir, L. Herrero, Mitochondrial fatty acid oxidation in obesity, Antioxid. Redox Signal. 19 (2013) 269-284, doi: 10.1089/ars.2012.4875.

[170] R. Weiss, A.A. Bremer, R.H. Lustig, What is metabolic syndrome, and why are children getting it?, Ann. N. Y. Acad. Sci. 1281 (2013) 123-140, doi: 10.1111/nyas.12030.

[171] S.K. Powers, E.E. Talbert, P.J. Adhihetty, Reactive oxygen and nitrogen species as intracellular signals in skeletal muscle, J. Physiol. (Lond.). 589 (2011) 2129-2138, doi: 10.1113/jphysiol.2010.201327.

[172] K. M, P. K, J. A, D. J, The role of oxidative stress in skeletal muscle injury and regeneration: focus on antioxidant enzymes., J Muscle Res Cell Motil. 36 (2015) 377-393, doi: 10.1007/s10974-015-9438-9.

[173] H. Yu, D. Zhou, W. Jia, Z. Guo, Locating the source of hyperglycemia: Liver versus muscle, Journal of diabetes. 4 (2012) 30-36, doi: 10.1111/j.1753-0407.2011.00170.x.

[174] B. Mittendorfer, Origins of metabolic complications in obesity: adipose tissue and free fatty acid trafficking, Curr Opin Clin Nutr Metab Care. 14 (2011) 535-541, doi: 10.1097/MCO.0b013e32834ad8b6.

[175] K.H. Collins, W. Herzog, G.Z. MacDonald, R.A. Reimer, J.L. Rios, I.C. Smith, R.F. Zernicke, D.A. Hart, Obesity, Metabolic Syndrome, and Musculoskeletal Disease: Common Inflammatory Pathways Suggest a Central Role for Loss of Muscle Integrity, Front Physiol. 9 (2018) 112, doi: 10.3389/fphys.2018.00112.

[176] K.H.M. Kwok, K.S.L. Lam, A. Xu, Heterogeneity of white adipose tissue: molecular basis and clinical implications, Exp. Mol. Med. 48 (2016) e215, doi: 10.1038/emm.2016.5.

[177] T. Schoettl, I.P. Fischer, S. Ussar, Heterogeneity of adipose tissue in development and metabolic function, J. Exp. Biol. 221 (2018), doi: 10.1242/jeb.162958.

[178] M. Gabbs, S. Leng, J.G. Devassy, M. Monirujjaman, H.M. Aukema, Advances in Our Understanding of Oxylipins Derived from Dietary PUFAs, Adv Nutr. 6 (2015) 513-540, doi: 10.3945/an.114.007732.

[179] A. Gil-de-la-Fuente, J. Godzien, S. Saugar, R. Garcia-Carmona, H. Badran, D.S. Wishart, C. Barbas, A. Otero, CEU Mass Mediator 3.0: A Metabolite Annotation Tool, J. Proteome Res. 18 (2019) 797-802, doi: 10.1021/acs.jproteome.8b00720.

[180] A.C. Schrimpe-Rutledge, S.G. Codreanu, S.D. Sherrod, J.A. McLean, Untargeted Metabolomics Strategies—Challenges and Emerging Directions, J. Am. Soc. Mass Spectrom. 27 (2016) 1897-1905, doi: 10.1021/jasms.8b05178.

[181] E. Kendrick, A Mass Scale Based on CH2 = 14.0000 for High Resolution Mass Spectrometry of Organic Compounds., Anal. Chem. 35 (1963) 2146-2154, doi: 10.1021/ac60206a048.

[182] J. Godzien, E.G. Armitage, S. Angulo, M.P. Martinez-Alcazar, V. Alonso-Herranz, A. Otero, A. Lopez-Gonzalvez, C. Barbas, In-source fragmentation and correlation analysis as tools for metabolite identification exemplified with CE-TOF untargeted metabolomics, ELECTROPHORESIS. 36 (2015) 2188-2195, doi: 10.1002/elps.201500016.

[183] H. Sato, S. Nakamura, K. Teramoto, T. Sato, Structural Characterization of Polymers by MALDI Spiral-TOF Mass Spectrometry Combined with Kendrick Mass Defect Analysis, J. Am. Soc. Mass Spectrom. 25 (2014) 1346-1355, doi: 10.1021/jasms.8b04839.

[184] A.G. Marshall, R.P. Rodgers, Petroleomics: The Next Grand Challenge for Chemical Analysis, Acc. Chem. Res. 37 (2004) 53-59, doi: 10.1021/ar020177t.

[185] M. Ubukata, K.J. Jobst, E.J. Reiner, S.E. Reichenbach, Q. Tao, J. Hang, Z. Wu, A.J. Dane, R.B. Cody, Non-targeted analysis of electronics waste by comprehensive two-dimensional gas chromatography combined with high-resolution mass spectrometry: Using accurate mass information and mass defect analysis to explore the data, Journal of Chromatography A. 1395 (2015) 152-159, doi: 10.1016/j.chroma.2015.03.050.

[186] K.J. Jobst, L. Shen, E.J. Reiner, V.Y. Taguchi, P.A. Helm, R. Mccrindle, S.M. Backus, The use of mass defect plots for the identification of (novel) halogenated contaminants in the environment, Analytical and Bioanalytical Chemistry (2013), doi: 10.1007/s00216-013-6735-2.

[187] S. Naz, A. Garcia, C. Barbas, Multiplatform Analytical Methodology For Metabolic Fingerprinting Of Lung Tissue, Anal. Chem. 85 (2013) 10941-10948, doi: 10.1021/ac402411n.

[188] V. González-Ruiz, Y. Gagnebin, N. Drouin, S. Codesido, S. Rudaz, J. Schappler, ROMANCE: A new software tool to improve data robustness and feature identification in CE-MS metabolomics, ELECTROPHORESIS. 39 (2018) 1222-1232, doi: 10.1002/elps.201700427.

[189] W. Chang, G.M. Hatch, Y. Wang, F. Yu, M. Wang, The relationship between phospholipids and insulin resistance: From clinical to experimental studies, J. Cell. Mol. Med. 23 (2019) 702-710, doi: 10.1111/jcmm.13984 [doi].

[190] J. Graessler, D. Schwudke, P.E. Schwarz, R. Herzog, A. Shevchenko, S.R. Bornstein, Top-down lipidomics reveals ether lipid deficiency in blood plasma of hypertensive patients, PLoS One. 4 (2009) e6261, doi: 10.1371/journal.pone.0006261 [doi].

[191] K.H. Pietiläinen, M. Sysi-Aho, A. Rissanen, T. Seppänen-Laakso, H. Yki-Järvinen, J. Kaprio, M. Oresic, Acquired obesity is associated with changes in the serum lipidomic profile independent of genetic effects--a monozygotic twin study, PLoS One. 2 (2007) e218, doi: e218.

[192] M.N. Barber, S. Risis, C. Yang, P.J. Meikle, M. Staples, M.A. Febbraio, C.R. Bruce, Plasma lysophosphatidylcholine levels are reduced in obesity and type 2 diabetes, PLoS One. 7 (2012) e41456, doi: 10.1371/journal.pone.0041456 [doi].

[193] U. Schwab, T. Seppänen-Laakso, L. Yetukuri, J. Ågren, M. Kolehmainen, D.E. Laaksonen, A. Ruskeepää, H. Gylling, M. Uusitupa, M. Orešič, for the GENOBIN, Study Group, Triacylglycerol Fatty Acid Composition in Diet-Induced Weight Loss in Subjects with Abnormal Glucose Metabolism – the GENOBIN Study, PLOS ONE. 3 (2008) e2630.

[194] S. Heimerl, M. Fischer, A. Baessler, G. Liebisch, A. Sigruener, S. Wallner, G. Schmitz, Alterations of plasma lysophosphatidylcholine species in obesity and weight loss, PLoS One. 9 (2014) e111348, doi: 10.1371/journal.pone.0111348 [doi].

[195] V. Kumar, A.K. Abbas, J.C. Aster, Robbins Y Cotran Patología Estructural Y Funcional, Elsevier, 2015.

[196] A. Bolsoni-Lopes, M.I. Alonso-Vale, Lipolysis and lipases in white adipose tissue - An update, Arch. Endocrinol. Metab. 59 (2015) 335-342, doi: S2359-39972015000400335 [pii].

[197] P. Mount, M. Davies, S.W. Choy, N. Cook, D. Power, Obesity-Related Chronic Kidney Disease-The Role of Lipid Metabolism, Metabolites. 5 (2015) 720-732, doi: 10.3390/metabo5040720 [doi].

[198] K. Fukuchi, S. Nozaki, T. Yoshizumi, S. Hasegawa, T. Uehara, T. Nakagawa, T. Kobayashi, Y. Tomiyama, S. Yamashita, Y. Matsuzawa, T. Nishimura, Enhanced myocardial glucose use in patients with a deficiency in long-chain fatty acid transport (CD36 deficiency), J. Nucl. Med. 40 (1999) 239-243.

[199] C.T. Coburn, F.F. Knapp Jr, M. Febbraio, A.L. Beets, R.L. Silverstein, N.A. Abumrad, Defective uptake and utilization of long chain fatty acids in muscle and adipose tissues of CD36 knockout mice, J. Biol. Chem. 275 (2000) 32523-32529, doi: S0021-9258(20)89128-5 [pii].

[200] van der Veen, Jelske N., J.P. Kennelly, S. Wan, J.E. Vance, D.E. Vance, R.L. Jacobs, The critical role of phosphatidylcholine and phosphatidylethanolamine metabolism in health and disease, Biochimica et Biophysica Acta (BBA) - Biomembranes. 1859 (2017) 1558-1572, doi: https://doi.org/10.1016/j.bbamem.2017.04.006.

[201] P.R. Baker 2nd, K.E. Boyle, T.R. Koves, O.R. Ilkayeva, D.M. Muoio, J.A. Houmard, J.E. Friedman, Metabolomic analysis reveals altered skeletal muscle amino acid and fatty acid handling in obese humans, Obesity (Silver Spring). 23 (2015) 981-988, doi: 10.1002/oby.21046 [doi].

[202] T. Shimizu, Lipid mediators in health and disease: enzymes and receptors as therapeutic targets for the regulation of immunity and inflammation, Annu. Rev. Pharmacol. Toxicol. 49 (2009) 123-150, doi: 10.1146/annurev.pharmtox.011008.145616 [doi].

[203] C.A. Pickens, L.M. Sordillo, C. Zhang, J.I. Fenton, Obesity is positively associated with arachidonic acid-derived 5- and 11-hydroxyeicosatetraenoic acid (HETE), Metab. Clin. Exp. 70 (2017) 177-191, doi: 10.1016/j.metabol.2017.01.034.

[204] J. Zhou, L. Chen, Z. Liu, L. Sang, Y. Li, D. Yuan, Changes in erythrocyte polyunsaturated fatty acids and plasma eicosanoids level in patients with asthma, Lipids Health Dis. 17 (2018) 206, doi: 10.1186/s12944-018-0853-y.

[205] B. Rigas, I.S. Goldman, L. Levine, Altered eicosanoid levels in human colon cancer, J. Lab. Clin. Med. 122 (1993) 518-523.

[206] J. Yang, J.P. Eiserich, C.E. Cross, B.M. Morrissey, B.D. Hammock, Metabolomic profiling of regulatory lipid mediators in sputum from adult cystic fibrosis patients, Free Radic. Biol. Med. 53 (2012) 160-171, doi: 10.1016/j.freeradbiomed.2012.05.001.

[207] M. Masoodi, O. Kuda, M. Rossmeisl, P. Flachs, J. Kopecky, Lipid signaling in adipose tissue: Connecting inflammation & metabolism, Biochim. Biophys. Acta. 1851 (2015) 503-518, doi: S1388-1981(14)00209-1 [pii].

[208] G.C. Shearer, R.E. Walker, An overview of the biologic effects of omega-6 oxylipins in humans, Prostaglandins Leukot. Essent. Fatty Acids. 137 (2018) 26-38, doi: 10.1016/j.plefa.2018.06.005.

[209] S.A. Khan, A. Ali, S.A. Khan, S.A. Zahran, G. Damanhouri, E. Azhar, I. Qadri, Unraveling the complex relationship triad between lipids, obesity, and inflammation, Mediators Inflamm. 2014 (2014) 502749, doi: 10.1155/2014/502749.

[210] J. Yeung, M. Hawley, M. Holinstat, The expansive role of oxylipins on platelet biology, J. Mol. Med. 95 (2017) 575-588, doi: 10.1007/s00109-017-1542-4.

[211] C. Vigor, J. Bertrand-Michel, E. Pinot, C. Oger, J. Vercauteren, P. Le Faouder, J. Galano, J.C. Lee, T. Durand, Non-enzymatic lipid oxidation products in biological systems: assessment of the metabolites from polyunsaturated fatty acids, J. Chromatogr. B Analyt. Technol. Biomed. Life Sci. 964 (2014) 65-78, doi: 10.1016/j.jchromb.2014.04.042.

[212] J. Yang, H. Dong, B.D. Hammock, Profiling the regulatory lipids: another systemic way to unveil the biological mystery, Curr. Opin. Lipidol. 22 (2011) 197-203, doi: 10.1097/MOL.0b013e3283468c10.

[213] C. Arnold, M. Markovic, K. Blossey, G. Wallukat, R. Fischer, R. Dechend, A. Konkel, C. von Schacky, F.C. Luft, D.N. Muller, M. Rothe, W. Schunck, Arachidonic acid-metabolizing cytochrome P450 enzymes are targets of {omega}-3 fatty acids, J. Biol. Chem. 285 (2010) 32720-32733, doi: 10.1074/jbc.M110.118406.

[214] A. Chen, S. Mumick, C. Zhang, J. Lamb, H. Dai, D. Weingarth, J. Mudgett, H. Chen, D.J. MacNeil, M.L. Reitman, S. Qian, Diet induction of monocyte chemoattractant protein-1 and its impact on obesity, Obes. Res. 13 (2005) 1311-1320, doi: 10.1038/oby.2005.159.

[215] G.S. Hotamisligil, P. Arner, J.F. Caro, R.L. Atkinson, B.M. Spiegelman, Increased adipose tissue expression of tumor necrosis factor-alpha in human obesity and insulin resistance, J. Clin. Invest. 95 (1995) 2409-2415, doi: 10.1172/JCI117936.

[216] G.S. Hotamisligil, B.M. Spiegelman, Tumor necrosis factor alpha: a key component of the obesity-diabetes link, Diabetes. 43 (1994) 1271-1278, doi: 10.2337/diab.43.11.1271.

[217] N. Ouchi, S. Kihara, T. Funahashi, Y. Matsuzawa, K. Walsh, Obesity, adiponectin and vascular inflammatory disease, Curr. Opin. Lipidol. 14 (2003) 561-566, doi: 10.1097/00041433-200312000-00003.

[218] N. Ouchi, A. Higuchi, K. Ohashi, Y. Oshima, N. Gokce, R. Shibata, Y. Akasaki, A. Shimono, K. Walsh, Sfrp5 is an anti-inflammatory adipokine that modulates metabolic dysfunction in obesity, Science. 329 (2010) 454-457, doi: 10.1126/science.1188280.

[219] A.H. Berg, P.E. Scherer, Adipose tissue, inflammation, and cardiovascular disease, Circ. Res. 96 (2005) 939-949, doi: 10.1161/01.RES.0000163635.62927.34.

[220] I.-. Tsai, K.D. Croft, T.A. Mori, J.R. Falck, L.J. Beilin, I.B. Puddey, A.E. Barden, 20-HETE and F2-isoprostanes in the metabolic syndrome: the effect of weight reduction, Free Radic. Biol. Med. 46 (2009) 263-270, doi: 10.1016/j.freeradbiomed.2008.10.028.

[221] M.H. Shishehbor, R. Zhang, H. Medina, M. Brennan, D.M. Brennan, S.G. Ellis, E.J. Topol, S.L. Hazen, Systemic elevations of free radical oxidation products of arachidonic acid are associated with angiographic evidence of coronary artery disease, Free Radic. Biol. Med. 41 (2006) 1678-1683, doi: 10.1016/j.freeradbiomed.2006.09.001.

[222] M.L. Foegh, Y. Zhao, L. Madren, M. Rolnick, T.O. Stair, K.S. Huang, P.W. Ramwell, Urinary thromboxane A2 metabolites in patients presenting in the emergency room with acute chest pain, Journal of Internal Medicine. 235 (1994) 153-161, doi: 10.1111/j.1365-2796.1994.tb01049.x.

[223] D. Tsikas, Application of gas chromatography-mass spectrometry and gas chromatography-tandem mass spectrometry to assess in vivo synthesis of prostaglandins, thromboxane, leukotrienes, isoprostanes and related compounds in humans, J. Chromatogr. B Biomed. Sci. Appl. 717 (1998) 201-245, doi: 10.1016/s0378-4347(98)00210-2.

[224] R. Berkecz, M. Lísa, M. Holčapek, Analysis of oxylipins in human plasma: Comparison of ultrahigh-performance liquid chromatography and ultrahigh-performance supercritical fluid chromatography coupled to mass spectrometry, J Chromatogr A. 1511 (2017) 107-121, doi: 10.1016/j.chroma.2017.06.070.

[225] V. Simon, D. Cota, Mechanisms In Endocrinology: Endocannabinoids and metabolism: past, present and future, Eur J Endocrinol. 176 (2017) R309-R324, doi: 10.1530/EJE-16-1044.

[226] D. Piomelli, The molecular logic of endocannabinoid signalling, Nature Reviews Neuroscience. 4 (2003) 873-884, doi: 10.1038/nrn1247.

[227] Y. Okamoto, J. Morishita, K. Tsuboi, T. Tonai, N. Ueda, Molecular characterization of a phospholipase D generating anandamide and its congeners, J Biol Chem. 279 (2004) 5298-5305, doi: 10.1074/jbc.M306642200.

[228] S.S. Choe, J.Y. Huh, I.J. Hwang, J.I. Kim, J.B. Kim, Adipose Tissue Remodeling: Its Role in Energy Metabolism and Metabolic Disorders, Front Endocrinol (Lausanne). 7 (2016) 30, doi: 10.3389/fendo.2016.00030.

[229] I. Willenberg, A.K. Meschede, F. Gueler, M. Jang, N. Shushakova, N.H. Schebb, Food Polyphenols Fail to Cause a Biologically Relevant Reduction of COX-2 Activity, PLoS One. 10 (2015), doi: 10.1371/journal.pone.0139147.

[230] A.A. Spector, H. Kim, Cytochrome P450 epoxygenase pathway of polyunsaturated fatty acid metabolism, Biochim. Biophys. Acta. 1851 (2015) 356-365, doi: 10.1016/j.bbalip.2014.07.020.

[231] C.M. Spickett, A.R. Pitt, Oxidative lipidomics coming of age: advances in analysis of oxidized phospholipids in physiology and pathology, Antioxid. Redox Signal. 22 (2015) 1646-1666, doi: 10.1089/ars.2014.6098.

[232] S.L. Lundström, B. Levänen, M. Nording, A. Klepczynska-Nyström, M. Sköld, J.Z. Haeggström, J. Grunewald, M. Svartengren, B.D. Hammock, B. Larsson, A. Eklund, ÅM. Wheelock, C.E. Wheelock, Asthmatics exhibit altered oxylipin profiles compared to healthy individuals after subway air exposure, PLoS ONE. 6 (2011) e23864, doi: 10.1371/journal.pone.0023864.

[233] J. Yang, K. Schmelzer, K. Georgi, B.D. Hammock, Quantitative profiling method for oxylipin metabolome by liquid chromatography electrospray ionization tandem mass spectrometry, Anal. Chem. 81 (2009) 8085-8093, doi: 10.1021/ac901282n.

[234] R.A. Colas, M. Shinohara, J. Dalli, N. Chiang, C.N. Serhan, Identification and signature profiles for pro-resolving and inflammatory lipid mediators in human tissue, Am. J. Physiol. , Cell Physiol. 307 (2014) 39, doi: 10.1152/ajpcell.00024.2014.

[235] I. Willenberg, A.I. Ostermann, N.H. Schebb, Targeted metabolomics of the arachidonic acid cascade: current state and challenges of LC-MS analysis of oxylipins, Anal Bioanal Chem. 407 (2015) 2675-2683, doi: 10.1007/s00216-014-8369-4.

[236] D.S. Dumlao, M.W. Buczynski, P.C. Norris, R. Harkewicz, E.A. Dennis, High-throughput lipidomic analysis of fatty acid derived eicosanoids and N-acylethanolamines, Biochim. Biophys. Acta. 1811 (2011) 724-736, doi: 10.1016/j.bbalip.2011.06.005.

[237] M. Chocholoušková, R. Jirásko, D. Vrána, J. Gatěk, B. Melichar, M. Holčapek, Reversed phase UHPLC/ESI-MS determination of oxylipins in human plasma: a case study of female breast cancer, Anal Bioanal Chem. 411 (2019) 1239-1251, doi: 10.1007/s00216-018-1556-y.

[238] G.C. Shearer, W.S. Harris, T.L. Pedersen, J.W. Newman, Detection of omega-3 oxylipins in human plasma and response to treatment with omega-3 acid ethyl esters, J. Lipid Res. 51 (2010) 2074-2081, doi: 10.1194/M900193-JLR200.

[239] S. Gouveia-Figueira, J. Späth, A.M. Zivkovic, M.L. Nording, Profiling the Oxylipin and Endocannabinoid Metabolome by UPLC-ESI-MS/MS in Human Plasma to Monitor Postprandial Inflammation, PLoS ONE. 10 (2015) e0132042, doi: 10.1371/journal.pone.0132042.

[240] S. Gouveia-Figueira, M.L. Nording, Validation of a tandem mass spectrometry method using combined extraction of 37 oxylipins and 14 endocannabinoid-related compounds including prostamides from biological matrices, Prostaglandins Other Lipid Mediat. 121 (2015) 110-121, doi: 10.1016/j.prostaglandins.2015.06.003.

[241] J.P. Schuchardt, S. Schmidt, G. Kressel, H. Dong, I. Willenberg, B.D. Hammock, A. Hahn, N.H. Schebb, Comparison of free serum oxylipin concentrations in hyper- vs. normolipidemic men, Prostaglandins Leukot. Essent. Fatty Acids. 89 (2013) 19-29, doi: 10.1016/j.plefa.2013.04.001.

[242] M.Y. Golovko, E.J. Murphy, An improved LC-MS/MS procedure for brain prostanoid analysis using brain fixation with head-focused microwave irradiation and liquid-liquid extraction, J. Lipid Res. 49 (2008) 893-902, doi: 10.1194/jlr.D700030-JLR200.

[243] G. Astarita, A.C. Kendall, E.A. Dennis, A. Nicolaou, Targeted lipidomic strategies for oxygenated metabolites of polyunsaturated fatty acids, Biochim. Biophys. Acta. 1851 (2015) 456-468, doi: 10.1016/j.bbalip.2014.11.012.

[244] B.H. Maskrey, V.B. O'Donnell, Analysis of eicosanoids and related lipid mediators using mass spectrometry, Biochem. Soc. Trans. 36 (2008) 1055-1059, doi: 10.1042/BST0361055.

[245] Y. Satomi, M. Hirayama, H. Kobayashi, One-step lipid extraction for plasma lipidomics analysis by liquid chromatography mass spectrometry, J. Chromatogr. B Analyt. Technol. Biomed. Life Sci. 1063 (2017) 93-100, doi: 10.1016/j.jchromb.2017.08.020.

[246] S. Tumanov, J.J. Kamphorst, Recent advances in expanding the coverage of the lipidome, Curr. Opin. Biotechnol. 43 (2017) 127-133, doi: 10.1016/j.copbio.2016.11.008.

[247] J. Folch, M. Lees, G.H. Sloane Stanley, A simple method for the isolation and purification of total lipides from animal tissues, J. Biol. Chem. 226 (1957) 497-509.

[248] E.G. Bligh, W.J. Dyer, A rapid method of total lipid extraction and purification, Can J Biochem Physiol. 37 (1959) 911-917, doi: 10.1139/o59-099.

[249] M. Puppolo, D. Varma, S.A. Jansen, A review of analytical methods for eicosanoids in brain tissue, Journal of Chromatography B. 964 (2014) 50-64, doi: 10.1016/j.jchromb.2014.03.007.

[250] Y. Wang, A.M. Armando, O. Quehenberger, C. Yan, E.A. Dennis, Comprehensive ultra-performance liquid chromatographic separation and mass spectrometric analysis of eicosanoid metabolites in human samples, J Chromatogr A. 1359 (2014) 60-69, doi: 10.1016/j.chroma.2014.07.006.

[251] T. Frömel, B. Jungblut, J. Hu, C. Trouvain, E. Barbosa-Sicard, R. Popp, S. Liebner, S. Dimmeler, B.D. Hammock, I. Fleming, Soluble epoxide hydrolase regulates hematopoietic progenitor cell function via generation of fatty acid diols, Proc. Natl. Acad. Sci. U. S. A. 109 (2012) 9995-10000, doi: 10.1073/pnas.1206493109.

[252] S.A. Brose, A.G. Baker, M.Y. Golovko, A Fast One Step Extraction and UPLC-MS/MS Analysis for E2/D2 Series Prostaglandins and Isoprostanes, Lipids. 48 (2013) 411-419, doi: 10.1007/s11745-013-3767-5.

[253] S. Sigma-Aldrich, Guide to solid phase extraction-bulletin 910, Bull. 910 (1998).

[254] J. Späth, Oxylipins in human plasma – method development and dietary effects on levels (2014).

[255] Y. H, S. Ki, B. Mr, B. Mf, R. Lj, J. Sa, Determination of bioactive eicosanoids in brain tissue by a sensitive reversed-phase liquid chromatographic method with fluorescence detection., J Chromatogr B Analyt Technol Biomed Life Sci. 803 (2004) 267-277, doi: 10.1016/j.jchromb.2003.12.027.

[256] W. Wang, S. Qin, L. Li, X. Chen, Q. Wang, J. Wei, An Optimized High Throughput Clean-Up Method Using Mixed-Mode SPE Plate for the Analysis of Free Arachidonic Acid in Plasma by LC-MS/MS, Int J Anal Chem. 2015 (2015), doi: 10.1155/2015/374819.

[257] Z. Yuan, S. Majchrzak-Hong, G.S. Keyes, M.J. Iadarola, A.J. Mannes, C.E. Ramsden, Lipidomic profiling of targeted oxylipins with ultra-performance liquid

chromatography-tandem mass spectrometry, Anal Bioanal Chem. 410 (2018) 6009-6029, doi: 10.1007/s00216-018-1222-4.

[258] M. Takabatake, T. Hishinuma, N. Suzuki, S. Chiba, H. Tsukamoto, H. Nakamura, T. Saga, Y. Tomioka, A. Kurose, T. Sawai, M. Mizugaki, Simultaneous quantification of prostaglandins in human synovial cell-cultured medium using liquid chromatography/tandem mass spectrometry, Prostaglandins Leukot. Essent. Fatty Acids. 67 (2002) 51-56, doi: 10.1054/plef.2002.0381.

[259] M. Masoodi, A. Nicolaou, Lipidomic analysis of twenty-seven prostanoids and isoprostanes by liquid chromatography/electrospray tandem mass spectrometry, Rapid Commun. Mass Spectrom. 20 (2006) 3023-3029, doi: 10.1002/rcm.2697.

[260] C.S. Ejsing, E. Duchoslav, J. Sampaio, K. Simons, R. Bonner, C. Thiele, K. Ekroos, A. Shevchenko, Automated Identification and Quantification of Glycerophospholipid Molecular Species by Multiple Precursor Ion Scanning, Anal. Chem. 78 (2006) 6202-6214, doi: 10.1021/ac060545x.

[261] S.K. Abbott, A.M. Jenner, T.W. Mitchell, S.H.J. Brown, G.M. Halliday, B. Garner, An improved high-throughput lipid extraction method for the analysis of human brain lipids, Lipids. 48 (2013) 307-318, doi: 10.1007/s11745-013-3760-z.

[262] M.M. Yore, I. Syed, P.M. Moraes-Vieira, T. Zhang, M.A. Herman, E.A. Homan, R.T. Patel, J. Lee, S. Chen, O.D. Peroni, A.S. Dhaneshwar, A. Hammarstedt, U. Smith, T.E. McGraw, A. Saghatelian, B.B. Kahn, Discovery of a class of endogenous mammalian lipids with anti-diabetic and anti-inflammatory effects, Cell. 159 (2014) 318-332, doi: 10.1016/j.cell.2014.09.035.

[263] B. Neises, W. Steglich, Simple Method for the Esterification of Carboxylic Acids, Angewandte Chemie International Edition in English. 17 (1978) 522-524, doi: 10.1002/anie.197805221.

[264] A.H. Morgan, V.J. Hammond, L. Morgan, C.P. Thomas, K.A. Tallman, Y.R. Garcia-Diaz, C. McGuigan, M. Serpi, N.A. Porter, R.C. Murphy, V.B. O'Donnell, Quantitative assays for esterified oxylipins generated by immune cells, Nat Protoc. 5 (2010) 1919-1931, doi: 10.1038/nprot.2010.162.

[265] O. Kuda, M. Brezinova, M. Rombaldova, B. Slavikova, M. Posta, P. Beier, P. Janovska, J. Veleba, J. Kopecky, E. Kudova, T. Pelikanova, J. Kopecky, Docosahexaenoic Acid-Derived Fatty Acid Esters of Hydroxy Fatty Acids (FAHFAs) With Anti-inflammatory Properties, Diabetes. 65 (2016) 2580-2590, doi: 10.2337/db16-0385.

[266] D.Z. Brunengraber, B.J. McCabe, T. Kasumov, J.C. Alexander, V. Chandramouli, S.F. Previs, Influence of diet on the modeling of adipose tissue triglycerides during

growth, Am J Physiol Endocrinol Metab. 285 (2003) 917, doi: 10.1152/ajpendo.00128.2003.

[267] S.K. Chakrabarti, Y. Wen, A.D. Dobrian, B.K. Cole, Q. Ma, H. Pei, M.D. Williams, M.H. Bevard, G.E. Vandenhoff, S.R. Keller, J. Gu, J.L. Nadler, Evidence for activation of inflammatory lipoxygenase pathways in visceral adipose tissue of obese Zucker rats, Am J Physiol Endocrinol Metab. 300 (2011) 175, doi: 10.1152/ajpendo.00203.2010.

[268] E.N. Kuipers, V. Kantae, B.C.E. Maarse, van den Berg, Susan M., R. van Eenige, K.J. Nahon, A. Reifel-Miller, T. Coskun, de Winther, Menno P. J., E. Lutgens, S. Kooijman, A.C. Harms, T. Hankemeier, M. van der Stelt, P.C.N. Rensen, M.R. Boon, High Fat Diet Increases Circulating Endocannabinoids Accompanied by Increased Synthesis Enzymes in Adipose Tissue, Front Physiol. 9 (2018) 1913, doi: 10.3389/fphys.2018.01913.

[269] K.M. Starowicz, L. Cristino, I. Matias, R. Capasso, A. Racioppi, A.A. Izzo, V. Di Marzo, Endocannabinoid dysregulation in the pancreas and adipose tissue of mice fed with a high-fat diet, Obesity (Silver Spring). 16 (2008) 553-565, doi: 10.1038/oby.2007.106.

[270] J. Clària, J. Dalli, S. Yacoubian, F. Gao, C.N. Serhan, Resolvin D1 and Resolvin D2 Govern Local Inflammatory Tone in Obese Fat, J Immunol. 189 (2012) 2597-2605, doi: 10.4049/jimmunol.1201272.

[271] B.Q. Starley, C.J. Calcagno, S.A. Harrison, Nonalcoholic fatty liver disease and hepatocellular carcinoma: A weighty connection, Hepatology. 51 (2010) 1820-1832, doi: 10.1002/hep.23594.

[272] S.L. Friedman, B. Neuschwander-Tetri, M. Rinella, A.J. Sanyal, Mechanisms of NAFLD development and therapeutic strategies, Nat. Med. 24 (2018) 908-922, doi: 10.1038/s41591-018-0104-9.

[273] M.R. Charlton, J.M. Burns, R.A. Pedersen, K.D. Watt, J.K. Heimbach, R.A. Dierkhising, Frequency and Outcomes of Liver Transplantation for Nonalcoholic Steatohepatitis in the United States, Gastroenterology. 141 (2011) 1249-1253, doi: //doi.org/10.1053/j.gastro.2011.06.061.

[274] D. Li, J. Li, G. Wang, Y. Qin, Z. Niu, Z. Li, C. Xu, Delayed Liver Regeneration after Partial Hepatectomy in Aged Nos2 Knockout Mice, Cell journal. 19 (2017) 218-230, doi: 10.22074/cellj.2016.4878.

[275] M. Alejandro Fernández-Rojo, C. Restall, C. Ferguson, N. Martel, S. Martin, M. Bosch, A. Kassan, G.M. Leong, S.D. Martin, S.L. McGee, G.E.O. Muscat, R.L. Anderson, C. Enrich, A. Pol, R.G. Parton, Caveolin-1 orchestrates the balance between glucose and lipid-dependent energy metabolism: Implications for liver regeneration, Hepatology. 55 (2012) 1574-1584, doi: 10.1002/hep.24810.

[276] S. Hoppe, C.v. Loeffelholz, J.F. Lock, S. Doecke, B.V. Sinn, A. Rieger, M. Malinowski, A.F.H. Pfeiffer, P. Neuhaus, M. Stockmann, Nonalcoholic Steatohepatits and Liver Steatosis Modify Partial Hepatectomy Recovery, Journal of Investigative Surgery. 28 (2015) 24-31, doi: 10.3109/08941939.2014.971206.

[277] C. Alonso, D. Fernández-Ramos, M. Varela-Rey, I. Martínez-Arranz, N. Navasa, S. M. Van Liempd, J.L. Lavín Trueba, R. Mayo, C. P. Ilisso, V. G. de Juan, M. Iruarrizaga-Lejarreta, L. delaCruz-Villar, I. Mincholé, A. Robinson, J. Crespo, A. Martín-Duce, M. Romero-Gómez, H. Sann, J. Platon, J. Van Eyk, P. Aspichueta, M. Noureddin, J.M. Falcón-Pérez, J. Anguita, A. M. Aransay, M.L. Martínez-Chantar, S. C. Lu, J.M. Mato, Metabolomic Identification of Subtypes of Nonalcoholic Steatohepatitis, Gastroenterology. 152 (2017) 1449-1461.e7, doi: //doi.org/10.1053/j.gastro.2017.01.015.

[278] Sara Samino, Jesús Revuelta-Cervantes, Maria Vinaixa, Miguel Ángel Rodríguez, Ángela M. Valverde, Xavier Correig, A 1H NMR metabolic profiling to the assessment of protein tyrosine phosphatase 1B role in liver regeneration after partial hepatectomy, Biochimie. 95 (2013) 808-816, doi: //doi.org/10.1016/j.biochi.2012.11.015.

[279] M.P. Valdecantos, L. Ruiz, V. Pardo, L. Castro-Sanchez, C. García-Monzón, B. Lanzón, J. Rupérez, C. Barbas, J. Naylor, J.L. Trevaskis, J. Grimsby, C.M. Rondinone, Á Valverde, Differential Effects of a Glucagon-Like Peptide 1 Receptor Agonist in Non-Alcoholic Fatty Liver Disease and in Response to Hepatectomy, Scientific Reports. 8 (2018) 16461, doi: 10.1038/s41598-018-33949-z.

[280] M.P. Valdecantos, V. Pardo, L. Ruiz, L. Castro-Sánchez, B. Lanzón, E. Fernández-Millán, C. García-Monzón, A.I. Arroba, Á González-Rodríguez, F. Escriva, C. Álvarez, F.J. Rupérez, C. Barbas, A. Konkar, J. Naylor, D. Hornigold, A.D. Santos, M. Bednarek, J. Grimsby, C.M. Rondinone, Á Valverde, A novel glucagon-like peptide 1/glucagon receptor dual agonist improves steatohepatitis and liver regeneration in mice, Hepatology. 65 (2017) 950-968, doi: 10.1002/hep.28962.

[281] E.N. Maldonado, I. Delgado, N.E. Furland, X. Buqué, A. Iglesias, M.I. Aveldaño, A. Zubiaga, O. Fresnedo, B. Ochoa, The E2F2 transcription factor sustains hepatic glycerophospholipid homeostasis in mice, PloS one. 9 (2014) e112620, doi: 10.1371/journal.pone.0112620.

[282] I.P. Pogribny, K. Dreval, I. Kindrat, S. Melnyk, L. Jimenez, A. de Conti, V. Tryndyak, M. Pogribna, J.F. Ortega, S.J. James, I. Rusyn, F.A. Beland, Epigenetically mediated inhibition of S-adenosylhomocysteine hydrolase and the associated dysregulation of 1-carbon metabolism in nonalcoholic steatohepatitis and hepatocellular carcinoma, The FASEB Journal. 32 (2018) 1591-1601, doi: 10.1096/fj.201700866R.

[283] G. Rizki, L. Arnaboldi, B. Gabrielli, J. Yan, G.S. Lee, R.K. Ng, S.M. Turner, T.M. Badger, R.E. Pitas, J.J. Maher, Mice fed a lipogenic methionine-choline-deficient diet

develop hypermetabolism coincident with hepatic suppression of SCD-1, J. Lipid Res. 47 (2006) 2280-2290.

[284] N. Sunny, E. Parks, J. Browning, S. Burgess, Excessive Hepatic Mitochondrial TCA Cycle and Gluconeogenesis in Humans with Nonalcoholic Fatty Liver Disease, Cell Metabolism. 14 (2011) 804-810, doi: 10.1016/j.cmet.2011.11.004.

[285] S. De Matteis, A. Ragusa, G. Marisi, S. De Domenico, A. Casadei Gardini, M. Bonafè, A.M. Giudetti, Aberrant Metabolism in Hepatocellular Carcinoma Provides Diagnostic and Therapeutic Opportunities, https://www.hindawi.com/journals/omcl/2018/7512159/. 2019 (2018), doi: 10.1155/2018/7512159.

[286] A. Sekowska, H. Ashida, A. Danchin, Revisiting the methionine salvage pathway and its paralogues, Microb. Biotechnol. 12 (2019) 77-97, doi: 10.1111/1751-7915.13324.

[287] M.K. Schneider, A. Mohs, K. Kilic, S.L. Candels, C. Elfers, E. Bennek, B.L. Schneider, F. Heymann, N. Gassler, J. Penders, C. Trautwein, Intestinal Microbiota Protects against MCD Diet-Induced Steatohepatitis, International Journal of Molecular Sciences. 20 (2019), doi: 10.3390/ijms20020308.

[288] Dong S, Zhan ZY, Cao HY, Wu C, Bian YQ, Li JY, Cheng GH, Liu P, Sun MY., Urinary metabolomics analysis identifies key biomarkers of different stages of nonalcoholic fatty liver disease. , World J Gastroenterol (2017) 23(15): 2771-2784.

[289] A.D. Lake, P. Novak, P. Shipkova, N. Aranibar, D.G. Robertson, M.D. Reily, L.D. Lehman-McKeeman, R.R. Vaillancourt, N.J. Cherrington, Branched chain amino acid metabolism profiles in progressive human nonalcoholic fatty liver disease, Amino Acids. 47 (2015) 603-615, doi: 10.1007/s00726-014-1894-9.

[290] K. Begriche, J. Massart, M. Robin, F. Bonnet, B. Fromenty, Mitochondrial adaptations and dysfunctions in nonalcoholic fatty liver disease, Hepatology. 58 (2013) 1497-1507, doi: 10.1002/hep.26226.

[291] A.P. Rolo, J.S. Teodoro, C.M. Palmeira, Role of oxidative stress in the pathogenesis of nonalcoholic steatohepatitis, Free Radical Biology and Medicine. 52 (2012) 59-69, doi: //doi.org/10.1016/j.freeradbiomed.2011.10.003.

[292] P. Puri, K. Daita, A. Joyce, F. Mirshahi, P.K. Santhekadur, S. Cazanave, V.A. Luketic, M.S. Siddiqui, S. Boyett, H. Min, D.P. Kumar, R. Kohli, H. Zhou, P.B. Hylemon, M.J. Contos, M. Idowu, A.J. Sanyal, The presence and severity of nonalcoholic steatohepatitis is associated with specific changes in circulating bile acids, Hepatology. 67 (2018) 534-548, doi: 10.1002/hep.29359.

[293] J.L. Rosa, R. Bartrons, A. Tauler, Gene expression of regulatory enzymes of glycolysis/gluconeogenesis in regenerating rat liver, Biochem. J. 287 (Pt 1) (1992) 113-116.

[294] G.K. Michalopoulos, Hepatostat: Liver regeneration and normal liver tissue maintenance, Hepatology. 65 (2017) 1384-1392, doi: 10.1002/hep.28988.

[295] Y. Simon, S.M. Kessler, R.M. Bohle, J. Haybaeck, A.K. Kiemer, The insulin-like growth factor 2 (*IGF2*) mRNA-binding protein p62/IGF2BP2-2 as a promoter of NAFLD and HCC?, Gut. 63 (2014) 861-863, doi: 10.1136/gutjnl-2013-305736.

Annexes

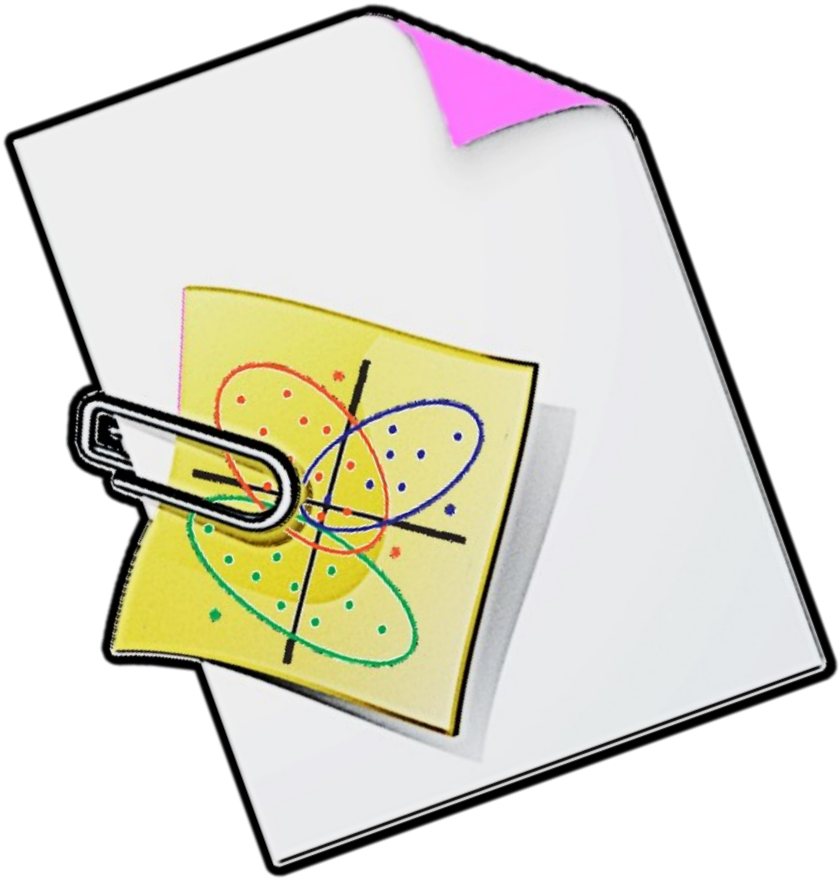

[Annex 1.1.1]: Specifications of HFD used for feeding mice in compartmentomics study (Chapter 1).

Teklad Custom Diet

TD.06414

Adjusted Calories Diet (60/Fat)

ENVIGO

Formula	g/Kg
Casein	**265.0**
L-Cystine	**4.0**
Maltodextrin	**160.0**
Sucrose	**90.0**
Lard	**310.0**
Soybean Oil	**30.0**
Cellulose	**65.5**
Mineral Mix, AIN-93G-MX (94046)	**48.0**
Calcium Phosphate, dibasic	**3.4**
Vitamin Mix, AIN-93-VX (94047)	**21.0**
Choline Bitartrate	**3.0**
Blue Food Color	**0.1**

Key Features

+ **Purified Diet**
+ **Diet Induced Obesity**
+ **High Fat**

Key Planning Information

+ *Products are made fresh to order*
+ Store product at 4°C or lower
+ Use within 6 months (applicable to most diets)
+ Box labeled with product name, manufacturing date, and lot number
+ Replace diet at minimum once per week
  More frequent replacement may be advised
+ Lead time:
  - 2 weeks non-irradiated
  - 4 weeks irradiated

Product Specific Information

+ 1/2" Pellet or Powder (free flowing)
+ Minimum order 3 Kg
+ Irradiation available upon request

Footnote

Approx. 60% of total calories come from fat. Designed with similarities to Research Diets, Inc. formula D12492. For the series TD 06414-TD 06416. Approximate fatty acid profile (% of total fat): 36% saturated, 41% monounsaturated, 23% polyunsaturated.

Options (fees will apply)

+ Rush order (pending availability)
+ Irradiation (see Product Specific Information)
+ Vacuum packaging (1 and 2 Kg)

Selected Nutrient Information[1]

	% by weight	% kcal from
Protein	23.5	18.3
Carbohydrate	27.3	21.4
Fat	34.3	60.3

Kcal/g **5.1**

[1] Values are calculated from ingredient analysis or manufacturer data

Contact Us

Obtain pricing · Check order status

+ teklad@envigo.com
+ **(800) 483·5523**

International Inquiry *(outside USA or Canada)*

+ askanutritionist@envigo.com

Speak With A Nutritionist

+ **(800) 483·5523**
+ askanutritionist@envigo.com

Teklad diets are designed & manufactured for research purposes only.

Place Your Order (USA & Canada)

Please Choose One

+ www.envigo.com/teklad-orders
+ tekladorders@envigo.com
+ **(800) 483·5523**
+ **(608) 277·2066** *facsimile*

DHR 02/18/19

Phenotype of C57BL/6NHsd Male Mice Fed TD.06414 or TD.08810

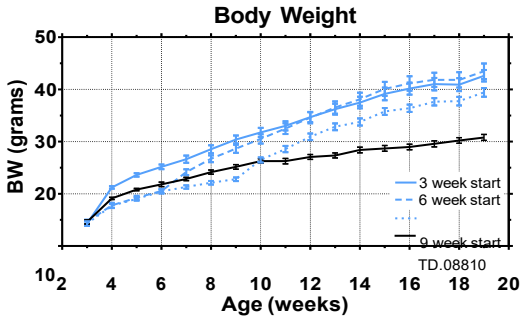

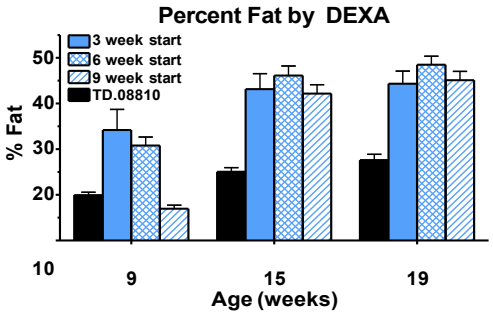

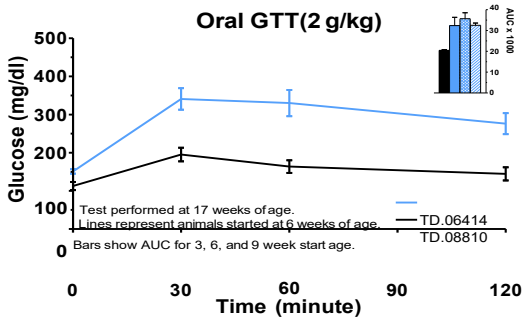

Key Findings

Male C57BL6/N mice started on TD.06414 at 3, 6, or 9 weeks of age develop similar degrees of obesity shown by rapid increase in body weight and percent fat mass.

Mice started on TD.06414 between 3-9 weeks of age develop impaired glucose tolerance by 17 weeks of age.

Mice fed TD.06414 develop hyperinsulinemia, hyperleptinemia, and exhibit increased liver accumulation of lipids.

The graphs ***above*** represent data obtained from male C57BL/6NHsd mice started on irradiated TD.06414 at 3, 6, or 9 weeks of age (16 mice/start age). Control animals were fed an irradiated purified diet TD.08810, or autoclaved natural ingredient diet 2018S. The data in the tables ***below*** is from a second cohort of mice started on the diets at 3 weeks of age. Prior to oral glucose tolerance test and collection of fasting values, mice were fasted for 6 hours (6am-12pm). Data are shown as mean ± SEM.

Additional Phenotype Data

11-12 weeks of age	TD.06414	TD.08810[t]	2018S[tt]
Body Weight (g, n=20)	32.1 ± 0.5	25.6 ± 0.3	25.0 ± 0.3
Percent Fat by NMR (n=20)	33.7 ± 1.1	19.2 ± 0.6	17.7 ± 0.4
Liver Triglyceride (mg/g liver, n=5)	75.5 ± 7.1	27.2 ± 3.9	34.9 ± 2.4
Fasted Total Cholesterol (mg/dl, n=20)	193 ± 7	119 ± 3	141 ± 3
Fasted Glucose (mg/dl, n=20)	166 ± 4	113 ± 2	120 ± 2
Fasted Insulin (ng/ml, n=20)	2.5 ± 0.2	0.8 ± 0.1	0.7 ± 0.1
Non-fasted Leptin (ng/ml, n=20)	37.2 ± 3.9	3.0 ± 0.6	2.5 ± 0.2
19-20 weeks of age	**TD.06414**	**TD.08810[t]**	**2018S[tt]**
Body Weight (g, n=14-20)	43.1 ± 0.9	29.4 ± 0.5	28.1 ± 0.5
Percent Fat by NMR (n=14-20)	45.2 ± 1.1	24.1 ± 0.7	21.8 ± 1.2
Liver Triglyceride (mg/g liver, n=5)	162.9 ± 46.3	40.6 ± 7.1	47.5 ± 4.8
Fasted Total Cholesterol (mg/dl, n=14-20)	253 ± 11	107 ± 3	142 ± 4
Fasted Glucose (mg/dl, n=14-20)	146 ± 5	115 ± 3	116 ± 5
Fasted Insulin (ng/ml, n=14-20)	5.0 ± 0.6	0.9 ± 0.1	0.8 ± 0.1
Non-fasted Leptin (ng/ml, n=14-20)	*86.9 ± 6.1	5.2 ± 0.8	5.4 ± 0.9

*11 of 16 mice had values greater than the detection limit and were set to 100 ng/ml.

[t]TD.120445 is a replacement for TD.08810 with 6% sucrose and majority of carbohydrate from resistant starch. Additional ingredient matched, low fat control diets are available.

[tt]Depending on what your main comparisons are, it may be suitable to have a grain-based diet as your control. 2018S is just one of many grain-based Teklad diets.

For additional study details, please refer to the **poster on our website**
or contact a nutritionist at **askanutritionist@envigo.com**

[Annex 1.1.2]: CE-MS: PCA-X scores scattered plot from CEMS acquisition data. Figure A: PCA-X of Plasma tissue (P) CE-MS results; Figure B: PCA-X of Kidney tissue(K) CEMS results; Figure C: PCA-X Heart tissue (H) CE-MS results and Figure D: PCA-X of Skeletal muscle tissue (SK) CE-MS results LC/MS positive polarity. Legend of groups:1.green: CHD; 2.dark blue: HFD; 3.red:QCs (Quality Controls)

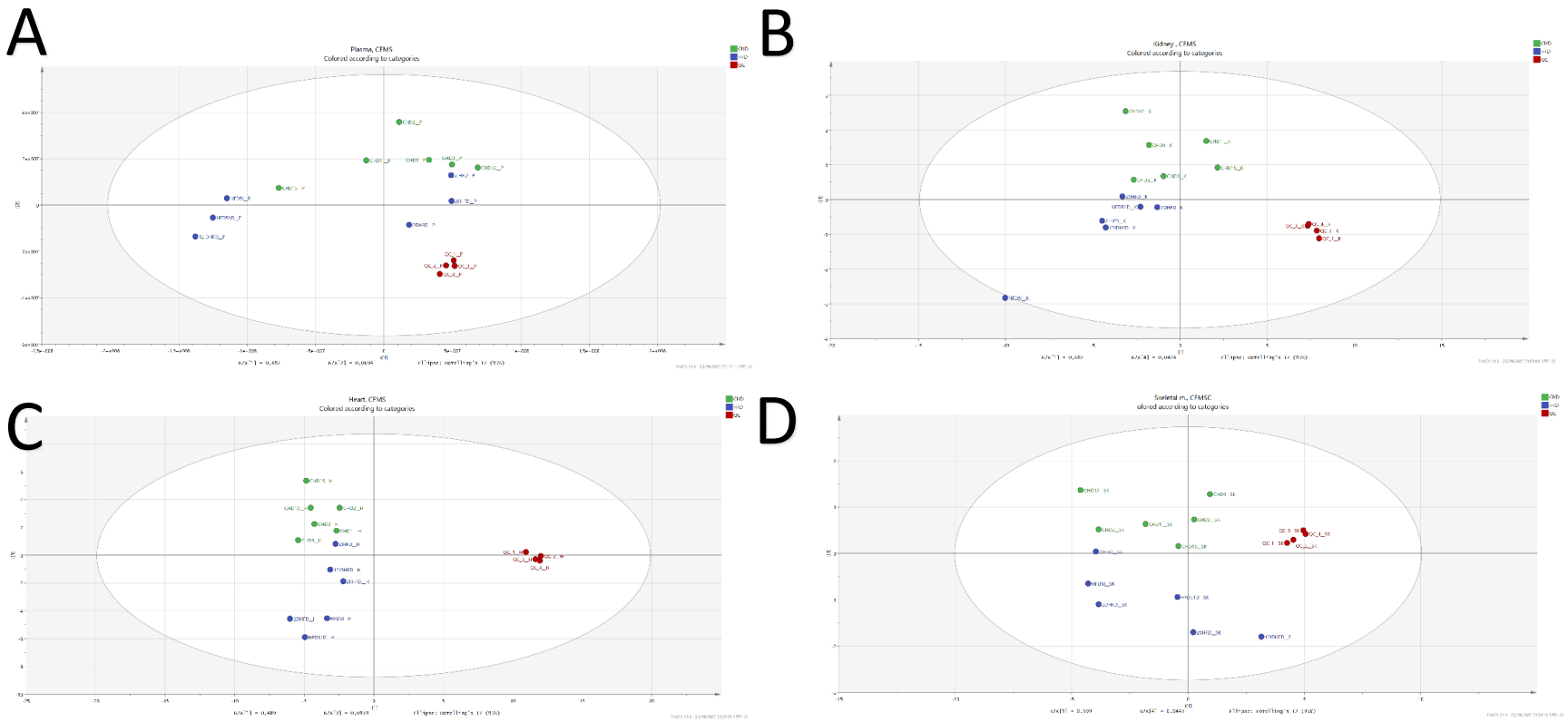

[Annex 1.1.3]:GC-MS: PCA-X scores scattered plot from GCMS acquisition data. Figure A: PCA-X of (P) GCMS results; Figure B: PCA-X of (K) GCMS results; Figure C: PCA-X of (H) GC-MS results; Figure D: PCA-X of (SK) GC-MS results; Figure E: PCA-X of Brown Adipose Tissue (BAT) GC-MS results; Figure F: PCA-X of epididymal White Adipose Tissue (WATe) GC-MS results; Figure G: PCA-X of inguinal White Adipose Tissue (WATi) GCMS results and Figure H: PCA-X of perirenal White Adipose Tissue (WATp) GC-MS results. Legend of groups:1.green: CHD; 2.dark blue: HFD; 3.red:QCs (Quality Controls)

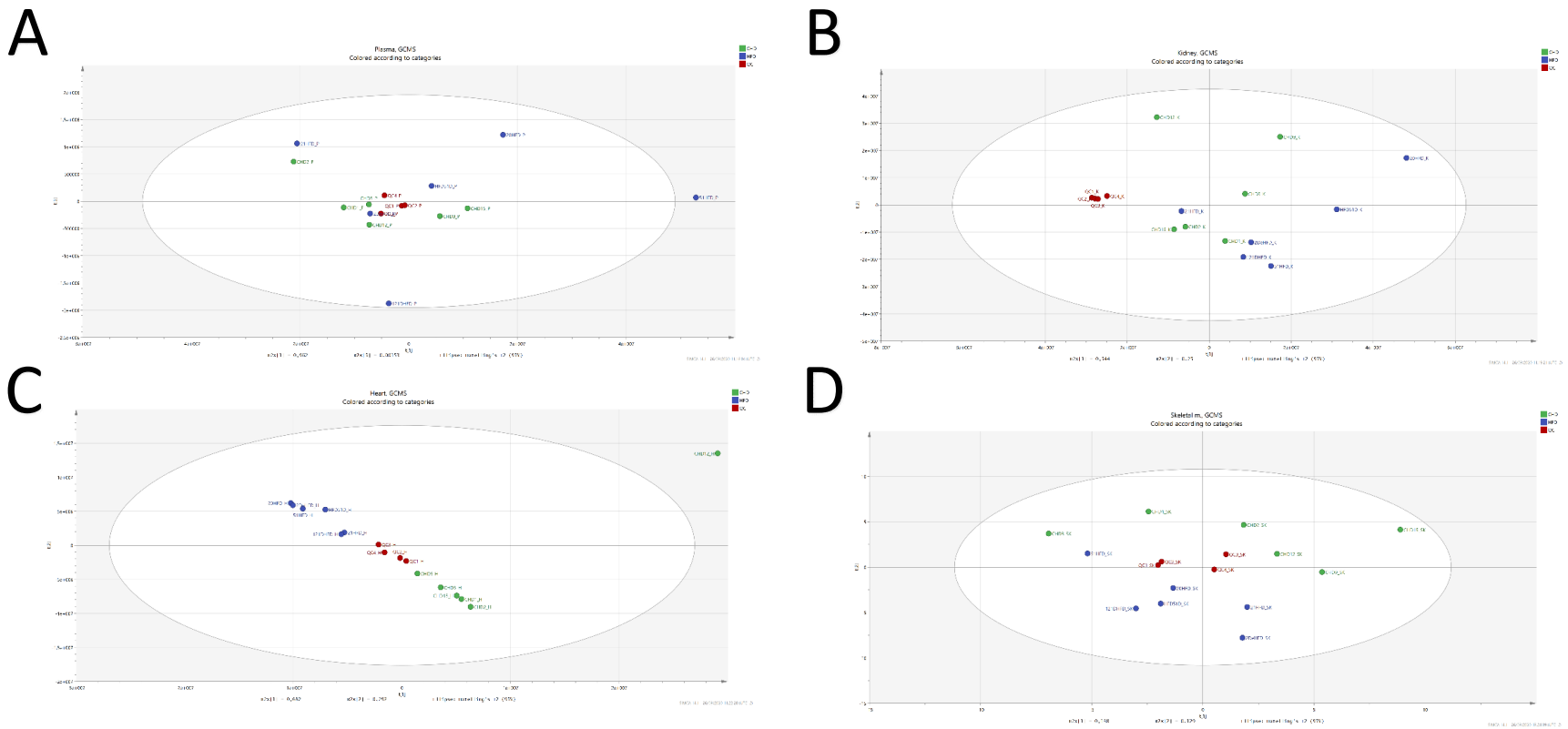

E

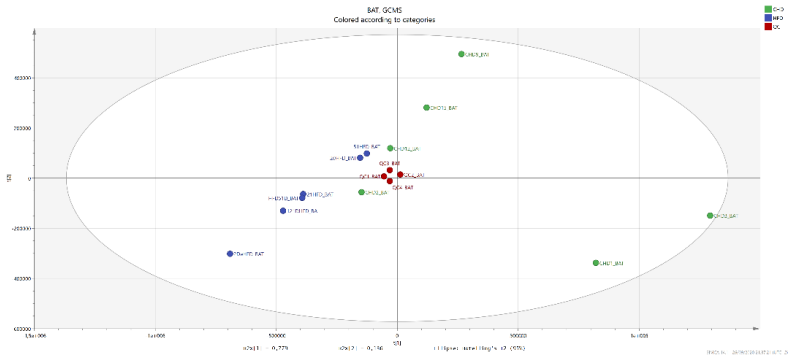
BAT, GCMS
Colored according to categories

F

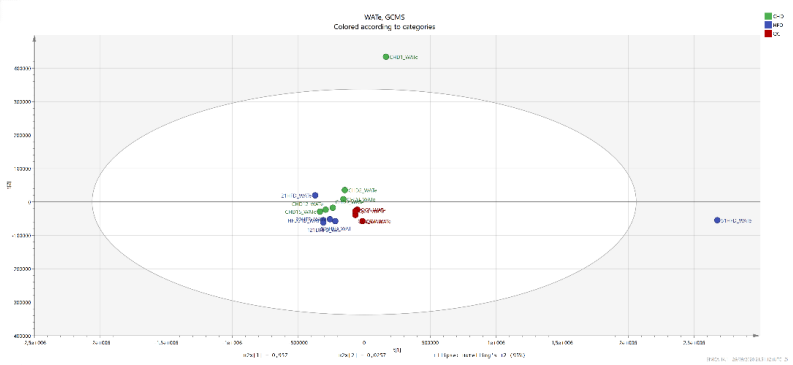
WATe, iGCMS
Colored according to categories

G

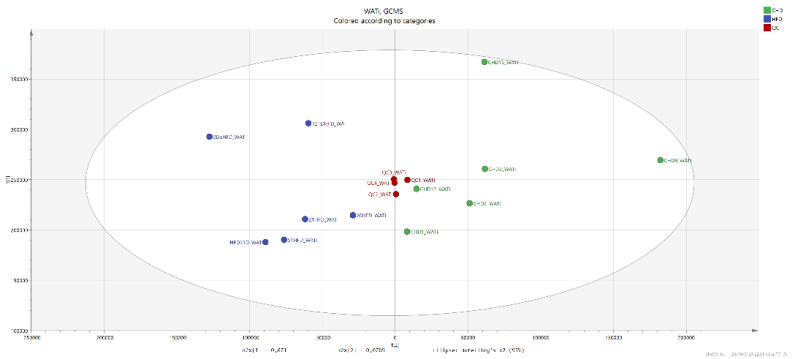
WATi, GCMS
Colored according to categories

H

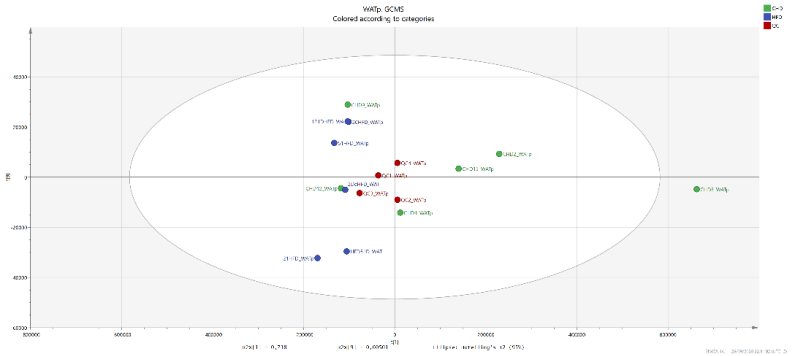
WATp, GCMS
Colored according to categories

[Annex 1.1.4]:LC-MS (-): PCA-X scores scattered plot from LCMS (-) acquisition data. Figure A:PCA-X of (P) LC-MS (-) results; Figure B: PCA-X of (K) LC-MS (-) results; Figure C: PCA-X of (H) LCMS (-) results; Figure D: PCA-X of (SK) LCMS (-) results; Figure E: PCA-X of Brown Adipose Tissue (BAT) LC-MS (-) results; Figure F: PCA-X of epididymal White Adipose Tissue (WATe) LC-MS (-) results; Figure G: PCA-X of inguinal White Adipose Tissue (WATi) LC-MS (-) results and Figure H: PCA-X of perirenal White Adipose Tissue (WATp) LCMS (-) results. Legend of groups:1.green: CHD; 2.dark blue: HFD; 3.red:QCs (Quality Controls)

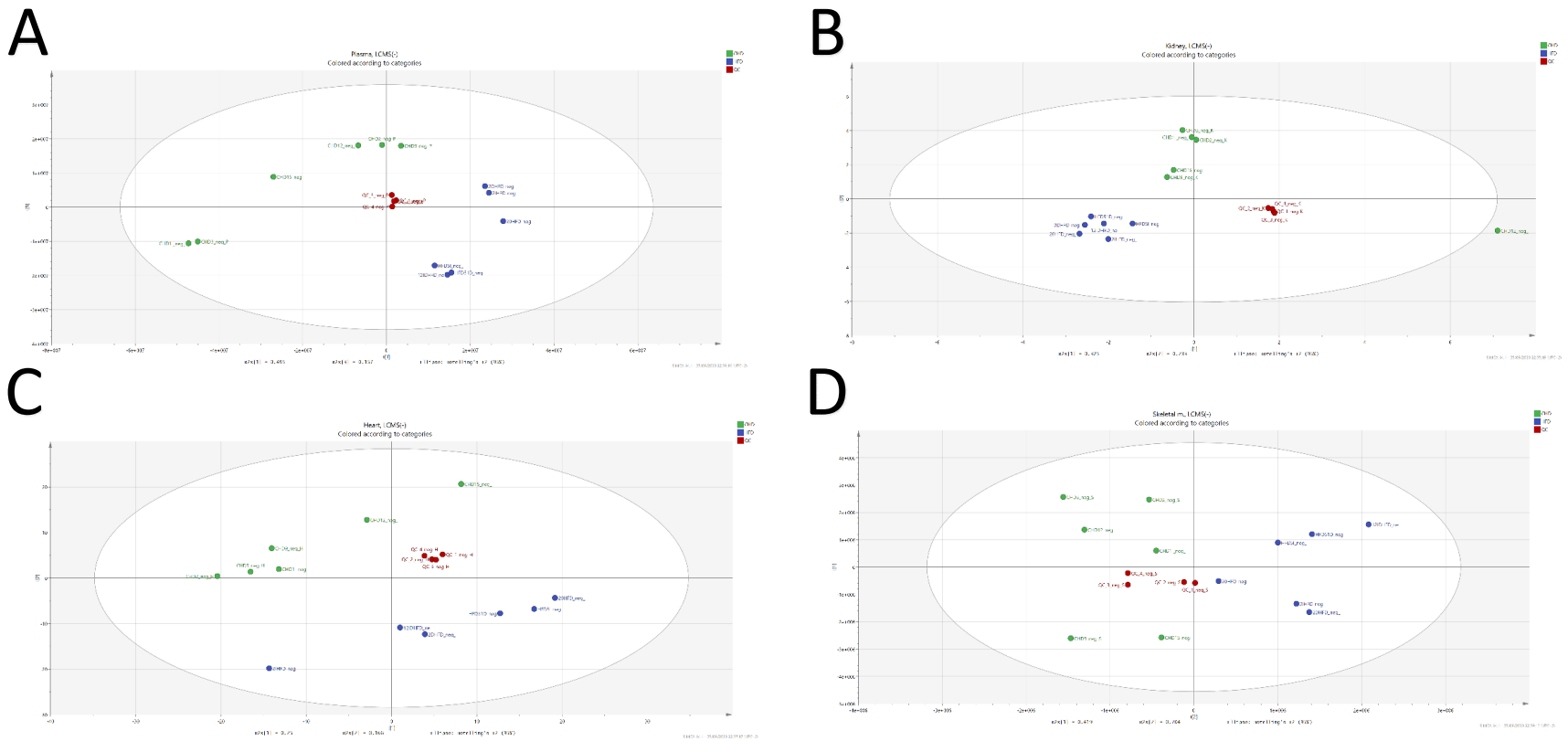

E

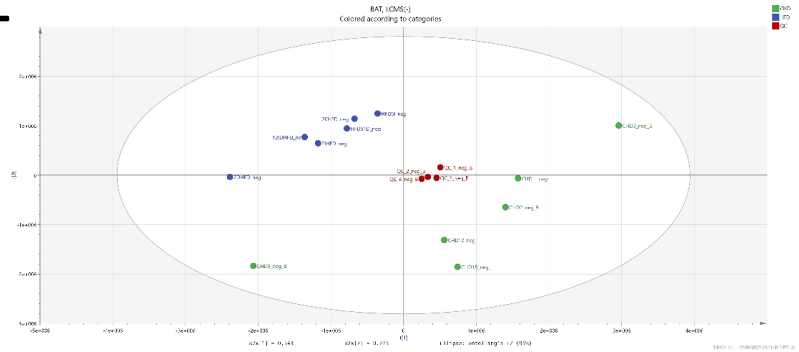
BAT, LCMS(-)
Colored according to categories
CNTL
ITD
QC

F

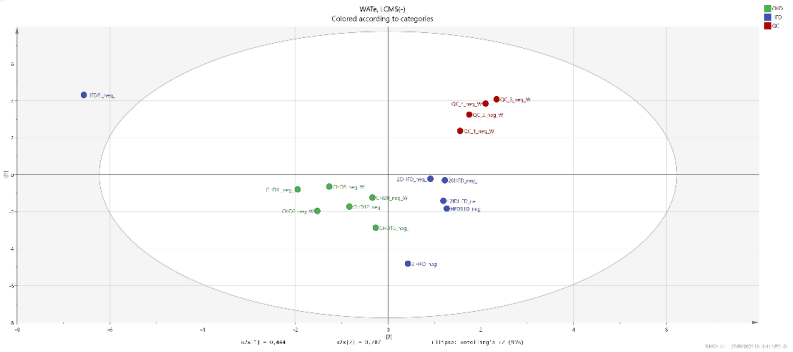
WATe, LCMS(-)
Colored according to categories
CNTL
ITD
QC

G

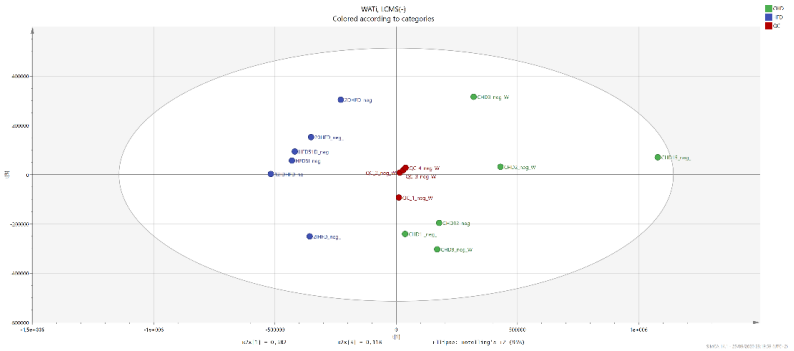
WATi, LCMS(-)
Colored according to categories
CNTL
ITD
QC

H

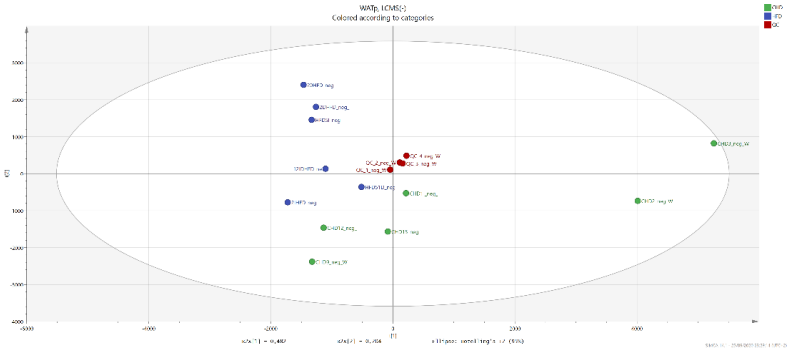
WATp, LCMS(-)
Colored according to categories
CNTL
ITD
QC

[Annex 1.1.5]: LC-MS (+):PCA-X scores scattered plot from LCMS (+) acquisition data. Figure A:PCA-X of (P) LCMS (+) results; Figure B: PCA-X of (K) LC-MS (+) results; Figure C: PCA-X of (H) LC-MS (+) results; Figure D: PCA-X of (SK) LC-MS (+) results; Figure E: PCA-X of Brown Adipose Tissue (BAT) LC-MS (+) results; Figure F: PCA-X of epididymal White Adipose Tissue (WATe) LC-MS (+) results; Figure G: PCA-X of inguinal White Adipose Tissue (WATi) LC-MS (+) results and Figure H: PCA-X of perirenal White Adipose Tissue (WATp) LCMS (+) results. Legend of groups:1.green: CHD; 2.dark blue: HFD; 3.red:QCs (Quality Controls)

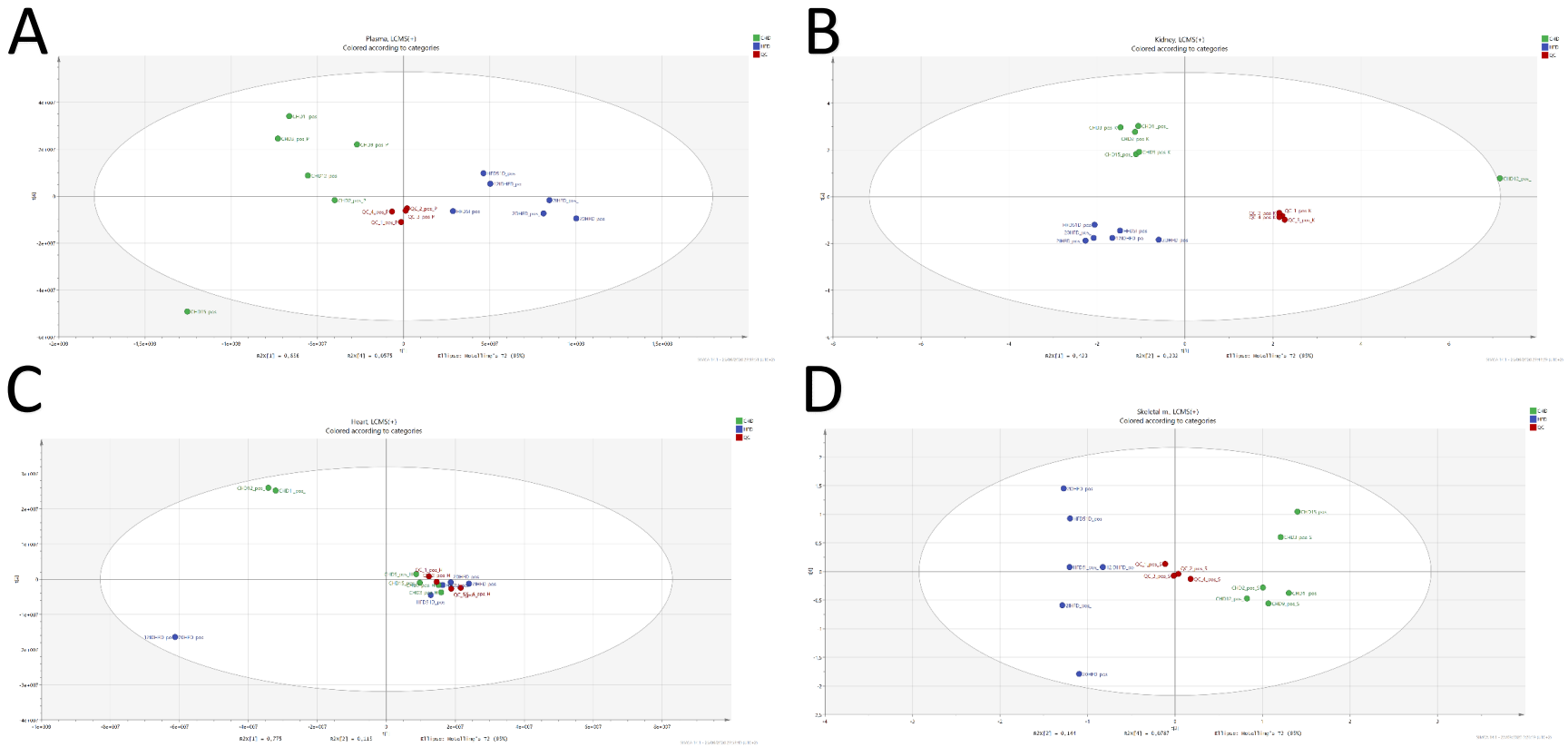

E

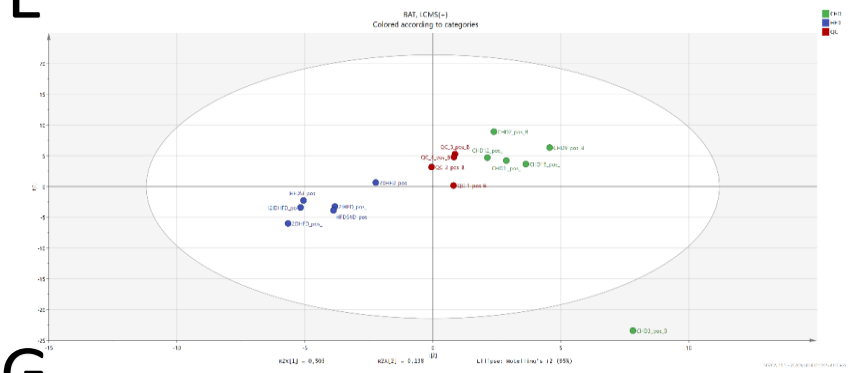
BAT, LCMS(−)
Colored according to categories

F

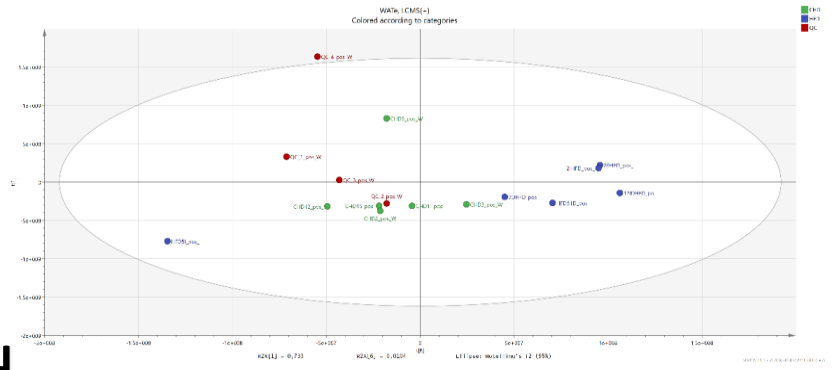
WATe, LCMS(+)
Colored according to categories

G

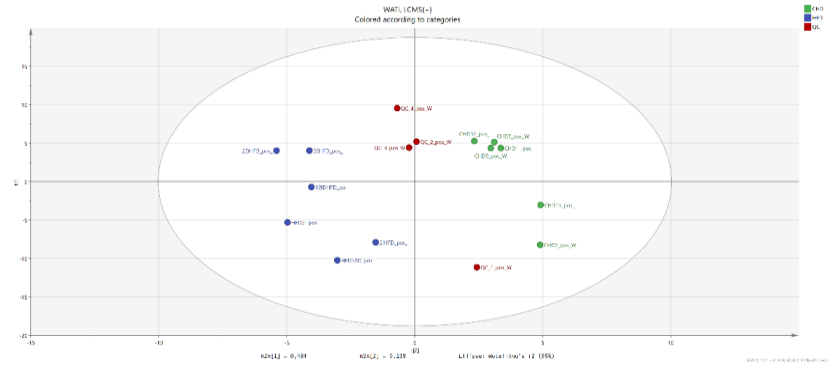
WAT, LCMS(−)
Colored according to categories

H

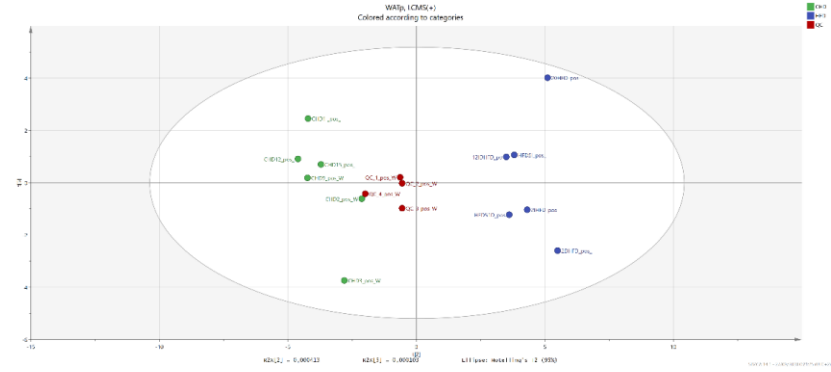
WATp, LCMS(+)
Colored according to categories

[Annex 2.1]: Specifications of MCD diet used for feeding mice in the study of NASH and PH (Chapter 2).

Teklad Custom Diet

TD.90262

Methionine/Choline Deficient Diet

ENVIGO

Formula	g/Kg
Sucrose	455.294
Corn Starch	200.0
Corn Oil	100.0
Cellulose	30.0
Mineral Mix, AIN-76 (170915)	35.0
Calcium Phosphate, dibasic	3.0
L-Alanine	3.5
L-Arginine HCl	12.1
L-Asparagine	6.0
L-Aspartic Acid	3.5
L-Cystine	3.5
L-Glutamic Acid	40.0
Glycine	23.3
L-Histidine HCl, monohydrate	4.5
L-Isoleucine	8.2
L-Leucine	11.1
L-Lysine HCl	18.0
L-Phenylalanine	7.5
L-Proline	3.5
L-Serine	3.5
L-Threonine	8.2
L-Tryptophan	1.8
L-Tyrosine	5.0
L-Valine	8.2
Vitamin Mix, w/o choline, A, D, E (83171)	5.0
Vitamin E, DL-alpha tocopheryl acetate (500 IU/g)	0.242
Vitamin A Palmitate (500,000 IU/g)	0.0396
Vitamin D_3, cholecalciferol (500,000 IU/g)	0.0044
Ethoxyquin, antioxidant	0.02

Footnote

Designed for rodents. TD.94149 is a possible ingredient matched control with L-Methionine included at 8.2 g/kg diet and choline at 1.4 g/kg diet. For questions about this or other AA and vitamin adjusted diets askanutritionist@envigo.com.

Key Features

+ **Amino Acid Defined Diet**
+ **Methionine**
+ **Choline**
+ **Rodent**

Selected Nutrient Information[1]

	% by weight	% kcal from
Protein	14.9	14.6
CHO	64.3	63.2
Fat	10.0	22.1
Kcal/g	**4.1**	

[1] Calculated values

[2] Protein based on N x 6.25

Teklad Diets are designed & manufactured for research purposes only.

Key Planning Information

+ *Products are made fresh to order*
+ Store product at 4°C or lower
+ Use within 6 months (applicable to most diets)
+ Box labeled with product name, manufacturing date, and lot number
+ Replace diet at minimum once per week
  More frequent replacement may be advised
+ Lead time:
  · 2 weeks non-irradiated
  · 4 weeks irradiated

Product Specific Information

+ 1/2" Pellet or Powder (free flowing)
+ Minimum order 3 Kg
+ Irradiation available upon request

Options (Fees Will Apply)

+ Rush order (pending availability)
+ Irradiation (see Product Specific Information)
+ Vacuum packaging (1 and 2 Kg)

Speak With A Nutritionist

+ **(800) 483·5523**
+ **askanutritionist@envigo.com**

Contact Us

Obtain Pricing · Check Order Status

+ **teklad@envigo.com**
+ **(800) 483·5523**

International Inquiry *(Outside USA or Canada)*

+ **askanutritionist@envigo.com**

Place Your Order (USA & Canada)

Please Choose One

+ **www.envigo.com/teklad-orders**
+ **tekladorders@envigo.com**
+ **(800) 483·5523**
+ **(608) 277·2066** *facsimile*

06/28/16